USC
UNIVERSIDADE
DE SANTIAGO
DE COMPOSTELA

Departamento de Física de Partículas

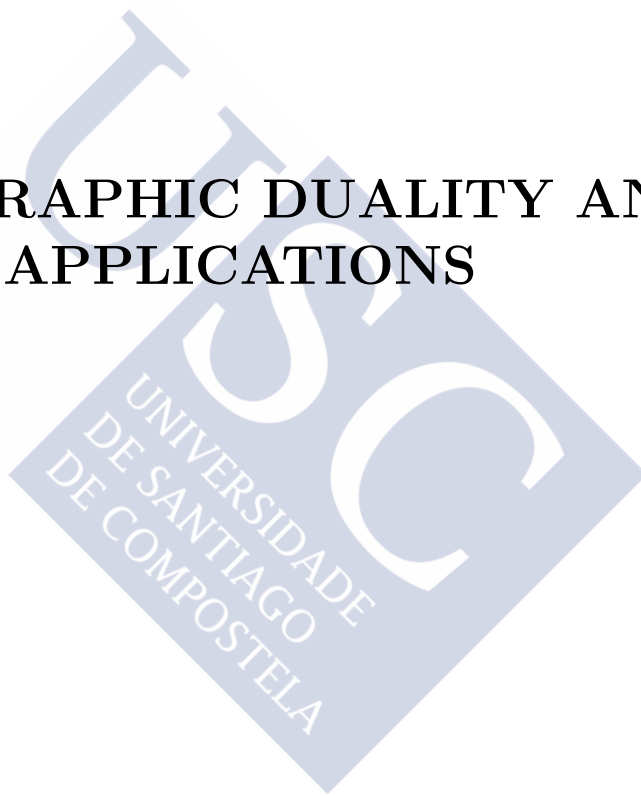# HOLOGRAPHIC DUALITY AND APPLICATIONS

Yago Bea Besada

Santiago de Compostela, setembro de 2016.

UNIVERSIDADE DE SANTIAGO DE COMPOSTELA

Departamento de Física de Partículas

HOLOGRAPHIC DUALITY AND APPLICATIONS

Yago Bea Besada

Santiago de Compostela, setembro de 2016.

UNIVERSIDADE DE SANTIAGO DE COMPOSTELA

Departamento de Física de Partículas

HOLOGRAPHIC DUALITY AND APPLICATIONS

Tese presentada para optar ao grao
de Doutor en Física por:

Yago Bea Besada

Setembro, 2016

UNIVERSIDADE DE SANTIAGO DE COMPOSTELA

Departamento de Física de Partículas

Alfonso Vázquez Ramallo, Catedrático de Física Teórica da Universidade de Santiago de Compostela,

CERTIFICO: que a memoria titulada *Holographic duality and applications* foi realizada, baixo a miña dirección, por Yago Bea Besada, no departamento de Física de Partículas desta Universidade e constitúe o traballo de Tese que presenta para optar ao grao de Doutor en Física.

Asinado:

Alfonso Vázquez Ramallo.
Santiago de Compostela, setembro de 2016.

A mi familia

Agradecimientos

Me gustaría agradecer profundamente a mi director de tesis Alfonso Vázquez Ramallo, quien me ha ofrecido la oportunidad de iniciarme en el ámbito de la investigación bajo una tutela inmejorable. Su inmenso conocimiento y su gran dedicación a la física han sido una enorme fuente de inspiración y motivación en la realización de esta tesis. Además, no sólo es una excelente persona en el ámbito académico, sino también en el personal, haciendo que la investigación se haya desarrollado en un entorno más que agradable.

I want to deeply thank Niko Jokela. With his patience and rigor, he devoted a lot of time explaining me an infinite amount of physics, and many other important things. From my point of view, he is not only a collaborator, I also consider him a co-advisor.

Otra persona que ha sido especialmente importante en mi iniciación en el ámbito de la investigación es Carlos Núñez, con quien he tenido la gran oportunidad de trabajar durante mi estancia en la universidad de Swansea. Aunque todo aquel que le conoce sabe que su devoción por la física y su conocimiento no tienen límites, también hay que destacar la infinita paciencia y dedicación con la que trata a sus estudiantes.

I am deeply grateful to Diego Trancanelli, who gave me the opportunity of staying in São Paulo university. During this stay I could learn a lot of new things, most of them different from the main topic of my thesis, that gave me a broader point of view.

I am also deeply grateful to Johanna Erdmenger, who offered me the possibility of staying at the Max-Planck-Institut für Physik, where I could meet a lot of new people in a very active atmosphere. My experience was very fruitful, I had a lot of discussions with many different people and I could attend a lot of lectures. Moreover, we started new collaborations.

Finally, I would like to thank my collaborators, from whom I have learned a lot of new physics and techniques, and with whom I have had very interesting and fruitful discussions: Daniel Areán, Paolo Benincasa, Eduardo Conde, José Edelstein, Georgios Itsios, Matthew Lippert, Aníbal Sierra and Dimitrios Zoakos.

Contents

Motivation

This thesis is based on the gauge/gravity duality, which emerged from string theory in the nineties. We give a historical introduction and contextualize the work that we will present.

In the twentieth century it took place the consolidation of two fundamental developments in physics. On the one hand, the theory of general relativity was constructed to explain gravity, one of the four fundamental forces of nature, and became very successful describing the macroscopic physics. On the other hand, the birth of quantum field theory gave a natural framework for elementary particle physics, which explains the other three fundamental forces of nature, weak, strong and electromagnetic, obtaining a very accurate description of the subatomic physics. However, these two developments are incompatible, and a desirable unification in a quantum theory of gravity remained as an open problem. In the seventies the string theory was constructed, and it turned out to be a promising candidate to perform such unification. Thus, string theory can be considered as a 'theory of everything', in the sense that it aims to explain the four fundamental forces of nature in a unified and common way.

String theory was originally formulated in the context of the strong interactions. In 1968 Veneziano proposed an amplitude [1] to explain some characteristics of the new hadronic experimental data. Soon after Veneziano's proposal, a theory which reproduced the amplitude was found in the form of a quantized string. In 1970 the Nambu-Goto action for the bosonic string was formulated [2] and in 1971 Ramond, Neveu and Schwarz constructed the fermionic string [3]. Nevertheless, at the beginning of the seventies the Veneziano amplitude became unable to explain the new experimental results, and a new theory, quantum chromodynamics, revealed itself as a much more promising candidate for the description of strong interactions. Therefore, string theory ceased to be a good candidate for the strong interactions. In 1974, Scherk and Schwarz [4] reinterpreted the string theory as a much more fundamental theory: a quantum theory of gravity. The scale of the theory was reduced from the strong interaction scale to the Planck scale. Previously, as a theory of strong interactions, the massless spin 2 particle present in the spectrum of the theory was absent in the experimental results, giving rise to an unsolved puzzle, but now, as a theory of quantum gravity, this particle had a natural interpretation as the graviton. String theory became a good candidate for the unification of the four fundamental forces, as in the low energy limit only the massless modes are left, including the graviton and lower spin particles, which could account for the matter and gauge bosons. Also, Einstein gravity is correctly recovered in the classical limit.

In 1976 Gliozzi Scherk and Olive [5] imposed the so-called GSO projection which removed

vice versa. This means that if we want to compute observables in a strong coupling region of a quantum field theory, we can consider its supergravity description, were the coupling constant is weak, and perform the computations. Then, performing an easy computation in classical supergravity we can obtain results in the strong coupling regime of a quantum field theory, where other tools are limited or inexistent. The drawback of this powerful method is that the quantum field theories with known gravity dual are very limited, and still far from realistic theories. The hope is that we can extract universal properties that are valid for a set of similar theories, and then extrapolate to the realistic theories. Another drawback of the gauge/gravity duality is that even if it has undergone many non trivial tests, there is no proof of the conjecture.

T-duality in string theory was discovered in the eighties. It relates two seemingly different theories that are compactified on a circle. These two theories are two different descriptions of the same physics, and they are said to be T-dual to each other. For example, type IIA and B string theories on Minkowski spacetime compactified on a circle are T-dual to each other. Locally, T-duality is given by the Buscher rules [11] [12], and globally, it corresponds to an exchange of the Chern number of a $U(1)$-fibration and the H_3 flux on its base [13]. On the other hand, non-abelian T-duality (NATD) was introduced at the end of the eighties [14] as a generalization of T-duality to non-abelian isometry groups. Buscher rules were known for the NSNS sector, and it was applied in the context of sigma models. Nevertheless, the transformation rules for the RR sector remained unclarified until 2010 [15]. With the complete Buscher rules, the NATD was used to obtain new supergravity solutions of type IIA/B and, then, new examples of the AdS/CFT duality. In particular, new AdS solutions were found by this method. Nevertheless, the global properties of the transformation are not known, and then the dual solution is only known locally (sometimes stated as "the range of the dual coordinates is not known"). As a consequence, the dual field theory to this new NATD background can not be understood with full detail. In this thesis we construct new supersymmetric solutions of type IIA/B and eleven-dimensional supergravity using NATD.

In the original formulation of the gauge/gravity duality, all the fields of the field theory are in the adjoint representation of the gauge group. In order to make contact with phenomenological theories, it is convenient to introduce fundamental matter (recall that fundamental matter corresponds to quarks in QCD or electrons in condensed matter physics). The fundamental matter was introduced in the correspondence in 2002 by Karch and Katz [16], using D7 probe branes in the $AdS_5 \times S^5$ solution. Using probe branes in the gravity side corresponds to having quenched fundamental matter in the field theory side. In order to take into account the full effect of the fundamental matter, one has to solve the equations of motion of supergravity coupled to the D-brane sources. In general, it is a difficult problem to obtain such backgrounds. For a stack of localized flavor branes, the problem has reduced symmetries, Dirac deltas and dependence on several variables. In order to simplify it, one can consider a continuous distribution of sources (as in electromagnetism a continuous source of charges), recovering the symmetries, the dependence in one variable and avoiding Dirac deltas. This method is known in the literature as the smearing technique. In this thesis, the smearing technique is used to obtain a new supergravity background that generalizes the

ABJM model by including massive fundamental matter.

The holographic duality has found a lot of applications, mostly in QCD and condensed matter physics. In particular, after the conjecture was formulated, the applications to condensed matter physics have increased continuously, and we can find applications to the description of superconductors, superfluids, insulators, metals, strange metals, topological insulators, Hall effect, Kondo model, etc. In this thesis we present a new model for the fractional quantum Hall effect based on the ABJM model. Besides, we also present a new model exhibiting quantum phase transitions.

About this thesis

This thesis is based on the papers [17, 18, 19, 20] and has the following structure:

- The first chapter is a general introduction to the gauge/gravity duality. First, we review the fundamental aspects of supergravity. Second, we review T-duality in the context of supergravity, and consider its non-abelian generalization. Third, we introduce the AdS/CFT correspondence and analyze the addition of flavor to it. Finally, we comment on some applications of the AdS/CFT conjecture.

- The second chapter reviews some applications of non-abelian T-duality. In the context of type IIA/B supergravity, the non-abelian T-duality is used to obtain new solutions from previously know solutions. The aim is to obtain new interesting cases of the gauge/gravity duality. In particular, new AdS_3 fixed points are constructed. Also, we analyze the field theory duals of the new supergravity solutions, via the computation of some observables.

- In the third chapter we construct a new supergravity IIA background with D6-branes sources, whose field theory dual corresponds to a generalization of the ABJM theory that includes unquenched massive flavors. This construction uses the smearing technique. Several observables are analyzed, confirming a RG flow between two fixed points at the IR and UV.

- In the fourth chapter we construct a supergravity solution based on the ABJM model, dual to a quantum Hall system. The fundamental matter is introduced in the supergravity dual via probe D6-branes, in which non-trivial woldvolume gauge fields are turned on. This set up allows to have Hall states, and the filling fraction is computed. For particular values of the parameters, supersymmetric solutions are found.

- In the fifth chapter, we construct a supergravity solution based on the ABJM model, dual to a condensed matter system exhibiting quantum phase transitions. The fundamental matter is introduced via D6-branes, and charge density is turned on. In the ABJM background, the probe brane undergoes a second order phase transition at zero charge density. In the partially backreacted ABJM solution, the phase transition becomes first order, and takes place at a finite value of the charge density.

Chapter 1

Introduction

We start this chapter by a review of the fundamental aspects of supergravity, which is the basic ground where this thesis is formulated. Besides, the elementary aspects of T-duality and non-abelian T-duality in the context of supergravity are reviewed. We also give a brief introduction to the AdS/CFT conjecture, and analyze the addition of flavor to it. Finally, we comment on the applications of the duality.

1.1 Supergravity

Supergravity is obtained by gauging supersymmetry, *i.e.*, by considering local supersymmetry, instead of global. In a natural way, supergravity theories contain Einstein gravity, and due to its supersymmetric character, they are well behaved theories and thus good candidates for a quantum theory of gravity.

The string theories at low energies are described by supergravity theories. For example, type IIA(B) string theory at low energies is described by IIA(B) supergravity, and M-theory at low energies is described by eleven-dimensional supergravity. These supergravity theories are particularly interesting in the context of AdS/CFT. The AdS/CFT conjecture was born from string theory, and it relates a string theory background with a quantum field theory. But the duality is actually useful in a particular regime, precisely in the low energy limit of the string theory side, when it is well described by classical supergravity.

In general, supergravity theories can be constructed in different dimensions, with different gauge groups and with different amounts of supersymmetry. The different supergravity theories are very heterogeneous, and it is difficult to consider a common treatment. In order to define what a supergravity theory is, let us consider the eleven-dimensional supergravity. This theory was predicted by Nahm [8] and constructed soon thereafter by Cremmer, Julia and Scherk [9].

Eleven-dimensional supergravity

The bosonic geometrical data of eleven-dimensional supergravity [21] consists of (M, g, F), where (M, g) is an eleven-dimensional lorentzian manifold with a Spin structure and $F \in \Omega^4(M)$, $dF = 0$, is a closed four-form. There is also fermionic data, but we will restrict to

bosonic solutions. The bosonic equations of motion of eleven-dimensional supergravity are a generalization of the Einstein and Maxwell equations in four dimensions. The generalization of the Einstein equation is:

$$\text{Ric}(X,Y) = \frac{1}{2}\langle i_X F, i_Y F \rangle - \frac{1}{6}g(X,Y)\langle F, F \rangle \ , \tag{1.1.1a}$$

where the left hand side is the Ricci tensor and the right hand side is related to the energy momentum tensor of the field F, and $X, Y \in \mathfrak{X}(M)$ are vector fields in M. The scalar product on forms $\langle -, - \rangle$ is the natural one inherited from the metric. Rewriting the same equation in local coordinates:

$$R_{\mu\nu} = \frac{1}{12}F_{\mu\sigma_1\sigma_2\sigma_3}F_{\nu}{}^{\sigma_1\sigma_2\sigma_3} - \frac{1}{144}g_{\mu\nu}F_{\sigma_1\sigma_2\sigma_3\sigma_4}F^{\sigma_1\sigma_2\sigma_3\sigma_4} \ . \tag{1.1.1b}$$

The generalization of the Maxwell equation is:

$$d * F = \frac{1}{2}F \wedge F \ . \tag{1.1.2}$$

A set (M, g, F) verifying equations (1.1.1) and (1.1.2) is a classical bosonic solution to eleven-dimensional supergravity.

Equations (1.1.1) and (1.1.2) can be obtained from an effective action:

$$S = \frac{1}{2\kappa^2}\int_M \left(*1 \ R - \frac{1}{2}F \wedge *F + \frac{1}{6}A \wedge F \wedge F \right) \ , \tag{1.1.3}$$

where A is a three form verifying $F = dA$, assuming that F is exact. The same expression in local coordinates reads (let U be a local chart of M):

$$S = \frac{1}{2\kappa^2}\int_{U \subset M} d\xi^{11}\sqrt{-g}\left(R - \frac{1}{48}F_{\sigma_1\sigma_2\sigma_3\sigma_4}F^{\sigma_1\sigma_2\sigma_3\sigma_4} \right) + \frac{1}{2\kappa^2}\int_{U \subset M}\frac{1}{6}A \wedge F \wedge F \ . \tag{1.1.4}$$

We have chosen a Lorentz manifold with a Spin structure. A time-oriented and space-oriented Lorentz manifold (M, g) has a Spin structure if the frame bundle can be lifted according to:

$$Spin_+(1, 10) \mapsto SO_+(1, 10) \ . \tag{1.1.5}$$

Not every manifold admits a Spin structure, and a topological obstruction can exist. A characterization for a Lorentz manifold to have a Spin structure is given in terms of Stiefel-Whitney classes [22].

An equivalent and useful way of describing the Spin structure is to consider a Clifford bundle on M, and then take the subbundle that is obtained by restriction to the Spin group inside the Clifford algebra at each point $p \in M$ (the obstruction to this reduction is the same as for the Spin structure). The Clifford algebra $Cl(1, 10)$ can be read off from the classification of Clifford algebras [23]:

$$Cl(1, 10) \cong Mat_{32}(\mathbb{R}) \oplus Mat_{32}(\mathbb{R}) \ . \tag{1.1.6}$$

Let \$ be the Spin bundle and $\varepsilon \in \Gamma(\$)$ a section, usually called spinor. There is a natural action of the exterior algebra on the Spin bundle:

$$c : \Lambda T^*M \cong Cl(T^*M) \to End \ \$ \quad , \qquad (1.1.7)$$

where the fist map is the bundle isomorphism induced by the vector space isomorphism between the exterior and Clifford algebras and the second map is induced from the action of the Clifford algebra $Cl(1,10)$ on the spinor representation S of $Spin(1,10)$.

The supersymmetric character of the theory is given by a list of rules to transform bosons and fermions that leave invariant the equations of motion, the so called supersymmetry transformations. For bosonic solutions, where the fermionic fields are set to zero, the supersymmetric variation of bosonic fields is automatically zero, and the supersymmetric variation of the fermionic field is given by:

$$\delta_\varepsilon \Psi = D\varepsilon \quad , \qquad (1.1.8)$$

where D, the supercovariant connection, is defined as:

$$D_X \varepsilon := \nabla_X \varepsilon + \frac{1}{6}c\left(\imath_X F\right)\varepsilon - \frac{1}{12}c\left(X^\flat \wedge F\right)\varepsilon \qquad \forall X \in \mathfrak{X}(M) \quad , \qquad (1.1.9a)$$

where ∇ is the spin connection and $X^\flat$ is the one-form dual to X. In components:

$$D_\mu \varepsilon := \nabla_\mu \varepsilon + \frac{1}{36}\Gamma^{\sigma_1 \sigma_2 \sigma_3} F_{\mu \sigma_1 \sigma_2 \sigma_3}\varepsilon - \frac{1}{288}\Gamma_\mu{}^{\sigma_1 \sigma_2 \sigma_3 \sigma_4} F_{\sigma_1 \sigma_2 \sigma_3 \sigma_4}\varepsilon \quad . \qquad (1.1.9b)$$

We say that a classical bosonic solution of eleven-dimensional supergravity (M, g, F) is supersymmetric if there is a nonzero spinor $\varepsilon \in \Gamma(\$)$ which is parallel with respect to the supercovariant connection D, *i.e.*, $D_X \varepsilon = 0 \ \ \forall X \in \mathfrak{X}(M), \ \varepsilon \neq 0$.

A nonzero spinor satisfying $D\varepsilon = 0$ is called a Killing spinor. As equation (1.1.9) is linear, the solutions form a vector space. The dimension of this vector space can range from 0 to 32, and it is common to use the parameter $\nu := \dim\{\text{Killing spinors}\}/32$ to refer to the supersymmetry of a given background.

It has been proven that the algebraic structure generated by the infinitesimal isometries and the Killing spinors form a superalgebra for any bosonic supersymmetric solution of eleven-dimensional supergravity [24]. This superalgebra is known as 'Killing superalgebra'. For example, for $AdS_4 \times S^7$ the Killing superalgebra is $\mathfrak{osp}(1|32)$. It has been also proven that this superalgebra is a filtered deformation of a subsuperalgebra of the Poincare superalgebra [25], and it is thought that the classification of the filtered subalgebras could allow a classification of the supersymmetric backgrounds (using this technique, it has been already rederived the classification of maximally supersymmetric backgrounds [25]).

The definition of Killing spinor could be generalized. We have considered a Spin structure on the manifold, and this can be generalized to Pin structures, or Clifford structures, restricting to the Pin group or Clifford group inside the Clifford algebra. Besides, complex Clifford algebras can be considered and Spin^c structures instead of Spin structures, or more generally Pin^c and Clifford^c [26]. The conditions for the existence of these structures can be

dim	Holonomy	Geometry	n
4k+2	SU_{2k+1}	Calabi-Yau	(1,1)
4k	SU_{2k}	Calabi-Yau	(2,0)
4k	Sp_k	hyperkähler	(k+1,0)
7	G_2	exceptional	1
8	$Spin_7$	exceptional	(1,0)

Table 1.1: Manifolds admitting parallel spinors

also found in [22]. This kind of generalizations correspond to a generalization of the definition of supergravity as usually considered in the literature, and are still under investigation. It could be interesting to consider the potential applications to AdS/CFT.

Supersymmetric solutions

A general classification of bosonic supersymmetric solutions of eleven-dimensional supergravity is an open and difficult problem. Nevertheless, there are some partial classifications for some particular regions of the theory.

Let us consider the classification attending to the amount of supersymmetry. For eleven-dimensional supergravity it has been classified the solutions of maximal supersymmetry $\nu = 1$ [27], corresponding to symmetric spaces (basically, they are Minkowski, $AdS_4 \times S^7$, $AdS_7 \times S^4$ and the common Penrose limit of the last two cases). It has been proven that for $\nu = 31/32$ [28, 29] and $\nu = 30/32$ [30] there are no solutions. Besides, it has been proven that for $\nu > 1/2$ the solutions are locally homogeneous [31]. For the following values there are known solutions: 1/32, 1/16, 3/32, 1/8, 5/32, 3/16, 1/4, 3/8, 1/2, 9/16, 5/8, 11/16, 3/4, 1, but for the other fractions of supersymmetry it is not known if there exist solutions.

Let us consider the classification for particular values of the four-form $F \in \Omega^4(M)$. First, for $F = 0$, the superconnection D reduces to the spin connection ∇, and it suffices to classify the spin manifolds admitting parallel spinors with respect to the spin connection. In order to simplify this problem, it is commonly assumed that the eleven-dimensional manifold M is a product of a Lorentz and a Riemann manifolds, $M = L \times R$. Choosing L as the Minkowski space, then the problem reduces to find a riemannian manifold R admitting parallel spinors. The classification of simply connected, complete (in this subsection all manifolds will be simply connected and complete) Riemann manifolds admitting parallel spinors was obtained in [32]. The idea is that the Riemann manifolds admitting parallel spinors are manifolds of special holonomy groups. The special holonomy groups where classified by Berger in 1957, and Wang [32] used this result to classify those admitting parallel spinors. The result of Wang is that manifolds admitting parallel spinors are in one of the classes presented in Table 1.1. To be precise, what is classified is not the whole set of manifolds admitting parallel spinors, but only the set of possible holonomy groups that the manifolds admitting parallel spinors can have. Knowing the special holonomy group allows to know the structure of the manifold.

We have considered an eleven-dimensional manifold as the product of a Minkowski space and a Riemann manifold $M = L \times R$, so we reduced the problem to the riemannian case. This has been the usual point of view adopted in the literature of string theory since its birth. Nevertheless, it is also interesting to consider parallel spinors in Lorentz manifolds. This problem was recently solved by Thomas Leistner. He obtained the classification of special holonomy manifolds for the lorentzian case, and as a corollary, the classification of the lorentzian manifolds admitting parallel spinors. In summary, the lorentzian manifolds admitting parallel spinors are the symmetric lorentzian spaces (in the riemannian case, symmetric spaces do not admit parallel spinors) and lorentzian manifolds with special holonomy group equal to $G \rtimes \mathbb{R}$, with G a group of the riemannian case of Table 1.1.

Let us now consider $F \neq 0$, for the particular case of F being related to the volume form of the manifolds involved. Then the Killing spinor equation reduces to the geometrical Killing spinor equation [1], namely:

$$\nabla_X \varepsilon = \lambda X \varepsilon \qquad \forall X \in \mathfrak{X}(M) \ , \tag{1.1.10}$$

with $\lambda \in \mathbb{C}$. As in the previous case, let us consider the simplification of considering the eleven-dimensional manifold as the product of a lorentzian manifold and a riemannian manifold. It turns out that the classification of riemannian manifolds admitting geometrical Killing spinors can be reduced to the classification of riemannian manifolds admitting parallel spinors with respect to the spin connection. This result was obtained by Bär [33], who used the cone construction. Given a manifold X admitting geometrical Killing spinors, on the product manifold $\mathbb{R}^+ \times X$ the following metric can be constructed:

$$ds^2_{\mathbb{R}^+ \times X} = dr^2 + r^2 ds^2_X \ . \tag{1.1.11}$$

The geometrical Killing spinors on the base manifold X are in 1 to 1 correspondence with the parallel spinors of the cone manifold $C = \mathbb{R}^+ \times X$. The corresponding geometries admitting geometrical Killing spinors are shown in Table 1.2.

An interesting question is if this cone construction can be extended to the lorentzian case. The answer is that it has not been done yet, because the classification in this case reduces to the classification of the manifolds with signature $(2, n-2)$ admitting parallel spinors, and the classification of special holonomy manifolds in signature $(2, n-2)$ is still unfinished.

For more general cases, with F arbitrary, there are no known classifications for the manifolds admitting Killing spinors. For these backgrounds, the study must be done case by case, checking the existence of globally defined Killing spinors.

Finally, it is also interesting to mention that there are some classifications for the more general case of supergravity defined using Spin^c manifolds. For example, it has been classified the riemannian Spin^c manifolds admitting parallel spinors [26].

These partial classifications have important applications to AdS/CFT. For example, it has allowed to extend the conjecture from the initial case of D3-branes in flat space to cone D3-branes, at the first stages of the formulation. One of the most remarkable examples is

---

[1]We use "Killing spinor" for a spinor satisfying the general equation (1.1.9) and "geometrical Killing spinor" for a spinor satisfying the particular equation (1.1.10)

dim X	Holonomy of C	Geometry of X	(n_+, n_-)
k	$\{1\}$	round sphere	$(2^{\lfloor k/2 \rfloor}, 2^{\lfloor k/2 \rfloor})$
4k-1	Sp_k	3-Sasaki	(k+1,0)
4k-1	SU_{2k}	Sasaki-Einstein	(2,0)
4k+1	SU_{2k+1}	Sasaki-Einstein	(1,1)
6	G_2	nearly Kähler	(1,1)
7	$Spin_7$	weak G_2 holonomy	(1,0)

Table 1.2: Manifolds admitting geometrical Killing spinors

the Klebanov-Witten solution [34].

We have described in detail the basic aspects of eleven-dimensional supergravity. An analog study can be done for type IIA/B supergravity, but we will only outline the basic expressions that we will use. Along this thesis, we will mostly use type IIA and B supergravities.

Type IIA supergravity

It is a non-chiral maximally supersymmetric supergravity in ten dimensions. Type IIA supergravity can be obtained by dimensional reduction from eleven-dimensional supergravity.

The bosonic geometrical data consists of $(M, g, \phi, B_2, A_1, A_3)$, where (M, g) is a ten-dimensional Lorentz manifold with Spin structure, $\phi \in \Omega^0(M)$, $B_2 \in \Omega^2(M)$, $A_1 \in \Omega^1(M)$, $A_3 \in \Omega^3(M)$. Let us define:

$$H_3 = dB_2 , \tag{1.1.12}$$

$$F_2 = dA_1 , \tag{1.1.13}$$

$$F_4 = dA_3 + H_3 \wedge A_1 . \tag{1.1.14}$$

The equations of motion are obtained from the action (in string frame):

$$S_{IIA} = \frac{1}{2\kappa_{10}^2} \int d\xi^{10} \sqrt{-g} \left\{ e^{-2\phi} \left(R + 4\partial_\mu \phi \partial^\mu \phi - \frac{1}{2 \cdot 3!} H_3^2 \right) - \frac{1}{2 \cdot 2!} F_2^2 - \frac{1}{2 \cdot 4!} F_4^2 \right\}$$

$$- \frac{1}{4\kappa_{10}^2} \int B_2 \wedge dA_3 \wedge dA_3 , \tag{1.1.15}$$

where $2\kappa_{10}^2 = (2\pi)^7 \alpha'^4 g_s^2$, and g_s is the string coupling constant.

The SUSY transformations for the dilatino λ and the gravitino ψ_m for type IIA supergravity in string frame are [35],

$$\delta_\epsilon \lambda = \left[\frac{1}{2} \Gamma^m \partial_m \Phi + \frac{1}{4 \cdot 3!} H_{mnp} \Gamma^{mnp} \Gamma_{11} + \frac{e^\Phi}{8} \left(\frac{3}{2!} F_{mn} \Gamma^{mn} \Gamma_{11} - \frac{1}{4!} F_{mnpq} \Gamma^{mnpq} \right) \right] \epsilon ,$$

$$\delta_\epsilon \psi_m = \left[\nabla_m + \frac{1}{4 \cdot 2!} H_{mnp} \Gamma^{np} \Gamma_{11} - \frac{e^\Phi}{8} \left(\frac{1}{2} F_{np} \Gamma^{np} \Gamma_{11} + \frac{1}{4!} F_{npqr} \Gamma^{npqr} \right) \Gamma_m \right] \epsilon , \quad (1.1.16)$$

where Γ_{11} is the product of all gamma matrices, and $m, n, p, q, r \in \{1, ..., 10\}$.

Type IIB supergravity

There exists also a chiral maximal supergravity in ten dimensions, type IIB supergravity. It is related to type IIA supergravity by T-duality, and it can not be obtained by dimensional reduction from eleven-dimensional supergravity.

The bosonic geometrical data consists of $(M, g, \phi, B_2, \chi, A_2, A_4)$, where (M, g) is a ten-dimensional Lorentz manifold with Spin structure, $\chi \in \Omega^0(M)$, $B_2, A_2 \in \Omega^2(M)$, $A_4 \in \Omega^4(M)$. Let us define:

$$H_3 = dB_2 , \tag{1.1.17}$$
$$F_1 = d\chi , \tag{1.1.18}$$
$$F_3 = dA_2 + \chi H_3 , \tag{1.1.19}$$
$$F_5 = dA_4 + H_3 \wedge A_2 . \tag{1.1.20}$$

The equations of motion are obtained from the action (in string frame):

$$S_{IIB} = \frac{1}{2\kappa_{10}^2} \int d\xi^{10} \sqrt{-g} \left\{ e^{-2\phi} \left(R + 4\partial_\mu \phi \partial^\mu \phi - \frac{1}{2 \cdot 3!} H_3^2 \right) - \frac{1}{2} \partial_\mu \chi \partial^\mu \chi - \frac{1}{2 \cdot 3!} F_3^2 - \frac{1}{4 \cdot 5!} F_5^2 \right\}$$

$$+ \frac{1}{4\kappa_{10}^2} \int dA_2 \wedge H_3 \wedge \left(A_4 + \frac{1}{2} B_2 \wedge A_2 \right) , \tag{1.1.21}$$

where $2\kappa_{10}^2 = (2\pi)^7 \alpha'^4 g_s^2$. The equations of motion obtained from this action are supplemented by a further condition, which states that the F_5 form is self-dual:

$$F_5 = *F_5 . \tag{1.1.22}$$

The SUSY transformations for the dilatino λ and the gravitino ψ_m for type IIB supergravity in string frame are [35],

$$\delta_\epsilon \lambda = \left[\frac{1}{2} \Gamma^m \partial_m \Phi + \frac{1}{4 \cdot 3!} H_{mnp} \Gamma^{mnp} \tau_3 - \frac{e^\Phi}{2} F_m \Gamma^m (i\tau_2) - \frac{e^\Phi}{4 \cdot 3!} F_{mnp} \Gamma^{mnp} \tau_1 \right] \epsilon , \tag{1.1.23}$$

$$\delta_\epsilon \psi_m = \left[\nabla_m + \frac{1}{4 \cdot 2!} H_{mnp} \Gamma^{np} \tau_3 + \frac{e^\Phi}{8} \left(F_n \Gamma^n (i\tau_2) + \frac{1}{3!} F_{npq} \Gamma^{npq} \tau_1 + \frac{1}{2 \cdot 5!} F_{npqrt} \Gamma^{npqrt} (i\tau_2) \right) \Gamma_m \right] \epsilon ,$$

where τ_i , $i = 1, 2, 3$, are the Pauli matrices.

1.2 T-duality

T-duality was introduced in string theory in the eighties, and it has been applied in different contexts. Here we will review T-duality in the particular context of type IIA/B supergravity. We will first explain abelian T-duality and then non-abelian T-duality.

1.2.1   Abelian T-duality

Let us start from a type IIA/B supergravity background with a global $U(1)$-isometry, which leaves invariant not only the metric but all the fields of the solution. Abelian T-duality is properly defined only for backgrounds with such isometry. What T-duality does is to start from a background with a global $U(1)$-isometry in type IIA (IIB) supergravity and obtain a background with a global $U(1)$-isometry in type IIB (IIA) supergravity. The map is an involution, and performing T-duality again we recover the original background. It is conjectured that T-dual backgrounds are actually dual to each other, *i.e.*, they are two different descriptions of the same physics.

Locally, T-duality is given by the Buscher rules [11] [12]. Given a local expression for the metric and fields in terms of coordinates, and denoting by θ an adapted coordinate for the isometry, $(x^0, x^\alpha) = (\theta, x^\alpha)$, $\alpha = 1, 2, ..., 9$, then the Buscher rules for the NSNS sector are:

$$
\begin{aligned}
&\hat{g}_{00} = 1/g_{00} , \qquad \hat{g}_{0\alpha} = B_{0\alpha}/g_{00} , \\
&\hat{g}_{\alpha\beta} = g_{\alpha\beta} - (g_{0\alpha}g_{0\beta} - B_{0\alpha}B_{0\beta})/g_{00} , \\
&\hat{B}_{0\alpha} = g_{0\alpha}/g_{00} , \\
&\hat{B}_{\alpha\beta} = B_{\alpha\beta} - (g_{0\alpha}B_{0\beta} - g_{0\beta}B_{0\alpha})/g_{00} , \\
&\hat{\phi} = \phi - \frac{1}{2}\log g_{00} .
\end{aligned}
\tag{1.2.24}
$$

For the RR sector let us define:

$$
\text{IIB} \quad P := \frac{e^\Phi}{2}\sum_{n=0}^{4}\slashed{F}_{2n+1} , \quad \text{IIA} \quad P := \frac{e^\Phi}{2}\sum_{n=0}^{5}\slashed{F}_{2n} ,
\tag{1.2.25}
$$

where $\slashed{F}_i := 1/i!\,\Gamma_{\mu_1...\mu_i}F_i^{\mu_1...\mu_i}$. Then, the transformation is given by:

$$
\hat{P} = P\,\Omega^{-1} ,
\tag{1.2.26}
$$

where:

$$
\Omega = \frac{1}{\sqrt{g_{00}}}\Gamma_{11}\Gamma_0 .
\tag{1.2.27}
$$

Globally, the initial 10-dim background that has a $U(1)$-isometry, can be equivalently described by a $U(1)$-principal fibration over a 9-manifold. On the one hand, the $U(1)$-fibrations are classified by the Chern number (an integer positive number). On the other hand, the projection of the H_3 field over the base of the fibration gives a 2-form field, that integrated over the base manifold gives an integer number. Under T-duality, these two integer numbers are exchanged [13], and the global properties of the transformation are cleanly specified.

One interesting question is if supersymmetry is preserved along the procedure of T-duality. Locally the supersymmetry is preserved and is the same before and after the T-duality. Nevertheless, in topologically non-trivial manifolds where the existence of global Killing spinors is non-trivial (as in the interesting AdS/CFT solutions), the question is not

easy to answer. Following the conjecture, both theories are two different descriptions of the same physics, so the supersymmetry must be the same. But there are simple examples where the supersymmetry after the T-duality is lost, and the phenomenon of 'supersymmetry without supersymmetry' appears. For example, in [36] it is performed T-duality along the S^1 fibre of the '$S^5 = \mathbb{CP}^2 \times S^1$' fibration in the $AdS_5 \times S^5$ solution, obtaining an $AdS_5 \times \mathbb{CP}^2 \times S^1$ solution in type IIA supergravity. This solution is not supersymmetric in the usual sense because $\mathbb{CP}^2$ is not Spin. But if the theory is T-dual to $AdS_5 \times S^5$ it is expected to have the same supersymmetry. The solution to this puzzle turns out to be that we have to consider Spin^c Killing spinors, and $\mathbb{CP}^2$ is a Spin^c manifold (for the definition of Spin^c see section 1.1).

The Buscher rules are derived from the T-dual action, via the following procedure. The idea is to start from the sigma model action for the NSNS fields, and gauge the $U(1)$ isometry $\partial \to D = \partial + A$ introducing a gauge field A. Then, a Lagrange multiplier term is introduced, ensuring that the gauge field is not dynamical. Finally, integrating out the gauge field we are left with the dual action. The Lagrange multiplier acts as the new coordinate. In the next section the computation is preformed for the more general case of non-abelian T-duality.

We have considered the definition of abelian T-duality for a background with a global $U(1)$-isometry, or equivalently, with a $U(1)$-principal fibration. This definition can be extended to more general cases, for example, when the fibration is not a principal bundle.

1.2.2 Non-abelian T-duality

Abelian T-duality can be generalized to non-abelian T-duality (NATD). The idea is to consider a background with a global G-isometry, where G is a Lie group, which leaves invariant not only the metric but all the fields of the theory. Along this thesis, we will consider the particular case of $G = SU(2)$.

The non-abelian T-duality was originally presented in [14] and was further developed and carefully inspected in [37]-[40]. See the lectures [41] for a nice account of some of the dualities that follow from a Buscher procedure.

Locally, we can consider the generalization of the Buscher rules to the $SU(2)$ case (for more details on notation and conventions see [42]). If L^i, ($i = 1, 2, 3$) are the $SU(2)$ Maurer-Cartan one-forms, we can write the metric and NSNS B_2 form as:

$$ds^2 = G_{\mu\nu}dx^\mu dx^\nu + 2G_{\mu i}dx^\mu L^i + g_{ij}L^i L^j \ , \tag{1.2.28}$$

$$B_2 = \frac{1}{2}B_{\mu\nu}dx^\mu \wedge dx^\nu + B_{\mu i}dx^\mu \wedge L^i + \frac{1}{2}b_{ij}L^i \wedge L^j \ , \tag{1.2.29}$$

where $\mu, \nu \in \{1, 2, ..., 7\}$. Let us define:

$$Q_{\mu\nu} := G_{\mu\nu} + B_{\mu\nu} \ , \quad Q_{\mu i} := G_{\mu i} + B_{\mu i} \ , \quad Q_{i\mu} := G_{i\mu} + B_{i\mu} \ , \quad E_{ij} := g_{ij} + b_{ij} \ , \tag{1.2.30}$$

and from them the following block matrix:

$$Q_{AB} := \begin{pmatrix} Q_{\mu\nu} & Q_{\mu i} \\ Q_{\nu j} & E_{ij} \end{pmatrix} \ , \tag{1.2.31}$$

where $A, B \in \{1, 2, ..., 10\}$. We can identify the dual metric and B_2 field as the symmetric and antisymmetric components, respectively, of:

$$\hat{Q}_{AB} := \begin{pmatrix} Q_{\mu\nu} - Q_{\mu i} M_{ij}^{-1} Q_{j\nu} & Q_{\mu j} M_{ji}^{-1} \\ -M_{ij}^{-1} Q_{j\mu} & M_{ij}^{-1} \end{pmatrix} , \tag{1.2.32}$$

where:

$$M_{ij} := E_{ij} + \epsilon_{ij}^k v_k , \tag{1.2.33}$$

and v_k, $(k = 1, 2, 3)$ are the new dual coordinates. Moreover, one finds that the dilaton receives a contribution at the quantum level just as in abelian case:

$$\hat{\Phi} = \Phi - \frac{1}{2} \ln (\det M) . \tag{1.2.34}$$

In order to transform the RR fluxes, one must construct the following quantity out of the RR forms:

$$\text{IIB} \quad P := \frac{e^\Phi}{2} \sum_{n=0}^{4} \slashed{F}_{2n+1} , \quad \text{IIA} \quad P := \frac{e^\Phi}{2} \sum_{n=0}^{5} \slashed{F}_{2n} , \tag{1.2.35}$$

where $\slashed{F}_i := \frac{1}{i!} \Gamma_{\mu_1 ... \mu_i} F_i^{\mu_1 ... \mu_i}$. Then, the dual RR fluxes are obtained from:

$$\hat{P} = P \, \Omega^{-1} , \tag{1.2.36}$$

where $\Omega = (\Gamma^1 \Gamma^2 \Gamma^3 + \zeta_a \Gamma^a) \Gamma_{11} / \sqrt{1 + \zeta^2}$, $\zeta^2 = \zeta_a \zeta^a$, $\zeta^a = \kappa_i^a z^i$, $\kappa_i^a \kappa_j^a = g_{ij}$ and $z_i = (b_i + v_i) / \det \kappa$, $b_{ij} = \epsilon_{ijk} b_k$.

Let us review how to obtain the NSNS Buscher rules above from the T-dual action. The lagrangian density for the NSNS sector of the initial solution is:

$$\mathcal{L} = Q_{AB} \partial_+ X^A \partial_- X^B , \tag{1.2.37}$$

where $\partial_\pm X^A = (\partial_\pm X^\mu, L_\pm^i)$. We omit the dilaton contribution. We then gauge the $SU(2)$ isometry by replacing the derivatives by covariant derivatives $\partial_\pm g \to D_\pm g = \partial_\pm g - A_\pm g$. The next step is to add a Lagrange multiplier term to ensure that the gauge fields are non-dynamical:

$$- i \text{Tr}(v F_\pm) , \quad F_\pm = \partial_+ A_- - \partial_- A_+ - [A_+, A_-] . \tag{1.2.38}$$

Now a gauge fixing choice must be done. We choose the 3 Lagrange multipliers v_i as the new coordinates. Finally, in the last step we integrate out the gauge fields, obtaining the dual lagrangian density:

$$\hat{\mathcal{L}} = \hat{Q}_{AB} \partial_+ \hat{X}^A \partial_- \hat{X}^B , \tag{1.2.39}$$

where $\partial_\pm \hat{X}^B = (\partial_\pm X^\mu, \partial_\pm v^i)$.

Globally, the rules for NATD are not known. This is a major difficulty, as without the global properties of the dual manifold, a lot of information is lost. For example, it is not known if NATD is in fact a duality, in the sense that the dual background is an equivalent description of the same theory, or it is a solution generation technique, *i.e.*, a systematic

method to obtain new backgrounds.

The amount of supersymmetry preserved by a supergravity solution after a NATD transformation follows from the argument of [15], which has been proven in [43]. According to this, one just has to check the vanishing of the Lie-Lorentz (or Kosmann) derivative [44] of the Killing spinor along the Killing vector that generates the isometry of the NATD transformation. More concretely, suppose that we want to transform a supergravity solution by performing a NATD transformation with respect to some isometry of the background that is generated by the Killing vector k^μ. Then there is a simple criterion which states that if the Lie-Lorentz derivative of the Killing spinor along k^μ vanishes, then the transformed solution preserves the same amount of SUSY as the original solution. In the opposite scenario one has to impose more projection conditions on the Killing spinor in order to make the Lie-Lorentz derivative vanish. Thus in that case the dual background preserves less supersymmetry than the original one. Nevertheless, this is only a local description of the spinors, and for the analysis of globally defined spinors it is needed the global properties of the NATD.

Let us summarize the basic differences between abelian T-duality and NATD:

- The abelian T-duality is an involution, *i.e.*, performing T-duality twice, the original background is recovered. Nevertheless, NATD is not an involution, as in the NATD background the isometries are no longer present (if there is no $SU(2)$ isometry it has no sense to apply NATD again).

- For compact commuting isometries one may argue that T-duality is actually a true symmetry of string theory. There is no analogous statement for the non-abelian cases.

- The global properties of the abelian T-duality are understood. Nevertheless, for the NATD they are not known yet. This problem is commonly stated as 'the variables of the T-dual background are generically non-compact'.

- In the abelian case we flip between type IIA and type IIB, but in the non-abelian case we might change or stay within the same theory. If the dimension of the isometry group G is odd, we flip from type IIA and B, and if the dimension is even, we stay within the same theory.

In chapter 2, we will perform NATD on backgrounds with $SU(2)$ isometry, to obtain new local solutions, and in particular, new AdS_3 solutions, which may be interesting for AdS/CFT applications.

1.3 The AdS/CFT correspondence

The AdS/CFT duality was originally formulated in 1997 by Juan Maldacena [10], who conjectured that type IIB string theory on $AdS_5 \times S^5$ is dual to $3 + 1$ $\mathcal{N} = 4$ $SU(N)$ superconformal Yang-Mills theory.

The conjecture is based on two alternative descriptions of a D3-brane. Let us start by considering type IIB string theory on 9+1 Minkowski spacetime, and a stack of N parallel

D3-branes extended along 3+1 dimensions. String theory in this background contains two
kinds of perturbative excitations, open strings and closed strings. The open strings end
on the D3-branes, and describe their excitations, while the closed strings are excitations of
empty space. If we consider the system at energies lower than the string scale $1/l_s$, then
only the massless string states can be excited. On the one hand, the closed string massless
states give a gravity supermultiplet in ten dimensions, whose low energy effective action is
the one of type IIB supergravity. On the other hand, the open string massless states give an
$\mathcal{N} = 4$ vector supermultiplet in 3+1 dimensions, whose low energy effective action is that of
$\mathcal{N} = 4$ $SU(N)$ super-Yang-Mills theory. To be precise, the complete action of the massless
excitations is:

$$S = S_{bulk} + S_{brane} + S_{int} \quad , \tag{1.3.40}$$

where S_{bulk} is the action of ten dimensional supergravity plus higher derivative corrections,
S_{brane} is defined on the brane worldvolume and it contains the $\mathcal{N} = 4$ $SU(N)$ SYM action
plus some higher derivative corrections, and S_{int} describes the interactions between the brane
and bulk excitations.

Now we can take the low energy limit. In fact, the so-called decoupling limit or Maldacena
limit consists in keeping the energy fixed and $\alpha' \to 0$, keeping also fixed N and g_s (the string
coupling constant). In this limit the interaction action S_{int} vanishes. In addition, all the
higher derivative terms in the brane action vanish, leaving only the pure 3+1 $\mathcal{N} = 4$ $SU(N)$
SYM conformal field theory, and the supergravity theory in the bulk becomes free. So, in
the low energy limit we have two decoupled systems: free gravity in the bulk and the 3+1
gauge theory.

Let us now consider a different description of the same stack of D3-branes. Recall that
in the low energy limit, type IIB string theory is well described by type IIB supergravity.
The D3-brane solution in type IIB supergravity has the following form:

$$ds^2 = h(r)^{-\frac{1}{2}}(-dt^2 + dx^2 + dy^2 + dz^2) + h(r)^{\frac{1}{2}}\left(dr^2 + r^2 d\Omega_{S^5}^2\right) \quad ,$$
$$F_5 = (1 + *)dt \wedge dx \wedge dy \wedge dz \wedge d(h(r)^{-1}) \quad , \quad F_3 = 0 \quad , \quad F_1 = 0 \quad , \quad e^\phi = 1 \quad , \tag{1.3.41}$$

where,

$$h(r) := 1 + \frac{R^4}{r^4} \quad , \quad R^4 := 4\pi g_s \alpha'^2 N \ . \tag{1.3.42}$$

The D3-brane is charged under the F_5 self-dual form, and it is a massive object since
it has some tension. Now notice that the g_{tt} component of the metric is not constant, and
depends on r. Then, the energy E_r of an object as measured by an observer at a position r
and the energy E_∞ measured by an observer at infinity are related by a redshift factor:

$$E_r \, h(r)^{-\frac{1}{4}} = E_\infty \quad , \tag{1.3.43}$$

This means that a object moving towards $r = 0$ will have less and less energy from the
point of view of the observer at infinity.

Let us now take the low energy limit of the D3-brane solution 1.3.41. In this low energy
limit there are two kind of excitations, from the point of view of the observer at infinity. On

the one hand, there are massless particles propagating in the bulk with increasing wavelength, and, on the other hand, there are any kind of excitation getting closer to $r = 0$. In the low energy limit, these two kinds of modes decouple from each other. So, finally we end with two decoupled sectors, one is free bulk supergravity and the other is the near horizon region of the geometry. This near horizon geometry is obtained from 1.3.41 by approximating $h(r) = R^4/r^4$, obtaining a new exact solution to the supergravity equations of motion:

$$ds^2 = \frac{r^2}{R^2}(-dt^2 + dx^2 + dy^2 + dz^2) + \frac{R^2}{r^2}dr^2 + R^2 d\Omega_{S^5}^2 \ ,$$

$$F_5 = (1+*)4\frac{r^3}{R^4}dt \wedge dx \wedge dy \wedge dz \wedge dr \ , \quad F_3 = 0 \ , \quad F_1 = 0 \ , \quad e^\phi = 1 \ , \quad (1.3.44)$$

which is the geometry of $AdS_5 \times S^5$.

In summary, we have described a D3-brane as a string theory object where the open strings can end, and alternatively, as a solution to supergravity. In both cases we have two decoupled sectors in the low energy limit. In each case, one of the two decoupled sectors is supergravity in flat space. Thus, it is natural to identify the second system which appears in both descriptions. This leads to conjecture that 3+1 $\mathcal{N} = 4$ $SU(N)$ SMY theory is dual to type IIB string theory on $AdS_5 \times S^5$

If the theories are conjectured to be the same, then the global symmetries must match. On the one hand, the isometry group of AdS_5 [2] is $SO(2,4)$, and it matches with the conformal group of 3+1 Minkowski space, which is also $SO(2,4)$. On the other hand, the isometry group of S^5 is $SO(6)$, and the R-symmetry of the field theory is $SO(6)_R$. Also these bosonic symmetries match when extended to the full supergroups on both sides of the duality. This supergroup is $SU(2,2|4)$, and its maximal bosonic subgroup is precisely $SO(2,4) \times SO(6)$.

Moreover, if the theories are conjectured to be dual, also the supersymmetry preserved by them must match. In both cases the supersymmetry is maximal, namely $\nu = 1$. Notice that the initial configuration of D3-branes have only $\nu = 1/2$ supersymmetries, but after the decoupling limit, the supersymmetry is enhanced to $\nu = 1$.

Besides, we can write down a dictionary for the parameters on both sides of the duality. The string coupling g_s and the Yang-Mills coupling g_{YM} are related by:

$$g_{YM}^2 = 4\pi g_s \ . \tag{1.3.45}$$

Moreover, the θ parameter on the gauge theory is identified with the expectation value of the RR scalar χ on the gravity side. These relations can be put together:

$$\tau := \frac{4\pi i}{g_{YM}^2} + \frac{\theta}{2\pi} = \frac{i}{g_s} + \frac{\chi}{2\pi} \ , \tag{1.3.46}$$

---

[2]In the AdS/CFT context, by 'AdS_d space' it is meant 'universal covering of AdS_d space'. The reason is because in AdS_d cyclic causal curves are allowed, but not in its universal covering. The topology of the first is $S^1 \times \mathbb{R}^{d-1}$ and the topology of the second is $\mathbb{R}^d$. The isometries of the AdS_d space are $O(2, d-1)$ (the connected component of the neutral element is $SO_+(2, d-1)$), and the isometries of the universal covering of AdS_d space are $SO(2, d-1)$.

We have written the couplings in this way because both the string theory and gauge theory have an $Sl(2,\mathbb{Z})$ self duality symmetry, under which $\tau \to (a\tau+b)/(c\tau+d)$, where a, b, c, d are integer numbers satisfying $ad - bc = 1$. This transformation is related to S-duality, another important duality in string theory. The number of initial D3-branes N, after the low energy limit, corresponds to the flux of the F_5 form through the S^5 sphere:

$$N = \int_{S^5} F_5 \ . \tag{1.3.47}$$

and on the field theory side, it is the range of the gauge group $SU(N)$.

The AdS/CFT conjecture can be formulated at three different levels of generality. The correspondence as formulated above is the strong statement of the duality, which assumes that both theories are dual for any values of the parameters g_s and N. The conjecture can also be formulated in a mild version, that states that 3+1 $\mathcal{N} = 4$ $SU(N)$ SYM theory in the large N limit is dual to type IIB classical string theory $(g_s \to 0)$ on $AdS_5 \times S^5$. The large N limit in the field theory side is also known as the t'Hooft limit. Recall that the t'Hooft limit is obtained by taking $g_{YM} \to 0$ and $N \to \infty$ while keeping fixed $\lambda := g_{YM}^2 N$, the t'Hooft coupling constant. It corresponds to a topological expansion of the Feynman diagrams of the field theory where the quantity $1/N$ acts as the coupling constant, and at leading order in $1/N$ only the planar diagrams contribute. Corrections $1/N$ on the field side corresponds to g_s corrections on the string side.

We can also consider a weak version of the duality, by taking the large t'Hooft coupling limit $\lambda \to \infty$. On the string theory side this corresponds to take the limit $\alpha' \to 0$, where classical string theory reduces to classical supergravity. So, the duality in its weak form states that $\mathcal{N} = 4$ $SU(N)$ SYM theory in the large N limit and large t'Hooft coupling λ is dual to classical type IIB supergravity on $AdS_5 \times S^5$. This weak formulation of the duality is the most useful, because using classical supergravity we can access to strong coupling results in field theory. This will be the formulation that we will use along this thesis.

In fact, the duality is a weak/strong duality. This means that if on one side of the duality the coupling constant is strong, then on the other side is weak, and vice versa. This makes the duality very useful, when we consider a field theory at strong coupling, where the perturbative techniques are not available, and other tools are very limited (like lattice field theory, localization or integrability). In this case, we can consider the gravity dual, which is weakly coupled, and compute the observables using classical supergravity. For the particular case of $\mathcal{N} = 4$ $SU(N)$ SYM theory in the large N limit and large λ limit, the theory is strongly coupled. Taking into account that $R^4/\alpha'^2 = \lambda$, then the supergravity theory has a large AdS_5 and S^5 radius, and is classical supergravity.

We have stated that the AdS/CFT duality establishes a relation between a gravity theory and a field theory. Let us now be more precise and write down the dictionary relating observables on both sides of the duality.

A conformal gauge theory is specified by a complete set of conformal operators. We are interested in the gauge invariant conformal operators polynomial in the canonical fields

since these operators will have a definite conformal dimension and, moreover, will form finite multiplets of increasing dimension. In order to compute correlators for a given operator $\mathcal{O}$, its generating functional $\Gamma(\mathcal{O})$ is constructed by adding a source term to the lagrangian of the conformal field theory:

$$e^{\Gamma(\mathcal{O})} = \langle e^{\int h\mathcal{O}} \rangle \; , \tag{1.3.48}$$

where h is a source for $\mathcal{O}$.

On the gravity side of the duality, the closed string excitations can be described by fields living on $AdS_5 \times S^5$. When compactifying along the S^5, these fields can be decomposed in terms of spherical harmonics, thus giving rise to an infinite tower of modes. Therefore, the observables of the string theory are a set of five-dimensional fields living on AdS_5, and, according to the correspondence, they have to be matched to the observables of the gauge theory.

Recall, the metric of AdS_5 space with radius R can be written as:

$$ds^2 = \frac{r^2}{R^2}dx_{1,3}^2 + \frac{R^2}{r^2}dr^2 \; , \tag{1.3.49}$$

In these variables the boundary of AdS_5 is at $r \to \infty$ and is isomorphic to four-dimensional Minkowski space, spanned by the coordinates $x_0, ..., x_3$. Now let us consider a scalar field $\hat{h}(x,r)$ on AdS_5, to be associated to the operator $\mathcal{O}$ of the gauge theory. The asymptotic dependence of $\hat{h}$ on the radial coordinate is given by the two independent solutions:

$$\hat{h} \sim r^{\Delta-4} \; , \qquad \hat{h} \sim r^{-\Delta} \; , \qquad (r \to \infty) \; , \tag{1.3.50}$$

where $\Delta = 2 + \sqrt{4 + m^2R^2}$, and m is the five-dimensional mass. Then, the first solution dominates near the boundary, and we can write:

$$\hat{h}(x,r) \to r^{\Delta-4}\hat{h}_\infty(x) \; , \qquad (r \to \infty) \; , \tag{1.3.51}$$

where $\hat{h}_\infty(x)$ is a four-dimensional function living on the boundary and is defined only up to conformal transformations, under which it has conformal dimension $\Delta - 4$. Finally, we can establish a relation between the field $\hat{h}$ and the operator $\mathcal{O}$, by identifying the generating functional of correlators of $\mathcal{O}$ with the five dimensional action $S_{AdS_5}(\hat{h})$ restricted to the solutions of $\hat{h}$ with boundary value $\hat{h}_\infty(x)$:

$$\langle e^{\int h\mathcal{O}} \rangle = e^{-S_{AdS_5}(\hat{h})} \; . \tag{1.3.52}$$

This relation was proposed in [45], [46]. Here we have considered the case of a scalar field, and a similar relation can be obtained for fields of other spins.

After the original formulation in 1997 of the duality by Maldacena [10], the conjecture was extended to other cases, with less supersymmetry and without conformal invariance. Let us mention some of the most important solutions that appeared soon afterwards. In 1998 it was published the Klebanov-Witten solution [34], a solution with reduced supersymmetry based on the conifold geometry. The conifold is a concrete case of the special holonomy manifolds revisited in section 1.1. This solution was followed by several generalizations,

like the Klebanov-Tseytlin solution [47], which use fractional D3-branes on the conifold, and the Klebanov-Strassler solution [48], which use fractional D3-branes on the deformed conifold, both solutions being non-conformal. Another non-conformal solution with reduced supersymmetry, formulated in 2000, is the Pilch-Warner solution [49], a massive deformation of the $\mathcal{N} = 4$ $SU(N)$ SYM theory, usually known as $\mathcal{N} = 2^*$. Also, in 2000, it was published the Maldacena-Nuñez solution [50], in which D5-branes are wrapped in a calibrated cycle of a special holonomy manifold.

A huge amount new examples of the correspondence were constructed until these days. One of the most important examples of the duality was formulated in 2008 by Aharony, Bergman, Jafferis and Maldacena [51], and it is known as the ABJM theory. This thesis is mostly based on this solution, so we devote the next subsection to explain this example in full detail.

1.3.1   The ABJM theory

The ABJM theory is one of the most important examples of the AdS/CFT duality. In the same way that the $\mathcal{N} = 4$ $SU(N)$ SYM theory is the best understood example of the $\text{AdS}_5/\text{CFT}_4$ correspondence, the ABJM theory is the best understood example of the $\text{AdS}_4/\text{CFT}_3$ correspondence.

In the seminal paper by Maldacena in 1997 [10], it was conjectured the duality between the maximally supersymmetric $AdS_5 \times S^5$ type IIB supergravity solution and the $\mathcal{N} = 4$ $SU(N)$ SYM field theory based on the decoupling limit of D3-branes in flat space. Besides, it is also noticed that there are two other maximally supersymmetric cases, $AdS_4 \times S^7$ and $AdS_7 \times S^4$, in eleven-dimensional supergravity, corresponding to the decoupling limit of the M2- and M5-branes on flat space, respectively. Nevertheless, the concrete field theories living inside the M-branes were not known.

The gauge theory living on the M5-brane in flat space was known to be a $5+1$ $\mathcal{N} = (2,0)$ superconformal theory with number of degrees of freedom scaling as N^3 in the large N limit. Nowadays, the details of the theory still remain unknown.

The gauge theory living on the M2-branes in flat space was known to be a conformal $2+1$ $\mathcal{N} = 8$ supersymmetric Chern-Simons-matter theory, with R-symmetry $SO(8)$ and a specific matter content, and that should scale as $N^{3/2}$ in the large N limit. But the details of the theory where not known. An important step towards the understanding of this theory was obtained in [52], where $2+1$ $\mathcal{N} = 1$ and $\mathcal{N} = 2$ superconformal $U(N)$ Chern-Simons-matter theories where constructed [3]. Nevertheless, it seemed not possible to obtain interacting theories with more supersymmetry and, besides, these theories were parity violating (the theory on the M2-branes must be parity preserving). Another important step was obtained by Bagger and Lambert [54] [55] [56] and Gustavsson [57] [58] who constructed a maximally supersymmetric $\mathcal{N} = 8$ Chern-Simons-matter theory which was proven to be equivalent [59] to a theory with the particular gauge group $SU(2) \times SU(2)$ and opposite levels k and $-k$ [4].

Inspired by the previous results, in 2008 Aharony, Bergman, Jafferis and Maldacena

---

[3]Interestingly, the gravity duals of these theories where recently found in [53].

[4]Notice that this theory is different from the ABJM for $N = 2$ because the gauge group is $SU(2) \times SU(2)$ and not $U(2) \times U(2)$.

(ABJM) [51] constructed a $2+1$ dimensional $\mathcal{N} = 6$ superconformal Chern-Simons-matter theory with gauge group $U(N) \times U(N)$ and opposite levels k and $-k$. The bosonic matter content of the theory is four complex scalar fields C_I ($I = 1, 2, 3, 4$) transforming in the bifundamental representation $(\mathbf{N}, \bar{\mathbf{N}})$ of the gauge group and their corresponding complex conjugate fields in the anti-bifundamental representation $(\bar{\mathbf{N}}, \mathbf{N})$. The fermionic matter content is 4 Majorana fermions, ψ_I ($I = 1, 2, 3, 4$).

The action of the ABJM theory is:

$$S_{ABJM} = \int_{\mathcal{M}_3} d^3x \ \text{Tr} \left[\frac{k}{4\pi} \left(A \wedge dA + \frac{2}{3} A \wedge A \wedge A - \hat{A} \wedge d\hat{A} - \frac{2}{3} \hat{A} \wedge \hat{A} \wedge \hat{A} \right) \right.$$

$$- D_\mu C_I^\dagger D^\mu C^I - i\psi^{I\dagger} \gamma^\mu D_\mu \psi_I$$

$$+ \frac{4\pi^2}{3k^2} \left(C^I C_I^\dagger C^J C_J^\dagger C^K C_K^\dagger + C_I^\dagger C^I C_J^\dagger C^J C_K^\dagger C^K + 4 C^I C_J^\dagger C^K C_I^\dagger C^J C_K^\dagger - 6 C^I C_J^\dagger C^J C_I^\dagger C^K C_K^\dagger \right)$$

$$+ \frac{2\pi i}{k} \left(C_I^\dagger C^I \psi^{J\dagger} \psi_J - \psi^{\dagger J} C^I C_I^\dagger \psi_J - 2 C_I^\dagger C^J \psi^{\dagger I} \psi_j + 2\psi^{\dagger J} C^I C_J^\dagger \psi_I \right.$$

$$\left. \left. + \epsilon^{IJKL} \psi_I C_J^\dagger \psi_K C_L^\dagger - \epsilon_{IJKL} \psi^{\dagger I} C^J \psi^{\dagger K} C^L \right) \right) , \tag{1.3.53}$$

where the covariant derivative acts as:

$$D_\mu C^I = \partial_\mu C^I + i(A_\mu C^I - C^I \hat{A}_\mu) . \tag{1.3.54}$$

The first line contains the Chern-Simons terms of the two gauge fields A and $\hat{A}$ corresponding to the two gauge groups $U(N) \times U(N)$, with levels k and $-k$ respectively. The second line contains the kinetic terms for the complex scalar fields and the Majorana spinors. The rest of the action is the potential. The potential is particularly chosen in order to preserve $\mathcal{N} = 6$ supersymmetry and it is very constrained.
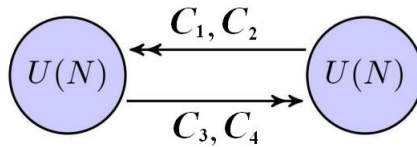
Figure 1.1: ABJM quiver diagram. The nodes correspond to the gauge groups, and the arrows represent the bosonic matter content C_I ($I = 1, 2, 3, 4$) transforming in the bifundamental and anti-bifundamental representations.

The field content of the $2+1$ ABJM theory is similar to the $3+1$ Klebanov-Witten theory [34], and also has a similar superpotential for the chiral fields. If we relabel $\{C_1, C_2, C_3, C_4\} = \{A_1, A_2, B_1^\dagger, B_2^\dagger\}$ the superpotential is:

$$W = \frac{2\pi}{k} \epsilon^{ij} \epsilon^{kl} \ \text{Tr}[A_i B_k A_j B_l] . \tag{1.3.55}$$

The ABJM theory is formulated on a 3 dimensional manifold $\mathcal{M}_3$. For the purpose of holography, this manifold will be chosen to be $\mathbb{R} \times S^2$ with the natural lorentzian metric, as this is the boundary of AdS_4. For the purpose of localization, the manifold will be chosen to be the euclidean manifold S^3 with the usual round metric.

The R symmetry of the theory is $U(4)_R = U(1)_R \times SU(4)_R$. The scalars C_I and the fermions ψ_I are in the fundamental $\mathbf{4}$ representation of $SU(4)_R$, and have charge $+1$ under $U(1)_R$.

One can take the t'Hooft limit in the ABJM theory, which is given by:

$$N, \ k \to \infty \quad , \qquad \lambda := \frac{N}{k} = fixed \ , \tag{1.3.56}$$

where λ is the t'Hooft coupling. It turns out that in the large N limit, the degrees of freedom scale as $N^{3/2}$, a different behavior than in $\mathcal{N} = 4$ $SU(N)$ SYM, which scales as N^2.

In general, the ABJM theory is not maximally supersymmetric, but for specific values of the parameters N and k the supersymmetry is enhanced from $\mathcal{N} = 6$ to $\mathcal{N} = 8$. It happens when $N = 2$ or $k = 1, 2$. In particular, the case $k = 1$ is interesting, as it corresponds to N M2-branes in flat space, which in the decoupling limit give rise to the maximally supersymmetric solution $AdS_4 \times S^7$.

The ABJM theory is a conformal highly supersymmetric field theory that has nice mathematical properties. Using localization and matrix model techniques it has been obtained the exact interpolating function for the free energy of ABJM theory on the three-sphere in the large N limit, which implies in particular the $N^{3/2}$ behavior at strong coupling [60]. This constitutes a non trivial check of the AdS/CFT correspondence. Using localization also the Wilson Loops can be obtained. Besides, the ABJM theory has many integrability properties.

Let us now consider the gravity dual description to the ABJM field theory. In order to motivate the conjecture, the authors of [51] constructed a specific brane set up in type IIB string theory, involving D3-branes, D5-branes and NS5-branes, where one of the coordinates is compactified on S^1. Next, they performed a T-duality along this compact coordinate and obtained a solution in type IIA string theory. Afterwards, this solution is lifted to M theory, where it is shown to be the theory of M2-branes on a $\mathbb{C}^4/\mathbb{Z}_n$ singularity.

So, the conjecture in its strong version states that the ABJM field theory is dual to M2-branes on a $\mathbb{C}^4/\mathbb{Z}_n$ singularity in M theory.

In the large N limit, the gravitational background becomes $AdS_4 \times S^7/\mathbb{Z}_k$ in eleven-dimensional supergravity. The $S^7/\mathbb{Z}_k$ space is a lens space, $i.e.$, a fibre bundle with base $\mathbb{CP}^3$ and fiber S^1, and the possible fibrations are classified by an integer, in this case k. When the Chern-Simons level k is large ($k^5 \gg N$) the size of the fiber is small and the system is better described in terms of type IIA supergravity, after performing a dimensional reduction to ten dimensions along the Hopf fiber S^1. In the type IIA description, the geometry is $AdS_4 \times \mathbb{CP}^3$, where $\mathbb{CP}^3$ inherits the natural metric from the total space $S^7/\mathbb{Z}_k$, known as the Fubini-Study metric. The solution also has a constant dilaton, and F_2 and F_4 forms.

The $\mathbb{CP}^3$ manifold with the Funibi-Study metric has an isometry group $U(4)$. This precisely corresponds with the R-symmetry of the ABJM field theory $U(4)_R = U(1) \times SU(4)$. The manifold $\mathbb{CP}^3$ has a spin structure, and in particular a Kähler structure with Kähler

form J. The dilaton ϕ and the F_2 and F_4 forms are:

$$e^\phi = \frac{2k}{L} \ , \qquad F_2 = 2kJ \ , \qquad F_4 = \frac{3k}{2}L^2\Omega_{AdS_4} \ , \qquad (1.3.57)$$

where Ω_{AdS_4} is the volume form of AdS_4 and L is the radius of AdS_4, $L^4 = 2\pi^2 N/k$.

This type IIA description of the ABJM theory is the one that we will use in chapters 3, 4 and 5 of this thesis.

The ABJM theory has been generalized in several directions. By adding fractional M2-branes it can be generalized (ABJ) to the case in which the ranges of the two gauge groups are different, $U(N) \times U(N+M)$, and in the type IIA description this corresponds to adding a topologically non trivial B_2 field proportional to M [61]. It can be generalized to the case where the two levels are not opposite, k and $-k'$ with $k - k' \neq 0$ and in the type IIA description this corresponds to a generalization to massive type IIA with mass parameter proportional to $k - k'$ [62] [63]. Moreover, the ABJM model admits a mass deformation (mABJM) that preserves the whole $\mathcal{N} = 6$ supersymmetry [64]. The ABJM theory has been extended to different quivers and groups with different amount os supersymmetry in [65] [66] [67] [68] [69] [70] [71].

Another generalization is obtained by including fundamental matter. One of the purposes of this thesis is to consider the ABJM theory with unquenched massive fundamental matter, and this question will be addressed in chapter 3. In chapters 4 and 5 we will use the ABJM background and we will add quenched fundamental matter with gauge fields turned on and we will study its properties.

1.4 Flavor in the gauge/gravity correspondence

In the original formulation of the gauge/gravity correspondence by Maldacena [10], all the fields of the gauge theory are in the adjoint representation of the gauge group $SU(N)$. In the subsequent years, new examples of the correspondence where constructed, either with one gauge group and adjoint matter or quiver groups and adjoint or bifundamental matter (as in the ABJM theory). Soon, the need for fundamental matter appeared, and the way of how to introduce it was clarified in [16].

The main motivation for introducing fundamental matter is to get closer to the phenomenological models, like QCD or those of condensed matter physics. In QCD the fundamental matter are the quarks, and in condensed matter physics the fundamental matter are the electrons.

1.4.1 Brane construction

Let us start with the theory of $\mathcal{N} = 4$ $SU(N)$ SYM and add flavor to it, as was first explained in [16].

Let us consider a stack of N_c D3-branes and a stack of N_f D7-branes in type IIB string theory, in 10-dim Minkowski spacetime. The D3-branes are extended along 3+1 dimensions, and the D7-branes are extended along the same 3+1 dimensions and 4 transverse spatial

directions. In this configuration, there are closed strings and open strings, and the open strings can have both ends on the D3-brane, both ends on the D7-brane or one end on the D3-brane and the other in the D7-brane. The lightest modes of these branes after quantization give rise to field theories living inside the D3 and the D7, with adjoint matter coming from the strings with both ends on the same brane, and bifundamental matter with one end in each brane. To be precise, after quantization we will have a $SU(N_c)$ gauge theory on the D3-branes, with adjoint matter $(\mathbf{N}_c \otimes \bar{\mathbf{N}}_c = \mathbf{1} \oplus (\mathbf{N}_c^2 - 1))$ coming from the strings with both ends on the D3-brane (3-3), we will have a $SU(N_f)$ gauge theory on the D7-branes, with adjoint matter $(\mathbf{N}_f \otimes \bar{\mathbf{N}}_f = \mathbf{1} \oplus (\mathbf{N}_f^2 - 1))$ coming from the strings with both ends on the D7-brane (7-7), and bifundamental matter $\mathbf{N}_c \otimes \bar{\mathbf{N}}_f$ and $\mathbf{N}_f \otimes \bar{\mathbf{N}}_c$ coming from the strings (3-7) and (7-3) [5].

Starting from this configuration, let us consider the near horizon limit for the D3-branes. The lightest modes of the 3-3 string give rise to the $\mathcal{N} = 4$ $SU(N)$ SYM with adjoint matter, as in the original case of Maldacena. Now, there is also the contribution from the 3-7 and 7-3 strings lightest modes, which give rise to a $\mathcal{N} = 2$ hypermultiplet of matter transforming in the bifundamental representation of $SU(N_c) \times SU(N_f)$. The gauge group of the D7-brane becomes a global group in the gauge side, precisely the flavor group. The (7-7) strings then correspond to matter in the adjoint of the global group $SU(N_f)$ (it is common to abuse of language and refer to these bound states as mesons, but the theory is not confining, so they are just bound states). On the gravity side, we will have some geometry, and in general it will be difficult to find. If we reduce to the particular case $N_f \ll N_c$, *i.e.*, we take the t'Hooft limit with N_f finite, then on the gravity side the geometry is not modified by the presence of the D7-branes, so we have $AdS_5 \times S^5$ where the D7-branes are treated as probe branes. On the gauge theory side, this corresponds to the 'quenched approximation', a terminology used in lattice QCD, which means that the quark determinant is set to one. Under the quenched approximation, many features of the fundamental matter can be captured, and it has turned out to be a very successful regime where many computations in the gauge/gravity duality have been carried out.

Unquenched flavor

If the full effect of the fundamental matter has to be taken into account, then we can consider a number of N_f D7-branes comparable to the number N_c of D3-branes. To be precise, this corresponds in the large N_c limit to take $N_c, N_f \to \infty$ and $N_f/N_c = fixed$, and this is known as the Veneziano limit [72]. In this case, the low energy theory corresponds to type IIB supergravity coupled to the dynamics of the D7-branes, which is dictated by the DBI +WZ action. The total action of the problem is:

$$S = S_{IIB} + S_{DBI+WZ} \ , \tag{1.4.58}$$

In practice, to find a backreacted solution one starts with a solution of pure supergravity where the gauge/gravity duality has been well understood. Then, one considers an ansatz

---

[5]Recall that for $SU(N)$ with $N \geq 3$ there are two fundamental representations, $\mathbf{N}$ and $\bar{\mathbf{N}}$, for $SU(2)$ there is only one, $\mathbf{2}$, and $U(1)$ is not semisimple, so there is no definition of fundamental representation. In the text we assume $N \geq 3$ for simplicity.

that generalizes the solution and allow the backreaction of the flavor. Next, one introduces this ansatz in the general equations of motion obtained from 1.4.58. Usually finding solutions to this equations is a difficult task, and in order to simplify the problem it is common to restrict to supersymmetric solutions. In that case, under an appropriate ansatz, it is enough to solve the dilatino and gravitino variations of type IIB, and the problem simplifies considerably.

A concrete supersymmetric solution to the unquenched D3-D7 problem was found in [73]. This solution is no longer conformal, and presents a Landau pole in the UV. For an example of a non-supersymmetric backreacted solution, see [74].

An interesting question is what are the new features of the flavor that are captured when considering backreaction. For example, the beta function can get corrections, and the originally flavorless conformal background becomes non-conformal after backreaction [73]. Another interesting feature is that some conformal dimensions become anomalous after backreaction (even if the backreacted background is still conformal) [75]. Also, the meson spectrum, after backreaction, will mix with the glueball spectrum. Besides, new dualities, like Seiberg-like dualities, may appear.

We can classify the approaches to the backreaction problem in two cases: the case in which the flavor branes are localized, and the case where the flavor branes are smeared. Let us consider the case in which the flavor branes are localized. This means that we have a stack of D7-branes at the same point. Then, the flavor symmetry is $SU(N_f)$, the source terms for the supergravity equations will have a Dirac delta at the location of the stack. Furthermore, the symmetries of the original (unflavored) background will be reduced, and dependence in more variables is introduced. Solving a problem with these features is a difficult task. In some cases exact solutions are found, for an example see [76].

The smearing technique

The smearing technique consists in delocalizing the brane sources. The idea is the same as in electromagnetism, when a point charge is substituted by a continuous volume charge. In this way, no Dirac deltas are present, the symmetries of the original theory are restored, and the dependence on several variables disappear. As the branes are at different locations, the flavor group is $U(1)^{N_f}$ instead of $SU(N_f)$.

This approach of the smearing technique was proposed in [77] in the context of non-critical holography. In practice, the smearing technique has been very useful and has lead to the discovery of a large amount of new backgrounds with backreacted flavor (for a review see [73]). In general, obtaining a solution using the smearing technique is easier that with localized sources, and in many cases, even analytical solutions are obtained.

In chapter 3 we will construct a model that generalizes the ABJM theory by including massive unquenched fundamental matter, using the smearing technique. In the next subsection we review a more elementary case where the fundamental matter is included in the ABJM theory in the quenched approximation.

1.4.2   The ABJM theory with quenched flavor

The ABJM theory can be generalized by including fundamental matter. One of the main interests of including fundamental matter are the applications in phenomenological models like QCD or condensed matter physics.

   The easiest way of including fundamental matter is using the quenched approximation. Starting from the gravity description of ABJM theory in the type IIA regime, this can be obtained by including N_f flavor probe D6-branes [78], [79], with N_f fixed when $N_c \to \infty$.

   The resulting field theory is the original ABJM plus a fundamental hypermultiplet in each node of the quiver diagram, as shown in Fig. 1.2, preserving $\mathcal{N} = 3$ supersymmetry of the original $\mathcal{N} = 6$.

   Let us comment on the precise brane construction. In order to introduce flavor in the ABJM theory, one can start by introducing two sets of N_f D5-branes in the initial type IIB configuration. Each stack of D5-branes is situated at a specific position at the x_6 compact direction, in opposite places, and not coincident with the NS5 and NS5'. The open strings with ends 3-5 and 5-3 give rise to fields transforming in the $(\mathbf{N}_c, \bar{\mathbf{N}}_f,)$ and $(\bar{\mathbf{N}}_c, \mathbf{N}_f)$ representations. After T-dualizing to type IIA and lifting to M-theory, the D5-branes become KK-monopoles. In the type IIA description, they become D6-branes extended along AdS_4 and wrapping a lagrangian cycle $\mathbb{RP}^3$ inside $\mathbb{CP}^3$, which preserve half of the supersymmetries ($\mathcal{N} = 3$).

   This construction allows to conjecture that these probe D6-branes are dual to fundamental hypermultiplets in the ABJM theory, transforming in the fundamental $(\mathbf{N}, 1)$, $(1, \mathbf{N})$ and anti-fundamental $(\bar{\mathbf{N}}, 1)$, $(1, \bar{\mathbf{N}})$ representations. The action of the ABJM field theory with this fundamental matter is the ABJM action plus the kinetic terms of the fundamental matter and the superpotential:

$$W = \frac{2\pi}{k} Tr[(A_a B_a + Q_1 \tilde{Q}_1)^2 - (B_a A_a - Q_2 \tilde{Q}_2)^2] \ . \tag{1.4.59}$$
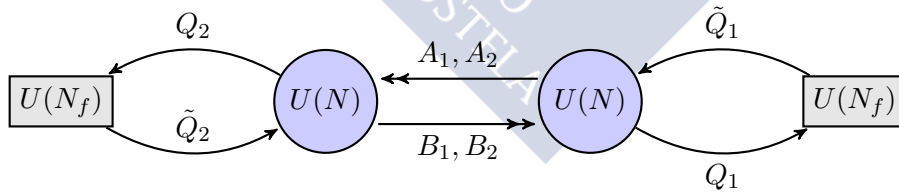
Figure 1.2: ABJM quiver diagram with flavor hypermultiplets

If the N_f flavor branes are located at the same point, the flavor group is $SU(N_f)$.

   Here we have reviewed the addition of flavor in the ABJM theory using probe D6-branes. This construction of adding flavor to ABJM using D6-branes will be the one that we will use along this thesis. Nevertheless, there are other brane set-ups for adding different kinds of fundamental matter to ABJM. For a list of supersymmetric flavor branes that allows to add different kinds of fundamental matter to ABJM see [80].

For the reader who is familiar with the flavor D7-brane in $AdS_5 \times S^5$, we can compare it with the flavor D6-brane in $AdS_4 \times \mathbb{CP}^3$:

- In both cases the codimension of the flavor brane is zero, *i.e.*, the D6-brane fills the 2+1 dimensions of the ABJM theory and the D7-brane is extended along the 3+1 dimensions of the $\mathcal{N} = 4$ $SU(N)$ SYM theory.

- The D7-brane adds a fundamental hypermultiplet to the only $SU(N)$ node of the quiver diagram, while the D6-brane adds a fundamental hypermultiplet to each node $U(N) \times U(N)$ quiver.

- For the D7-brane embedding only the DBI part of the action contributes, while for the D6-brane embedding both DBI+WZ contribute.

- The D7-brane worldvolume is $AdS_5 \times S^3 \subset AdS_5 \times S^5$, while the D6-brane worldvolume is $AdS_4 \times \mathbb{RP}^3 \subset AdS_4 \times \mathbb{CP}^3$.

- For massive embeddings, where there is some brane profile, the brane terminates at some point before reaching the IR. At this point, in the D7 case the S^3 collapses to a point, and in the D6 case the $\mathbb{RP}^3$ becomes a S^2 (the S^1 fibre of $\mathbb{RP}^3$ collapses to a point but the base S^2 remains unaffected).

1.5   The D-brane action

The D-branes play a fundamental role in the derivation of the AdS/CFT correspondence. After taking the decoupling limit, the D-branes disappear, and we are left with the field theory and the supergravity theory. Nevertheless, in the previous section it has been shown how to add flavor to the AdS/CFT duality via D-branes. This flavor branes remain after the decoupling limit, so it is necessary to deal with its dynamics. If we restrict to the quenched approximation for the fundamental matter in the field theory, this corresponds to consider a probe Dp-brane in the supergravity background. In this section we will review the action of a D-brane in a generic supergravity background (for a review see [81]), which will be used in chapters 3, 4 and 5.

D-branes are extended objects where open strings can end. The open strings ending on the brane must satisfy Dirichlet boundary conditions in the directions orthogonal to the hyperplane. Let us first recall that in the absence of any such object the massless bosonic sector of the open string consists of a ten-dimensional vector and, accordingly, the low energy effective field theory for the open superstring in flat space with Neumann boundary conditions is $\mathcal{N} = 1$ SYM. However, the zero modes of the open string along the directions with Dirichlet boundary conditions are not dynamical and so the low energy fields corresponding to the massless modes of the open string sector do not depend on these directions. Therefore, the low energy effective theory one gets is the dimensional reduction of the ten-dimensional one, with the components of the gauge field along directions with Dirichlet boundary conditions becoming scalars representing the fluctuations of the D-brane. The hyperplane is then a dynamical object whose fluctuations correspond to states of the open string spectrum.

The bosonic action of a Dp-brane can be computed by requiring that the non-linear sigma model describing the propagation of an open string with Dirichlet boundary conditions in a general supergravity background is conformally invariant. The constraints arising for the bosonic fields are the same as the equations of motion resulting from the following action (in string frame):

$$S_{DBI} = -T_p \int_{\Sigma_{p+1}} d^{p+1}\xi \, e^{-\phi} \sqrt{-\det\left(g + \mathcal{F}\right)}, \tag{1.5.1}$$

which is known as the Dirac-Born-Infeld (DBI) action. The presence of the dilaton ϕ is due to the fact that the Dp-brane is an object of the open string spectrum, hence the coupling g_s^{-1} inside $T_p = (2\pi)^{-p} g_s^{-1} \alpha'^{-\frac{p+1}{2}}$, where T_p is the tension of the brane. In (1.5.1) Σ_{p+1} denotes the Dp-brane worldvolume, and g is the induced metric on the Dp-brane resulting from the pullback to the worldvolume of the background metric:

$$g_{ab} = \frac{\partial X^M}{\partial \xi^a} \frac{\partial X^N}{\partial \xi^b} G_{MN} , \tag{1.5.2}$$

where ξ^a, $(a = 0, \cdots, p)$ are the worldvolume coordinates, and X^M and G_{MN} are the coordinates and metric of the background. By making use of the worldvolume and spacetime diffeomorphism invariance one can go to the so-called 'static gauge' where the worldvolume of the Dp-brane is aligned with the first $p+1$ spacetime coordinates. In this gauge the embedding of the Dp-brane is given by the functions $X^m(\xi^a)$, where X^m, $(m = 1, \cdots, 9-p)$ are the spacetime coordinates transverse to the Dp-brane. Actually, in this 'static gauge' the induced metric for a Dp-brane in flat space takes the form:

$$g_{ab} = \eta_{ab} + \frac{\partial X^m}{\partial \xi^a} \frac{\partial X^n}{\partial \xi^b} \delta_{mn} . \tag{1.5.3}$$

The two-form $\mathcal{F}$ present in eq. (1.5.1) is given by:

$$\mathcal{F}_{ab} = P[B]_{ab} + 2\pi \, \alpha' \, F_{ab} , \tag{1.5.4}$$

where $F = dA$ is the field strength of the gauge field living on the worldvolume of the Dp-brane, $P[\cdots]$ denotes the pullback to the worldvolume and B is the NSNS two-form potential.

The DBI action (1.5.1) not only describes the massless open string modes given by the worldvolume gauge field A_a and the scalars X^m, but also couples the Dp-brane to the massless closed string modes of the NSNS sector, namely ϕ, G_{MN} and B_{MN}. Moreover, this action is an abelian $U(1)$ gauge theory and when the target space is flat, it reduces (at leading order in α') to YM in $p+1$ dimensions with $9-p$ scalar fields plus higher derivative terms. Indeed, the quadratic expansion of (1.5.1) for a Dp-brane in flat space is:

$$S_{DBI} \approx -\int_{\Sigma_{p+1}} d^{p+1}\xi \, e^{-\phi} \left[T_p + \frac{1}{g_{YM}^2} \left(\frac{1}{2} F_{ab} F^{ab} + \partial_a \Phi^m \, \partial^a \Phi^m \right) \right], \tag{1.5.5}$$

where we have applied the usual relation between coordinates and fields: $\Phi^m = 1/(2\pi \, \alpha') \, X^m$, and that $g_{YM}^2 = 2(2\pi)^{p-2} g_s (\alpha')^{\frac{p-3}{2}}$. After taking into account the fermionic superpartners

coming from the fermionic completion of the action for the super D-brane, the low energy effective theory living on the worldvolume becomes the maximally supersymmetric SYM theory in $p + 1$ dimensions (for a D-brane in flat space). In particular, for $p = 3$ it is obtained the $\mathcal{N} = 4$ $SU(N)$ SYM theory of the original Maldacena conjecture.

The worldvolume of a Dp-brane naturally couples to a $(p+1)$-form RR potential $C_{(p+1)}$, whose field strength is a $(p+2)$-form. Apart from the natural coupling term $\int_{\Sigma_{p+1}} C_{p+1}$, the action coupling a Dp-brane to the RR potentials must contain additional terms involving the worldvolume gauge field. By making use of T-duality one can show that the part of the action of a Dp-brane describing its coupling to the RR potentials is given by the following Wess-Zumino (WZ) term:

$$S_{WZ} = T_p \int_{\Sigma_{p+1}} \sum_{r=0}^{p+1} P\left[C_{(r)}\right] \wedge e^{\mathcal{F}} . \tag{1.5.6}$$

Although the integrand above involves forms of various ranks, the integral only picks out those proportional to the volume form of the Dp-brane worldvolume.

Finally, the action of a Dp-brane is given by the sum of the DBI and WZ terms, (1.5.1) and (1.5.6) respectively, which reads (in string frame):

$$S_{Dp} = -T_p \int_{\Sigma_{p+1}} d^{p+1}\xi\, e^{-\phi} \sqrt{-\det\left(g + \mathcal{F}\right)} \pm T_p \int_{\Sigma_{p+1}} \sum_{r=0}^{p+1} P\left[C_{(r)}\right] \wedge e^{\mathcal{F}} , \tag{1.5.7}$$

where the + (-) in front of the second term corresponds to a Dp-brane (anti-Dp-brane).

1.5.1 Kappa symmetry

The kappa symmetry is a fermionic gauge symmetry of the worldvolume theory which is an important ingredient in the covariant formulation of superstrings and supermembranes [82]. It turns out to be a useful tool to find supersymmetric embeddings of probe D-branes in a given background, and it will be used in chapters 3 and 4.

The bosonic Dp-brane is described by a map $X^m\left(\Sigma_{p+1}\right)$, where Σ_{p+1} is the worldvolume of the brane and X^m are the coordinates of the ten-dimensional target space. In order to construct the action of the super Dp-brane, this map is replaced with a supermap $\{Z^M\} = (X^m, \theta^\alpha)$ and, accordingly, the bosonic fields with the corresponding superfields. In this subsection we will use the indices $M, N, \cdots$, for the superspace coordinates and the indices $m, n, \cdots$, for the bosonic coordinates of the ten-dimensional spacetime. Superspace forms can be expanded in the coordinate basis dZ^M, or alternatively, in the one-form frame $E^{\underline{M}} = E_N^{\underline{M}} dZ^N$, where the underlined indices are flat and $E_N^{\underline{M}}$ is the supervielbein. Under the action of the Lorentz group $E^{\underline{M}}$ decomposes into a vector $E^{\underline{m}}$ and a spinor $E^{\underline{\alpha}}$, which is a 32-component Majorana spinor for IIA superspace and a doublet of chiral Majorana spinors for IIB superspace. In particular, for flat superspace one can write:

$$E^m = dX^m + \bar{\theta}\Gamma^m\, d\theta , \qquad E^\alpha = d\theta^\alpha , \tag{1.5.8}$$

where the indices are already flat. The supersymmetric generalization of the DBI plus WZ terms of the action (1.5.7) for a super Dp-brane reads:

$$S = -T_p \int_{\Sigma_{p+1}} d^{p+1}\xi \, \sqrt{-\det(g + \mathcal{F})} + T_p \int_{\Sigma_{p+1}} \sum_{r=0}^{p+1} P\left[C_{(r)}\right] \wedge e^{\mathcal{F}}, \qquad (1.5.9)$$

with:

$$g_{ab} = E_a^m \, E_b^n \, \eta_{\underline{mn}}\,,$$

$$\mathcal{F}_{ab} = F_{ab} - E_a^M E_b^N B_{\underline{MN}}\,,$$

$$C_{(r)} = \frac{1}{r!}\, dZ^{M_1} \wedge \cdots \wedge dZ^{M_r}\, C_{M_1 \cdots M_r}\,, \qquad (1.5.10)$$

where the indices a, b run over the worldvolume, F is the field strength of the worldvolume gauge field A $(F = dA)$[6], B is the NSNS two-form potential superfield, $C_{(r)}$ is the RR r-form gauge potential superfield and g_{ab} is the induced metric on the worldvolume expressed in terms of the pullback to the worldvolume of the supervielbein, which is given by:

$$E_a^m = \partial_a Z^M \, E_M^m\,. \qquad (1.5.11)$$

In ref. [83] the action (1.5.9) was shown to be invariant under the local fermionic transformations:

$$\delta_\kappa E^{\underline{m}} = 0\,,$$

$$\delta_\kappa E^{\underline{\alpha}} = (1 + \Gamma_\kappa)\kappa\,, \qquad (1.5.12)$$

where $\delta_\kappa E^{\underline{M}} = (\delta_\kappa Z^N) E_N^{\underline{M}}$. This generalizes to curved backgrounds the kappa symmetry variations of the flat superspace coordinates:

$$\delta_\kappa \theta = (1 + \Gamma_\kappa)\kappa\,, \qquad \delta_\kappa X^m = \bar{\theta}\Gamma^m \delta_\kappa \theta\,. \qquad (1.5.13)$$

One can easily check, reading the supervielbein from (1.5.8), that these transformations fulfill eq. (1.5.12).

In terms of the induced gamma matrices $\gamma_a = E_a^m \Gamma_{\underline{m}}$, the matrix Γ_κ takes the form [83]:

$$\Gamma_\kappa = \frac{1}{\sqrt{-\det(g + \mathcal{F})}} \sum_{n=0}^{\infty} \frac{(-1)^n}{2^n n!} \gamma^{a_1 b_1 \cdots a_n b_n} \mathcal{F}_{a_1 b_1} \cdots \mathcal{F}_{a_n b_n} J_{(p)}^{(n)}\,, \qquad (1.5.14)$$

where g and $\mathcal{F}$ are those defined in (1.5.10), and $J_{(p)}^{(n)}$ is the following matrix:

$$J_{(p)}^{(n)} = \begin{cases} (\Gamma_{11})^{n+(p-2)/2}\, \Gamma_{(0)} & \text{(IIA)}\,, \\[2mm] (-1)^n (\sigma_3)^{n+(p-3)/2}\, i\sigma_2 \otimes \Gamma_{(0)} & \text{(IIB)}\,, \end{cases} \qquad (1.5.15)$$

---

[6]With respect to eq. (1.5.7) F has been made dimensionless by means of the redefinition $2\pi\,\alpha'\, F \to F$.

with $\Gamma_{(0)}$ being:

$$\Gamma_{(0)} = \frac{1}{(p+1)!} \, \epsilon^{a_1 \cdots a_{p+1}} \, \gamma_{a_1 \cdots a_{p+1}} \; , \tag{1.5.16}$$

and $\gamma_{a_1 \cdots a_{p+1}}$ denoting the antisymmetrized product of the induced gamma matrices. In eq. (1.5.15) σ_2 and σ_3 are Pauli matrices that act on the two Majorana-Weyl components (arranged as a two-dimensional vector) of the type IIB spinors.

What makes this fermionic symmetry a key ingredient in the formulation of the super Dp-brane is that, upon gauge fixing, it eliminates the extra fermionic degrees of freedom of the worldvolume theory, guaranteeing the equality of fermionic and bosonic degrees of freedom on the worldvolume. Recall that the number of bosonic degrees of freedom coming from the transverse scalars is $9 - p$. After adding up the $p - 1$ physical degrees of freedom corresponding to the worldvolume gauge field, the total number of bosonic degrees of freedom is 8. On the other hand, one has 32 spinors θ which are cut in half by the equation of motion. We will see that by gauge fixing the local kappa symmetry the spinorial degrees of freedom are also halved, thus resulting the expected 8 physical spinors.

Kappa symmetry is a useful tool for finding embeddings of Dp-branes preserving some supersymmetry [84]. In particular, we are interested in bosonic configurations where the fermionic degrees of freedom vanish, *i.e.* $\theta = 0$, so we only need the variations of θ up to linear terms in θ. The supersymmetry plus kappa symmetry transformations of θ is:

$$\delta\theta = \epsilon + (1 + \Gamma_\kappa)\kappa \; , \tag{1.5.17}$$

where ϵ is the supersymmetric variation parameter. Therefore, although generically these transformations do not leave θ invariant, one can choose an appropriate value of κ such that $\delta\theta = 0$. Of course, this amounts to gauge fixing the kappa symmetry. Indeed, let us impose the following gauge fixing condition:

$$\mathcal{P}\theta = 0 \; , \tag{1.5.18}$$

where $\mathcal{P}$ is a field independent projector, $\mathcal{P}^2 = 1$, so the non-vanishing components of θ are given by $(1 - \mathcal{P})\theta$. The condition for preserving the gauge fixing condition $\mathcal{P}\delta\theta = 0$ results in:

$$\mathcal{P}\delta\theta = \mathcal{P}\epsilon + \mathcal{P}(1 + \Gamma_\kappa)\kappa = 0 \; , \tag{1.5.19}$$

which determines $\kappa = \kappa(\epsilon)$. Then, after gauge fixing the kappa symmetry, the transformation (1.5.17) becomes a global supersymmetry transformation. The condition of unbroken supersymmetry for the non-vanishing components of θ, namely $(1 - \mathcal{P})\theta$, reads:

$$(1 - \mathcal{P})\,\delta\theta = (1 - \mathcal{P})\,\epsilon + (1 - \mathcal{P})(1 + \Gamma_\kappa)\,\kappa(\epsilon) = \epsilon + (1 + \Gamma_\kappa)\,\kappa(\epsilon) = 0 \; , \tag{1.5.20}$$

where in the last equality we have used eq. (1.5.19). Multiplying the last equality by $(1 - \Gamma_\kappa)$ one gets:

$$(1 - \Gamma_\kappa)\,\epsilon = 0 \; . \tag{1.5.21}$$

Then, the fraction of supersymmetry preserved by the brane is given by the number of solutions to this equation. Notice that Γ_κ, defined in eq. (1.5.14) depends on the first derivatives of the embedding trough the induced metric and the pullback of the B field. Finally, for backgrounds of reduced supersymmetry, ϵ (the target space supersymmetry parameter) must be substituted by the Killing spinor of the ten-dimensional geometry where the Dp-brane is embedded.

1.6   Applications of the gauge/gravity duality

The gauge/gravity duality can be used to explore quantum field theories using gravity theories or vice versa. In most of its applications, classical supergravity is used to explore quantum field theories at strong coupling. The traditional method to explore quantum field theories was to use a perturbative approach, which is only valid at weak coupling regime. In general, few tools existed to address quantum field theories at strong coupling: lattice quantum field theory, integrability and localization, basically. The gauge/gravity duality has become a new powerful tool to address strongly coupled quantum field theories.

Given a quantum field theory at strong coupling, the hope would be to find the exact gravity dual. Nevertheless, it is still not known how to obtain the gravity dual of any phenomenological theory of nature. Starting from highly supersymmetric and conformal theories, there has been large efforts to introduce new elements to get closer to the phenomenological theories, but even the more sophisticated models are still far from the real theories. So, a natural question is: why is the duality useful if it is not known the gravity dual? What is expected from the duality is that we can extract universal properties. Indeed, we can consider several field theories with known gravity dual, that share some features with a given phenomenological theory, and then extract some universal behavior from them. If a result holds for all of them, then we can conjecture that the result will be also valid for the phenomenological theory. So, the hope is that from the duality we can predict general behaviors, but not concrete numbers.

Let us consider a list of fields were the AdS/CFT conjecture has found applications:

- Applications to QCD. Even if there have been large efforts devoted to find a theory as close as possible to the gravity dual of QCD (see, for example, Sakai-Sugimoto-Witten model [85]), it seems that finding the exact gravity dual of QCD is a very challenging problem. Using models that share some properties with QCD, there have been efforts to understand different aspects of the theory, like the physics of the collisions happening at the particle accelerators (see for example [86]), the phases of the QCD phase diagram (for example [74]), the physics of QCD with non vanishing theta angle (for example [87]), the glueball spectrum and other particles of the spectrum (for example [88]), the behavior of the jet events (for example [89]),etc.

- Applications to condensed matter physics. Condensed matter physics is one of the fields where the gauge/gravity duality has found more applications. Models have been constructed to describe holographic superconductors, fractional quantum Hall systems, fractional topological insulators, Kondo models, Weyl semimetals, holographic superfluids, dirty materials, etc. In condensed matter physics applications it is common to use the 'bottom-up' approach, in which the gravity systems are not necessarily embedded in string theory. In these cases, the fact that the gravity model has a dual field theory is less clear. The models that are embedded in string theory are usually called 'top-down' models.

- Applications to astrophysics. For example, in [90] it is studied the cold quark matter

just above the deconfinement transition, using a D3-D7 system, in order to describe some phases of neutron stars.

- Applications to cosmology. Cosmological models can be studied from its field theory dual, see for example [91].

- Applications to hydrodynamics. This concrete case of the duality is known as fluid/gravity duality, see [92] for a review.

- Applications to non-equilibrium systems. In the last years real time evolution has been considered in gravitational systems, and a lot of numerical efforts in solving them have lead to a new branch of the duality, known as numerical holography. See for example [93] [94].

- Applications to entanglement entropy and quantum information theory. The famous Ryu-Takayanagi prescription offers a simple geometrical method to compute the entanglement entropy in a quantum field theory with known gravity dual. For a review see [95].

- Applications to black hole physics. The black hole physics can be analyzed via its field theory dual, for an example see [96].

Here we have mentioned some applications of the duality, and a complete list would probably involve much more items. The subject has vastly extended in the last years, and the correspondence has found applications in many areas.

The KSS bound

Let us mention one of the first and most famous successes of the AdS/CFT conjecture. The duality can be used to compute transport properties in strongly coupled quantum field theories. In particular, in 2001 Policastro, Son and Starinets [97] computed the shear viscosity in a holographic model, and the result, expressed in terms of the entropy density, is very simple:

$$\frac{\eta}{s} = \frac{1}{4\pi} \ . \tag{1.6.22}$$

This value turned out to be the same for different holographic models, and in 2004 Kotvun, Son y Starinets (KSS) [98] conjectured that this is a lower bound for a set of theories (there are counterexamples where the bound is not satisfied, like in Gauss-Bonnet theories).

The ratio of shear viscosity to entropy density can be used to characterize how close a given fluid is to being perfect. Ordinary fluids, like water, have shear viscosities much higher than this value. Even the liquid helium has much higher viscosity. Nevertheless, there is a fluid whose shear viscosity is close to this ratio. It is the quark-gluon plasma, one of the phases of the phase diagram of QCD. This state of matter was first observed in the Relativistic Heavy Ion Collider (RHIC) at Brookhaven National Laboratory in 2005. After 10 years since this first measurement, the recent values obtained in the experiments are still

compatible with the KSS bound (for a review of recent results see [99]). Also, there are condensed matter systems whose shear viscosity is close to the conjectured bound, like for example, in graphene [100].

Applications in this thesis

In this thesis we will use the AdS/CFT correspondence to obtain new results in condensed matter physics. In chapter 4 we construct a gravity dual of a fractional quantum Hall system and in chapter 5 we construct a gravity dual of a system exhibiting quantum phase transitions.

The quantum Hall effect is a phenomenon present in gapped (2+1)-dimensional systems with broken parity symmetry. When electrons are confined in a heterojunction at low temperature and strong magnetic fields, the response to an applied electric field displays a striking behavior: the conductivity in the direction of the electric field vanishes, while the transverse conductivity is quantized and given by $(e^2/h)\nu$, where ν is the filling fraction, defined as the ratio of the charge density to the magnetic flux. In the integer quantum Hall effect (IQHE) $\nu \in \mathbb{Z}$, whereas ν is a rational number in the fractional quantum Hall effect (FQHE). The integer quantum Hall effect is well explained by field theories at weak coupling. However, in a natural way the fractional quantum Hall effect is described by field theories at strong coupling, and then the AdS/CFT is a good arena to explore its properties. In chapter 4 a holographic model for a fractional quantum Hall system is constructed. In particular, supersymmetric Hall states are found.

Quantum phase transitions are phase transitions that happen at zero temperature, and the phase transition parameter is not the temperature but other parameter like the doping of the material, chemical potential, etc. In general, the approach to computing observables in quantum phase transitions is a theoretical challenge, as lowering the temperature near zero turns out to be a difficult process. Nevertheless, the AdS/CFT correspondence offers a very good scenario for this set up, as in its original formulation the temperature is already vanishing. Besides, the quantum phase transitions happen in systems at strong coupling. Then, the gauge/gravity duality is an ideal tool for studying these systems, and in chapter 5 we will construct a gravity dual of a system exhibiting quantum phase transition as the chemical potential is tuned.

Both models are based in the ABJM theory. This theory is particularly interesting to use for condensed matter physics purposes, as it is a Chern-Simons matter theory in 2+1 dimensions, and many condensed matter systems are based in Chern-Simons theories. In the original paper of Aharony, Bergman, Jafferis and Madacena [51], it is stated that one of the main motivations to construct the theory is to obtain new condensed matter physics applications. Nevertheless, after almost ten years, the theory has not been yet fully exploited, and in this thesis we give a further step in this direction.

Chapter 2

Non-abelian T duality and new AdS_3 backgrounds

2.1 Introduction

The aim of this chapter is to construct new solutions of type IIA/B and eleven-dimensional supergravity via non-abelian T-duality (NATD) and interpret the dual field theory of these new solutions according to the gauge/gravity correspondence.

In particular, we are interested in new $AdS_3 \times M_7$ supersymmetric solutions, but non-supersymmetric non-AdS solutions are also obtained. As explained in section 1.2, the NATD is performed locally, and the global properties of the manifold M_7 are not known. Consequently, we will be able to obtain only some details of the dual field theories, as the full information requires the global details of the manifold[1].

The NATD was used for the first time in the context of the gauge/gravity duality in the paper [15]. Indeed, Sfetsos and Thompson applied NATD to the maximally supersymmetric example of $AdS_5 \times S^5$, finding a metric and RR-fields that preserved $\mathcal{N} = 2$ SUSY. When lifted to eleven dimensions, the background fits (not surprisingly) into the classification of [101]. What is interesting is that Sfetsos and Thompson [15] *generated* a new solution to the Gaiotto-Maldacena differential equation [102], describing $\mathcal{N} = 2$ SUSY CFTs of the Gaiotto-type [103], [104]. This logic was profusely applied to less supersymmetric cases in [105]-[107]; finding new metrics and defining new QFTs by the calculation of their observables.

Nevertheless, various puzzles associated with NATD remain. As explained above, the global properties of the new manifold are not known. In more concrete terms, the periodicity (if any) of the dual coordinates (the Lagrange multipliers in the sigma-model) is not known. In the same vein, the precise field theory dual to the backgrounds generated by NATD is not clear.

In this chapter we present possible solutions to these puzzles— at least in particular examples. Our study begins with type IIB backgrounds dual to a compactification of the Klebanov-Witten CFT [34] to a 2-d CFT. We will present these backgrounds for different compactifications and perform a NATD transformation on them, hence generating new

---

[1] For example, the solutions $AdS_5 \times S^5$ and $AdS_5 \times S^5/\mathbb{Z}_2$ are locally equivalent, but globally different, and the field theories are different. The first one has gauge group $SU(N)$ and the second one $SU(N) \times SU(N)$

smooth and SUSY solutions with AdS_3-factors in type IIA and M-theory. Application of a further T-duality generates new backgrounds in type IIB with an AdS_3-factor which are also smooth and preserve the same amount of SUSY. We will make a proposal for the dual QFT and interpret the range of the dual coordinates in terms of a field theoretic operation.

The picture that emerges is that our geometries describe QFTs that become conformal at low energies. These CFTs live on the intersection of D2- and D6-branes suspended between NS5-branes. While crossing the NS5-branes, charge for D4-branes is induced and new nodes of the quiver appear.

We will present the calculation of different observables of the associated QFTs that support the proposal made above. These calculations are performed in smooth supergravity solutions, hence they are trustable and capture the strong dynamics of the associated 2-d CFTs.

The work performed in this chapter is a continuation of the previous works of Sfetsos-Thompson [15] and Itsios-Nunez-Sfetsos-Thompson (INST) [105], [42]. The connection between the material in this work and those papers is depicted in Fig. 2.1 below.
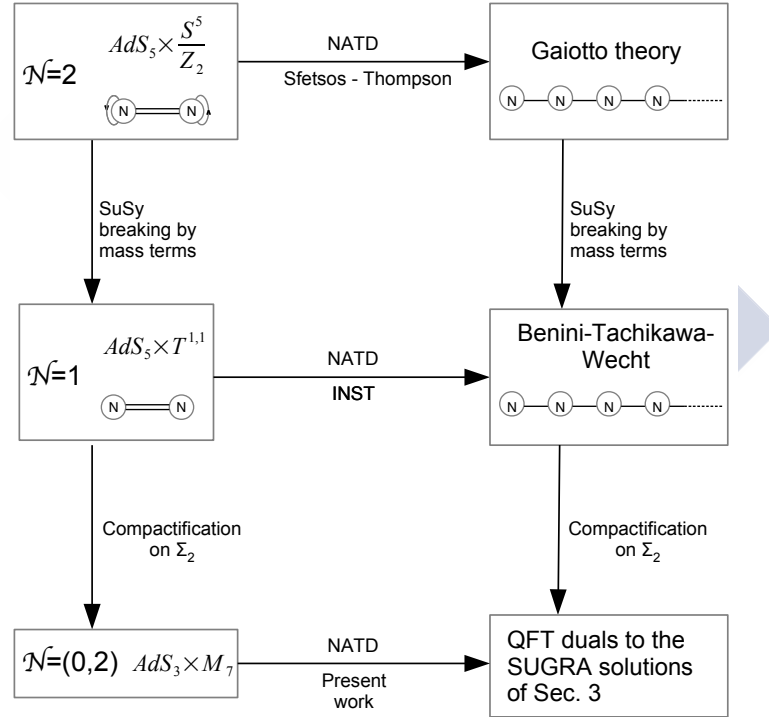
Figure 2.1: On the left: known solutions on which NATD is performed. On the right: QFT's that correspond to the NATD SUGRA solutions.

The organization of this chapter is as follows. In the first part of this work, covered in sections 2.2 to 2.5, we present type IIB backgrounds that are already known and the new ones (in type IIA, IIB and M-theory) that we construct. Table 2.1 summarizes these solutions. In the second part of this work, starting in section 2.6, we begin the study of the field theoretical aspects encoded by the backgrounds presented in the first part. Section 2.7 deals with the quantized charges, defining ranks of the gauge groups. Section 2.8 studies the

central charge computed holographically, either at the fixed points or along the anisotropic flows (where a proposal for a c-function is analyzed). This observable presents many clues towards the understanding of the associated QFTs. Section 2.9 presents a detailed study of Wilson loops and entanglement entropy of the QFT at the fixed points and along the flow. We discuss the results in section 2.10. The computations of the supersymmetry preserved by the solutions is relegated to appendix 2.A.1.

Solutions	IIB	NATD	NATD-T	Uplift
Flow from $AdS_5 \times T^{1,1}$ to $AdS_3 \times H_2 \times T^{1,1}$ $(\mathcal{N} = 1)$ Fixed points $AdS_3 \times \Sigma_2 \times T^{1,1} : \Sigma_2 = S^2, T^2, H_2$	2.2.1	2.3.1	2.4	2.5.1
The Donos-Gauntlett solution	2.2.2	2.3.2	-	2.5.2

Table 2.1: Summary of solutions contained in sections 2.2 to 2.5. The numbers indicate the section where they are discussed.

To be more precise, in the first part of this chapter (sections 2.2 to 2.5) we will exhaustively present a large set of backgrounds solving the type IIB or type IIA supergravity equations. Most of them are new, but some are already present in the bibliography. New solutions in eleven-dimensional supergravity will also be discussed. These geometries, for the most part, preserve some amount of SUSY.

The common denominator of these backgrounds will be the presence of an AdS_3 submanifold in the ten or eleven-dimensional metric. This will be interpreted as the dual description of strongly coupled two dimensional conformal dynamics. In most of the cases, there is also a flow, connecting from an AdS_3 fixed point to an AdS_5, with boundary $R^{1,1} \times \Sigma_2$. The manifold Σ_2 will be a constant curvature Riemann surface. As a consequence we conjecture that the full geometry is describing the strongly coupled dynamics of a four dimensional QFT, that is conformal at high energies and gets compactified on Σ_2 (typically preserving some amount of SUSY). The QFT flows at low energies to a 2-d CFT that is also strongly coupled.

The solutions that we are going to present in this section, can be found by inspection of the type II equations. This requires a quite inspired ansatz. More practical is to search for solutions of this kind in five dimensional gauged supergravity, see the papers [108, 109] for a detailed account of the lagrangians. Some other solutions are efficiently obtained by the use of generating techniques, for example a combination of abelian and non-abelian T-duality, that are applied to known (or new) backgrounds, as we show below.

We now present in detail, the solutions we will work with in this chapter.

2.2 Simple flows from $AdS_5 \times T^{1,1}$ to $AdS_3 \times M_7$ in type IIB

We start this section by proposing a simple background in type IIB. In the sense of the Maldacena duality, this describes the strongly coupled dynamics of an $\mathcal{N} = 1$ SUSY QFT

in four dimensions, that is compactified to two dimensions on a manifold Σ_2. In order to allow such a compactification we turn on a 1-form field, A_1, on the Riemann surface Σ_2. Motivated by the works [108, 109], where the authors consider dimensional reductions to five dimensions of type IIB supergravity backgrounds on any Sasaki-Einstein manifold, we propose the following ansatz,

$$\frac{ds^2}{L^2} = e^{2A}\left(-dy_0^2 + dy_1^2\right) + e^{2B}ds_{\Sigma_2}^2 + dr^2 + e^{2U}ds_{KE}^2 + e^{2V}\left(\eta + zA_1\right)^2,$$

$$\frac{F_5}{L^4} = 4e^{-4U-V}\text{Vol}_5 + 2J \wedge J \wedge (\eta + zA_1) - z\text{Vol}_{\Sigma_2} \wedge J \wedge (\eta + zA_1) \tag{2.2.1}$$

$$- ze^{-2B-V}\text{Vol}_{AdS_3} \wedge J,$$

$$\Phi = 0, \qquad C_0 = 0, \qquad F_3 = 0, \qquad B_2 = 0.$$

We will focus on the case in which the Sasaki-Einstein space is $T^{1,1}$, hence the Kähler-Einstein manifold is

$$ds_{KE}^2 = \frac{1}{6}(\sigma_1^2 + \sigma_2^2 + \omega_1^2 + \omega_2^2), \tag{2.2.2}$$

where we have defined,

$$\sigma_1 = d\theta_1, \qquad\qquad \sigma_2 = \sin\theta_1 d\phi_1, \qquad\qquad \sigma_3 = \cos\theta_1 d\phi_1,$$

$$\omega_1 = \cos\psi\sin\theta_2 d\phi_2 - \sin\psi d\theta_2, \qquad \omega_2 = \sin\psi\sin\theta_2 d\phi_2 + \cos\psi d\theta_2, \qquad \omega_3 = d\psi + \cos\theta_2 d\phi_2,$$

$$\text{Vol}_{AdS_3} = e^{2A}dy_0 \wedge dy_1 \wedge dr, \qquad \text{Vol}_5 = e^{2B}\text{Vol}_{AdS_3} \wedge \text{Vol}_{\Sigma_2}, \qquad z \in \mathbb{R},$$

$$\eta = \tfrac{1}{3}\left(d\psi + \cos\theta_1 d\phi_1 + \cos\theta_2 d\phi_2\right), J = \tfrac{-1}{6}\left(\sin\theta_1 d\theta_1 \wedge d\phi_1 + \sin\theta_2 d\theta_2 \wedge d\phi_2\right). \tag{2.2.3}$$

The forms η and J verify the relation $d\eta = 2J$. The range of the angles in the $\sigma_i's$ and the ω_i's —the left invariant forms of $SU(2)$— is given by $0 \leq \theta_{1,2} < \pi$, $0 \leq \phi_{1,2} < 2\pi$ and $0 \leq \psi < 4\pi$. The ω_i satisfy $d\omega_i = \frac{1}{2}\,\epsilon_{ijk}\,\omega_j \wedge \omega_k$. We also defined a one form A_1, that verifies $dA_1 = \text{Vol}_{\Sigma_2}^2$. As usual $ds_{\Sigma_2}^2$ is the metric of the two dimensional surface of curvature $\kappa = (1, -1, 0)$, denoting a sphere, hyperbolic plane[2] or a torus respectively. In local coordinates these read,

$$A_1 = -\cos\alpha\, d\beta, \quad \text{Vol}_{\Sigma_2} = \sin\alpha\, d\alpha \wedge d\beta, \quad ds_{\Sigma_2}^2 = d\alpha^2 + \sin^2\alpha d\beta^2, \quad (\kappa = 1),$$

$$A_1 = \cosh\alpha\, d\beta, \quad \text{Vol}_{\Sigma_2} = \sinh\alpha\, d\alpha \wedge d\beta, \quad ds_{\Sigma_2}^2 = d\alpha^2 + \sinh^2\alpha d\beta^2, \quad (\kappa = -1),$$

$$A_1 = \alpha\, d\beta, \qquad \text{Vol}_{\Sigma_2} = d\alpha \wedge d\beta, \qquad ds_{\Sigma_2}^2 = d\alpha^2 + d\beta^2, \qquad (\kappa = 0). \tag{2.2.4}$$

---

[2]To be precise, we do not consider the hyperbolic plane H_2, as it has infinite volume. What we consider is a compact space H_2/Γ obtained by quotient by a proper Fuchsian group [110], and its volume is given by $4\pi(g-1)$, where g is the genus of H_2/Γ.

A natural vielbein for the metric (2.2.1) is,

$$e^{y_0} = Le^A dy_0 \ , \qquad e^{y_1} = Le^A dy_1 \ , \qquad e^\alpha = Le^B d\alpha \ , \qquad e^\beta = Le^B A_0 d\beta \ , \qquad e^r = Ldr \ ,$$

$$e^{\sigma_1} = L\frac{e^U}{\sqrt{6}}\sigma_1 \ , \qquad e^{\sigma_2} = L\frac{e^U}{\sqrt{6}}\sigma_2 \ , \qquad e^1 = L\frac{e^U}{\sqrt{6}}\omega_1 \ , \qquad e^2 = L\frac{e^U}{\sqrt{6}}\omega_2 \ , \qquad e^3 = Le^V(\eta + zA_1) \ ,$$

$$(2.2.5)$$

with $A_0 = \sinh\alpha$ for H_2, $A_0 = \sin\alpha$ for S^2 and $A_0 = 1$ for T^2.

As anticipated, the background above describes the strong dynamics for a compactification of a four dimensional QFT to two dimensions. In the case that we are interested in this work — in which the Kähler-Einstein manifold is the one in eq. (2.2.2)— the four dimensional QFT at high energy asymptotes to the Klebanov-Witten quiver [34] on $R^{1,1} \times \Sigma_2$. As it will be clear, most of our results will be valid for the case of a general $Y^{p,q}$ or any other Sasaki-Einstein manifold and their associated QFT. Indeed, these solutions can be obtained by lifting to type IIB, simpler backgrounds of the five-dimensional supergravity in [109]. In fact, the 5-d supergravity lagrangian was written for any Sasaki-Einstein internal space.

Assuming that the functions A, B, U, V depend only on the radial coordinate r, we can calculate the BPS equations describing the SUSY preserving flow from $AdS_5 \times T^{1,1}$ at large values of the radial coordinate to $AdS_3 \times M_7$. The end-point of the flow will be dual to a 2-d CFT obtained after taking the low energy limit of a twisted KK compactification of the Klebanov-Witten QFT on Σ_2. Imposing a set of projections on the SUSY spinors of type IIB—see appendix 2.A.1 for details— we find,

$$A' - e^{-V-4U} \pm \frac{z}{2}e^{-2B-2U-V} = 0,$$

$$B' - e^{-V-4U} \mp \frac{z}{2}e^{-2B-2U-V} \mp \frac{z}{2}e^{-2B+V} = 0,$$

$$U' + e^{-V-4U} - e^{V-2U} = 0, \qquad (2.2.6)$$

$$V' - 3e^{-V} + 2e^{V-2U} + e^{-V-4U} \mp \frac{z}{2}e^{-2B-2U-V} \pm \frac{z}{2}e^{-2B+V} = 0 \ ,$$

where the upper signs are for H_2, the lower signs for S^2, and $z = -\frac{1}{3}$ for both cases. In the case of the torus the variation of the gravitino will force $z = 0$, obtaining $A' = B'$, which does not permit an AdS_3 solution. We now attempt to find simple solutions to the eqs.(2.2.6).

2.2.1 Solution of the form $AdS_3 \times H_2$, $AdS_3 \times S^2$ and $AdS_3 \times T^2$ with 'twisting'

At this point we are going to construct a flow between $AdS_5 \times T^{1,1}$ and $AdS_3 \times \Sigma_2 \times M_5$. To simplify the task, we propose that the functions U, V are constant, then the BPS equations imply that $U = V = 0$, leaving us—in the case of H_2 with,

$$A' = 1 + \frac{e^{-2B}}{6}, \quad B' = 1 - \frac{e^{-2B}}{3} \ , \qquad (2.2.7)$$

that can be immediately integrated,

$$A = \frac{3}{2}r - \frac{1}{4}\ln\left(1 + e^{2r}\right) + a_0 \ , \qquad B = \ln\frac{1}{\sqrt{3}} + \frac{1}{2}\ln\left(1 + e^{2r}\right) . \qquad (2.2.8)$$

One of the integration constants associated with these solutions corresponds to a choice of the origin of the holographic variable and the other constant, e^{2a_0}, sets the size of the three dimensional space (y_0, y_1, r). We will choose $a_0 = 0$ in what follows.

In the limit $r \to \infty$ (capturing the UV-dynamics of the QFT) we recover a Klebanov-Witten metric

$$A \sim r - \frac{1}{4}e^{-2r} + \frac{1}{8}e^{-4r} \ , \qquad B \sim r - \frac{1}{2}\ln 3 + \frac{1}{2}e^{-2r} - \frac{1}{4}e^{-4r} \ , \tag{2.2.9}$$

whilst in the limit $r \to -\infty$ (that is dual to the IR in the dual QFT) we obtain a supersymmetric solution of the form $AdS_3 \times H_2$,

$$A \sim \frac{3}{2}r - \frac{1}{4}e^{2r} + \frac{1}{8}e^{4r} \ , \qquad B \sim \ln\frac{1}{\sqrt{3}} + \frac{1}{2}e^{2r} - \frac{1}{4}e^{4r}. \tag{2.2.10}$$

Let us write explicitly this background using eq. (2.2.2),

$$\frac{ds_{10}^2}{L^2} = \frac{e^{3r}}{\sqrt{1+e^{2r}}}\left(-dy_0^2 + dy_1^2\right) + \frac{1+e^{2r}}{3}\left(d\alpha^2 + \sinh^2\alpha\, d\beta^2\right) + dr^2 + ds_{KE}^2 + \left(\eta - \frac{1}{3}A_1\right)^2 \ ,$$

$$\frac{F_5}{L^4} = \frac{4}{3}e^{3r}\sqrt{1+e^{2r}}\sinh\alpha\, dy_0 \wedge dy_1 \wedge d\alpha \wedge d\beta \wedge dr + 2J \wedge J \wedge \left(\eta - \frac{1}{3}A_1\right)$$

$$+ \frac{1}{3}\sinh\alpha\, d\alpha \wedge d\beta \wedge J \wedge \left(\eta - \frac{1}{3}A_1\right) + \frac{e^{3r}}{(1+e^{2r})^{\frac{3}{2}}}dy_0 \wedge dy_1 \wedge dr \wedge J \ , \tag{2.2.11}$$

$$A_1 = \cosh\alpha\, d\beta, \qquad \Phi = 0, \qquad C_0 = 0, \qquad F_3 = 0, \qquad B_2 = 0 \ .$$

The solution above was originally presented in [111].

We consider now the case of S^2. With the same assumptions about the functions U, V, the BPS equations (2.2.6) read,

$$A' = 1 - \frac{e^{-2B}}{6}, \qquad B' = 1 + \frac{e^{-2B}}{3}. \tag{2.2.12}$$

These can also be immediately integrated (with a suitable choice of integration constants),

$$A = \frac{3}{2}r - \frac{1}{4}\ln\left(e^{2r} - 1\right) \ , \qquad B = \ln\frac{1}{\sqrt{3}} + \frac{1}{2}\ln\left(e^{2r} - 1\right) \ , \qquad r > 0 \ . \tag{2.2.13}$$

This solution seems to be problematic close to $r = 0$. Indeed, if we compute the Ricci scalar we obtain $R = 0$, nevertheless, $R_{\mu\nu}R^{\mu\nu} \sim \frac{3}{32L^4r^4} + \dots$ close to $r = 0$. The solution is singular and we will not study it further.

It is interesting to notice that a family of *non-SUSY* fixed point solutions exists. Indeed, we can consider the situation where B, U, V and $A'(r) = a_1$ are constant. For S^2 and H_2, we find then that the Einstein equations impose $U = V = 0$ and

$$8 + e^{-4B}z^2 - 4\,a_1^2 = 0 \ , \qquad 4 - z^2 e^{-4B} + \kappa\,e^{-2B} = 0. \tag{2.2.14}$$

Where $\kappa = +1$ for S^2 and $\kappa = -1$ for H_2. The solution is,

$$z^2 = e^{2B} \left(4e^{2B} + \kappa \right) \ , \qquad a_1^2 = 3 + \kappa \, \frac{e^{-2B}}{4} \ . \tag{2.2.15}$$

For the S^2 case the range of parameters is,

$$B \in \mathbb{R} \ , \qquad z \in \mathbb{R} - \{0\} \ , \qquad a_1 \in \left(-\infty, \sqrt{3} \right) \cup \left(\sqrt{3}, +\infty \right) \ , \tag{2.2.16}$$

while for H_2 we find,

$$B \in \left[-\ln 2, +\infty \right) \ , \qquad z \in \mathbb{R} \ , \qquad a_1 \in \left(-\sqrt{3}, -\sqrt{2} \right] \cup \left[\sqrt{2}, \sqrt{3} \right) \ . \tag{2.2.17}$$

Notice that in the case of H_2, there is a non-SUSY solution with $z = 0$, hence no fibration between the hyperbolic plane and the Reeb vector η. The SUSY fixed point in eq. (2.2.12) is part of the family in eq. (2.2.17), with $z = -\frac{1}{3}$.

For the T^2 we also find an AdS_3 solution,

$$a_1^2 = 3 \ , \qquad z^2 = 4e^{4B} \ , \qquad U = 0 \ , \qquad V = 0 \ . \tag{2.2.18}$$

Notice that $z \in \mathbb{R} - \{0\}$. This completes our presentation of what we will refer as 'twisted' solutions. By twisted we mean solutions where a gauge field is switched on the Riemann surface generating a fibration between Σ_2 and the R-symmetry direction. In the following, we will present a background that also contains an AdS_3 factor, it flows in the UV to an AdS_5, but the field content and the mechanism of SUSY preservation are different from the ones above.

2.2.2 The Donos-Gauntlett-(Kim) background

In this section we revisit a beautiful solution written in [112]—this type of solution was first studied in [113]. Due to the more detailed study of [112], we will refer to it as the Donos-Gauntlett solution in the rest of this chapter.

The background in [112] describes a flow in the radial coordinate, from $AdS_5 \times T^{1,1}$ to $AdS_3 \times M_7$. The solution is very original. While the boundary of AdS_5 is of the form $R^{1,1} \times T^2$, the compactification on the Riemann surface (a torus) does not use a 'twist' of the 4d-QFT. This is reflected by the absence of a fibration of the Riemann surface on the R-symmetry direction η. Still, the background preserves SUSY [3]. The solution contains an active NS-three form H_3 that together with the RR five form F_5 implies the presence of a RR-three form F_3. The authors of [112] found this configuration by using a very inspired ansatz. We review this solution below, adding new information to complement that in [112].

The metric ansatz is given by,

$$\frac{ds^2}{L^2} = e^{2A} \left(-dy_0^2 + dy_1^2 \right) + e^{2B} \left(d\alpha^2 + d\beta^2 \right) + dr^2 + e^{2U} ds_{KE}^2 + e^{2V} \eta^2 \ , \tag{2.2.19}$$

---

[3]The solutions in Eqs.(63)-(80) of the paper [114], can be thought as an 'ugly' ancestor of the Donos-Gauntlett background.

where A, B, U, V are functions of the radial coordinate r only. The line element ds^2_{KE} is defined in eq. (2.2.2) and σ_i, ω_i, η are given in eq. (2.2.3). The natural vielbein is,

$$e^{y_0} = Le^A dy_0, \quad e^{y_1} = Le^A dy_1, \quad e^\alpha = Le^B d\alpha, \quad e^\beta = Le^B d\beta, \quad e^r = Ldr,$$

$$e^{\sigma_1} = L\frac{e^U}{\sqrt{6}}\sigma_1, \quad e^{\sigma_2} = L\frac{e^U}{\sqrt{6}}\sigma_2, \quad e^1 = L\frac{e^U}{\sqrt{6}}\omega_1, \quad e^2 = L\frac{e^U}{\sqrt{6}}\omega_2, \quad e^3 = Le^V \eta\ . \tag{2.2.20}$$

Note that compared to [112] we have relabelled $\phi_i \to -\phi_i$. To complete the definition of the background, we also need

$$\text{Vol}_1 = -\sigma_1 \wedge \sigma_2, \qquad \text{Vol}_2 = \omega_1 \wedge \omega_2, \tag{2.2.21}$$

and the fluxes,

$$\frac{1}{L^4}F_5 = 4e^{2A+2B-V-4U}dy_0 \wedge dy_1 \wedge d\alpha \wedge d\beta \wedge dr + \frac{1}{9}\eta \wedge \text{Vol}_1 \wedge \text{Vol}_2$$

$$+\frac{\lambda^2}{12}\Big[d\alpha \wedge d\beta \wedge \eta \wedge (\text{Vol}_1 + \text{Vol}_2) + e^{2A-2B-V}dy_0 \wedge dy_1 \wedge dr \wedge (\text{Vol}_1 + \text{Vol}_2)\Big],$$

$$\frac{1}{L^2}F_3 = \frac{\lambda}{6}d\beta \wedge (\text{Vol}_1 - \text{Vol}_2), \qquad \frac{1}{L^2}B_2 = -\frac{\lambda}{6}\alpha\ (\text{Vol}_1 - \text{Vol}_2), \tag{2.2.22}$$

where λ is a constant that encodes the deformation of the space (and the corresponding operator in the 4d CFT). The BPS equations for the above system are given by,

$$A' = \frac{1}{4}\lambda^2 e^{-2B-2U-V} + e^{-4U-V}, \qquad B' = e^{-4U-V} - \frac{1}{4}\lambda^2 e^{-2B-2U-V},$$

$$U' = e^{V-2U} - e^{-4U-V}, \qquad V' = -\frac{1}{4}\lambda^2 e^{-2B-2U-V} - e^{-4U-V} - 2e^{V-2U} + 3e^{-V}. \tag{2.2.23}$$

It is possible to recover the $AdS_5 \times T^{1,1}$ solution by setting $\lambda = 0$ and

$$A = B = r, \qquad U = V = 0. \tag{2.2.24}$$

Further we can recover the AdS_3 solution by setting $\lambda = 2$ (this is just a conventional value adopted in [112]) and

$$A = \frac{3^{3/4}}{\sqrt{2}}r, \qquad B = \frac{1}{4}\ln\left(\frac{4}{3}\right), \qquad U = \frac{1}{4}\ln\left(\frac{4}{3}\right), \qquad V = -\frac{1}{4}\ln\left(\frac{4}{3}\right). \tag{2.2.25}$$

A flow (triggered by the deformation parameterized by λ) between the asymptotic AdS_5 and the AdS_3 fixed point can be found numerically.

Up to this point, we have set the stage for our study, but most of the solutions discussed above have already been stated in the literature. Here we just added some new backgrounds and technical elaborations on the known ones. Below, we will present genuinely new type

IIA/B solutions. The technical tool that we have used is non-abelian T-duality. This technique, when applied to an $SU(2)$ isometry of the previously discussed solutions will generate new type IIA configurations. In our examples these new solutions are nonsingular. Their lift to eleven dimensions will produce new, smooth, AdS_3 configurations in M-theory. Moreover, performing an additional abelian T-duality transformation we generate new type IIB backgrounds with all fluxes turned on and an AdS_3 fixed point at the IR. We move on to describe these.

2.3 New backgrounds in type IIA: use of non-abelian T-duality

In this section we apply the technique of non-abelian T-duality on the type IIB backgrounds that we presented above. As a result we obtain new solutions of the type IIA supergravity.

2.3.1 The non-abelian T-dual of the twisted solutions

We will start by applying non-abelian T-duality (NATD) to the background obtained via a twisted compactification in section 2.2. The configuration we will focus on is a particular case of that in eq. (2.2.1). Specifically, in what follows we consider $U = V = 0$. These values for the functions U and V are compatible with the BPS system (2.2.6). In this case the background (2.2.1) simplifies to,

$$\frac{ds^2}{L^2} = e^{2A}\left(-dy_0^2 + dy_1^2\right) + e^{2B}ds_{\Sigma_2}^2 + dr^2 + \frac{1}{6}\left(\sigma_1^2 + \sigma_2^2\right) + \frac{1}{6}\left(\omega_1^2 + \omega_2^2\right) + \left(\eta + zA_1\right)^2 ,$$

$$\frac{F_5}{L^4} = 4\text{Vol}_5 + 2J \wedge J \wedge \left(\eta + zA_1\right) - z\text{Vol}_{\Sigma_2} \wedge J \wedge \left(\eta + zA_1\right) - ze^{-2B}\text{Vol}_{AdS_3} \wedge J .$$

$$(2.3.26)$$

As before, all other RR and NS fields are taken to vanish. Also, the 1-form A_1, the line element of the Riemann surface Σ_2 and the corresponding volume form, for each of the three cases that we consider here, are given in eq. (2.2.4).

We will now present the details for the background after NATD has been applied on the $SU(2)$ isometry described by the coordinates (θ_2, ϕ_2, ψ). As is well-known a gauge fixing has to be implemented during the NATD procedure. This leads to a choice of three 'new coordinates' among the Lagrange multipliers (x_1, x_2, x_3) used in the NATD procedure and the 'old coordinates' (θ_2, ϕ_2, ψ) [4]. In all of our examples we consider a gauge fixing of the form,

$$\theta_2 = \phi_2 = \psi = 0. \qquad (2.3.27)$$

As a result, the Lagrange multipliers x_1, x_2 and x_3 play the rôle of the dual coordinates in the new background. To display the natural symmetries of the background, we will quote the results using spherical coordinates (the expressions in cylindrical and cartesian coordinates

---

[4]The process of NATD and the needed gauge fixing was described in detail in [42], [106].

are written in appendix C of [19]). We define,

$$x_1 = \rho \cos \xi \sin \chi \, , \qquad x_2 = \rho \sin \xi \sin \chi \, , \qquad x_3 = \rho \cos \chi \, ,$$

$$\Delta = L^4 + 54\alpha'^2 \rho^2 \sin^2 \chi + 36\alpha'^2 \rho^2 \cos^2 \chi \, , \qquad \tilde{\sigma}_3 = \cos \theta_1 d\phi_1 + 3z A_1.$$

(2.3.28)

The NSNS sector of the transformed IIA background reads,

$$e^{-2\widehat{\Phi}} = \frac{L^2}{324\alpha'^3} \Delta,$$

$$\frac{d\hat{s}^2}{L^2} = e^{2A} \left(-dy_0^2 + dy_1^2 \right) + e^{2B} ds_{\Sigma_2}^2 + dr^2 + \frac{1}{6} \left(\sigma_1^2 + \sigma_2^2 \right) + \frac{\alpha'^2}{\Delta} \left[6 \left(\sin^2 \chi \left(d\rho^2 + \rho^2 (d\xi + \tilde{\sigma}_3)^2 \right) \right. \right.$$

$$\left. + \rho \sin(2\chi) d\rho d\chi + \rho^2 \cos^2 \chi d\chi^2 \right) + 9 \left(\cos \chi d\rho - \rho \sin \chi d\chi \right)^2 + \frac{324\alpha'^2}{L^4} \rho^2 d\rho^2 \right],$$

$$\widehat{B}_2 = \frac{\alpha'^3}{\Delta} \left[36\rho \cos \chi \left(\rho \tilde{\sigma}_3 \wedge d\rho + \rho \sin \chi d\xi \wedge \left(\sin \chi d\rho + \rho \cos \chi d\chi \right) \right) \right.$$

$$\left. + \left(\frac{L^4}{\alpha'^2} \tilde{\sigma}_3 - 54\rho^2 \sin^2 \chi d\xi \right) \wedge \left(\cos \chi d\rho - \rho \sin \chi d\chi \right) \right],$$

(2.3.29)

while the RR sector is, [5]

$$\widehat{F}_0 = 0, \qquad \widehat{F}_2 = \frac{L^4}{54\alpha'^{\frac{3}{2}}} \left(2\sigma_1 \wedge \sigma_2 + 3z \text{Vol}_{\Sigma_2} \right) \, ,$$

$$\widehat{F}_4 = \frac{L^4}{18\sqrt{\alpha'}} \left[3z e^{-2B} \left(d\rho \cos \chi - \rho \sin \chi d\chi \right) \wedge \text{Vol}_{AdS_3} + z \, \rho \, \cos \chi \text{Vol}_{\Sigma_2} \wedge \sigma_1 \wedge \sigma_2 \right.$$

$$- \frac{18\alpha'^2}{\Delta} \rho^2 \sin \chi \left(z \text{Vol}_{\Sigma_2} + \frac{2}{3} \sigma_1 \wedge \sigma_2 \right) \wedge \left(2 \cos \chi \left(\sin \chi d\rho + \rho \cos \chi d\chi \right) \right.$$ (2.3.30)

$$\left. \left. + 3 \sin \chi \left(\rho \sin \chi d\chi - \cos \chi d\rho \right) \right) \wedge \left(d\xi + \tilde{\sigma}_3 \right) \right].$$

The SUSY preserved by this background is discussed in appendix 2.A.1. We have checked that the equations of motion are solved by this background.

2.3.2   The non-abelian T-dual of the Donos-Gauntlett solution

In this section we will briefly present the result of applying NATD to the Donos-Gauntlett solution [112] that we described in section 2.2.2.

Like above, we will perform the NATD choosing a gauge such that the new coordinates are (x_1, x_2, x_3). We will quote the result in spherical coordinates (the expressions in cylindrical

---

[5] According to the democratic formalism, the higher rank RR forms are related to those of lower rank through the relation $F_p = (-1)^{[\frac{p}{2}]} * F_{10-p}$.

and cartesian coordinates are written in appendix C of [19]). The expressions below are naturally more involved than those in section 2.3.1. This is due to the fact that now there is a non-trivial NS 2-form that enters in the procedure (explicitly, in the string sigma model) which makes things more complicated. As above, we start with some definitions,

$$\mathcal{B}_\pm = \rho \cos \chi \pm \frac{L^2 \lambda}{6\alpha'} \alpha \ , \qquad \mathcal{B} = \mathcal{B}_+ \ , \qquad \Delta = L^4 e^{4U+2V} + 54 \alpha'^2 e^{2U} \rho^2 \sin^2 \chi + 36 \alpha'^2 \mathcal{B}^2 e^{2V} \ .$$

$$(2.3.31)$$

The NSNS sector is given by,

$$e^{-2\widehat{\Phi}} = \frac{L^2}{324 \ \alpha'^3} \Delta,$$

$$\frac{d\hat{s}^2}{L^2} = e^{2A} \left(-dy_0^2 + dy_1^2 \right) + e^{2B} \left(d\alpha^2 + d\beta^2 \right) + dr^2 + \frac{e^{2U}}{6} \left(\sigma_1^2 + \sigma_2^2 \right) +$$

$$+ \frac{\alpha'^2}{\Delta} \left[6 e^{2U+2V} \left(\sin^2 \chi \left(d\rho^2 + \rho^2 \left(d\xi + \sigma_3 \right)^2 \right) + \rho \sin(2\chi) d\rho d\chi + \rho^2 \cos^2 \chi d\chi^2 \right) \right.$$

$$\left. + 9 e^{4U} \left(\cos \chi d\rho - \rho \sin \chi d\chi \right)^2 + \frac{324 \alpha'^2}{L^4} \left(\left(\mathcal{B} \cos \chi + \rho \sin^2 \chi \right) d\rho + \rho \left(\rho \cos \chi - \mathcal{B} \right) \sin \chi d\chi \right)^2 \right],$$

$$(2.3.32)$$

$$\widehat{B}_2 = L^2 \frac{\lambda}{6} \ \alpha \ \sigma_1 \wedge \sigma_2 + \frac{\alpha'^3}{\Delta} \left[36 \ \mathcal{B} \ e^{2V} \left(\sigma_3 \wedge \left(\left(\mathcal{B} \cos \chi + \rho \sin^2 \chi \right) d\rho + \rho \left(\rho \cos \chi - \mathcal{B} \right) \sin \chi d\chi \right) \right. \right.$$

$$\left. + \rho \sin \chi d\xi \wedge \left(\sin \chi d\rho + \rho \cos \chi d\chi \right) \right) + e^{2U} \left(e^{2V+2U} \frac{L^4}{\alpha'^2} \sigma_3 - 54 \rho^2 \sin^2 \chi d\xi \right) \wedge \left(\cos \chi d\rho - \rho \sin \chi d\chi \right) \right].$$

The RR sector reads,

$$\widehat{F}_0 = 0, \qquad \widehat{F}_2 = \frac{L^2}{6\alpha'^{\frac{3}{2}}} \left(\lambda \alpha' d\mathcal{B}_- \wedge d\beta + \frac{2}{9} L^2 \sigma_1 \wedge \sigma_2 \right),$$

$$\widehat{F}_4 = \frac{L^4 \lambda}{36\sqrt{\alpha'}} \left[e^V \left(\frac{2L^2}{\alpha'} d\alpha - 3 e^{-2B-2V} \lambda \left(\cos \chi d\rho - \rho \sin \chi d\chi \right) \right) \wedge \text{Vol}_{AdS_3} \right.$$

$$- \frac{6\alpha'}{L^2} \left(\rho \sin \chi \left(\sin \chi d\rho + \rho \cos \chi d\chi \right) \mathcal{B} d\mathcal{B} \right) \wedge d\beta \wedge \sigma_1 \wedge \sigma_2 \qquad (2.3.33)$$

$$+ \frac{36\alpha'^2}{\Delta} \rho \sin \chi \left(\frac{3\alpha'}{L^2} d\beta \wedge d\mathcal{B}_- - \frac{2}{3\lambda} \sigma_1 \wedge \sigma_2 \right) \wedge \left(2 e^{2V} \mathcal{B} \left(\sin \chi d\rho + \rho \cos \chi d\chi \right) + \right.$$

$$\left. \left. + 3 e^{2U} \rho \sin \chi \left(\rho \sin \chi d\chi - \cos \chi d\rho \right) \right) \wedge \left(d\xi + \sigma_3 \right) \right] \ .$$

Here again, aspects of the SUSY preserved by this background are relegated to appendix 2.A.1. We have checked that the equations of motion are solved by this background.

2.4   T-dualizing back from type IIA to IIB

In this section, we will construct *new* type IIB Supergravity backgrounds with an AdS_3 factor at the IR. The idea is to obtain these new solutions by performing an (abelian) T-duality on the configurations described by eqs. (2.3.29)-(2.3.30) which, in turn, were obtained by performing NATD on the backgrounds of eq. (2.3.26). The full chain of dualities is NATD -T. The new solutions present an AdS_3 fixed point and all RR and NS fields are switched on.

It should be interesting to study if the AdS_3 fixed point of this geometry falls within known classifications [115]. If not, to use them as inspiring ansatz to extend these taxonomic efforts.

In order to perform the T-duality, we will choose a Killing vector that has no fixed points, in such a way that the dual geometry has no singularities. An adapted system of coordinates for that Killing vector is obtained through the change of variables,

$$\alpha = \operatorname{arccosh}\left(\cosh a \cosh b\right) \ , \qquad \beta = \arctan\left(\frac{\sinh b}{\tanh a}\right) \ , \tag{2.4.34}$$

obtaining [6],

$$A_1 = \sinh a \ db \ , \qquad \operatorname{Vol}_{\Sigma_2} = \cosh a \ da \wedge db \ , \qquad ds_{\Sigma_2}^2 = da^2 + \cosh^2 a \ db^2 \ . \tag{2.4.35}$$

The Killing vector that we choose is the one given by translations along the b direction. Its modulus is proportional to the quantity,

$$\Delta_T = 54\alpha'^2 z^2 \rho^2 \sin^2 \chi \sinh^2 a + e^{2B} \cosh^2 a \ \Delta \ , \tag{2.4.36}$$

where Δ is defined in eq.(2.3.28). Since Δ_T is never vanishing the isometry has no fixed points.

To describe these new configurations, we define,

$$A_3 = 3z \sinh a \left(\cos \chi d\rho - \rho \sin \chi d\chi\right) - db \ . \tag{2.4.37}$$

---

[6] In fact using the coordinate transformation eq. (2.4.34) we obtain $A_1 = \sinh a \ db +$ total derivative.

Then, we will have a NSNS sector,

$$e^{-2\widetilde{\Phi}} = \frac{L^4}{324\alpha'^4}\Delta_T \; ,$$

$$\frac{d\widetilde{s}^2}{L^2} = e^{2A}\left(-dy_0^2 + dy_1^2\right) + e^{2B}da^2 + dr^2 + \frac{1}{6}\left(\sigma_1^2 + \sigma_2^2\right)$$

$$+ \frac{\alpha'^2}{\Delta_T}\left[\frac{\Delta}{L^4}db^2 + 6e^{2B}\cosh^2 a\left(\rho^2\sin^2\chi\left(\sigma_3 + d\xi\right)^2 + \left(d\rho\,\sin\chi + \rho\,\cos\chi\,d\chi\right)^2\right)\right.$$

$$+ 9\left(z^2\sinh^2 a + e^{2B}\cosh^2 a\right)\left(\left(d\rho\,\cos\chi - \rho\,\sin\chi\,d\chi\right)^2 + \frac{36\alpha'^2}{L^4}\rho^2 d\rho^2\right)$$

$$\left. - 6z\sinh a\,db\left(\left(\frac{36\alpha'^2}{L^4}\rho^2 + 1\right)\cos\chi\,d\rho - \rho\,\sin\chi\,d\chi\right)\right] \; ,\tag{2.4.38}$$

$$\widetilde{B}_2 = \frac{\alpha'^3}{\Delta_T}\left[e^{2B}\cosh^2 a\left(36\rho\cos\chi\left[\rho\sigma_3 \wedge d\rho + \rho\sin\chi d\xi \wedge\left(\sin\chi d\rho + \rho\cos\chi d\chi\right)\right]\right.\right.$$

$$\left.\left. + \left(\frac{L^4}{\alpha'^2}\sigma_3 - 54\rho^2 d\xi\sin^2\chi\right)\wedge\left(d\rho\cos\chi - \rho\sin\chi d\chi\right)\right) - 18\,z\,\rho^2\,\sinh a\sin^2\chi\left(d\xi \wedge A_3 + db \wedge \sigma_3\right)\right] \; ,$$

and a RR sector that reads,

$$\widetilde{F}_1 = \frac{zL^4}{18\alpha'^2}\cosh a\,da \; ,$$

$$\widetilde{F}_3 = \frac{L^4}{54\alpha'}\left(2A_3 + 3z\rho\cos\chi\cosh a\,da\right)\wedge\sigma_1 \wedge \sigma_2$$

$$+ \frac{zL^4\alpha'\cosh a}{\Delta_T}\rho^2\sin\chi\left(\sigma_3 + d\xi\right)\wedge\left[e^{2B}\cosh^2 a\left(\left(2 + \sin^2\chi\right)d\chi - \sin\chi\cos\chi d\rho\right)\right.$$

$$\left. - z\sinh a\sin\chi A_3\right]\wedge da \; ,$$

$$\widetilde{F}_5 = \frac{L^4}{6}e^{-2B}\left(24e^{4B}\rho\cosh a\,da \wedge d\rho + z\left(d\rho\cos\chi - \rho d\chi\sin\chi\right)\wedge db\right)\wedge \text{Vol}_{AdS_3}\tag{2.4.39}$$

$$+ \frac{L^4\alpha'^2\cosh a}{18\Delta_T}\left[e^{2B}\cosh a\rho\sin\chi d\xi \wedge\left(\left(d\rho\sin\chi + \rho d\chi\cos\chi\right)\wedge\left[24\rho\cos\chi A_3\right.\right.\right.$$

$$\left.\left.\left. - z\left(\frac{L^4}{\alpha'^2} + 54\rho^2\sin^2\chi\right)\cosh a\,da\right] + 18\,\rho\,\sin\chi\left(3z\rho\cos\chi\cosh a\,da - 2d\beta\right)\wedge\left(d\rho\cos\chi - \rho d\chi\sin\chi\right)\right)\right.$$

$$\left. - 18z^2\,\rho^3\sinh a\,\sin^2\chi\,d\xi \wedge\left(3z\sinh a\left(\sin^2\chi d\rho + \rho\sin\chi\cos\chi d\chi\right) + \cos\chi A_3\right)\wedge da\right]\wedge\sigma_1 \wedge \sigma_2 \; .$$

We have checked that the equations of motion are solved by this background, either assuming the BPS equations (2.2.7) or the non-SUSY solution (2.2.17). We have also checked that the Kosmann derivative vanishes without the need to impose further projections. These facts point to the conclusion that this new and smooth solution is also SUSY preserving.

We will now present new backgrounds of eleven-dimensional supergravity.

2.5   Lift to M - theory

Here, we lift the solutions of sections 2.3.1 and 2.3.2 to eleven dimensions, presenting new and smooth backgrounds of M-theory that describe the strong dynamics of a SUSY 2d CFT.

It is well known that given a solution of the type IIA supergravity the metric of the uplifted to eleven dimensions solution, has the following form,

$$ds_{11}^2 = e^{-\frac{2}{3}\widehat{\Phi}}\, ds_{IIA}^2 \; + \; e^{\frac{4}{3}\widehat{\Phi}} \left(dx_{11} + \widehat{C}_1\right)^2 , \tag{2.5.40}$$

where $\widehat{\Phi}$ is the dilaton of the 10-dimensional solution of the Type IIA SUGRA and $\widehat{C}_1$ is the 1-form potential that corresponds to the RR 2-form of the Type IIA background. Also, by x_{11} we denote the 11$^{\text{th}}$ coordinate which corresponds to a $U(1)$ isometry as neither the metric tensor or flux explicitly depend on it.

The 11-dimensional geometry is supported by a 3-form potential C_3^M which gives rise to a 4-form $F_4^M = dC_3^M$. This 3-form potential can be written in terms of the 10-dimensional forms and the differential of the 11$^{\text{th}}$ coordinate as,

$$C_3^M = \widehat{C}_3 + \widehat{B}_2 \wedge dx_{11} . \tag{2.5.41}$$

The 3-form $\widehat{C}_3$ corresponds to the closed part of the 10-dimensional RR form $\widehat{F}_4 = d\widehat{C}_3 - \widehat{H}_3 \wedge \widehat{C}_1$. Here, $\widehat{B}_2$ is the NS 2-form of the 10-dimensional type-IIA theory and $\widehat{H}_3 = d\widehat{B}_2$. Hence we see that in order to describe the 11-dimensional solution we need the following ingredients,

$$ds_{IIA}^2 , \quad \widehat{\Phi} , \quad \widehat{B}_2 , \quad \widehat{C}_1 , \quad \widehat{C}_3 \;\text{ or }\; \widehat{F}_4 . \tag{2.5.42}$$

Let us now present these quantities for the cases of interest.

2.5.1   Uplift of the NATD of the twisted solutions

As we mentioned above, in order to specify the M-theory background we need to read the field content of the 10-dimensional solution. For the case at hand we wrote the metric ds_{IIA}^2, the dilaton $\widehat{\Phi}$ and the NS 2-form $\widehat{B}_2$ in eq. (2.3.29). Moreover, from the expression of the RR 2-form in eq. (2.3.30) we can immediately extract the 1-form potential $\widehat{C}_1$,

$$\widehat{C}_1 = \frac{L^4}{54\, a'^{\frac{3}{2}}} \left(3\, z\, A_1 - 2\, \sigma_3\right) . \tag{2.5.43}$$

The 3-form potential–$\widehat{C}_3$–can be obtained from the RR 4-form of eq. (2.3.30). After some algebra one finds,

$$
\widehat{C}_3 = \frac{L^4 \ e^{-2B}}{6 \ a'^{\frac{1}{2}}} \ z \ \rho \ \cos\chi \ \mathrm{Vol}_{AdS_3} + \frac{L^4 \ z \ \left(L^4 + 36a'^2\rho^2\right) \ \cos\chi}{6 \ \alpha'^{\frac{1}{2}} \ \Delta} A_1 \wedge \sigma_3 \wedge d\rho
$$
$$
+ \frac{L^4 \ \alpha'^{\frac{3}{2}} \ \rho^2 \sin\chi}{\Delta} \left(z \ A_1 - \frac{2}{3}\sigma_3 \right) \wedge d\xi \wedge \left(\rho \left(2 + \sin^2\chi\right) d\chi - \sin\chi \ \cos\chi \ d\rho \right) \quad (2.5.44)
$$
$$
+ \frac{L^4 \ z \ \rho}{18 \ \alpha'^{\frac{1}{2}} \ \Delta} \left(\Delta \ \cos\chi \ \left(\sigma_3 \wedge \mathrm{Vol}_{\Sigma_2} - 2A_1 \wedge d\sigma_3\right) - 3L^4 \sin\chi \ A_1 \wedge \sigma_3 \wedge d\chi \right) .
$$

We close this section by observing that, if the coordinate ρ takes values in a finite interval, then the radius of the M-theory circle, $e^{\frac{4}{3}\widehat{\Phi}}$ never blows up, because the function Δ that appears in the expression of the dilaton is positive definite. We have checked that the equations of motion of the 11-dimensional Supergravity are solved by this background.

2.5.2   Uplift of the NATD of the Donos-Gauntlett solution

Here, the NSNS fields of the 10-dimensional theory have been written in detail in eq. (2.3.32). In order to complete the description of the M-theory background we need also to consider the potentials $\widehat{C}_1$ and $\widehat{C}_3$ that are encoded in the RR fields of eq. (2.3.33). Hence from the RR 2-form potential we can easily read $\widehat{C}_1$,

$$
\widehat{C}_1 = \frac{L^2\lambda\mathcal{B}_-}{6\alpha'^{\frac{1}{2}}} \, d\beta - \frac{L^4}{27\alpha'^{\frac{3}{2}}} \, \sigma_3 \ , \qquad (2.5.45)
$$

where the function $\mathcal{B}_-$ has been defined in eq. (2.3.31). Also, from the RR 4-form we can obtain the potential $\widehat{C}_3$ which in this case is,

$$
\widehat{C}_3 = \frac{e^{-2B-V}L^4\lambda}{36\alpha'^{\frac{3}{2}}} \left(2e^{2B+2V} L^2\alpha - 3\lambda\alpha'\rho\cos\chi \right)\mathrm{Vol}_{AdS_3}
$$
$$
- \frac{\alpha'^{\frac{1}{2}}L^2\rho\sin\chi}{18\Delta} \left(18\alpha'\lambda\mathcal{B}_-\left(\sigma_3 + d\xi\right) \wedge d\beta + 4L^2\sigma_3 \wedge d\xi \right) \wedge \Sigma_1 \qquad (2.5.46)
$$
$$
+ \frac{L^2\lambda\alpha'^{\frac{1}{2}}}{12} \left(\mathcal{B}_-^2 + \mathcal{B}^2 + \rho^2\sin^2\chi \right)d\beta \wedge d\sigma_3 \ .
$$

Here for brevity we have defined the 1-form Σ_1 in the following way:

$$
\Sigma_1 = 6\alpha'e^{2V}\mathcal{B} \left(\sin\chi d\rho + \rho\cos\chi d\chi \right) - 9\alpha'e^{2U}\rho\sin\chi \left(\cos\chi d\rho - \rho\sin\chi d\chi \right) . \qquad (2.5.47)
$$

Finally, we observe that the radius of the M-theory circle is finite, for reasons similar to those discussed in the previous example. We have checked that the equations of motion of the 11-dimensional Supergravity are solved by this background.

This completes our presentation of this set of new and exact solutions. A summary of all the solutions can be found in Table 2.1. The expressions for these backgrounds in cartesian and cylindrical coordinates are written in appendix C of [19] .

We will now move on to the second part of this chapter. We will study aspects of the field theories that our new and smooth backgrounds are defining.

2.6   General comments on the Quantum Field Theory

Let us start our study of the correspondence between our new metrics with their respective field theory dual. We will state some general points that these field theories will fulfill.

In the case of the backgrounds corresponding to the compactifications described in section 2.2.1, our field theories are obtained by a twisted KK-compactification on a two dimensional manifold—that can be H_2, S^2 or T^2. The original field theory is, as we mentioned, the Klebanov-Witten quiver, that controls the high energy dynamics of our system. The bosonic part of the global symmetries for this QFT in the UV are

$$SO(1,3) \times SU(2) \times SU(2) \times U(1)_R \times U(1)_B, \qquad (2.6.48)$$

where, as we know the $SO(1,3)$ is enhanced to $SO(2,4)$. The theory contains two vector multiplets $\mathcal{W}^i = (\lambda^i, A^i_\mu)$, for $i = 1, 2$, together with four chiral multiplets $\mathcal{A}_\alpha = (A_\alpha, \psi_\alpha)$ for $\alpha = 1, 2$ and $\mathcal{B}_{\dot\alpha} = (B_{\dot\alpha}, \chi_{\dot\alpha})$ with $\dot\alpha = 1, 2$.

These fields transform as vector, spinors and scalars under $SO(1,3)$—that is $A_\alpha, B_{\dot\alpha}$ are singlets, the fermions transform in the $(\frac{1}{2}, \mathbf{0}) \oplus (\mathbf{0}, \frac{1}{2})$ and the vectors in the $(\frac{1}{2}, \frac{1}{2})$. The transformation under the 'flavor' quantum numbers $SU(2) \times SU(2) \times U(1)_R \times U(1)_B$ is,

$$
\begin{aligned}
A_\alpha &= (2, 1, \tfrac{1}{2}, 1), & B_{\dot\alpha} &= (1, 2, \tfrac{1}{2}, -1), \\
\psi_\alpha &= (2, 1, -\tfrac{1}{2}, 1), & \chi_{\dot\alpha} &= (1, 2, -\tfrac{1}{2}, -1), \\
\lambda^i &= (1, 1, 1, 0), & A^i_\mu &= (1, 1, 0, 0).
\end{aligned}
\qquad (2.6.49)
$$

The backgrounds in section 2.2.1, are describing the strong coupling regime of the field theory above, in the case in which we compactify the D3-branes on Σ_2 twisting the theory. This means, mixing the R-symmetry $U(1)_R$ with the $SO(2)$ isometry of Σ_2. This twisting is reflected in the metric fibration between the η-direction (the Reeb vector) and the Σ_2. The fibration is implemented by a vector field A_1 in eq. (2.2.1). The twisting mixes the R-symmetry of the QFT, represented by A_1 in the dual description, with (part of) the Lorentz group. In purely field theoretical terms, we are modifying the covariant derivative of different fields that under the combined action of the spin connection and the R-symmetry (on the curved part of the space) will read $D_\mu \sim \partial_\mu + \omega_\mu + A_\mu$.

In performing this twisting, the fields decompose under $SO(1,3) \rightarrow SO(1,1) \times SO(2)$. The decomposition is straightforward for the bosonic fields. For the fermions, we have that $(\frac{1}{2}, \mathbf{0})$ decomposes as $(+, \pm)$ and similarly for the $(\mathbf{0}, \frac{1}{2})$ spinors.

The twisting itself is the 'mixing' between the $\pm$ charges of the spinor and its R-symmetry charge. There is an analog operation for the vector and scalar fields. Some fields are scalars

under the diagonal group in $U(1)_R \times SO(2)_{\Sigma_2}$. Some are spinors and some are vectors. Only the scalars under the diagonal group are massless. These determine the SUSY content of the QFT. This particular example amounts to preserving two supercharges. There are two massless vector multiplets and two massless matter multiplets. The rest of the fields get a mass whose set by the inverse size of the compact manifold. In other words, the field theory at low energies is a two dimensional CFT (as indicated by the AdS_3 factor), preserving $(0,2)$ SUSY and obtained by a twisted compactification of the Klebanov-Witten CFT. The QFT is deformed in the UV by a relevant operator of dimension two, as we can read from eq. (2.2.9).

An alternative way to think about this QFT is as the one describing the low energy excitations of a stack of N_c D3-branes wrapping a calibrated space Σ_2 inside a Calabi-Yau 4-fold.

The situation with the metrics in section 2.2.2 is more subtle. In that case there is also a flow from the Klebanov-Witten quiver to a two-dimensional CFT preserving $(0,2)$ SUSY. The difference is that this second QFT is not apparently obtained via a twisting procedure. As emphasized by the authors of [112], the partial breaking of SUSY is due (from a five-dimensional supergravity perspective) to 'axion' fields depending on the torus directions. These axion fields are proportional to a deformation parameter—that we called λ in eq. (2.2.22). The deformation in the UV QFT is driven by an operator of dimension four that was identified to be $Tr(W_1^2 - W_2^2)$ and a dimension six operator that acquires a VEV, as discussed in [112].

To understand the dual field theory to the IIA backgrounds obtained after non-abelian T-duality and presented in section 2.3.1 involves more intricacy. Indeed, it is at present unclear what is the analog field theoretical operation of non-abelian T-duality. There are, nevertheless, important hints. Indeed, the foundational paper of Sfetsos and Thompson [15], that sparked the interest of the uses of non-abelian T-duality in quantum field theory duals, showed that if one starts with a background of the form $AdS_5 \times S^5/Z_2$, a particular solution of the Gaiotto-Maldacena system (after lifting to M-theory) is generated [102]. This is hardly surprising, as the backgrounds of eleven-dimensional supergravity with an AdS_5 factor and preserving $\mathcal{N} = 2$ SUSY in four dimensions, have been classified. What is interesting is that the solution generated by Sfetsos and Thompson appears as a zoom-in on the particular class of solutions in [50]. This was extended in [42] that computed the action of non-abelian T-duality on the end-point of the flow from the $\mathcal{N} = 2$ conformal quiver with adjoints to the Klebanov-Witten CFT. Again, not surprisingly, the backgrounds obtained correspond to the $\mathcal{N} = 1$ version of the Gaiotto T_N theories— these were called *Sicilian* field theories by Benini, Tachikawa and Wecht in [116], see Fig. 2.1. It is noticeable, that while the Sicilian theories can be obtained by a twisted compactification of M5-branes on H_2, S^2, T^2, the case obtained using non-abelian T-duality corresponds only to M5-branes compactified on S^2 and preserving minimal SUSY in four dimensions. What we propose in this paper is that the twisted compactification on Σ_2 of a Sicilian gauge theory can be studied by using the backgrounds we discussed in section 2.3.1 and their M-theory counterparts. We will elaborate more about the 2-d CFTs and their flows in the coming sections.

In the following, we will calculate different observables of these QFT's by using the backgrounds as a 'definition' of the 2d SCFT. The backgrounds are smooth and thus the ob-

servables have trustable results. Hence, we are defining a QFT by its observables, calculated in a consistent way by the dual solutions. The hope is that these calculations together with other efforts can help map the space of these new families of CFTs. To the study of these observables we turn now.

2.7 Quantized charges

In this section, we will study the quantized charges on the string side. This analysis appears in the field theory part of the chapter because these charges will, as in the canonical case of $AdS_5 \times S^5$, translate into the ranks of the gauge theory local symmetry groups.

The NATD produced local solutions to the 10-dim SUGRA equations of motion. Nevertheless, it is still not known how to obtain the global properties of these new geometries. Some quantities associated to a particular solution, like the Page charges below, are only well-defined when the global properties of the background are known. Since we have only a local description of our solution, we will propose very reasonable global results for the Page charges, mostly based on physical intuition.

Let us start by analyzing a quantity that is proposed to be periodic in the string theory. We follow the ideas introduced in [117] and further elaborated in [106]. To begin with, we focus on the NATD version of the twisted solutions; described in section 2.3.1. Let us define the quantity,

$$b_0 = \frac{1}{4\pi^2 \alpha'} \int_{\Pi_2} B_2 \quad \in [0,1] \,, \tag{2.7.50}$$

where the cycle Π_2 is defined as,

$$\Pi_2 = S^2 \quad \left\{ \chi, \xi, \alpha = 0, \rho = \text{const}, d\beta = -\frac{1}{3z} d\xi \right\} . \tag{2.7.51}$$

As the topology of the NATD theory is not known, we propose that this cycle is present in the geometry. This cycle will have a globally defined volume form, which in a local description can be written as $\text{Vol}_{\Pi_2} = \sin \chi \, d\xi \wedge d\chi$. We then find,

$$b_0 = \frac{1}{4\pi^2 \alpha'} \int_{\Pi_2} \alpha' \rho \sin \chi d\xi \wedge d\chi = \frac{\rho}{\pi} \quad \in [0,1]. \tag{2.7.52}$$

Again, we emphasize that this is a *proposal* made in [117] and used in [106]. Moving further than π along the variable ρ can be 'compensated' by performing a large gauge transformation on the B_2-field,

$$B_2 \to B_2' = B_2 - \alpha' n\pi \sin \chi d\xi \wedge d\chi. \tag{2.7.53}$$

We will make extensive use of this below.

Let us now focus on the conserved magnetic charges defined for our backgrounds. We will start the analysis for the case of the solutions in section 2.2.1.

2.7.1 Page charges for the twisted solutions

We will perform this study for the solutions before and after the NATD, and we will obtain how the Page charges transform under the NATD process. Page charges (in contrast to Maxwell charges) have proven fundamental in understanding aspects of the dynamics of field theories—see for example [118].

In the following, we use as definition of Page charge,

$$N_{Dp}\big|_{\Pi_{8-p}} = \frac{1}{2\kappa_{10}^2 T_{Dp}} \int_{\Pi_{8-p}} \left(\sum_i F_i \right) \wedge e^{-B_2}, \qquad N_{NS5}\big|_{\Pi_3} = \frac{1}{2\kappa_{10}^2 T_{NS5}} \int_{\Pi_3} H_3 \ , \tag{2.7.54}$$

$$2\kappa_{10}^2 = (2\pi)^7 \alpha'^4, \qquad T_{Dp} = \frac{1}{(2\pi)^p \alpha'^{\frac{p+1}{2}}}, \qquad T_{NS5} = T_{D5} \ .$$

In particular, for D3-branes we have,

$$N_{D3}\big|_{\Pi_5} = \frac{1}{2\kappa_{10}^2 T_{D3}} \int_{\Pi_5} \left(F_5 - B_2 \wedge F_3 + \frac{1}{2} B_2 \wedge B_2 \wedge F_1 \right).$$

The topology of the internal space is $\Sigma_2 \times S^2 \times S^3$. First, we consider the cycle $S^2 \times S^3$. Second, we can consider some cycles given by the product of Σ_2 with a generator of $H_3\left(S^2 \times S^3, \mathbb{Z}\right)$. Notice that the $S^2 \times S^3$ is realized as a $U(1)$ fibration over an $S_1^2 \times S_2^2$ base. A smooth 3-manifold, S_1^3, that can be used to generate $H_3\left(S^2 \times S^3, \mathbb{Z}\right)$ is provided by the circle bundle restricted to the S_1^2 factor. We can also choose S_2^3, defined to be the circle bundle restricted to the S_2^2 factor of the base space. In summary, the relevant cycles are,

$$\begin{aligned} \Pi_5^{(1)} &= \ S^2 \times S^3 \left\{ \theta_1, \phi_1, \theta_2, \phi_2, \psi \right\}, \qquad \Pi_5^{(2)} = \Sigma_2 \times S_1^3 \left\{ \alpha, \beta, \theta_1, \phi_1, \psi \right\}, \\ \Pi_5^{(3)} &= \ \Sigma_2 \times S_2^3 \left\{ \alpha, \beta, \theta_2, \phi_2, \psi \right\}. \end{aligned} \tag{2.7.55}$$

The background fields B_2, F_1 and F_3 are vanishing, and only F_5 contributes. The specific components of F_5 in eq. (2.3.26) that have non vanishing pullback on these cycles are,

$$F_5 = \frac{L^4}{9} \text{Vol}_1 \wedge \text{Vol}_2 \wedge \eta + \frac{L^4}{6} z \text{Vol}_{\Sigma_2} \wedge \left(\text{Vol}_1 + \text{Vol}_2\right) \wedge \eta + ... \tag{2.7.56}$$

We explicitly see that it is a globally defined form, as all the involved quantities (η, Vol_{Σ_2}, Vol_1, Vol_2) are well defined globally. The associated Page charges of D3-branes for the background around eq. (2.3.26) are,

$$N_{D3}\big|_{\Pi_5^{(1)}} = \frac{4L^4}{27\alpha'^2\pi} \ , \qquad \widehat{N}_{D3}\big|_{\Pi_5^{(2)}} = \widetilde{N}_{D3}\big|_{\Pi_5^{(3)}} = \frac{L^4}{\alpha'^2} \frac{z \ vol\left(\Sigma_2\right)}{18\pi^2} \ , \tag{2.7.57}$$

where $vol\left(\Sigma_2\right)$ is the total volume of the two-manifold Σ_2.[7] As usual, the first relation quantizes the size of the space,

$$L^4 = \frac{27\pi}{4} \alpha'^2 N_{D3}. \tag{2.7.58}$$

---

[7]Notice that we use Vol for volume elements (differential forms) and *vol* for the actual volumes of the manifolds (real numbers).

We have then defined three D3-charges. The one associated with N_{D3} is the usual one appearing also in the $AdS_5 \times S^5$ case. The other two can be thought as charges 'induced' by the wrapping of the D3-branes on the Riemann surface. The reader may wonder whether these charges are present in the backgrounds found after NATD. We turn to this now.

The particular expressions for Page charges in type IIA are,

$$N_{D6}\big|_{\Pi_2} = \frac{1}{2\kappa_{10}^2 T_{D6}} \int_{\Pi_2} \left(\widehat{F}_2 - \widehat{F}_0\, \widehat{B}_2 \right),$$

$$N_{D4}\big|_{\Pi_4} = \frac{1}{2\kappa_{10}^2 T_{D4}} \int_{\Pi_4} \left(\widehat{F}_4 - \widehat{B}_2 \wedge \widehat{F}_2 + \frac{1}{2}\widehat{F}_0\, \widehat{B}_2 \wedge \widehat{B}_2 \right), \qquad (2.7.59)$$

$$N_{D2}\big|_{\Pi_6} = \frac{1}{2\kappa_{10}^2 T_{D2}} \int_{\Pi_6} \left(\widehat{F}_6 - \widehat{B}_2 \wedge \widehat{F}_4 + \frac{1}{2}\widehat{B}_2 \wedge \widehat{B}_2 \wedge \widehat{F}_2 - \frac{1}{6}\widehat{F}_0\, \widehat{B}_2 \wedge \widehat{B}_2 \wedge \widehat{B}_2 \right).$$

We label the radius of the space of the geometry in eq. (2.3.29) by $\widehat{L}$, to distinguish it from L, the quantized radius before the NATD.

In order to properly define the cycles to be considered, we should know the topology of this NATD solution. However, we have obtained only a local expression for this solution, and we do not know the global properties. As we explained above, we will present a proposal to define the Page charges that would explain the transmutation of branes through the NATD. We propose the relevant cycles to be, [8]

$$\Pi_2^{(1)} \; \left\{\theta_1, \phi_1\right\}, \qquad \Pi_6^{(2)} = \left\{\alpha, \beta, \theta_1, \phi_1, \rho, \xi, \chi = \frac{\pi}{2}\right\}, \qquad \Pi_2^{(3)} \; \left\{\alpha, \beta\right\}. \qquad (2.7.60)$$

The associated charges are,

$$N_{D6}\big|_{\Pi_2^{(1)}} = \frac{2\widehat{L}^4}{27\alpha'^2}, \qquad \widetilde{N}_{D6}\big|_{\Pi_2^{(3)}} = \frac{\widehat{L}^4}{\alpha'^2}\frac{z\;vol\,(\Sigma_2)}{36\pi},$$

$$\widehat{N}_{D2}\big|_{\Pi_6^{(2)}} = \frac{\widehat{L}^4}{\alpha'^2}\frac{z\;vol\,(\Sigma_2)\,vol\,(\rho,\xi)}{144\pi^4} = \frac{n^2}{4}\frac{\widehat{L}^4}{\alpha'^2}\frac{z\;vol\,(\Sigma_2)}{36\pi}. \qquad (2.7.61)$$

In the last expression, we performed the integral over the ρ-coordinate in the interval $[0, n\pi]$. These three charges are in correspondence with the ones before the NATD in eq. (2.7.57). Indeed, we can compute the quotients,

$$\frac{\widehat{N}_{D3}}{N_{D3}} = \frac{\widetilde{N}_{D3}}{N_{D3}} = \frac{3}{8\pi}z\;vol\,(\Sigma_2), \qquad \frac{4\widehat{N}_{D2}}{n^2 N_{D6}} = \frac{\widetilde{N}_{D6}}{N_{D6}} = \frac{3}{8\pi}z\;vol\,(\Sigma_2). \qquad (2.7.62)$$

These quotients indicate a nice correspondence between charges before and after the duality.

---

[8]Intuitively, we can think that the branes transform under NATD as 3 consecutive T-dualities. For example, in the first 5-cycle of eq. (2.7.55), the NATD is performed along 3 of the coordinates, (θ_2, ϕ_2, ψ), in such a way that we end up with a 2-cycle, the first cycle in eq.(2.7.60), associated with D6-branes. In the second 5-cycle of eq.(2.7.55) the NATD only affects the ψ-direction, so it disappears, and two more directions are added in order to complete the 3 T-dualities, ending up with a 6-cycle in eq.(2.7.60), associated with D2-branes.

Using the first relation in eq. (2.7.61) we quantize the size $\widehat{L}$ of the space after NATD to be $\widehat{L}^4 = \frac{27}{2}\alpha'^2 N_{D6}$.

A small puzzle is presented by the possible existence of charge for D4-branes, as there would be no quantized number before the NATD to make them correspond to. To solve this puzzle, we propose that there should be a globally defined closed non-exact form that allows us to perform a large gauge transformation for the $\widehat{B}_2$, in such a way that all the D4 Page charges vanish. In local coordinates, we have a gauge transformation,

$$\widehat{B}_2 \to \widehat{B}_2' = \widehat{B}_2 + \alpha' d\left[\rho \cos \chi \ \tilde{\sigma}_3\right], \tag{2.7.63}$$

written in such a way that the integrand has at least one leg along a non-compact coordinate,

$$\widehat{F}_4 - \widehat{B}_2' \wedge \widehat{F}_2 = \frac{z\widehat{L}^4}{6\sqrt{\alpha'}}e^{-2B}\left(\cos \chi d\rho - \rho \sin \chi d\chi\right) \wedge \mathrm{Vol}_{AdS_3}. \tag{2.7.64}$$

Hence, any Page charge for D4-branes is vanishing. To be precise, the D2 charge $\widehat{N}_{D2}$ must be computed after choosing this gauge, as it depends on $\widehat{B}_2$, but it turns out to be the same as calculated in eq. (2.7.61).

The motion in the ρ-coordinate, as we discussed above, can be related to large gauge transformations of the $\widehat{B}_2$-field. The large transformation that 'compensates' for motions in ρ, namely $\widehat{B}_2 \to \widehat{B}_2' = \widehat{B}_2 - \alpha' n\pi \sin \chi d\xi \wedge d\chi$, has the effect of changing the Page charges associated with D4-branes, that were initially vanishing. Indeed, if we calculate for the following four cycles,

$$\Pi_4^{(1)} \ \left\{\theta_1, \phi_1, \chi, \xi\right\}, \qquad \Pi_4^{(2)} \ \left\{\alpha, \beta, \chi, \xi\right\}, \tag{2.7.65}$$

the Page charge of D4-branes varies according to,

$$\Delta N_{D4}\big|_{\Pi_4^{(1)}} = \frac{1}{2\kappa_{10}^2 T_{D4}} \int_{\Pi_4^{(1)}} \left(-\Delta \widehat{B}_2 \wedge \widehat{F}_2\right) = -n\frac{L'^4}{\alpha'^2}\frac{2}{27} = -nN_{D6},$$

$$\Delta N_{D4}\big|_{\Pi_4^{(2)}} = \frac{1}{2\kappa_{10}^2 T_{D4}} \int_{\Pi_4^{(2)}} \left(-\Delta \widehat{B}_2 \wedge \widehat{F}_2\right) = -n\frac{L'^4}{\alpha'^2}\frac{z}{36\pi}vol\left(\Sigma_2\right) = -n\widetilde{N}_{D6}. \tag{2.7.66}$$

We can interpret these findings in the following way. Our QFT (after the NATD) can be thought as living on the world-volume of a superposition of D2- and D6-branes. Motions in the ρ-coordinate induce charge of D4-branes, which can be interpreted as new gauge groups appearing. This suggest that we are working with a linear quiver, with many gauge groups. Moving $n\pi$-units in ρ generates or 'un-higgses' new gauge groups of rank nN_{D6} and $n\widetilde{N}_{D6}$. Computing volumes or other observables that involve integration on the ρ-coordinate amounts to working with a QFT with different gauge group, depending on the range in ρ we decide to integrate over. Notice that ρ is not a holographic coordinate. Motions in ρ are not changing the energy in the dual QFT. For the AdS-fixed points the theory is conformal and movements in ρ do not change that.

In the paper [106] , the motion in the ρ-coordinate was argued to be related to a form of 'duality' (a Seiberg-type of duality was argued to take place, in analogy with the mechanism

of the Klebanov-Strassler duality cascade, but in a CFT context). That can not be the whole story as other observables, like for example the number of degrees of freedom in the QFT, change according to the range of the ρ-integration. Hence the motion in ρ can not be just a duality. We are proposing here that moving in the ρ-coordinate amounts to changing the quiver, adding gauge groups, represented by the increasing D4 charge.

We will now present the same analysis we have performed above, but for the case of the background in section 2.2.2.

2.7.2   Page charges for the Donos-Gauntlett solution

Part of the analysis that follows was carefully done in the original work of [112] and here we will extend the study for the solution after the NATD that we presented in section 2.3.2. We will give an outline of the results as the general structure is similar to the one displayed by the twisted solutions of the previous section.

We focus on the original Donos-Gauntlett background first. We denote by d_α, d_β the two radii of the torus (the cycles of the torus are then of size $2\pi d_\alpha$ and $2\pi d_\beta$ respectively) and consider five different cycles in the geometry,

$$
\begin{aligned}
&\Pi_5^{(1)} = S^2 \times S^3 \ \left\{\theta_1, \phi_1, \theta_2, \phi_2, \psi\right\}, \quad \Pi_5^{(2)} = T^2 \times S_1^3 \ \left\{\alpha, \beta, \theta_1, \phi_1, \psi\right\}, \\
&\Pi_5^{(3)} = T^2 \times S_2^3 \ \left\{\alpha, \beta, \theta_2, \phi_2, \psi\right\}, \\
&\Pi_3^{(4)} = S_1^1 \times s(S) \ \left\{\alpha, \theta_1 = \theta_2, \phi_1 = -\phi_2, \psi = \text{const}\right\}, \\
&\Pi_3^{(5)} = S_2^1 \times s(S) \ \left\{\beta, \theta_1 = \theta_2, \phi_1 = -\phi_2, \psi = \text{const}\right\}.
\end{aligned}
\tag{2.7.67}
$$

The Page charges associated with D3-, D5- and NS5-branes are,

$$
\begin{aligned}
&N_{D3}\big|_{\Pi_5^{(1)}} = \frac{4L^4}{27\alpha'^2 \pi} \,, \qquad \widehat{N}_{D3}\big|_{\Pi_5^{(2)}} = -\widetilde{N}_{D3}\big|_{\Pi_5^{(3)}} = 2 \, \frac{L^4}{\alpha'^2} \frac{\lambda^2 \, d_\alpha d_\beta}{9} \,, \\
&N_{NS5}\big|_{\Pi_3^{(4)}} = -2 \, \frac{L^2 \lambda \, d_\alpha}{3\alpha'} \,, \qquad N'_{D5}\big|_{\Pi_3^{(5)}} = 2 \, \frac{L^2 \lambda \, d_\beta}{3\alpha'} \,.
\end{aligned}
\tag{2.7.68}
$$

After the NATD, we focus on the background around eqs. (2.3.32) (2.3.33). We consider the following cycles in the geometry,

$$
\begin{aligned}
&\Pi_2^{(1)} \ \left\{\theta_1, \phi_1\right\}, \quad \Pi_6^{(2)} \ \left\{\alpha, \beta, \theta_1, \phi_1, \rho, \xi, \chi = \frac{\pi}{2}\right\}, \quad \Pi_2^{(3)} \ \left\{\alpha, \beta\right\}, \\
&\Pi_6^{(4)} \ \left\{\beta, \theta_1, \phi_1, \rho, \chi, \xi\right\}, \quad \Pi_2^{(5)} \ \left\{\beta, \chi, \rho = \rho_0\right\}.
\end{aligned}
\tag{2.7.69}
$$

The correspondent Page charges defined on them (the ρ-coordinate is taken in the $[0, n\pi]$

interval),

$$N_{D6}\big|_{\Pi_2^{(1)}} = \frac{2\widehat{L}^4}{27\alpha'^2} \ , \qquad \widetilde{N}_{D6}\big|_{\Pi_2^{(3)}} = -\frac{\widehat{L}^4}{\alpha'^2}\frac{\lambda^2\pi}{18}d_\alpha d_\beta \ , \qquad N'_{D6}\big|_{\Pi_2^{(5)}} = \frac{L'^2}{\alpha'}\frac{\lambda}{3}\rho_0 \ d_\beta \ ,$$

$$\widehat{N}_{D2}\big|_{\Pi_6^{(2)}} = -\frac{\widehat{L}^4}{\alpha'^2}\frac{\lambda^2 \ vol\,(T^2)\,vol\,(\rho,\xi)}{288\pi^4} = -\frac{\widehat{L}^4}{\alpha'^2}\lambda^2\frac{n^2\pi}{72}d_\alpha d_\beta, \tag{2.7.70}$$

$$N_{D2}\big|_{\Pi_6^{(4)}} = \frac{\widehat{L}^2}{\alpha'}\frac{\lambda}{24\pi^3}d_\beta \ vol\,(\rho,\chi,\xi) = \frac{\widehat{L}^2}{\alpha'}\lambda\frac{n^3\pi}{18}d_\beta.$$

From the first relation we obtain, $\widehat{L}^4 = \frac{27}{2}\alpha'^2 N_{D6}$. Like in the case of the twisted solutions, we can choose a gauge for the $\widehat{B}_2$ field

$$\widehat{B}_2 \to \widehat{B}'_2 = \widehat{B}_2 + \delta\widehat{B}_2 \ ,$$

$$\delta\widehat{B}_2 = \frac{9\alpha'^2\lambda}{2L^2} \ d\beta \wedge \left(\rho\sin\chi \ d(\rho\sin\chi) + \mathcal{B} \ d\mathcal{B}\right) + L^2\frac{\lambda}{6}\big(d\alpha \wedge \sigma_3 - \alpha \ \sigma_1 \wedge \sigma_2\big), \tag{2.7.71}$$

such that the Page charge of D4-branes, when computed on every possible compact 4-cycle, is vanishing. Indeed, after the gauge transformation, we have

$$\widehat{F}_4 - \widehat{B}'_2 \wedge \widehat{F}_2 = \frac{L^4\lambda}{36\sqrt{\alpha'}}e^V\left(\frac{2L^2}{\alpha'}d\alpha - 3e^{-2B-2V}\lambda \ d(\rho\cos\chi)\right) \wedge \mathrm{Vol}_{AdS_3}. \tag{2.7.72}$$

Any integral over compact manifolds is vanishing. Like in the case of the twisted solutions, $\widehat{N}_{D2}$ and N_{D2} should be recalculated after choosing this gauge; but their value turns out to be unchanged.

We can apply the same string theory considerations on the quantity b_0 that now is defined as an integral over the cycle,

$$\Pi_2 = S^2 \ , \qquad \{\chi,\xi,\alpha = \mathrm{const}, \rho = \mathrm{const}\}. \tag{2.7.73}$$

We then calculate,

$$b_0 = \frac{1}{4\pi^2\alpha'}\int_{\Pi_2}\alpha'\rho\sin\chi d\xi \wedge d\chi = \frac{\rho}{\pi} \ \in \ [0,1]. \tag{2.7.74}$$

If we move further than π along the variable ρ, we can compensate this by performing the large gauge transformation $\widehat{B}_2 \to \widehat{B}'_2 = \widehat{B}_2 - \alpha'n\pi\sin\chi d\xi \wedge d\chi$. We now consider the correspondent variation of Page charges for D4-branes, that can be calculated using the following cycles,

$$\Pi_4^{(1)} \ \{\theta_1,\phi_1,\chi,\xi\} \ , \qquad \Pi_4^{(2)} \ \{\alpha,\beta,\chi,\xi\}, \tag{2.7.75}$$

to be,

$$\Delta Q_{D4}^P\big|_{\Pi_4^{(1)}} = \frac{1}{2\kappa_{10}^2 T_{D4}}\int_{\Pi_4^{(1)}}\left(-\Delta\widehat{B}_2 \wedge \widehat{F}_2\right) = -n\frac{L^4}{\alpha'^2}\frac{2}{27} = -nN_{D6} \ ,$$

$$\Delta Q_{D4}^P\big|_{\Pi_4^{(2)}} = \frac{1}{2\kappa_{10}^2 T_{D4}}\int_{\Pi_4^{(2)}}\left(-\Delta\widehat{B}_2 \wedge \widehat{F}_2\right) = -n\frac{L^4}{\alpha'^2}\frac{\pi\lambda^2}{18}d_\alpha d_\beta = n\widetilde{N}_{D6} \ . \tag{2.7.76}$$

The variation of the Page charges of D2-branes vanishes under this large gauge transformation. For the Donos-Gauntlett solution we observe a structure very similar to the one discussed for the twisted solutions. Again, here we would propose that the NATD background 'un-higgses' gauge groups of rank nN_{D6} as we move in units of $n\pi$ in the ρ-coordinate.

We move now to the study of another important observable of our dual 2-d and 4-d CFTs.

2.8   Central charges and c-theorem

In this section, we will study the central charge, an important observable of the different strongly coupled QFTs that our backgrounds in sections 2.2 to 2.5 are defining.

Let us start with a brief summary of the ideas behind this observable. The RG-flow can be understood as the motion of the different couplings of the QFT λ_i in terms of a parameter $t = -\ln\mu$, such that for a given operator $\widehat{O}$,

$$\frac{d\widehat{O}}{dt} = -\beta_i(\lambda)\frac{\partial\widehat{O}}{\partial\lambda_i}. \qquad (2.8.77)$$

Hence, the beta functions $\beta_i(\lambda)$ are the 'velocities' of the motion towards the IR. It is interesting to define a 'c-function' $c(t)$ with the property that it decreases when flowing to low energies,

$$\frac{dc(t)}{dt} \leq 0. \qquad (2.8.78)$$

Such that at stationary points $\frac{dc(t)}{dt} = 0$ implies that $\beta_i(\lambda) = 0$ and vice versa. The intuition behind this quantity is that massless degrees of freedom are lifted by relevant deformations, the flow to low energies then coarse-grains away these lifted modes. This intuition is realized in different situation: the two dimensional case, with Zamolodchikov's definition of $c(g)$ [119] or Cardy's conjecture for the 'a-theorem' [120], proven by Komargodski and Schwimmer in [121]. There are different versions of the c-theorem, varying in 'strength' and generality. See the paper [122] for a summary.

As we discussed, the c-function is properly defined only at the conformal points of a QFT. Hence, we can define it properly in all of our backgrounds only at the AdS_5 and AdS_3 fixed points. In those cases the central charge is basically proportional to the volume of the 'internal manifold' M_d (the complement-space of AdS_5 or AdS_3). Indeed, there exists a well-established formalism to calculate central charges that uses the relation between this quantity and the Weyl anomaly $\mathcal{A}$ in the QFT when placed on a generic curved space. This was first discovered in [123] (before the Maldacena conjecture was formulated!) and a complete understanding was developed in [124]. Indeed, for conformal field theories in two and four dimensions, associated with AdS_3 and AdS_5 geometries respectively, we have [9]

$$\text{2 dimensions:} \quad \mathcal{A} = -\frac{L\bar{R}}{16\pi G_N^{(3)}} = -\frac{c}{24\pi}\bar{R}, \qquad c = \frac{3}{2}\frac{L}{G_N^{(3)}} \ , \qquad (2.8.79)$$

---

[9]The central charges a and c are equal at the leading order in an N_c-expansion. This is the result captured by the Supergravity approximation used in this paper. Also notice that the L's entering in this formulas are relative to an AdS space expressed in the canonical form.

and

4 dimensions: $\quad \mathcal{A} = -\dfrac{L^3}{8\pi G_N^{(5)}}\left(-\dfrac{1}{8}\bar{R}^{ij}\bar{R}_{ij} + \dfrac{1}{24}\bar{R}^2\right) = \dfrac{1}{16\pi^2}\left[c\left(\bar{R}^{ijkl}\bar{R}_{ijkl} - 2\bar{R}^{ij}\bar{R}_{ij} + \dfrac{1}{3}\bar{R}^2\right)\right.$

$$\left. - a\left(\bar{R}^{ijkl}\bar{R}_{ijkl} - 4\bar{R}^{ij}\bar{R}_{ij} + \bar{R}^2\right)\right], \qquad c = a = \dfrac{\pi}{8}\dfrac{L^3}{G_N^{(5)}} ,$$

$$(2.8.80)$$

where $\bar{R}_{ijkl}$, $\bar{R}_{ij}$ and $\bar{R}$ are the Riemann and Ricci tensors and scalar of the boundary metric. The Newton constant in different dimensions is calculated according to (we take $g_s = 1$ as in the rest of this paper),

$$G_N^{(10)} = 8\pi^6\alpha'^4, \qquad G_N^{(10-d)} = \dfrac{G_N^{(10)}}{vol(M_d)}. \qquad (2.8.81)$$

For solutions presenting a flow between these fixed points (or generically, an RG flow), a quantity that gives an idea of the number of degrees of freedom can also be defined. This quantity measures an 'effective volume' of the internal space, that is a volume that is weighted together with the dilaton and other factors in the metric. To define such a quantity one goes back to a proposal by Freedman, Gubser, Pilch and Warner [125]—see also the paper [126] for earlier attempts. Indeed, for any background (that should be considered to be a solution of a D-dimensional supergravity, possibly connected with string theory) of the form,

$$ds_D^2 = e^{2A(r)}dx_{1,D-2}^2 + dr^2 , \qquad (2.8.82)$$

and assuming that the matter fields satisfy certain Energy conditions [125], it was proven using the Einstein equations that the quantity,

$$c \sim \dfrac{1}{(A')^{D-2}}, \qquad (2.8.83)$$

is monotonically increasing towards the UV [125]. This proposal was extended by Klebanov, Kutasov and Murugan in the paper [127], to account for an RG-flow in a $d+1$ dimensional QFT, dual to a generic metric and dilaton of the form,

$$ds^2 = \alpha_0(r)\left[dx_{1,d}^2 + \beta_0(r)dr^2\right] + g_{ij}(r,\vec{\theta})d\theta^i d\theta^j, \quad \Phi(r). \qquad (2.8.84)$$

In these cases and in cases where the functions α_0, Φ depend also on the internal coordinates $\alpha_0(r,\vec{\theta}), \Phi(r,\vec{\theta})$, the formulas of [127] were extended in [106] to be,

$$c = d^d\dfrac{\beta_0(r)^{\frac{d}{2}}\widehat{H}^{\frac{2d+1}{2}}}{\pi G_N^{(10)}(\widehat{H}')^d}, \quad \widehat{H} = \left(\int d\vec{\theta}\sqrt{e^{-4\Phi}\det[g_{int}]\alpha_0^d}\right)^2. \qquad (2.8.85)$$

At conformal points, i.e. when calculated in AdS backgrounds, this gives a constant result, in agreement with eq. (2.8.79). For backgrounds with a flow, the quantity in eq. (2.8.85) gives an idea of the number of degrees of freedom that participate in the dynamics of the QFT at a given energy.

In the following sections, we will quote the results for central charges according to eq. (2.8.79) for the conformal field theories in two and four dimensions. Following that, we will write the result that eq. (2.8.85) gives for the flows between theories.

2.8.1   Central charge at conformal points

As anticipated, we will quote here the results for eq. (2.8.79) for the different AdS_3 and AdS_5 fixed points. We start with the twisted solutions of section 2.2.1. We will use that the volume of the $T^{1,1}$ space is $vol(T^{1,1}) = 16\pi^3/27$.

Twisted geometries

For the IR AdS_3 fixed point, the volume of the internal compact manifold is $vol(M_7) = \frac{1}{3}L^7 vol(\Sigma_2) vol(T^{1,1})$, and the central charge is,

$$c = 9\left|N_{D3}\widehat{N}_{D3}\right| = \frac{L^8}{\alpha'^4}\frac{vol(\Sigma_2)vol(T^{1,1})}{24\pi^6}. \tag{2.8.86}$$

At the UV AdS_5 fixed point, the volume of the internal compact manifold is $vol(M_5) = L^5 vol(T^{1,1})$, and the result for the central charge is,

$$c = \frac{27}{64}N_{D3}^2 = \frac{L^8}{\alpha'^4}\frac{vol(T^{1,1})}{64\ \pi^5}\ . \tag{2.8.87}$$

After the NATD, we must consider the new radius of the space $\widehat{L}$ and the volume of the new 5-dim compact space $4\pi^2 vol(\rho, \chi, \xi)$. The computations turn out to be similar as the previous ones, and we obtain that the central charges before and after NATD, for both the two and four dimensional CFTs, are related by,

$$\frac{\hat{c}}{c} = \frac{\widehat{L}^8}{L^8}\frac{4\pi^2 vol(\rho, \chi, \xi)}{vol(T^{1,1})}. \tag{2.8.88}$$

Let us comment on the quantity $vol(\rho, \chi, \xi)$, that appears in the calculation of the Page charges in section 2.7—see for example, eq. (2.7.70) and also in the computation of the entanglement entropy of section 2.9. Indeed, if we calculate, [10]

$$vol(\rho, \chi, \xi) = \int_0^{n\pi} \rho^2 d\rho \int_0^{2\pi} d\xi \int_0^\pi \sin\chi d\chi = \frac{4\pi^4}{3}n^3\ ,$$

$$\frac{\hat{c}}{c} = \frac{\widehat{L}^8}{L^8}\frac{4\pi^2 vol(\rho, \chi, \xi)}{vol(T^{1,1})} = \frac{36\pi N_{D6}^2}{N_{D3}^2}n^3\ . \tag{2.8.89}$$

We have performed the ρ-integral in the interval $[0, n\pi]$. The logic behind this choice was spelt out in section 2.7, see below eq. (2.7.66). The proposal is that moving in units of π in the ρ-coordinate implies 'un-higgsing' a gauge group, hence we would have a linear quiver gauge theory. The central charge captures this un-higgsing procedure, increasing according to how many groups we 'create'. What is interesting is the n^3 behavior in eq. (2.8.89). Indeed, if n were associated with the rank of a gauge group, this scaling would be precisely the one obtained in Gaiotto-like CFTs (also valid for the $\mathcal{N} = 1$ 'Sicilian' theories of [116]). Indeed, the NATD procedure when applied to the $AdS_5 \times T^{1,1}$ background creates metric

---

[10]We identify the integral with the volume of the manifold spanned by the new coordinates. This becomes more apparent if we use the expressions in the appendix, in different coordinate systems.

and fluxes similar to those characterizing the Sicilian CFTs. The backgrounds in sections 2.2 to 2.5 are dual to a compactification of the Klebanov Witten CFT and (using the NATD background) the Sicilian CFT on a two space Σ_2. The two-dimensional IR fixed point of these flows is described by our 'twisted AdS_3' and its NATD. The central charge of the Sicilian CFT and its compactified version is presenting a behavior that goes like a certain rank to a third power $c \sim n^3$. This suggest that crossing $\rho = \pi$ amounts to adding D4-branes and Neveu-Schwarz five branes and n is the number of branes that were added —see eqs. (2.7.66) and (2.7.76)— or crossed[11]. Had we integrated on the interval $[n\pi, (n+1)\pi]$, we would have obtained a scaling like $c \sim N_{D_4}^2$ at leading order in n.

Donos-Gauntlett geometry

We study here the central charge for the Donos-Gauntlett background in section 2.2.2. For the AdS_3 fixed point, the volume of the internal compact manifold is

$$vol(M_7) = L^7 \left(4/3\right)^{5/4} 4\pi^2 d_\alpha d_\beta \, vol(T^{1,1}) \quad ,$$

and the central charge is,

$$c = 3 \left| N_{D3} \widehat{N}_{D3} \right| = \frac{2}{3} \frac{L^8}{\alpha'^4} \frac{d_\alpha d_\beta vol(T^{1,1})}{\pi^4} \quad . \tag{2.8.90}$$

For the AdS_5 fixed point, the volume of the internal compact manifold $vol(M_5) = L^5 vol(T^{1,1})$, and the central charge results in,

$$c = \frac{27}{64} N_{D3}^2 = \frac{L^8}{\alpha'^4} \frac{vol(T^{1,1})}{64 \, \pi^5} \quad . \tag{2.8.91}$$

The quotient of central charges before and after the NATD for the Donos-Gauntlett QFT, are given by a similar expression to that in eq. (2.8.88).

We move now to study a quantity that gives an idea of the degrees of freedom along a flow.

2.8.2 Central charge for flows across dimensions

In the previous section, we calculated the central charge for two and four dimensional CFTs dual to the AdS_3 and AdS_5 fixed points of the flow. In this section, we will use the developments in [125] and [127], to write a c-function along the flows between these fixed points. We will find various subtleties,

- When considered as a low energy two-dimensional CFT, the definition of the c-function evaluated on the flows will not detect the presence of the four dimensional CFT in the far UV.

- We attempt to generalize the formula of [127] for anisotropic cases (that is for field theories that undergo a spontaneous compactification on Σ_2). This new definition will detect both the two dimensional and four dimensional conformal points, but will not necessarily be decreasing towards the IR. This is not in contradiction with 'c-theorems' that assume Lorentz invariance.

---

[11]Thanks to Daniel Thompson for a discussion about this.

We move into discussing these different points in our particular examples. To start, we emphasize that the formulas in eqs.(2.8.82)-(2.8.85), contain the same information. Indeed, the authors of [127] present a 'spontaneous compactification' of a higher dimensional Supergravity (or String theory) to $d+2$ dimensions, see eq. (2.8.84). Moving the reduced system to Einstein frame and observing that the $T_{\mu\nu}$ of the matter in the lower dimension satisfies certain positivity conditions imposed in [125], use of eq. (2.8.83) implies eq. (2.8.85). Hence, we will apply eqs. (2.8.84)-(2.8.85) to our different compactifications in sections 2.2 to 2.5.

<u>Twisted and Donos-Gauntlett solutions.</u> For the purpose of the flows both twisted and Donos-Gauntlett solutions present a similar qualitative behavior. We start by considering the family of backgrounds in eq. (2.2.1) as dual to field theories in $1+1$ dimensions. In this case the quantities relevant for the calculation of the central charge are,

$$d = 1, \quad \alpha_0 = L^2 e^{2A}, \quad \beta_0 = e^{-2A}, \quad e^{\Phi} = 1,$$

$$\frac{ds_{int}^2}{L^2} = e^{2B} ds_{\Sigma_2}^2 + e^{2U} ds_{KE}^2 + e^{2V} (\eta + zA_1)^2 . \tag{2.8.92}$$

We calculate the quantity

$$\widehat{H} = \mathcal{N}^2 e^{2(B+4U+V+A)}, \qquad \mathcal{N} = \frac{(4\pi)^3 vol(\Sigma_2) L^8}{108}. \tag{2.8.93}$$

Then, we obtain

$$c = \frac{\mathcal{N} e^{2B+4U+V}}{2\pi G_N^{(10)}(2B' + 4U' + V' + A')}. \tag{2.8.94}$$

Using the BPS equations describing these flows in eq. (2.2.6) we can get an expression without derivatives. Specializing for the solution with an H_2 in section 2.2.1, we find

$$c = \frac{\mathcal{N}}{9\pi G_N^{(10)}} \frac{(1 + e^{2r})^2}{1 + 2e^{2r}}. \tag{2.8.95}$$

We can calculate this for the background we obtained in section 2.3.1, by application of NATD. The result and procedure will be straightforward, but we will pick a factor of the volume of the space parametrized by the new coordinates, $vol(\rho, \chi, \xi)$.

For the purposes of the RG-flow, the quotient of the central charges will be the same as the quotient in eq. (2.8.89). This was indeed observed in the past [42], [106] and is just a consequence of the invariance of the quantity $\left(e^{-2\Phi}\sqrt{\det[g]}\right)$ under NATD.

Coming back to eq. (2.8.95), we find that in the far IR, represented by $r \to -\infty$, the central charge is constant. But in the far UV ($r \to \infty$), we obtain a result that is not characteristic of a CFT. Hence, this suggest that the definition is only capturing the behavior of a 2-dim QFT. In other words, the four dimensional QFT may be thought as a two dimensional QFT, but with an infinite number of fields.

The absence of the four dimensional fixed point in our eq. (2.8.95) can be accounted if we generalize the prescription to calculate central charges for an anisotropic 4-dim QFT. Holographically this implies working with a background of the form,[12]

$$ds_{10}^2 = -\alpha_0 dy_0^2 + \alpha_1 dy_1^2 + \alpha_2 ds_{\Sigma_2}^2 + \left(\alpha_1 \alpha_2^2\right)^{\frac{1}{3}} \beta_0 dr^2 + g_{ij} d\theta^i d\theta^j. \tag{2.8.96}$$

---

[12]A natural generalization of eq. (2.8.96) is $ds^2 = -\alpha_0 dt^2 + \alpha_1 dy_1^2 + ... + \alpha_d dy_d^2 + \Pi_{i=1}^d \alpha_i^{\frac{1}{d}} \beta dr^2 + g_{ij} d\theta^i d\theta^j$.

In this case we define,

$$G_{ij}d\xi_i d\xi_j = \alpha_1 dy_1^2 + \alpha_2 ds_{\Sigma_2}^2 + g_{ij}d\theta^i d\theta^j,$$

$$\widehat{H} = \left(\int d\theta^i \sqrt{e^{-4\Phi} \det[G_{ij}]} \right)^2,$$

$$c = d^d \frac{\beta_0^{\frac{d}{2}} \widehat{H}^{\frac{2d+1}{2}}}{\pi G_N^{(10)}(\widehat{H}')^d}.$$

(2.8.97)

We can apply this generalized definition to the flow for the twisted H_2 background of section 2.2.1, and Donos-Gauntlett background of section 2.2.2 (for more examples the reader is referred to appendix D of [19]). In this case, we consider them as dual to a field theory in $3 + 1$ anisotropic dimensions (two of the dimensions are compactified on a Σ_2). The quantities relevant for the calculation of the central charge are,

$$d = 3, \;\; \alpha_1 = L^2 e^{2A}, \;\;\; \alpha_2 = L^2 e^{2B}, \;\;\; \beta_0 = e^{\frac{-2A-4B}{3}}, \;\;\; e^{\Phi} = 1,$$

$$G_{ij}d\xi_i d\xi_j = L^2 \left(e^{2A}dy_1^2 + e^{2B}ds_{\Sigma_2}^2 + e^{2U}ds_{KE}^2 + e^{2V}\left(\eta + zA_1\right)^2 \right).$$

(2.8.98)

We calculate

$$\widehat{H} = \mathcal{N}^2 e^{2(2B+4U+V+A)}, \;\;\; \mathcal{N} = \frac{(4\pi)^3 L^8}{108}.$$

(2.8.99)

Then, we obtain

$$c = \frac{27\mathcal{N}e^{4U+V}}{8\pi G_N^{(10)}(2B' + 4U' + V' + A')^3}.$$

(2.8.100)

Focusing on the H_2 case, if we use the solution that describe this flow—see eq. (2.2.8) we get an analytical expression,

$$c = \frac{\mathcal{N}}{\pi \, G_N^{(10)}} \left(\frac{1 + e^{2r}}{1 + 2e^{2r}} \right)^3.$$

(2.8.101)

Notice that, by definition, this quantity gives the correct central charge in the UV (a constant, characterizing the 4-d fixed point). In the IR, the quantity turns out to be constant too, so it is capturing the presence of a 2-d fixed point. Nevertheless, it is probably not an appropriate candidate for a 'c-function between dimensions' as it is not necessarily increasing towards the UV. This is not in contradiction with the logic of 'a-theorems' and proofs like the ones in [125] or [121], as the metric does not respect Lorentz invariance. Hence, it is not satisfying the assumptions of the theorems. For the Donos-Gauntlett case analogous things happen. It would be very nice to try to apply the recent ideas of [128] to this flow. Notice that this feature of a 'wrong monotonicity' for the central charge was also observed—for theories breaking Lorentz invariance in Higher Spin theories—see the papers [129].

Let us move now to study other observables defining the 2-d and 4-d QFTs.

2.9   Entanglement entropy and Wilson loops

In this section, we will complement the work done above, by studying a couple of fundamental observables in the QFTs defined by the backgrounds in sections 2.2 to 2.5.

Whilst at the conformal points the functional dependence of results is determined by the symmetries, the interest will be in the coefficients accompanying the dependence. Both observables interpolate smoothly between the fixed points.

2.9.1   Entanglement entropy

The aim of this section is to compute the entanglement entropy on a strip, which extends along the direction $y_1 \in [-\frac{d}{2}, \frac{d}{2}]$, and study how this observable transforms under NATD. The input backgrounds for our calculations will be the Donos-Gauntlett and the H_2 flow as well as their non-abelian T-duals. Since the procedure is the same in all of the cases and due to the similarity of the geometries we will present the results in a uniform way.

For the computation of the entanglement entropy one has to apply the Ryu-Takayanagi formula [95] for non-conformal metrics [130]. This prescription states that the holographic entanglement entropy between the strip and its complement is given by the minimal-area static surface that hangs inside the bulk, and whose boundary coincides with the boundary of the strip. The general form of the entanglement entropy for the non-conformal case is,

$$S = \frac{1}{4G_N^{(10)}} \int d^8\sigma e^{-2\Phi} \sqrt{G_{\text{ind}}^{(8)}} \; . \tag{2.9.102}$$

For the strip, we chose the embedding functions to be $y_0 = \text{const}$ and $r = r(y_1)$ and then using the conservation of the Hamiltonian we arrive at an expression for $r(y_1)$ that makes the area minimal under that embedding. With that we compute,

$$S = \frac{\tilde{L}^8}{54} \frac{\pi}{G_N^{(10)}} vol(\Sigma_2) V_3 \int\limits_{r_*}^{\infty} dr \; e^{-A} \frac{G^2}{\sqrt{G^2 - G_*^2}} \; , \tag{2.9.103}$$

where the form of the function G depends on the geometry of the background that we consider,

$$G = \begin{cases} e^{A+2B} & \text{for the twisted solutions} \\ e^{A+2B+4U+V} & \text{for the DG solution} \end{cases} . \tag{2.9.104}$$

Above, r_* is the radial position of the hanging surface tip and we define $G_* = G(r_*)$. Also, with $vol(\Sigma_2)$ we denote the volume of the Riemann surface Σ_2. Notice that the form of the function G is the same before and after NATD. Moreover we consider,

$$\tilde{L} = \begin{cases} L & \text{before NATD} \\ \widehat{L} & \text{after NATD} \end{cases} , \tag{2.9.105}$$

The quantity V_3 is defined as,

$$V_3 = \begin{cases} 16 \; \pi^2 & \text{before NATD} \\ \int d\chi \; d\xi \; d\rho \; \rho^2 \sin\chi & \text{after NATD} \end{cases} . \tag{2.9.106}$$

Before the NATD transformation V_3 comes from the 3-dimensional submanifold that is spanned by the coordinates (θ_2, ϕ_2, ψ), while after the NATD it comes from the submanifold that is spanned by the dual coordinates (ρ, χ, ξ). This implies that the entropies before and after NATD are proportional all along the flow, for any strip length. A discussion on possible values of the quantity $\int d\chi\, d\xi\, d\rho\, \rho^2 \sin\chi$ can be found in the quantized charges section 2.7 and in the discussion on central charges in section 2.8.

When computed by the Ryu-Takayanagi formula eq. (2.9.103) the entanglement entropy is UV divergent. In order to solve this we compute the regularized entanglement entropy (S^{reg}) by subtracting the divergent part of the integrand of eq. (2.9.103). The regularized entanglement entropy is given by,

$$S^{\text{reg}} = \frac{\tilde{L}^8}{54}\frac{\pi}{G_N^{(10)}} vol(\Sigma_2)V_3 \left\{ \int\limits_{r_*}^{\infty} dr\, \left(\frac{e^{-A}G^2}{\sqrt{G^2 - G_*^2}} - F_{UV} \right) - \int\limits^{r_*} dr\, F_{UV} \right\} , \qquad (2.9.107)$$

where the last integral is an indefinite integral with the result being evaluated at $r = r_*$ and

$$F_{UV} = \begin{cases} \frac{1+e^{2r}}{3} & \text{for the } H_2 \text{ twisted solution} \\ e^{2r} + \frac{\lambda^2}{3} & \text{for the Donos-Gauntlett solution} \end{cases} . \qquad (2.9.108)$$

From the formulas (2.9.105), (2.9.106) and (2.9.107) it is obvious that the regularized entanglement entropies before and after the NATD transformation differ by the factor

$$\frac{\widehat{S}^{\text{reg}}}{S^{\text{reg}}} = \frac{\widehat{L}^8}{L^8}\frac{\int d\chi\, d\xi\, d\rho\, \rho^2 \sin\chi}{16\, \pi^2} . \qquad (2.9.109)$$

In the formula above we denoted by $\widehat{S}^{\text{reg}}$ the value of the entanglement entropy after the NATD transformation. As discussed below eq. (2.8.95), the quantity $\left(e^{-2\Phi}\sqrt{\det[g]} \right)$ is invariant under NATD, and this explains why the ratio (2.9.109) is constant along the flow.

At this point let us normalize the regularized entanglement entropy by defining the quantity,

$$S' = \frac{54}{\tilde{L}^8}\frac{G_N^{(10)}}{\pi\, vol(\Sigma_2)V_3}\, S^{\text{reg}} . \qquad (2.9.110)$$

In what follows we present the behavior of S' in the UV and the IR for the geometries of interest. We express the results in terms of the width of the strip d,

$$d = 2G_* \int\limits_{r_*}^{\infty} dr\, \frac{e^{-A}}{\sqrt{G^2 - G_*^2}} . \qquad (2.9.111)$$

The UV/IR behavior written in eqs (2.9.113), (2.9.116), (2.9.119) and (2.9.121) below, are just consequences of the fact that in far UV and far IR the dual QFT is conformal. The functional forms are universal, so our main interest is the constant appearing in them, and also as a cross-check of numerical results.

Behavior in the UV

Twisted geometries

In the case of the twisted H_2 geometry we find that the width of the strip is,

$$d = e^{-r_*} \int\limits_1^\infty \frac{du}{u^2} \frac{2}{\sqrt{u^6 - 1}} = \frac{2\sqrt{\pi}\Gamma\left(\frac{2}{3}\right)}{\Gamma\left(\frac{1}{6}\right)} e^{-r_*} . \tag{2.9.112}$$

Here in the integration we changed the variable r by $u = \frac{e^r}{e^{r_*}}$. From the calculation of the normalized entropy S' we observe that in the UV this behaves like $\frac{1}{d^2}$, namely

$$S' = -\frac{\pi^{3/2}}{6}\left(\frac{\Gamma\left(\frac{2}{3}\right)}{\Gamma\left(\frac{1}{6}\right)}\right)^3 \frac{1}{d^2} + \frac{1}{3}\ln d + \frac{1}{3}\ln\left(\frac{\Gamma\left(\frac{1}{6}\right)}{2\sqrt{\pi}}\Gamma\left(\frac{2}{3}\right)\right) , \tag{2.9.113}$$

where we also included subleading and next-to subleading terms.

Donos-Gauntlett geometry

Similarly in the case of the Donos-Gauntlett geometry we find that the width of the strip in terms of r_* (considering also a subheading term) is,

$$d = \frac{2\sqrt{\pi}\Gamma\left(\frac{2}{3}\right)}{\Gamma\left(\frac{1}{6}\right)}e^{-r_*} + \lambda^2\left(\frac{5}{72} + \frac{11}{24}I_1\right)e^{-3r_*} , \tag{2.9.114}$$

where

$$I_1 = \int\limits_1^\infty dz \frac{z^2}{(z^4 + z^2 + 1)\sqrt{z^6 - 1}} = 0.1896\ldots \tag{2.9.115}$$

Here as well we end up with a $\frac{1}{d^2}$ behavior, a logarithmic subleading contribution and a constant c_1 for the regularized entropy,

$$S' = -2\pi^{3/2}\left(\frac{\Gamma\left(\frac{2}{3}\right)}{\Gamma\left(\frac{1}{6}\right)}\right)^3 \frac{1}{d^2} + \frac{\lambda^2}{3}\ln d + c_1 , \tag{2.9.116}$$

where c_1 ,

$$c_1 = \lambda^2\left(-\frac{1}{3}\ln\left(\frac{2\sqrt{\pi}\Gamma\left(\frac{2}{3}\right)}{\Gamma\left(\frac{1}{6}\right)}\right) + \left(\frac{\ln 2}{9} + \frac{11}{48}I_1\right) + \frac{\Gamma\left(-\frac{1}{3}\right)}{6\Gamma\left(\frac{2}{3}\right)}\left(\frac{5}{72} + \frac{11}{24}I_1\right)\right) . \tag{2.9.117}$$

Behavior in the IR

Twisted geometries

The calculation for the IR limit is more tricky. The origin of the subtlety is that the integrals we have to evaluate now run all along the flow and we do not know the analytical properties of the integrands. In order to address this issue we split the integration into the intervals $[r_*, a]$ and $[a, +\infty)$ choosing a to be in the deep IR but always greater than r_*.

Following this prescription in the calculation, for the width of the strip we find,

$$d = \frac{4}{3} \, e^{-\frac{3r_*}{2}} . \tag{2.9.118}$$

If we do the same analysis when we calculate the normalized entropy we find,

$$S' = \frac{2}{9} \ln d + \frac{2}{9} \ln \frac{3}{2} . \tag{2.9.119}$$

The logarithmic dependence of the leading term on d is the expected for a $1+1$ theory.

Donos-Gauntlett geometry

We close this section presenting the corresponding results for the Donos-Gauntlett geometry. As in the case of the twisted geometries we split the integrations in the same way. Then for the width of the strip we find,

$$d = e^{-a_0} \frac{2\sqrt{2}}{3^{\frac{3}{4}}} e^{-\frac{3^{\frac{3}{4}}}{\sqrt{2}} r_*} . \tag{2.9.120}$$

The normalized entropy displays again a logarithmic behavior in terms of the width of the strip,

$$S' = \frac{8}{9} \ln d + \frac{8}{9} \ln \left(e^{a_0} \frac{3^{\frac{3}{4}}}{\sqrt{2}} \right) + c_2 , \tag{2.9.121}$$

where the constant c_2 has the value,

$$c_2 = \int_0^\infty \left(e^{-A} G - e^{2r} - \frac{4}{3} \right) dr + \int_{-\infty}^0 \left(e^{-A} G - e^{2r} - \left(\frac{4}{3} \right)^{\frac{5}{4}} \right) dr = -0.0312\ldots \tag{2.9.122}$$

The results for the entanglement entropy are shown in Fig. 2.2. We will now perform a similar analysis for Wilson loops.

2.9.2 Wilson loop

In this section we calculate the potential energy as a function of the separation in the y_1 direction (denoted as d) for two non-dynamical sources added to the QFT [131]. In holography this observable can be represented by a hanging string whose ends are separated by a distance d along the y_1 direction. In our calculations we consider an embedding of the form $r = r(y_1)$ for the string. Such an embedding gives rise to the following induced metric on the string,

$$ds_{\text{st}}^2 = \tilde{L}^2 \left(e^{-2A} \, dy_0^2 + \left(e^{2A} + r'^2 \right) dy_1^2 \right) , \tag{2.9.123}$$

where $\tilde{L}$ is defined in (2.9.105). It is obvious that the above induced metric is the same for all of the geometries that we have discussed in this chapter so far (even for the duals). For this reason we believe that it is not necessary to make any distinction with respect to these geometries for the moment. Moreover, this means that the observable is 'uncharged' under NATD and thus it has the same functional form when computed in the initial and dualized geometries. The interest will be in the numerical coefficients our calculation will give.
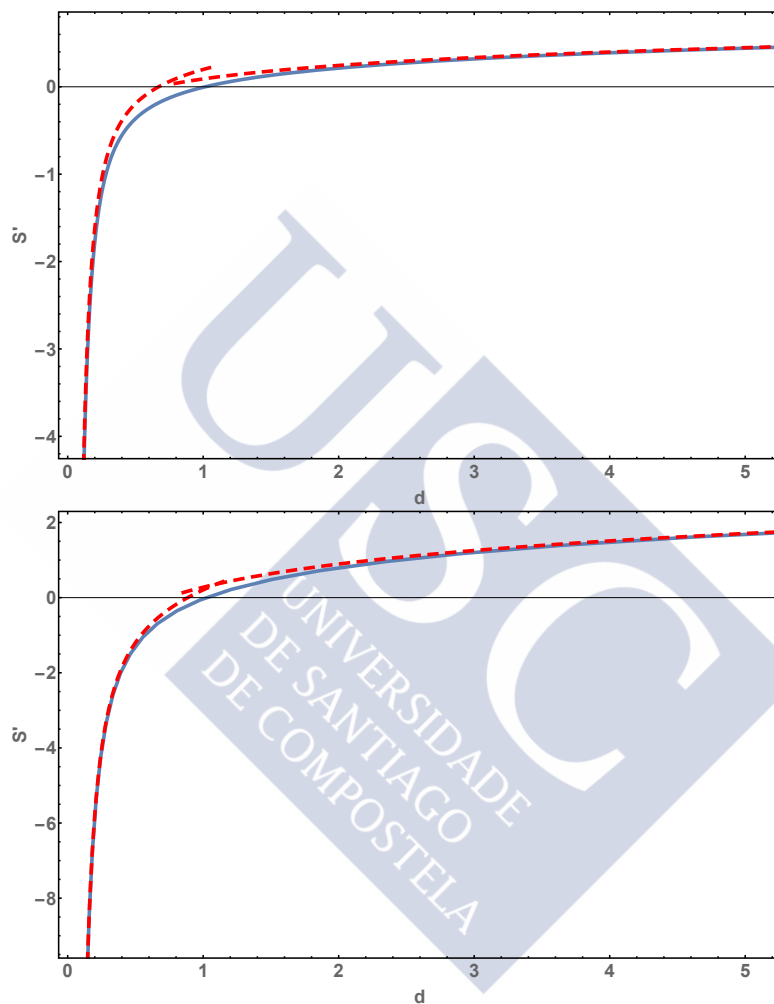
Figure 2.2: S' as a function of d for twisted H_2 (left) and Donos-Gauntlett solution (right). The continuous curves correspond to the numerical value, while the dashed red ones to the UV and IR limits.

The Nambu-Goto lagrangian density for the string takes the form,

$$\mathcal{L} = \frac{1}{2\pi\alpha'}\sqrt{-\det(g_{\text{ind}})} = \frac{\tilde{L}^2}{2\pi\alpha'} \, e^A \, \sqrt{e^{2A} + r'^2} \, , \tag{2.9.124}$$

where g_{ind} stands for the induced metric (2.9.123). The conservation of the Hamiltonian implies that,

$$\frac{e^{3A}}{\sqrt{e^{2A} + r'^2}} = e^{2A_*} \, , \tag{2.9.125}$$

where A_* is the value of the function $A(r)$ at the tip of the hanging string $r = r_*$. We can solve the last equation for r' and use the result to calculate the distance between the endpoints of the string. If we do this we can express d in terms of r_*

$$d = e^{2A_*} \int_{r_*}^{\infty} dr \, \frac{e^{-A}}{\sqrt{e^{4A} - e^{4A_*}}} \, . \tag{2.9.126}$$

The Nambu-Goto action now reads

$$S = \frac{T\tilde{L}^2}{\pi\alpha'} \int_{r_*}^{\infty} dr \, \frac{e^{3A}}{\sqrt{e^{4A} - e^{4A_*}}} \, , \tag{2.9.127}$$

where $T = \int dt$. The integral in eq. (2.9.127) is divergent since we are considering quarks of infinite mass sitting at the endpoints of the string. We can regularize this integral by subtracting the mass of the two quarks and dividing by T as it is shown below

$$\frac{E}{\tilde{L}^2}\alpha' = \frac{1}{\pi} \int_{r_*}^{\infty} dr e^A \left(\frac{e^{2A}}{\sqrt{e^{4A} - e^{4A_*}}} - 1 \right) - \frac{1}{\pi} \int_{-\infty}^{r_*} dr \, e^A \, . \tag{2.9.128}$$

This formula gives us the quark-antiquark energy. In order to calculate the same observable starting with the NATD geometries one must take into account that the AdS radius L is different from that of the original geometries. In fact both results are related in the following way

$$\frac{\widehat{E}}{E} = \frac{\widehat{L}^2}{L^2} \, . \tag{2.9.129}$$

In the last expression the hats refer to the dual quantities.

At this point we will explore the UV and IR limits of the quark-antiquark energy both for the twisted and the Donos-Gauntlett geometries.

Behavior in the UV

Twisted and Donos Gauntlett geometry

First we focus on the twisted solution where the Riemann surface is the hyperbolic space, i.e. $\Sigma_2 = H_2$. In section 2.2.1 we saw that in this case the function $A(r)$ behaves like

$A(r) \sim r$. Taking this into account we can compute the distance between the quarks from the formula (2.9.126). The result of this is

$$d = \frac{2\sqrt{2}\,\pi^{\frac{3}{2}}}{\Gamma\left(\frac{1}{4}\right)^2} e^{-r_*} \, . \tag{2.9.130}$$

Solving this equation for r_* we can substitute into the result coming from the formula (2.9.128). This will give the quark-antiquark energy in terms of d which in our case is

$$E = -\frac{\tilde{L}^2}{\alpha'}\,\frac{4\,\pi^2}{\Gamma\left(\frac{1}{4}\right)^4}\,\frac{1}{d} \, , \tag{2.9.131}$$

as expected for a CFT. The main point of interest in the previous formula is in the numerical coefficient.

Similar considerations for the case of the Donos-Gauntlett geometry give the same results as in the twisted case above. This is because the asymptotic behavior of the function $A(r)$ in the UV is the same in both cases.

Behavior in the IR

Twisted geometry

Again in the IR region we address again the same difficulty that we found in the computation of the entanglement entropy. We use the same trick to overcome it, that is we split the integrations into the intervals $[r_*, a]$ and $[a, +\infty)$ where a has value in the deep IR but always greater than r_*.

In section 2.2.1 we saw that in the case where $\Sigma_2 = H_2$, the IR behavior of the function $A(r)$ is $A(r) \sim \frac{3}{2}\,r$. Applying this into the formula (2.9.126) we obtain the following result,

$$d = \frac{4\sqrt{2}\,\pi^{\frac{3}{2}}}{3\,\Gamma\left(\frac{1}{4}\right)^2} e^{-\frac{3}{2}r_*} \, . \tag{2.9.132}$$

As before we solve the previous result for r_* and we substitute it into the expression that we find from the calculation of the quark-antiquark potential. This way we express the energy as a function of the distance between the quarks,

$$E = -\frac{\tilde{L}^2}{\alpha'}\,\frac{16\,\pi^2}{9\,\Gamma\left(\frac{1}{4}\right)^4}\,\frac{1}{d} \, . \tag{2.9.133}$$

Donos-Gauntlett geometry

Repeating the same steps for the case of the Donos-Gauntlett geometry we find that the distance between the quarks is,

$$d = \frac{4\pi^{\frac{3}{2}}}{3^{\frac{3}{2}}\Gamma\left(\frac{1}{4}\right)^2} e^{-a_0 - \frac{3^{\frac{3}{4}}}{\sqrt{2}}r_*} \, . \tag{2.9.134}$$

Then, expressing the energy in terms of the distance d we find again a dependence proportional to $\frac{1}{d}$,

$$E = -\frac{\tilde{L}^2}{\alpha'} \frac{8\pi^2}{3^{\frac{3}{2}} \Gamma\left(\frac{1}{4}\right)^4} \frac{1}{d} \ . \tag{2.9.135}$$

Let us point out that the behavior in eqs (2.9.131), (2.9.133) and (2.9.135) are just consequences of the fact that far in the UV and far in the IR the QFT is conformal.

The results for the quark-antiquark potential are shown in Fig. 2.3.
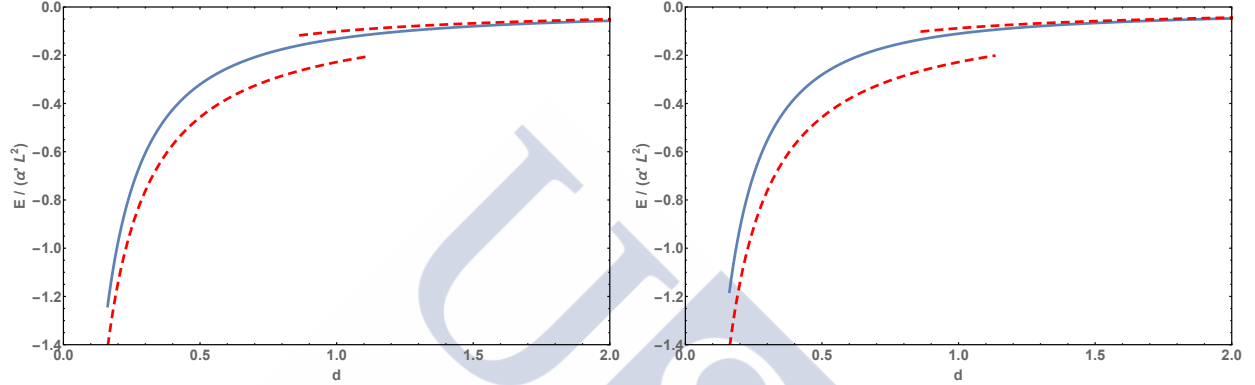
Figure 2.3: The quark-antiquark potential $\frac{E}{\alpha' L^2}$ as a function of the distance d in the cases of the twisted H_2 (left) and Donos-Gauntlett (right) solutions. The continuous curves correspond to the numerical results and the dashed ones to the UV and IR limits.

2.10 Discussion

We started by studying backgrounds dual to two-dimensional SUSY CFTs. The 2-d CFTs were obtained by compactification of the four-dimensional Klebanov-Witten CFT on a torus or on a compact hyperbolic plane. The 2-d CFT preserves (0,2) SUSY.

On those type IIB backgrounds we performed a NATD transformation, using an $SU(2)$-isometry of the 'internal space' (or, equivalently, a global symmetry of the dual CFT). As a result, we constructed *new, smooth* and SUSY preserving backgrounds in type IIA and 11 supergravity with an AdS_3 fixed point. A further T-duality was used to construct new, smooth and SUSY type IIB background whose IR is of the form $AdS_3 \times M_7$ and all fluxes are active.

We analyzed the dual QFT by computing its observables, using the smooth backgrounds mentioned above. By studying the Page charges, we observed that there is a correspondence between the branes of the starting type IIB solution and those of the type IIA solution after NATD.

The behavior of the central charge in the original CFT (the compactification of the Klebanov-Witten theory to 2-d) is $c \sim N_{D3}^2$, while after the NATD goes like $c \sim N_{D6}^2 n^3$. This new (cubic) dependence suggest a relation with long linear quivers, which would imply that n is measuring the number of D4- and NS5-branes. The picture that emerges is that of

a 2-d CFT living on the intersection of D2- , D6- and NS5-branes, with induced D4 charge every time an NS-brane is crossed. Quantized charges support this interpretation.

Entanglement entropy and Wilson loops had the expected universal dependence on d (the quark-antiquark separation or the length of strip separating the two regions) at the fixed points. The interest of the expressions is on the coefficients, not determined by conformal invariance. Interestingly, along the flow the observables smoothly interpolate between the IR and the UV behaviors, which are fixed points of different dimensionality. Both for the entanglement entropy and the Wilson loops we found that the quotient of their values before and after NATD is constant along the flow, as it is expected.

It would be interesting to connect these studies with previous calculations done for AdS_3, either at the sigma model or the supergravity level. We are presenting new backgrounds, hence new 2-d CFTs on which studies done in the past could be interesting to revisit. It would be also interesting to make more precise the QFT dual to these backgrounds. The key point needed for this purpose is to understand the global properties of the supergravity background after the NATD. Besides, it could be interesting to check whether our solutions fall within the existent classifications of, for example [115], [132]. Probably, for this purpose the global properties of the solution are needed. Another interesting point would be to further study new observables that select (or explore) the values of $\rho = n\pi$ argued in this work to be special values of the ρ-coordinate, in the line of [133]

2.A   Appendix

2.A.1   SUSY analysis

SUSY preserved by the twisted solutions

In this appendix we write explicitly the variations of the dilatino and gravitino for the ansatz (2.1-2.4), for the 3 cases H_2, S^2 and T^2. The SUSY transformations for the dilatino λ and the gravitino ψ_m for type IIB supergravity in string frame are [35],

$$\delta_\epsilon \lambda = \left[\frac{1}{2}\Gamma^m \partial_m \Phi + \frac{1}{4 \cdot 3!}H_{mnp}\Gamma^{mnp}\tau_3 - \frac{e^\Phi}{2}F_m\Gamma^m(i\tau_2) - \frac{e^\Phi}{4 \cdot 3!}F_{mnp}\Gamma^{mnp}\tau_1\right]\epsilon ,\qquad(2.A.1)$$

$$\delta_\epsilon \psi_m = \left[\nabla_m + \frac{1}{4 \cdot 2!}H_{mnp}\Gamma^{np}\tau_3 + \frac{e^\Phi}{8}\left(F_n\Gamma^n(i\tau_2) + \frac{1}{3!}F_{npq}\Gamma^{npq}\tau_1 + \frac{1}{2 \cdot 5!}F_{npqrt}\Gamma^{npqrt}(i\tau_2)\right)\Gamma_m\right]\epsilon ,$$

where τ_i , $i = 1, 2, 3$, are the Pauli matrices. Let us consider the H_2 case in detail (the S^2 case is obtained analogously) . Recall that the vielbein is written in (2.2.5).

The dilatino variation vanishes identically, as the fields involved are vanishing. The $m = 0$ component of the gravitino reads,

$$\delta_\epsilon \psi_0 = \left[\frac{A'}{2L}\Gamma_{04} - \frac{e^{-4U-V}}{2L}\Gamma_{04}\Gamma_{0123}i\tau_2 + \frac{e^{-2B-2U-V}}{16L}z\big(\Gamma_{014} - \Gamma_{239}\big)\big(\Gamma_{78} - \Gamma_{56}\big)\Gamma_0 i\tau_2\right]\epsilon .$$
$$(2.A.2)$$

First, we use the chiral projection of type IIB,

$$\Gamma_{11}\epsilon = \epsilon \ , \tag{2.A.3}$$

where we define $\Gamma_{11} = \Gamma_{0123456789}$. We also impose the following projections (Kähler projections),

$$\Gamma_{56}\epsilon = -\Gamma_{78}\epsilon = -\Gamma_{49}\epsilon \ . \tag{2.A.4}$$

Then, expression (2.A.2) simplifies to,

$$\delta_\epsilon \psi_0 = \Gamma_{04}\left[\frac{A'}{2L} - \frac{e^{-V-4U}}{2L} + \frac{e^{-2B-2U-V}}{4L}z\Gamma_{0178}i\tau_2 \right]\epsilon \ . \tag{2.A.5}$$

We now impose the usual projection for the D3-brane,

$$\Gamma_{0123}\ i\tau_2\epsilon = \epsilon \ , \tag{2.A.6}$$

and also a further projection related to the presence of the twisting,

$$\Gamma_{23}\epsilon = \Gamma_{78}\epsilon \ . \tag{2.A.7}$$

Then, imposing that expression (2.A.5) vanishes we obtain,

$$A' - e^{-V-4U} + \frac{z}{2}e^{-2B-2U-V} = 0 \ . \tag{2.A.8}$$

For the component $m = 1$ of the gravitino equation, we obtain that it is zero when we impose the projections and equation (2.A.8). For the component $m = 2$ we have,

$$\delta_\epsilon \psi_2 = \left[\frac{B'}{2L}\Gamma_{24} + \frac{e^{-2B+V}}{4L}z\Gamma_{39} - \frac{e^{-V-4U}}{2L}\Gamma_{24}\Gamma_{0123}i\tau_2 - \frac{e^{-2B-2U-V}}{4L}z\Gamma_{24}\Gamma_{0178}i\tau_2 \right]\epsilon \ . \tag{2.A.9}$$

Combining projections (2.A.4) and (2.A.7) we get $\Gamma_{39}\epsilon = -\Gamma_{24}\epsilon$. Then, (2.A.9) gives the condition,

$$B' - e^{-V-4U} - \frac{z}{2}e^{-2B-2U-V} - \frac{z}{2}e^{-2B+V} = 0 \ . \tag{2.A.10}$$

For $m = 3$, after imposing the projections and equation (2.A.10) we arrive at,

$$\delta_\epsilon \psi_3 = -\frac{e^{-B}}{2L}\cot\alpha\ (1+3z)\Gamma_{23}\epsilon \ . \tag{2.A.11}$$

There are two contributions to this term, one coming from the curvature of the H_2 (through the spin connection) and another coming from the twisting A_1. That is, here we explicitly see that the twisting is introduced to compensate the presence of the curvature, in such a way that some SUSY can be still preserved. Then, we impose,

$$z = -\frac{1}{3} \ . \tag{2.A.12}$$

For $m = 4$, the variation is,

$$\delta_\epsilon \psi_4 = \frac{1}{L}\partial_r \epsilon - \frac{1}{2L}\left[e^{-4U} + 2e^{-2B-2U-V}\right]\epsilon \ . \tag{2.A.13}$$

From the condition $\delta_\epsilon \psi_4 = 0$, we obtain a differential equation for ϵ. Solving for it we arrive at the following form for the Killing spinor,

$$\epsilon = e^{1/2 \int (e^{-4U} + 2e^{-2B-2U-V})dr}\, \epsilon_0 \ , \tag{2.A.14}$$

where ϵ_0 is spinor which is independent of the coordinate r. For $m = 5, 6, 7, 8$ the variations vanish as long as,

$$U' + e^{-V-4U} - e^{V-2U} = 0 \ . \tag{2.A.15}$$

Finally, for $m = 9$ the graviton variation vanishes if,

$$V' - 3e^{-V} + 2e^{V-2U} + e^{-V-4U} - \frac{z}{2}e^{-2B-2U-V} + \frac{z}{2}e^{-2B+V} = 0 \ . \tag{2.A.16}$$

Summarizing, the variations of the dilatino and gravitino vanish if we impose the following projections on the Killing spinor,

$$\Gamma_{11}\epsilon = \epsilon \ , \qquad \Gamma_{56}\epsilon = -\Gamma_{78}\epsilon = -\Gamma_{49}\epsilon \ , \qquad \Gamma_{0123}\, i\tau_2 \epsilon = \epsilon \ , \qquad \Gamma_{23}\epsilon = \Gamma_{49}\epsilon \ , \tag{2.A.17}$$

and the BPS equations (2.2.6), together with the condition $z = -1/3$. For the case of the 2-torus, if we focus on the $m = 3$ component,

$$\delta_\epsilon \psi_3 = \left[-\frac{ze^{-2B+V}}{4L}\Gamma_{29} - \frac{3ze^{-B}}{2L}\,\alpha\,\Gamma_{78} + \frac{B'}{2L}\Gamma_{34} - \frac{e^{-V-4U}}{2L}\Gamma_{34} - \frac{ze^{-2B-2U-V}}{4L}\Gamma_{34}\right]\epsilon \ , \tag{2.A.18}$$

we see that there is one term depending on α, due to the twisting. Contrary to the H_2 and S^2 cases, here there is no curvature term that could cancel it. This will force $z = 0$, obtaining $A' = B'$, which does not permit an AdS_3 solution.

Finally, after all this analysis we deduce that the Killing spinor does not depend explicitly on the coordinates (θ_2, ϕ_2, ψ) on which we perform the NATD transformation. In fact it only has a dependence on the coordinate r.

SUSY preserved by the NATD solutions

In the above subsection we calculated the amount of SUSY that is preserved by the type IIB supergravity solutions of the section 2.2.1 by examining the dilatino and the gravitino variations. Here we compute the portion of SUSY that is preserved by a supergravity solution after a NATD transformation following the argument of [15], which has been proven in [43]. According to this, one just has to check the vanishing of the Lie-Lorentz (or Kosmann) derivative [44] of the Killing spinor along the Killing vector that generates the isometry of the NATD transformation. More concretely, suppose that we want to transform a supergravity solution by performing a NATD transformation with respect to some isometry of the background that is generated by the Killing vector k^μ. Then there is a simple criterion

which states that if the Lie-Lorentz derivative of the Killing spinor along k^μ vanishes, then the transformed solution preserves the same amount of SUSY as the original solution. In the opposite scenario one has to impose more projection conditions on the Killing spinor in order to make the Lie-Lorentz derivative vanish. Thus in that case the dual background preserves less supersymmetry than the original one.

We recall that given a Killing vector k^μ the Lie-Lorentz derivative on a spinor ϵ along k^μ maps the spinor ϵ to another spinor and is defined as,

$$\mathcal{L}_k \epsilon = k^\mu D_\mu \epsilon + \frac{1}{4}\big(\nabla_\mu k_\nu\big)\Gamma^{\mu\nu}\epsilon = k^\mu D_\mu \epsilon + \frac{1}{8}(dk)_{\mu\nu}\Gamma^{\mu\nu}\epsilon \ , \tag{2.A.19}$$

where $D_\mu \epsilon = \partial_\mu \epsilon + \frac{1}{4}\omega_{\mu\rho\sigma}\Gamma^{\rho\sigma}\epsilon$. For further details about the Lie-Lorentz derivative we urge the interested reader to consult [134].

In this chapter we constructed type IIA supergravity solutions by applying a NATD transformation with respect to the $SU(2)$ isometry of the original backgrounds that corresponds to the directions (θ_2, ϕ_2, ψ). The non-vanishing components of the associated Killing vectors are,

$$\begin{aligned}
&k^{\theta_2}_{(1)} = \sin\phi_2 \ , \quad k^{\phi_2}_{(1)} = \cot\theta_2 \cos\phi_2 \ , \quad k^{\psi}_{(1)} = -\frac{\cos\phi_2}{\sin\theta_2} \ , \\
&k^{\theta_2}_{(2)} = \cos\phi_2 \ , \quad k^{\phi_2}_{(2)} = -\cot\theta_2 \sin\phi_2 \ , \quad k^{\psi}_{(2)} = \frac{\sin\phi_2}{\sin\theta_2} \ , \\
&k^{\phi_2}_{(3)} = 1 \ .
\end{aligned} \tag{2.A.20}$$

In what follows we will compute the Lie-Lorentz derivative along the three Killing vectors $(k_{(1)}, k_{(2)}, k_{(3)})$ using the geometries of the sections 2.2.1 and 2.2.2. It turns out that in all cases the Lie-Lorentz derivative vanishes without the requirement of imposing further projections on the Killing spinor. This means that the new solutions that we found using the technique of NATD preserve the same SUSY as the original solutions.

Let us now compute the Lie-Lorentz derivative along the Killing vector (2.A.20) for the twisted geometries that are described by the formulas (2.2.1)-(2.2.5). In the previous section, which deals with the supersymmetry of the starting solutions, we mentioned that the Killing spinor does not depend on the isometry coordinates (θ_2, ϕ_2, ψ). This means that the first term in (2.A.19) reduces to,

$$k^\mu_{(i)} D_\mu \epsilon = \frac{1}{4}\, \omega_{\mu\rho\sigma}\, k^\mu_{(i)}\, \Gamma^{\rho\sigma}\epsilon \ , \quad i = 1, 2, 3 \ . \tag{2.A.21}$$

Hence for each of the three Killing vectors we find,

$$
k_{(1)}^\mu D_\mu \epsilon = \frac{z}{12}\, e^{2V-2B}\ \cos\phi_2 \sin\theta_2 \Gamma^{23}\epsilon - \frac{e^{2V-2U}}{6}\ \cos\phi_2 \sin\theta_2 \left(\Gamma^{56} - \Gamma'^{78}\right)\epsilon
$$
$$
- \frac{1}{2}\ \cos\phi_2 \sin\theta_2 \Gamma'^{78}\epsilon + \frac{e^{V-U}}{2\sqrt{6}}\ \left(\cos\theta_2 \cos\phi_2 \Gamma'^{8} - \sin\phi_2 \Gamma'^{7}\right)\Gamma^9\epsilon
$$
$$
+ \frac{e^U\, U'}{2\sqrt{6}}\left(\cos\theta_2 \cos\phi_2 \Gamma'^{7} + \sin\phi_2 \Gamma'^{8}\right)\Gamma^4\epsilon + \frac{e^V\, V'}{6}\ \sin\theta_2 \cos\phi_2 \Gamma^{49}\epsilon\ ,
$$

$$
k_{(2)}^\mu D_\mu \epsilon = -\frac{z}{12}\, e^{2V-2B}\ \sin\phi_2 \sin\theta_2 \Gamma^{23}\epsilon + \frac{e^{2V-2U}}{6}\ \sin\phi_2 \sin\theta_2 \left(\Gamma^{56} - \Gamma'^{78}\right)\epsilon
$$
$$
+ \frac{1}{2}\ \sin\phi_2 \sin\theta_2 \Gamma'^{78}\epsilon - \frac{e^{V-U}}{2\sqrt{6}}\ \left(\cos\theta_2 \sin\phi_2 \Gamma'^{8} + \cos\phi_2 \Gamma'^{7}\right)\Gamma^9\epsilon
$$
$$
\tag{2.A.22}
$$
$$
- \frac{e^U\, U'}{2\sqrt{6}}\left(\cos\theta_2 \sin\phi_2 \Gamma'^{7} - \cos\phi_2 \Gamma'^{8}\right)\Gamma^4\epsilon - \frac{e^V\, V'}{6}\ \sin\theta_2 \sin\phi_2 \Gamma^{49}\epsilon\ ,
$$

$$
k_{(3)}^\mu D_\mu \epsilon = -\frac{z}{12}\, e^{2V-2B}\ \cos\theta_2 \Gamma^{23}\epsilon + \frac{e^{2V-2U}}{6}\ \cos\theta_2 \left(\Gamma^{56} - \Gamma'^{78}\right)\epsilon + \frac{1}{2}\ \cos\theta_2 \Gamma'^{78}\epsilon
$$
$$
+ \frac{e^{V-U}}{2\sqrt{6}}\ \sin\theta_2 \Gamma'^{8}\Gamma^9\epsilon - \frac{e^U\, U'}{2\sqrt{6}}\ \sin\theta_2 \Gamma^4\Gamma'^{7}\epsilon - \frac{e^V\, V'}{6}\ \cos\theta_2 \Gamma^{49}\epsilon\ .
$$

For convenience we have defined the rotated Γ-matrices,

$$
\Gamma'^{7} = \cos\psi\ \Gamma^7 + \sin\psi\ \Gamma^8\ ,\quad \Gamma'^{8} = -\sin\psi\ \Gamma^7 + \cos\psi\ \Gamma^8\ . \tag{2.A.23}
$$

Let us now compute the 1-forms that are dual to the Killing vectors. What one has to do is to lower the index of the Killing vectors (2.A.20) using the metric (2.2.1) which gives the following result,

$$
k_{(1)} = -\frac{L^2}{3}e^{2V} \sin\theta_2 \cos\phi_2 \left(\eta + zA_1\right) + \frac{L^2}{6}e^{2U}\left(\sin\phi_2 d\theta_2 + \sin\theta_2 \cos\theta_2 \cos\phi_2 d\phi_2\right)\ ,
$$
$$
k_{(2)} = \frac{L^2}{3}e^{2V} \sin\theta_2 \sin\phi_2 \left(\eta + zA_1\right) + \frac{L^2}{6}e^{2U}\left(\cos\phi_2 d\theta_2 - \sin\theta_2 \cos\theta_2 \sin\phi_2 d\phi_2\right)\ ,
$$
$$
k_{(3)} = \frac{L^2}{3}e^{2V} \cos\theta_2 \left(\eta + zA_1\right) + \frac{L^2}{6}e^{2U} \sin^2\theta_2 d\phi_2\ .
$$
$$
\tag{2.A.24}
$$

The second term of (2.A.19) can be computed by acting with the exterior derivative on the above 1-forms and contracting the result with Γ-matrices. Notice that in order to compare with (2.A.22) one has to express the components of $dk_{(i)}$, $i = 1, 2, 3$ using the flat frame (2.2.5). Finally for the second term of (2.A.19) we find,

$$
\frac{1}{8}(dk_{(i)})_{\mu\nu}\Gamma^{\mu\nu}\epsilon = -k_{(i)}^\mu D_\mu\epsilon,\ \ i = 1, 2, 3, \tag{2.A.25}
$$

which means that the Lie-Lorentz derivative along the Killing vectors $k_{(i)}$, $i = 1, 2, 3$ vanishes.

In the case of the Donos-Gauntlett geometry (2.2.19) we notice that all the necessary expressions are quite similar to those computed in the previous subsection. This is because the only significant difference between the line element of the twisted geometries and that of the Donos-Gauntlett geometry is just a fiber term. As in the previous case, the Killing spinor does not depend on the isometry coordinates (θ_2, ϕ_2, ψ). This implies that the derivative term $k^\mu \partial_\mu \epsilon$ in eq. (2.A.19) has no contribution to the result. Then the first term of eq. (2.A.19), for each of the three Killing vectors, can be easily obtained from eq. (2.A.22) by setting $z = 0$. Similarly, if we set $z = 0$ into eq. (2.A.24) we find the 1-forms $k_{(1)}, k_{(2)}, k_{(3)}$ for the Donos-Gauntlett case. Once we know these 1-forms we can follow the same prescription as in the previous subsection and compute the second term of (2.A.19) for each Killing vector. It happens again that this term, when computed for every Killing vector, is related to the first term by a minus sign and thus the Lie-Lorentz derivative vanishes without imposing further projections on the Killing spinor.

Chapter 3

Unquenched massive flavored ABJM

3.1   Introduction

In section 1.3.1 we introduced the ABJM model, which is an $\mathcal{N} = 6$ supersymmetric $U(N) \times U(N)$ gauge theory with Chern-Simons levels k and $-k$, coupled to matter fields which transform in the bifundamental representations $(N, \bar{N})$ and $(\bar{N}, N)$ of the gauge group. When N and k are large the ABJM theory admits a gravity dual in type IIA supergravity in ten dimensions. The corresponding background is a geometry of the form $AdS_4 \times \mathbb{CP}^3$ with fluxes.

The ABJM model constitutes one of the most important examples of the AdS/CFT correspondence in which the high amount of supersymmetry allows to perform a large amount of checks and computations. Nevertheless, in its original formulation it only has fields in the bifundamental representation of the gauge group, and for condensed matter physics purposes it would be interesting to generalize it to a theory also with fundamental matter, *i.e.*, with fields transforming in the $(N, 1)$ and $(1, N)$ representations of the gauge group. In section 1.4.2 it was explained how to add fundamental matter to ABJM in the quenched approximation. Recall that in the supergravity description these flavors were added by considering D6-branes extended along the AdS_4 directions and wrapping a three-dimensional submanifold of $\mathbb{CP}^3$.

In order to go beyond the quenched approximation, one must be able to solve the supergravity equations of motion including the backreaction induced by the source terms generated by the flavor branes. The sources modify the Bianchi identities satisfied by the forms and the Einstein equations satisfied by the metric. These equations with sources are, in general, very difficult to solve, since they contain Dirac δ-functions whose support is the worldvolume of the branes. In order to bypass this difficulty we will follow the smearing approach, explained in section 1.4.1 . When the branes are introduced in this way there are no δ-function sources in the equations of motion and they become more tractable. This approach is valid in the so-called Veneziano limit [72], in which both N and N_f are large and their ratio N_f/N is fixed.

A holographic dual to ABJM with unquenched *massless* flavors in the Veneziano limit was found in [75]. In this setup the flavor branes fill the AdS_4 and are smeared in the internal $\mathbb{CP}^3$ space in such a way that $\mathcal{N} = 1$ supersymmetry is preserved. Notice, that since

the flavor branes are not coincident, the flavor symmetry is $U(1)^{N_f}$ rather than $U(N_f)$. A remarkable feature of the solution found in [75] is its simplicity and the fact that the ten-dimensional geometry is of the form $AdS_4 \times \mathcal{M}_6$, where $\mathcal{M}_6$ is a compact six-dimensional manifold whose metric is a squashed version of the unflavored Fubini-Study metric of $\mathbb{CP}^3$. The radii and squashing factors of this metric depend non-linearly on the flavor deformation parameter $\frac{N_f}{N}\lambda$, where $\lambda = N/k$ is the 't Hooft coupling of the theory. Moreover, the dilaton is also constant and, since the metric contains an AdS_4 factor, the background is the gravity dual of a three-dimensional conformal field theory with flavor. Actually, it was checked in perturbation theory in [135] that the ABJM theory has conformal fixed points even after the addition of flavor. This solution captures rather well many of the effects due to loops of the fundamentals in several observables [75]. Its generalization at non-zero temperature in [136] leads to thermodynamics which passes several non-trivial tests required to a flavored black hole.

Contrary to other backgrounds with unquenched flavors, the supergravity solutions dual to ABJM with smeared sources are free of pathologies, both at the IR and the UV. This fact offers us a unique opportunity to study different flavor effects holographically in a well-controlled setup. In this chapter, we will study such effects when *massive* flavors are considered. The addition of massive flavors breaks conformal invariance explicitly and, therefore, the corresponding dual geometry should not contain an Anti-de Sitter factor anymore. Actually, for massive flavors the quark mass is an additional parameter at our disposal which we can vary and see what is the effect on the geometry and observables. Indeed, let m_q denote the quark mass. In the IR limit in which m_q is very large we expect the quarks to be integrated out and their effects to disappear from the different observable quantities. Thus, in the IR limit we expect to find a geometry which reduces to the unflavored ABJM background. On the contrary, when $m_q \to 0$, we are in the UV regime and we should recover the deformed Anti-de Sitter background of [75]. The important point to stress here is that the quark mass triggers a non-trivial renormalization group flow between two fixed points and that we can vary m_q to enhance or suppress the effects due to the loops of the fundamentals.

To find the supergravity solutions along the flow, we will adopt an ansatz with brane sources in which the metric and forms are squashed as in [75]. By imposing the preservation of $\mathcal{N} = 1$ supersymmetry, the different functions of the ansatz must satisfy a system of first-order BPS equations, which reduce to a single second-order master equation. The full background can be reconstructed from the solution to the master equation.

The flavor branes corresponding to massive flavors do not extend over the full range of the holographic coordinate. Indeed, their tip should lie at a finite distance (related to the quark mass) from the IR end of the geometry. Moreover, in the asymptotic UV region, the geometry we are looking for should reduce to the one in [75], since the quarks should be effectively massless in that region. Therefore, we have to solve the BPS equations without sources at the IR and match this solution with another one in which the D6-brane charge is non-vanishing and such that it reduces to the massless flavored solution of [75] in the deep UV. Amazingly, we have been able to find an analytic solution in the region without sources which contains a free parameter which can be tuned in such a way that the background reduces to the massless flavored geometry in the asymptotic UV. This semi-analytic solution interpolates between two different conformal AdS geometries and contains the quark mass

and the number of flavors as control parameters.

With the supergravity dual at our disposal, we can study the holographic flow for different observables. The general picture we get from this analysis is the following. Let l be a length scale characterizing the observable. Then, the relevant parameter to explore the flow is the dimensionless quantity $m_q l$. When $m_q l$ is very large (small) the observable is dominated by the IR unflavored (UV massless flavored) conformal geometry, whereas for intermediate values of $m_q l$ we move away from the fixed points. We will put a special emphasis on the study of the holographic entanglement entropy, following the prescription of [95]. In particular, we study the refined entanglement entropy for a disk proposed in [137], which can be used as a central function for the F-theorem [138]. We check the monotonicity of the refined entropy along the flow (see [139] for a general proof of this monotonic character in three-dimensional theories). Other observables we analyze are the Wilson loop and quark-antiquark potential, the two-point functions of high-dimension bulk operators, and the mass spectrum of quark-antiquark bound states.

The rest of this chapter is divided into two parts. The first part starts in section 3.2 with a brief review of the ABJM solution. In section 3.3 we introduce the squashed ansatz, write the master equation for the BPS geometries with sources, and classify its solutions according to their UV behavior. In section 3.4 we write the analytic solution of the unflavored system that was mentioned above while, in section 3.5 we construct solutions which interpolate between an unflavored IR region and a UV domain with D6-brane sources. The backgrounds corresponding to ABJM flavors with a given mass are studied in section 3.6.

In the second part of the chapter we study the different observables. In section 3.7 we analyze the holographic entanglement entropy for a disk. section 3.8 is devoted to the calculation of the quark-antiquark potential from the Wilson loop. In section 3.9 we study the two-point functions of bulk operators with high mass, while the meson spectrum is obtained in section 3.10. Section 3.11 contains a summary of our results and some conclusions. The chapter is completed with several appendices with detailed calculations and extensions of the results of the main text.

3.2 Review of the ABJM solution

The ABJM theory was reviewed in detail in section 1.3.1, and in this section we will fix the notation for the expression of the metric, dilaton and forms in local coordinates. The ten-dimensional metric of the ABJM solution in string frame is given by:

$$ds^2 = L^2_{ABJM} \, ds^2_{AdS_4} + 4 \, L^2_{ABJM} \, ds^2_{\mathbb{CP}^3} \ , \tag{3.2.1}$$

where $ds^2_{AdS_4}$ and $ds^2_{\mathbb{CP}^3}$ are respectively the AdS_4 and $\mathbb{CP}^3$ metrics. The former, in Poincaré coordinates, is given by:

$$ds^2_{AdS_4} = r^2 \, dx^2_{1,2} + \frac{dr^2}{r^2} \ , \tag{3.2.2}$$

where $dx^2_{1,2}$ is the Minkowski metric in 2+1 dimensions. In (3.2.1) L_{ABJM} is the radius of the AdS_4 part of the metric and is given, in string units, by:

$$L^4_{ABJM} = 2\pi^2 \, \frac{N}{k} \ , \tag{3.2.3}$$

where N and k correspond, in the gauge theory dual, to the rank of the gauge groups and the Chern-Simons level, respectively. The ABJM background contains a constant dilaton, which can be written in terms of N and k as:

$$e^{\phi_{ABJM}} \;=\; \frac{2 L_{ABJM}}{k} \;=\; 2\sqrt{\pi} \left(\frac{2N}{k^5} \right)^{\frac{1}{4}} . \qquad (3.2.4)$$

Apart from the metric and the dilaton written above, the ABJM solution of type IIA supergravity contains a RR two-form F_2 and a RR four-form F_4, whose expressions can be written as:

$$F_2 \;=\; 2k\,J \;, \qquad\qquad F_4 \;=\; \frac{3}{2}\,k\,L_{ABJM}^2\,\Omega_{AdS_4} \;=\; \frac{3\pi}{\sqrt{2}}\,\sqrt{kN}\,\Omega_{AdS_4} \;, \qquad (3.2.5)$$

where J is the Kähler form of $\mathbb{CP}^3$ and Ω_{AdS_4} is the volume element of the AdS_4 metric (3.2.2). It follows from (3.2.5) that F_2 and F_4 are closed forms (*i.e.*, $dF_2 = dF_4 = 0$).

The metric of the $\mathbb{CP}^3$ manifold in (3.2.1) is the canonical Fubini-Study metric. Following the approach of [75], we will regard $\mathbb{CP}^3$ as an $\mathbb{S}^2$-bundle over $\mathbb{S}^4$, where the fibration is constructed by using the self-dual $SU(2)$ instanton on the four-sphere. This representation of $\mathbb{CP}^3$ is the one obtained when it is constructed as the twistor space of the four-sphere. As in [75], this $\mathbb{S}^4$-$\mathbb{S}^2$ representation will allow us to deform the ABJM background by squashing appropriately the metric and forms, while keeping some amount of supersymmetry. More explicitly, we will write $ds^2_{\mathbb{CP}^3}$ as:

$$ds^2_{\mathbb{CP}^3} \;=\; \frac{1}{4} \left[ds^2_{\mathbb{S}^4} + \left(dx^i + \epsilon^{ijk}\,A^j\,x^k \right)^2 \right] , \qquad (3.2.6)$$

where $ds^2_{\mathbb{S}^4}$ is the standard metric for the unit four-sphere, x^i ($i = 1, 2, 3$) are Cartesian coordinates that parameterize the unit two-sphere ($\sum_i (x^i)^2 = 1$) and A^i are the components of the non-abelian one-form connection corresponding to the $SU(2)$ instanton. Let us now introduce a specific system of coordinates to represent the metric (3.2.6) and the two-form F_2. First of all, let ω^i ($i = 1, 2, 3$) be a set of $SU(2)$ left-invariant one-forms satisfying $d\omega^i = \frac{1}{2}\,\epsilon_{ijk}\,\omega^j \wedge \omega^k$. Together with a new coordinate ξ, the ω^i's can be used to parameterize the metric of the four-sphere $\mathbb{S}^4$ as:

$$ds^2_{\mathbb{S}^4} \;=\; \frac{4}{(1+\xi^2)^2} \left[d\xi^2 + \frac{\xi^2}{4} \left((\omega^1)^2 + (\omega^2)^2 + (\omega^3)^2 \right) \right] , \qquad (3.2.7)$$

where $0 \le \xi < +\infty$ is a non-compact coordinate. The $SU(2)$ instanton one-forms A^i can be written in these coordinates as:

$$A^i \;=\; -\frac{\xi^2}{1+\xi^2}\,\omega^i \;. \qquad (3.2.8)$$

Let us next parameterize the x^i coordinates of the unit $\mathbb{S}^2$ by two angles θ and φ ($0 \le \theta < \pi$, $0 \le \varphi < 2\pi$),

$$x^1 \;=\; \sin\theta\,\cos\varphi \;, \qquad\qquad x^2 \;=\; \sin\theta\,\sin\varphi \;, \qquad\qquad x^3 \;=\; \cos\theta \;. \qquad (3.2.9)$$

Then, it is straightforward to demonstrate that the $\mathbb{S}^2$ part of the Fubini-Study metric can be written as:

$$\left(dx^i + \epsilon^{ijk}\,A^j\,x^k \right)^2 \;=\; (E^1)^2 + (E^2)^2 \;, \qquad (3.2.10)$$

where E^1 and E^2 are the following one-forms:

$$E^1 = d\theta + \frac{\xi^2}{1+\xi^2} \left(\sin\varphi\,\omega^1 - \cos\varphi\,\omega^2\right),$$

$$E^2 = \sin\theta \left(d\varphi - \frac{\xi^2}{1+\xi^2}\,\omega^3\right) + \frac{\xi^2}{1+\xi^2}\,\cos\theta \left(\cos\varphi\,\omega^1 + \sin\varphi\,\omega^2\right). \quad (3.2.11)$$

Therefore, the $\mathbb{CP}^3$ metric can be written in terms of the one-forms defined above as:

$$ds^2_{\mathbb{CP}^3} = \frac{1}{4}\left[ds^2_{\mathbb{S}^4} + (E^1)^2 + (E^2)^2\right]. \quad (3.2.12)$$

We will now write the expression of F_2 in such a way that the $\mathbb{S}^4$-$\mathbb{S}^2$ split structure is manifest. Accordingly, we define three new one-forms S^i ($i = 1, 2, 3$) as:

$$S^1 = \sin\varphi\,\omega^1 - \cos\varphi\,\omega^2,$$

$$S^2 = \sin\theta\,\omega^3 - \cos\theta \left(\cos\varphi\,\omega^1 + \sin\varphi\,\omega^2\right),$$

$$S^3 = -\cos\theta\,\omega^3 - \sin\theta \left(\cos\varphi\,\omega^1 + \sin\varphi\,\omega^2\right). \quad (3.2.13)$$

Notice that the S^i are just the ω^i rotated by the two angles θ and φ. In terms of the forms defined in (3.2.13) the line element of the four-sphere is obtained by substituting $\omega^i \to S^i$ in (3.2.7). Let us next define the one-forms $\mathcal{S}^\xi$ and $\mathcal{S}^i$ as:

$$\mathcal{S}^\xi = \frac{2}{1+\xi^2}\,d\xi, \qquad \mathcal{S}^i = \frac{\xi}{1+\xi^2}\,S^i, \qquad (i = 1, 2, 3), \quad (3.2.14)$$

in terms of which the metric of the four-sphere is $ds^2_{\mathbb{S}^4} = (\mathcal{S}^\xi)^2 + \sum_i (\mathcal{S}^i)^2$. Moreover, the RR two-form F_2 in (3.2.5) can be written in terms of the one-forms defined in (3.2.11) and (3.2.14) as:

$$F_2 = \frac{k}{2}\left(E^1 \wedge E^2 - \left(\mathcal{S}^\xi \wedge \mathcal{S}^3 + \mathcal{S}^1 \wedge \mathcal{S}^2\right)\right). \quad (3.2.15)$$

The solution of type IIA supergravity reviewed above is a good gravity dual of the $U(N)_k \times U(N)_{-k}$ ABJM field theory when the AdS radius L_{ABJM} is large in string units and when the string coupling constant e^ϕ is small. From (3.2.3) and (3.2.4) it is straightforward to prove that these conditions are satisfied if k and N are in the range $N^{\frac{1}{5}} \ll k \ll N$.

3.3 Squashed solutions

Let us consider the deformations of the ABJM background which preserve the $\mathbb{S}^4$-$\mathbb{S}^2$ splitting. These deformed backgrounds will solve the equations of motion of type IIA supergravity (with sources) and will preserve at least two supercharges. We will argue below that some of these backgrounds are dual to Chern-Simons matter theories with fundamental massive flavors.

The general ansatz for the ten-dimensional metric of our solutions in string frame takes the form:

$$ds_{10}^2 = h^{-1/2}dx_{1,2}^2 + h^{1/2}\left[dr^2 + e^{2f}ds_{\mathbb{S}^4}^2 + e^{2g}\left(\left(E^1\right)^2 + \left(E^2\right)^2\right)\right], \tag{3.3.16}$$

where the warp factor h and the functions f and g depend on the holographic coordinate r. Notice that f and g determine the sizes of the $\mathbb{S}^4$ and $\mathbb{S}^2$ within the internal manifold. Actually, their difference $f-g$ determines the squashing of the $\mathbb{CP}^3$ and will play an important role in characterizing our solutions. We will measure this squashing by means of the function q, defined as:

$$q \equiv e^{2f-2g}. \tag{3.3.17}$$

Clearly, the ABJM solution has $q = 1$. A departure from this value would signal a non-trivial deformation of the metric. Similarly, the RR two- and four-forms will be given by:

$$F_4 = K\,d^3x \wedge dr, \tag{3.3.18}$$

$$F_2 = \frac{k}{2}\left(E^1 \wedge E^2 - \eta\left(\mathcal{S}^\xi \wedge \mathcal{S}^3 + \mathcal{S}^1 \wedge \mathcal{S}^2\right)\right), \tag{3.3.19}$$

where k is a constant and $K = K(r)$, $\eta = \eta(r)$ are new functions. The background is also endowed with a dilaton $\phi = \phi(r)$. As compared with the ABJM value (3.2.15), the expression of F_2 in our ansatz contains the function $\eta(r)$ which generically introduces an asymmetry between the $\mathbb{S}^4$ and $\mathbb{S}^2$ terms. Moreover, when $\eta \neq 1$ the two-form F_2 is no longer closed and the corresponding Bianchi indentity is violated. Indeed, one can check that:

$$dF_2 = -\frac{k}{2}\,(\eta-1)\left[E^1 \wedge (\mathcal{S}^\xi \wedge \mathcal{S}^2 - \mathcal{S}^1 \wedge \mathcal{S}^3) + E^2 \wedge (\mathcal{S}^\xi \wedge \mathcal{S}^1 + \mathcal{S}^2 \wedge \mathcal{S}^3)\right] - $$

$$-\frac{k}{2}\,\eta'\,dr \wedge \left(\mathcal{S}^\xi \wedge \mathcal{S}^3 + \mathcal{S}^1 \wedge \mathcal{S}^2\right). \tag{3.3.20}$$

The violation of the Bianchi identity of F_2 means that we have D6-brane sources in our model. Indeed, since $F_2 = *F_8$, if $dF_2 \neq 0$ then the Maxwell equation of F_8 contains a source term, which is due to the presence of D6-branes since the latter are electrically charged with respect to F_8. The charge distribution of the D6-brane sources is determined by the function η, which we will call the profile function.

The function K of the RR four-form can be related to the other functions of the ansatz by using its equation of motion $d*F_4 = 0$ and the flux quantization condition for the integral of $*F_4$ over the internal manifold. The result is [75]:

$$K = 3\pi^2\,N\,h^{-2}\,e^{-4f-2g}, \tag{3.3.21}$$

where the integer N is identified with the ranks of the gauge groups in the gauge theory dual (*i.e.*, with the number of colors).

It is convenient to introduce a new radial variable x, related to r through the differential equation:

$$x\,\frac{dr}{dx} = e^g. \tag{3.3.22}$$

From now on, all functions of the holographic variable are considered as functions of x, unless otherwise specified. The ten-dimensional metric in this new variable takes the form:

$$ds_{10}^2 = h^{-\frac{1}{2}} dx_{1,2}^2 + h^{\frac{1}{2}} \left[e^{2g} \frac{dx^2}{x^2} + e^{2f} ds_{\mathbb{S}^4}^2 + e^{2g} \left(\left(E^1 \right)^2 + \left(E^2 \right)^2 \right) \right] . \tag{3.3.23}$$

It was shown in [75] that the background given by the ansatz written above preserves $\mathcal{N} = 1$ supersymmetry in three dimensions if the functions satisfy a system of first-order differential equations. It turns out that this BPS system can be reduced to a unique second-order differential equation for a particular combination of the functions of the ansatz. The details of this reduction are given in appendix 3.A.1. Here we will just present the final result of this analysis. First of all, let us define the function $W(x)$ as:

$$W(x) \equiv \frac{4}{k} h^{\frac{1}{4}} e^{2f-g-\phi} x . \tag{3.3.24}$$

Then, the BPS system can be reduced to the following second-order non-linear differential equation for $W(x)$:

$$W'' + 4\eta' + (W' + 4\eta) \left[\frac{W' + 10\eta}{3W} - \frac{W' + 4\eta + 6}{x(W' + 4\eta)} \right] = 0 . \tag{3.3.25}$$

We will refer to (3.3.25) as the master equation and to $W(x)$ as the master function. Interestingly, the BPS equations do not constrain the profile function η. Therefore, we can choose $\eta(x)$ (which will fix the type of supersymmetric sources of our system) and afterwards we can solve (3.3.25) for $W(x)$. Given $\eta(x)$ and $W(x)$ one can obtain the other functions that appear in the metric. Indeed, as proved in appendix 3.A.1, $g(x)$ and $f(x)$ are given by:

$$e^{g(x)} = \frac{x}{W^{\frac{1}{3}}} \exp \left[\frac{2}{3} \int^x \frac{\eta(\xi)d\xi}{W(\xi)} \right] ,$$

$$e^{f(x)} = \sqrt{\frac{3x}{W' + 4\eta}} W^{\frac{1}{6}} \exp \left[\frac{2}{3} \int^x \frac{\eta(\xi)d\xi}{W(\xi)} \right] , \tag{3.3.26}$$

while the warp factor h can be written as:

$$h(x) = 4\pi^2 \frac{N}{k} e^{-g} (W' + 4\eta) \left[\int_x^{\infty} \frac{\xi e^{-3g(\xi)}}{W(\xi)^2} d\xi + \beta \right] , \tag{3.3.27}$$

where β is a constant that determines the behavior of h as $x \to \infty$ ($\beta = 0$ if we impose that $h \to 0$ as $x \to \infty$). Finally, the dilaton is given by:

$$e^{\phi(x)} = \frac{12}{k} \frac{x h^{\frac{1}{4}}}{W^{\frac{1}{3}}(W' + 4\eta)} \exp \left[\frac{2}{3} \int^x \frac{\eta(\xi)d\xi}{W(\xi)} \right] . \tag{3.3.28}$$

From the expression of f and g in (3.3.26) it follows that the squashing function q can be written in terms of the master function W and its derivative as:

$$q = \frac{3W}{x(W' + 4\eta)} . \tag{3.3.29}$$

3.3.1   Classification of solutions

Let us study the behavior of the solutions of the master equation in the UV region $x \to \infty$. This analysis will allow us to have a classification of the different solutions. We will assume that the profile function $\eta(x)$ reaches a constant value as $x \to \infty$, and we will denote:

$$\lim_{x\to\infty} \eta(x) = \eta_0 . \tag{3.3.30}$$

Let us restrict ourselves to the case in which $\eta_0 \neq 0$. We will assume that $W(x)$ behaves for large x as:

$$W(x) \approx A_0\, x^\alpha , \qquad\qquad x \to \infty , \tag{3.3.31}$$

where A_0 and α are constants. It is easy to check that this type of behavior is consistent only when the exponent $\alpha \geq 1$ or, in other words, when $W(x)$ grows at least as a linear function of x when $x \to \infty$.

We will also characterize the different solutions by the asymptotic value of the squashing function q, which determines the deformation of the internal manifold in the UV. Let us denote

$$q_0 = \lim_{x\to\infty} q(x) . \tag{3.3.32}$$

It follows from (3.3.29) that the asymptotic value of the squashing function and that of the profile function are closely related. Actually, this relation depends on whether the exponent α in (3.3.31) is strictly greater or equal to one. Indeed, plugging the asymptotic behavior (3.3.31) in (3.3.29) one immediately proves that:

$$q_0 = \begin{cases} \frac{3}{\alpha} , & \text{for } \alpha > 1 , \\[2ex] \frac{3A_0}{A_0 + 4\eta_0} , & \text{for } \alpha = 1 . \end{cases} \tag{3.3.33}$$

This result indicates that we have to study separately the cases $\alpha > 1$ and $\alpha = 1$. As we show in the next two subsections these two different asymptotics correspond to two qualitatively different types of solutions.

The asymptotic G_2 cone

Let us assume that the master function behaves as in (3.3.31) for some $\alpha > 1$. By plugging this asymptotic form in the master equation (3.3.25) and keeping the leading terms as $x \to \infty$, one readily verifies that the coefficient A_0 is not constrained and that the exponent α takes the value:

$$\alpha = \frac{3}{2} . \tag{3.3.34}$$

Therefore, it follows from (3.3.33) that the asymptotic squashing is:

$$q_0 = 2 . \tag{3.3.35}$$

Let us evaluate the asymptotic form of all the functions of the metric. From (3.3.26), we get, at leading order:

$$e^g \approx C \sqrt{x} , \tag{3.3.36}$$

where C is a constant of integration. Moreover, since $q_0 = 2$, the asymptotic value of the function f is:

$$e^f \approx \sqrt{2}\, C\, \sqrt{x}\ . \tag{3.3.37}$$

Let us now evaluate the warp factor h from (3.3.27). Clearly, we have to compute the integral:

$$\int_x^\infty \frac{\xi\, e^{-3g(\xi)}}{W(\xi)^2}\, d\xi \sim x^{-\frac{5}{2}}\ , \tag{3.3.38}$$

which vanishes when $x \to \infty$. Therefore, by choosing the constant β in (3.3.27) to be non-vanishing we can neglect the integral (3.3.38) and, since $e^g\, W' \to$ constant, then the warp factor h becomes also a constant when $x \to \infty$. To clarify the nature of the asymptotic metric, let us change variables, from x to a new radial variable ρ, defined as $\rho = 2C\sqrt{x}$. Then, after some constant rescalings of the coordinates the metric becomes:

$$ds_{10}^2 \approx dx_{1,2}^2 + ds_7^2\ , \tag{3.3.39}$$

where ds_7^2 is:

$$ds_7^2 = d\rho^2 + \frac{\rho^2}{4}\left[2ds_{\mathbb{S}^4}^2 + \left(E^1\right)^2 + \left(E^2\right)^2\right]\ . \tag{3.3.40}$$

The metric (3.3.40) is a Ricci flat cone with G_2 holonomy, whose principal orbits at fixed ρ are $\mathbb{CP}^3$ manifolds with a squashed Einstein metric. In the asymptotic region of large ρ the line element (3.3.40) coincides with the metric of the resolved Ricci flat cone found in [140], which was constructed from the bundle of self-dual two-forms over $\mathbb{S}^4$ and is topologically $\mathbb{S}^4 \times \mathbb{R}^3$ (see [141] for applications of this manifold to the study of the dynamics of M-theory).

The asymptotic AdS metric

Let us now explore the second possibility for the exponent α in (3.3.31), namely $\alpha = 1$. In this case the coefficient A_0 cannot be arbitrary. Indeed, by analyzing the master equation as $x \to \infty$ we find that A_0 and η_0 must be related as:

$$A_0^2 + (9 - \eta_0)\, A_0 - 20\, \eta_0^2 = 0\ . \tag{3.3.41}$$

On the other hand, A_0 should be related to the asymptotic squashing q_0 as in (3.3.33), which we now write as:

$$A_0 = \frac{4q_0}{3 - q_0}\, \eta_0\ . \tag{3.3.42}$$

By plugging (3.3.42) into (3.3.41) we arrive at the following quadratic relation between q_0 and η_0:

$$q_0^2 - 3(1 + \eta_0)\, q_0 + 5\eta_0 = 0\ . \tag{3.3.43}$$

Using this equation we can re-express A_0 as:

$$A_0 = \frac{q_0(\eta_0 + q_0)}{2 - q_0}\ . \tag{3.3.44}$$

Moreover, we can solve (3.3.43) for q_0 and obtain the following two possible asymptotic squashings in terms of η_0:

$$q_0^{\pm} = \frac{1}{2}\left[3 + 3\eta_0 \mp \sqrt{9\eta_0^2 - 2\eta_0 + 9}\right] . \tag{3.3.45}$$

Thus, there are two possible branches in this case, corresponding to the two signs in (3.3.45). In this chapter we will only consider the q_0^+ case, since this is the one which has the same asymptotics as the ABJM solution when there are no D6-brane sources. Indeed, (3.3.45) gives $q_0^+ = 1$ when $\eta_0 = 1$, which means that the internal manifold in the deep UV is just the un-squashed $\mathbb{CP}^3$ (when $\eta_0 = 1$ there are no D6-brane sources in the UV, see (3.3.20)).

Let us now study in detail the asymptotic metric in the UV corresponding to the $x \to \infty$ squashing q_0^+ (which from now on we simply denote as q_0). By substituting $\eta \to \eta_0$ and $W \to A_0 x$ in (3.3.26) and performing the integral, we get:

$$e^{g(x)} \approx C\, x^{\frac{2}{3}\left(1 + \frac{\eta_0}{A_0}\right)} , \tag{3.3.46}$$

where C is a constant of integration. Using (3.3.42) this expression can be rewritten as:

$$e^{g(x)} \approx C\, x^{\frac{1}{b}} , \tag{3.3.47}$$

where b is given by:

$$b = \frac{2\,q_0}{q_0 + 1} . \tag{3.3.48}$$

The remaining functions of the metric can be found in a similar way. We get for f and h the following asymptotic expressions:

$$e^{f(x)} \approx C\,\sqrt{q_0}\, x^{\frac{1}{b}} , \qquad\qquad h(x) \approx 4\pi^2\,\frac{N}{k}\,\frac{2-b}{C^4\,A_0}\,\frac{1}{x^{\frac{4}{b}}} . \tag{3.3.49}$$

Let us write the above expressions in terms of the original r variable, which can be related to x by integrating the equation:

$$x\,\frac{dr}{dx} = e^g \approx C\, x^{\frac{1}{b}} . \tag{3.3.50}$$

For large x we get:

$$r \approx b\,C\, x^{\frac{1}{b}} , \tag{3.3.51}$$

and the functions g, f, and h can be written in terms of r as:

$$e^g \approx \frac{r}{b} , \qquad\qquad e^f \approx \frac{\sqrt{q_0}}{b}\, r , \qquad\qquad h \approx \frac{L_0^4}{r^4} , \tag{3.3.52}$$

where L_0 is given by:

$$L_0^4 = 4\pi^2\,\frac{N}{k}\,\frac{(2-b)\,b^4}{A_0} . \tag{3.3.53}$$

In terms of the asymptotic values η_0 and q_0, L_0 can be written as:

$$L_0^4 = 128\pi^2 \frac{N}{k} \frac{(2 - q_0)\, q_0^3}{(\eta_0 + q_0)\,(q_0 + 1)^5}\ . \tag{3.3.54}$$

Using these results we find that the asymptotic metric takes the form:

$$ds^2 \approx L_0^2\, ds_{AdS_4}^2 + \frac{L_0^2}{b^2}\left[q_0\, ds_{\mathbb{S}^4}^2 + (E^1)^2 + (E^2)^2 \right]\ , \tag{3.3.55}$$

where we have rescaled the Minkowski coordinates as $x^\mu \to L_0^2\, x^\mu$. The metric (3.3.55) corresponds to the product of AdS_4 space with radius L_0 and a squashed $\mathbb{CP}^3$. The parameter b will play an important role in the following. Its interpretation is rather clear from (3.3.55): it represents the relative squashing of the $\mathbb{CP}^3$ part of the asymptotic metric with respect to the AdS_4 part.

It is now straightforward to show that in the UV the dilaton reaches a constant value ϕ_0, related to q_0 and η_0 as:

$$e^{\phi_0} \approx 4\sqrt{2\pi}\left[\frac{(2 - q_0)^5}{q_0\,(q_0 + 1)\,(\eta_0 + q_0)^5} \right]^{\frac{1}{4}} \left(\frac{2N}{k^5} \right)^{\frac{1}{4}}\ , \tag{3.3.56}$$

while the RR four-form approaches the value:

$$F_4 \approx 12\sqrt{2}\,\pi \left[\frac{q_0^5\,(\eta_0 + q_0)}{(2 - q_0)\,(q_0 + 1)^7} \right]^{\frac{1}{2}} \sqrt{k\,N}\ \Omega_{AdS_4}\ , \tag{3.3.57}$$

where Ω_{AdS_4} is the volume element of AdS_4.

Interestingly, when the profile function η is constant and equal to η_0, the metric, dilaton, and forms written above solve the BPS equations not only in the UV, but also in the full domain of the holographic coordinate. Equivalently, $W = A_0\, x$ is an exact solution to the master equation (3.3.25) if η is constant and equal to η_0 and A_0 is given by (3.3.42). Actually, when $\eta_0 = 1$ one can check that $q_0 = b = 1$ and the asymptotic background becomes the ABJM solution ($W = 2x$ for this case). Moreover, when $\eta = \eta_0 > 1$ the background corresponds[1] to the one found in [75] for the ABJM model with unquenched massless flavors, if one identifies η_0 with $1 + \frac{3N_f}{4k}$, where N_f is the number of flavors.

The main objective of this chapter is the construction of solutions which interpolate between the $\eta = 1$ ABJM background in the IR and the AdS_4 asymptotics with $\eta_0 > 1$ in the UV. Equivalently, we are looking for backgrounds such that the squashing function $q(x)$ varies from the value $q = 1$ when $x \to 0$ to $q = q_0 > 1$ for $x \to \infty$. These backgrounds naturally

---

[1] Notice that the expression for b written in (3.3.48) is equivalent to the one obtained in [75], namely:

$$b = \frac{q_0(\eta_0 + q_0)}{2(q_0 + \eta q_0 - \eta_0)}\ .$$

In order to check this equivalence it is convenient to use the following relation between q_0 and η_0: $q_0 + \eta_0 q_0 - \eta_0 = (q_0 + 1)\,(\eta_0 + q_0)/4$.

correspond to gravity duals of Chern-Simons matter models with massive unquenched flavors. In the next section we present a one-parameter family of analytic unflavored solutions which coincide with the ABJM background in the deep IR and that have a squashing function q which grows as we move towards the UV. In sections 3.5 and 3.6 we show that these running solutions can be used to construct the gravity duals to massive flavor that we are looking for.

3.4   The unflavored system

In this section we will consider the particular case in which the profile is $\eta = 1$. In this case $dF_2 = 0$ and there are no flavor sources. It turns out that one can find a particular analytic solution of the BPS system written in appendix 3.A.1. This solution was found in [75] in a power series expansion around the IR. Amazingly, this series can be summed exactly and a closed analytic form can be written for all functions. Let us first write them in the coordinate r. The functions f and g are given by:

$$e^f = r \sqrt{\frac{1 + c\,r}{1 + 2c\,r}} \,, \qquad\qquad e^g = r\, \frac{1 + c\,r}{1 + 2c\,r} \,, \qquad (3.4.58)$$

where c is a constant. For $c = 0$ this solution is ABJM without flavor (*i.e.*, $AdS_4 \times \mathbb{CP}^3$ with fluxes), while for $c \neq 0$ it is a running background which reduces to ABJM in the IR, $r \to 0$. The squashing function q can be immediately obtained from (3.4.58):

$$q = \frac{1 + 2c\,r}{1 + c\,r} \,. \qquad (3.4.59)$$

For $c \neq 0$ the squashing function q interpolates between the ABJM value $q = 1$ in the IR and the UV value:

$$q_0 = 2 \,. \qquad (3.4.60)$$

The warp factor for this solution is:

$$h(r) = \frac{2\pi^2 N}{k} \frac{(1 + 2c\,r)^2}{r^4 (1 + c\,r)^2} \left[1 + 2c\,r\Big(3cr(1 + 2c\,r) - 1\Big) + \right.$$

$$\left. + 12c^3 (1 + c\,r)\,r^3 \left(\log\left[\frac{cr}{1 + cr}\right] + \alpha \right) \right] \,, \qquad (3.4.61)$$

where α is a constant which has to be fixed by adjusting the behavior of the metric in the UV. Finally, the dilaton can be related to the warp factor as:

$$e^\phi = \frac{2}{k} \frac{1 + c\,r}{(1 + 2c\,r)^2} r\, h^{\frac{1}{4}} \,. \qquad (3.4.62)$$

Let us now re-express this running analytic solution in terms of the variable x, related to r by (3.3.22), which in the present case becomes:

$$\frac{1}{x} \frac{dx}{dr} = \frac{1 + 2c\,r}{(1 + c\,r)r} \,. \qquad (3.4.63)$$

This equation can be easily integrated:

$$\gamma\, x \;=\; c\, r(1 + c\, r)\,, \tag{3.4.64}$$

where γ is a constant of integration which parameterizes the freedom from passing to the x variable. By solving (3.4.64) for r we get:

$$r \;=\; \frac{1}{2c}\left[\sqrt{1 + 4\,\gamma\, x} - 1\right]\,. \tag{3.4.65}$$

It is straightforward to write the functions f and g in terms of x:

$$e^f \;=\; \frac{\gamma}{c}\, x \left[\frac{2}{\sqrt{1 + 4\,\gamma\, x}\,(\sqrt{1 + 4\,\gamma\, x} + 1)}\right]^{\frac{1}{2}},$$

$$e^g \;=\; \frac{\gamma}{c}\, \frac{x}{\sqrt{1 + 4\,\gamma\, x}}\,, \tag{3.4.66}$$

while the squashing function is:

$$q \;=\; 2\,\frac{\sqrt{1 + 4\,\gamma\, x}}{1 + \sqrt{1 + 4\,\gamma\, x}}\,. \tag{3.4.67}$$

The warp factor h in terms of the x variable is:

$$h \;=\; \frac{8\pi^2 N c^4}{k}\left(1 + \frac{1}{4\gamma\, x}\right)\left[\left(\frac{1}{2} + 6\gamma\, x + \frac{1 + (1 - 6\gamma\, x)\sqrt{1 + 4\,\gamma\, x}}{4\gamma\, x}\right)\frac{\sqrt{1 + 4\,\gamma\, x} + 1}{\gamma^2\, x^2} + \right.$$

$$\left. + 24\,\log\left[\frac{\sqrt{4\,\gamma\, x}}{\sqrt{1 + 4\,\gamma\, x} + 1}\right] + \alpha\right]\,. \tag{3.4.68}$$

By choosing appropriately the constant α in (3.4.68) this running solution behaves as the G_2-cone in the UV region $x \to \infty$. The dilaton as a function of x is:

$$e^\phi \;=\; \frac{2}{k}\,\frac{\gamma}{c}\,\frac{x}{1 + 4\,\gamma\, x}\,h^{\frac{1}{4}}\,. \tag{3.4.69}$$

Working in the variable x, it is very interesting to find the function $W(x)$. For the solution described above, W can be found by plugging the different functions in the definition (3.3.24). We find:

$$W(x) \;=\; \frac{4\,(1 + 4\,\gamma\, x)\, x}{1 + \sqrt{1 + 4\,\gamma\, x}}\,. \tag{3.4.70}$$

One can readily check that the function written in (3.4.70) solves the master equation (3.3.25) for $\eta = 1$. For large x, the function $W(x)$ behaves as:

$$W \sim 8\sqrt{\gamma}\, x^{\frac{3}{2}}\,, \tag{3.4.71}$$

which corresponds to an exponent $\alpha = 3/2$ in (3.3.31). This is consistent with the asymptotic value $q_0 = 2$ of the squashing found above.

Let us finally point out that we have checked explicitly that the geometry discussed in this section is free of curvature singularities.

3.5 Interpolating solutions

Let us now construct solutions to the BPS equations which interpolate between an IR region in which there are no D6-brane sources (*i.e.*, with $\eta = 1$) and a UV region in which $\eta > 1$ and, therefore, the Bianchi identity of F_2 is violated. In the r variable the profile $\eta(r)$ will be such that $\eta(r) = 1$ for $r \leq r_q$, while $\eta(r) > 1$ for $r > r_q$. In the region $r \leq r_q$ our interpolating solutions will reduce to the unflavored running solution of section 3.4 for some value of the constant c. In order to match this solution with the one in the region $r > r_q$ it is convenient to work in the x coordinate (3.4.64). The point $r = r_q$ will correspond to some $x = x_q$. Notice, however, that we have some freedom in performing the $r \to x$ change of variables. This freedom is parameterized by the constant γ in (3.4.64). We will fix this freedom by requiring that $x_q = 1$, *i.e.*, that the transition between the unflavored and flavored region takes place at the point $x = 1$. Then, (3.4.64) immediately implies that γ is given in terms of c and r_q:

$$\gamma = c\, r_q \, (1 + c\, r_q) \ . \tag{3.5.72}$$

We will use (3.5.72) to eliminate the constant c in favor of r_q and γ. Actually, if we define $\hat{\gamma}$ as:

$$\hat{\gamma} \equiv \sqrt{1 + 4\gamma} \ , \tag{3.5.73}$$

then c is given by

$$c = \frac{\hat{\gamma} - 1}{2\, r_q} \ . \tag{3.5.74}$$

In this running solution the squashing factor q is equal to one in the deep IR at $x = 0$. When $x > 0$ the function $q(x)$ grows monotonically until it reaches a certain value $\hat{q}$ at $x = 1$, which is related to the parameter $\hat{\gamma}$ as:

$$\hat{\gamma} = \frac{\hat{q}}{2 - \hat{q}} . \tag{3.5.75}$$

In the region $x \geq 1$ we have to solve the master equation (3.3.25) with $\eta(x) > 1$ and initial conditions given by the values of W and W' attained by the unflavored running solution at $x = 1$. These values depend on the parameter $\hat{\gamma}$. They can be straightforwardly found by taking $x = 1$ in the function (3.4.70) and in its derivative. We find:

$$W(x = 1) = \frac{4\,\hat{\gamma}^2}{1 + \hat{\gamma}} \ , \qquad W'(x = 1) = 6\,\hat{\gamma} - 4 \ . \tag{3.5.76}$$

Let us now write the different functions of these interpolating solutions in the two regions $x \leq 1$ and $x \geq 1$. For $x \leq 1$ we have to rewrite (3.4.66) after eliminating the constant c by using (3.5.74) (which implies that $\gamma/c = (\hat{\gamma} + 1)\, r_q/2$). For the functions f, g, and the

dilaton ϕ we get:

$$
e^f = r_q \frac{\hat{\gamma}+1}{\sqrt{2}} \frac{x}{\left[\sqrt{1+4\,\gamma\,x}\,(\sqrt{1+4\,\gamma\,x}+1)\right]^{\frac{1}{2}}} \, ,
$$

$$
e^g = r_q \frac{\hat{\gamma}+1}{2} \frac{x}{\sqrt{1+4\,\gamma\,x}} \, , \qquad (x \leq 1) \, ,
$$

$$
e^\phi = r_q \frac{\hat{\gamma}+1}{k} \frac{x}{1+4\,\gamma\,x} h^{\frac{1}{4}} \, , \qquad\qquad (3.5.77)
$$

where h is the function written in (3.4.68) for $c = (\hat{\gamma}-1)/(2\,r_q)$. By using the general equations of section 3.3, the solution for $x \geq 1$ can be written in terms of $W(x)$, which can be obtained by numerical integration of the master equation with initial conditions (3.5.76). This defines a solution in the full range of x for every γ and r_q. Notice that (3.3.26), (3.3.27), and (3.3.28) contain arbitrary multiplicative constants, which we will fix by imposing continuity of f, g, and h at $x = 1$. We get for f, g and ϕ:

$$
e^f = r_q \left[\frac{(\hat{\gamma}+1)^2}{2\,\hat{\gamma}}\right]^{\frac{1}{3}} \sqrt{\frac{3x}{W'+4\eta}} \; W^{\frac{1}{6}} \; \exp\left[\frac{2}{3}\int_1^x \frac{\eta(\xi)d\xi}{W(\xi)}\right] \, ,
$$

$$
e^g = r_q \left[\frac{(\hat{\gamma}+1)^2}{2\,\hat{\gamma}}\right]^{\frac{1}{3}} \frac{x}{W^{\frac{1}{3}}} \; \exp\left[\frac{2}{3}\int_1^x \frac{\eta(\xi)d\xi}{W(\xi)}\right] \, , \qquad (x \geq 1) \, ,
$$

$$
e^\phi = r_q \left[\frac{(\hat{\gamma}+1)^2}{2\,\hat{\gamma}}\right]^{\frac{1}{3}} \frac{12}{k} \frac{x\,h^{\frac{1}{4}}}{W^{\frac{1}{3}}(W'+4\eta)} \; \exp\left[\frac{2}{3}\int_1^x \frac{\eta(\xi)d\xi}{W(\xi)}\right] \, . \qquad (3.5.78)
$$

The warp factor $h(x)$ for $x \geq 1$ is given by (3.3.27), where the integration constant β is related to the constant α of (3.4.68) by the following matching condition at $x = 1$:

$$
\lim_{x\to 1^-} h(x) = \lim_{x\to 1^+} h(x) \, . \qquad\qquad (3.5.79)
$$

For a given profile function $\eta(x)$, the solution described above depends on the parameter γ, which determines $W(x)$ for $x \leq 1$ through (3.4.70) and sets the initial conditions (3.5.76) needed to integrate the master equation in the $x \geq 1$ region. The solution $W(x)$ obtained numerically in this way grows generically as $x^{3/2}$ for large x which, according to our analysis in section 3.3.1, gives rise to the geometry of the G_2-cone in the UV. We are, actually, interested in obtaining solutions with the *AdS* asymptotics discussed in section 3.3.1, for a set of profiles that correspond to flavor D6-branes with a non-zero quark mass. In order to get these geometries we have to fine-tune the parameter γ to some precise value which depends on the number of flavors. This analysis is presented in the next section.

3.6 Massive flavor

We now apply the formalism developed so far to find supergravity backgrounds representing massive flavors in ABJM. These solutions will depend on a deformation parameter $\hat{\epsilon}$, related

to the total number of flavors N_f and the Chern-Simons level k as:

$$\hat{\epsilon} \equiv \frac{3N_f}{4k} \ , \tag{3.6.80}$$

where the factor $3/4$ is introduced for convenience and N_f/k is just $\frac{N_f}{N}\lambda$ with $\lambda = N/k$ being the 't Hooft coupling. The profile η, which corresponds to a set of smeared flavor D6-branes ending at $r = r_q$, has been found in [75]. The main technique employed in [75] was the comparison between the smeared brane action for the distribution of flavor branes and the action for a fiducial embedding in a background of the type studied here. This fiducial embedding was determined by using kappa symmetry. With our present conventions,[2] assuming as above that $r = r_q$ corresponds to $x = x_q = 1$, the function $\eta(x)$ is given by:

$$\eta(x) = 1 + \hat{\epsilon}\left(1 - \frac{1}{x^2}\right)\Theta(x - 1) \ , \tag{3.6.81}$$

where $\Theta(x)$ is the Heaviside step function. It follows from (3.6.81) that the asymptotic value η_0 of the profile is:

$$\eta_0 = 1 + \hat{\epsilon} \ . \tag{3.6.82}$$

We want to find interpolating solutions of the type studied in section 3.5 which have the AdS asymptotic behavior in the UV corresponding to the value of η_0 written in (3.6.82). These solutions have an asymptotic squashing (corresponding to q_0^+ in (3.3.45)) given in terms of $\hat{\epsilon}$ as:

$$q_0 = 3 + \frac{3}{2}\hat{\epsilon} - 2\sqrt{1 + \hat{\epsilon} + \frac{9}{16}\hat{\epsilon}^2} \ . \tag{3.6.83}$$

It follows from (3.6.83) that the asymptotic squashing q_0 grows with the deformation parameter $\hat{\epsilon}$. Indeed, $q_0 = 1$ for $\hat{\epsilon} = 0$, whereas for $\hat{\epsilon} \to \infty$ the squashing reaches its maximum value: $q_0 \to 5/3$. By using the relation between b and q_0 (eq. (3.3.48)) we also conclude that $b \to 5/4$ when $\hat{\epsilon} \to \infty$.

To find the solution for $x \geq 1$ we have to solve numerically the BPS system in this region. The most efficient way to proceed is by looking at the master equation for $W(x)$ with the initial conditions (3.5.76). For a generic value of γ the numerical solution either gives rise to negative values of $W(x)$ (which is unphysical for $k > 0$, see the definition (3.3.24)) or behaves in the UV as $W(x) \sim x^{\frac{3}{2}}$, which corresponds to the G_2-cone asymptotics with $q_0 = 2$ discussed in section 3.3.1. Only when γ is fine-tuned to some particular value (which depends on $\hat{\epsilon}$) we get in the UV that $W(x) \sim x$ and that q_0 is given by (3.6.83). To determine this critical value of γ we have to perform a numerical shooting for every value of $\hat{\epsilon}$. In what follows we understand that $\gamma = \gamma(\hat{\epsilon})$ is the function of the deformation parameter which results of this shooting. The function $\gamma(\hat{\epsilon})$ is plotted in Fig. 3.1, where we notice that $\gamma(\hat{\epsilon} = 0) = 0$ and, therefore, we recover the unflavored ABJM background when the deformation parameter vanishes. In the opposite limit $\hat{\epsilon} \to \infty$, the function $\gamma(\hat{\epsilon})$ grows as $\hat{\epsilon}^2$. Actually, $\gamma(\hat{\epsilon})$ can be accurately represented by a function of the type:

$$\gamma(\hat{\epsilon}) = \gamma_1\hat{\epsilon} + \gamma_2\hat{\epsilon}^2 \ , \tag{3.6.84}$$

with $\gamma_1 = 0.351$ and $\gamma_2 = 0.309$. In Fig. 3.2 we plot the function $W(x)$ and the squashing function $q(x)$ for some selected values of $\hat{\epsilon}$.

---

[2] The variable ρ used in section 8 of [75] is related to x by $x = e^\rho$.
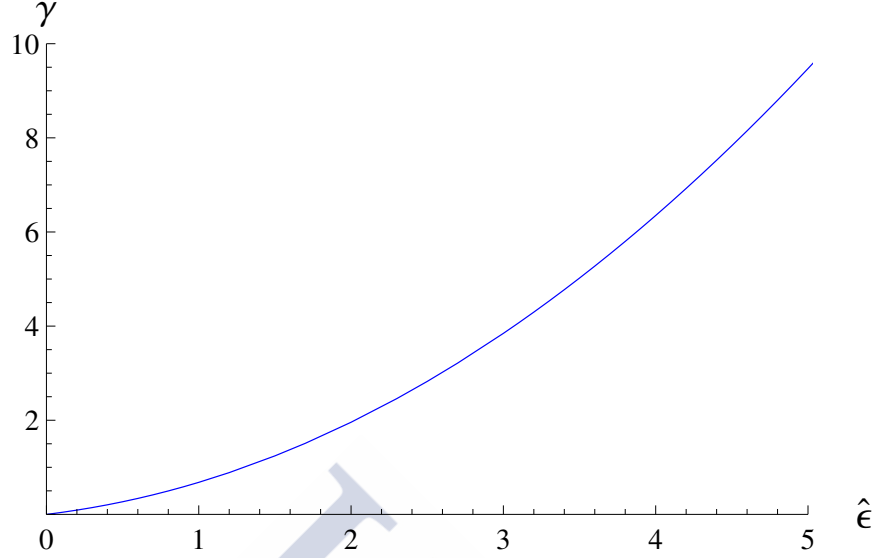
Figure 3.1: Representation of $\gamma(\hat{\epsilon})$.

Interestingly, we have found an analytical solution for small flavor parameter $\hat{\epsilon}$. We present the analytical solution up to order $\hat{\epsilon}^2$ in appendix 3.A.7. Along this chapter, we will present the results using the numerical solution, which is valid for any value of $\hat{\epsilon}$, but a similar analysis could be done analytically for small flavor.

From the function $W(x)$ we can obtain f and g by performing the integrals in (3.5.78). The whole metric is determined if h is known. We will compute h from (3.3.27) with $\beta = 0$, which corresponds to requiring that $h \to 0$ in the UV. In the $x \leq 1$ region the warp factor $h(x)$ is given by (3.4.68), with the constant α determined by the matching condition (3.5.79). The limit on the left-hand side of (3.5.79) can be determined explicitly from (3.4.68):

$$\lim_{x \to 1^-} h(x) = \frac{\pi^2}{8\,r_q^4} \frac{N}{k} \frac{(\hat{\gamma}-1)^4 (1+4\gamma)}{\gamma} \left[\left(\frac{1}{2} + 6\gamma + \frac{1+(1-6\gamma)\hat{\gamma}}{4\gamma} \right) \frac{\hat{\gamma}+1}{\gamma^2} + 24 \log \frac{\sqrt{4\gamma}}{\hat{\gamma}+1} + \alpha \right],$$
(3.6.85)

whereas $h(x \to 1^+)$ is given by:

$$\lim_{x \to 1^+} h(x) = \frac{48\,\pi^2}{r_q} \frac{N}{k} \frac{\hat{\gamma}^2}{\hat{\gamma}+1} \int_1^\infty \frac{\xi\, e^{-3g(\xi)}}{\left[W(\xi) \right]^2} \, d\xi \ .$$
(3.6.86)

Notice that r_q (the value of the r coordinate at the tip of the flavor branes) appears as a free parameter in eqs. (3.5.77) and (3.5.78). Actually, r_q can be easily related to the mass m_q of the quarks which deform the geometry. Indeed, by computing the Nambu-Goto action of a fundamental string stretching along the holographic direction between $r = 0$ and $r = r_q$ at fixed value of all the other spacelike coordinates in the geometry (3.3.16), we get that m_q and r_q are linearly related as:

$$m_q = \frac{r_q}{2\pi\alpha'} \ ,$$
(3.6.87)
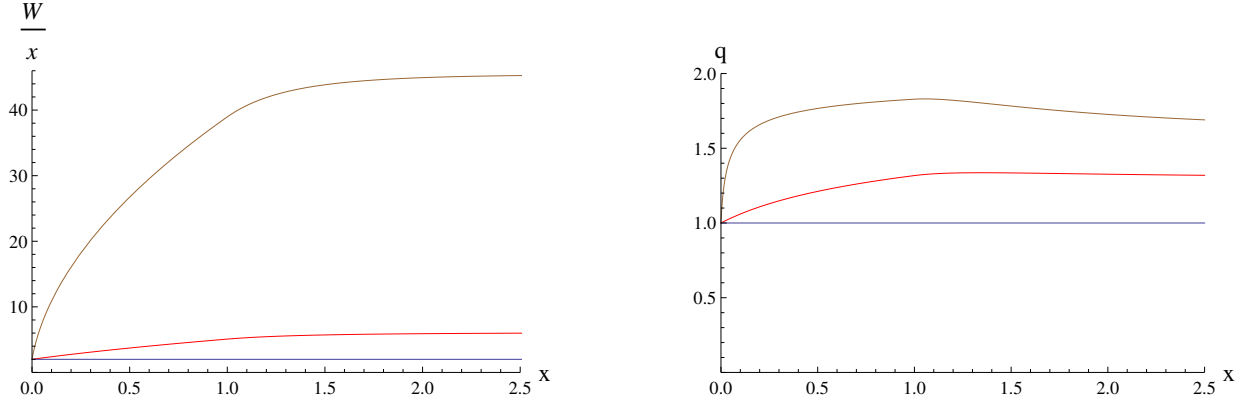
Figure 3.2: Representation of $W(x)/x$ and $q(x)$ for different numbers of flavors ($\hat{\epsilon} = 0$ (bottom, blue), $\hat{\epsilon} = 1$ (middle, red), and $\hat{\epsilon} = 9$ (top, brown)). The plots on the left show that $W(x)/x$ becomes constant as we approach the IR and UV conformal points at $x = 0$ and $x = \infty$, respectively. Similarly, the squashing function $q(x)$ interpolates between $q = 1$ at $x = 0$ and $q = q_0$ at large x.

where α' is the Regge slope (which we will take to be equal to one in most of our equations). Equivalently, we can relate m_q to the constant c appearing in the solution in the $x \leq 1$ region:

$$ m_q = \frac{\sqrt{1 + 4\gamma(\hat{\epsilon})} - 1}{4\pi} \frac{1}{c} \ , \tag{3.6.88} $$

where $\gamma(\hat{\epsilon})$ is the function obtained by the shooting and only depends on the deformation parameter $\hat{\epsilon}$.

We have computed the curvature invariants for the flavored metric and we have checked that the geometry is regular both in the IR ($x \to 0$) and UV ($x \to \infty$). However, the curvature has a finite discontinuity at $x = 1$, as can be directly concluded by inspecting Einstein's equations (see appendix 3.A.1). This "threshold" singularity occurs at the point where the sources are added and could be avoided by smoothing the introduction of brane sources with an additional smearing (see the last article in [142] for a similar analysis in other background).

3.6.1   UV asymptotics

The full background in the $x \geq 1$ region must be found by numerical integration and shooting, as described above. However, in the UV region $x \to \infty$ one can solve the master equation (3.3.25) in power series for large x. Indeed, one can find a solution where $W(x)$ is represented as:

$$ W(x) = x \sum_{i=0}^{\infty} \frac{A_{2i}}{x^{2i}} \ , \tag{3.6.89} $$

where the coefficients A_{2i} can be obtained recursively. The coefficient A_0 of the leading term was written in (3.3.42). The next two coefficients are:

$$A_2 = -\frac{40\,\eta_0 - 11\,A_0}{9 + 13\,\eta_0 - 2\,A_0}\,\hat{\epsilon}\,, \qquad\qquad A_4 = \frac{5A_2^2 + 20\,\hat{\epsilon}^2 + 25\,\hat{\epsilon}\,A_2}{9(1 + 3\eta_0 - 2A_0)}\,. \qquad (3.6.90)$$

Notice that a linear behavior of $W(x)$ with x corresponds to a conformal AdS background, whereas the deviations from conformality are encoded in the non-linear corrections.

From the result written above one can immediately obtain the asymptotic behavior of the squashing function for large x. Indeed, let us use in the expression of q in terms of W and W' (eq. (3.3.29)) the following large x expansion:

$$x\,(\,W' + 4\eta\,) \;=\; (A_0 + 4\eta_0)\,x \;-\; \frac{A_2 + 4(\eta_0 - 1)}{x} \;+\;\cdots\,. \qquad (3.6.91)$$

We get:

$$q(x) \;=\; q_0 \;+\; \frac{q_2}{x^2} \;+\;\cdots\,, \qquad (3.6.92)$$

where q_0 is the asymptotic value of the squashing (see (3.6.83)) and q_2 is given by:

$$q_2 \;=\; \frac{2b}{3(2-b)^2}\left[(3 - 2b)\,\frac{\eta_0 - 1}{\eta_0} + (3 - b)\,\frac{A_2}{A_0}\right]\,, \qquad (3.6.93)$$

where b is related to q_0 and $\hat{\epsilon}$ by (3.3.48) and (3.6.83). Similarly, we can find analytically the first corrections to the UV conformal behavior. The details of these calculations are given in appendix 3.A.2. In this section we just present the final results. First of all, let us define the constant κ (depending on the deformation $\hat{\epsilon}$) as:

$$\kappa \;\equiv\; b\left[\frac{(\hat{\gamma}+1)^2}{2\,\hat{\gamma}\,A_0}\right]^{\frac{1}{3}}\exp\left[\frac{2}{3}\int_1^\infty\left[\frac{\eta(\xi)}{W(\xi)} - \frac{\eta_0}{A_0\,\xi}\right]d\xi\right]\,. \qquad (3.6.94)$$

Then the functions g and f can be expanded for large x as:

$$e^g = \frac{\kappa\,r_q}{b}\,x^{\frac{1}{b}}\left[1 + \frac{g_2}{x^2} + \cdots\right]\,, \qquad e^f = \sqrt{q_0}\,\frac{\kappa\,r_q}{b}\,x^{\frac{1}{b}}\left[1 + \frac{f_2}{x^2} + \cdots\right]\,, \quad (3.6.95)$$

where the coefficients g_2 and f_2 are:

$$g_2 = \frac{3 - 2b}{6b}\,\frac{\eta_0 - 1}{\eta_0} + \frac{3 - 4b}{6b}\,\frac{A_2}{A_0}\,,$$

$$f_2 = \frac{1}{3}\left(\frac{3}{2b} + \frac{1}{2-b} - 1\right)\frac{A_2}{A_0} + \frac{(2+b)(3-2b)}{6b(2-b)}\,\frac{\eta_0 - 1}{\eta_0}\,. \qquad (3.6.96)$$

Moreover, the UV expansion of the warp factor h and the dilaton is:

$$h(x) = \frac{L_0^4}{\kappa^4\,r_q^4}\,x^{-\frac{4}{b}}\left[1 + \frac{h_2}{x^2} + \cdots\right]\,, \qquad e^\phi = e^{\phi_0}\left(1 + \frac{\phi_2}{x^2} + \cdots\right)\,, \qquad (3.6.97)$$

with the coefficients h_2 and ϕ_2 given by:

$$h_2 = \frac{3-2b}{2b}\left(1 + \frac{8}{3(b-2)} - \frac{3}{3+2b}\right)\frac{\eta_0 - 1}{\eta_0} + \left(1 + \frac{2}{3(b-2)} - \frac{2}{b} + \frac{3}{3+2b}\right)\frac{A_2}{A_0},$$

$$\phi_2 = \frac{3-2b}{8b}\left(1 + \frac{4b}{2-b} - \frac{3}{3+2b}\right)\frac{\eta_0 - 1}{\eta_0} - \frac{3}{4}\left(1 - \frac{2}{3(2-b)} - \frac{1}{3+2b}\right)\frac{A_2}{A_0}. \quad (3.6.98)$$

It is also interesting to write the previous expansions in terms of the r variable. Again, the details are worked out in appendix 3.A.2 and the final result is:

$$e^{g(r)} = \frac{r}{b}\left[1 + \tilde{g}_2\left(\frac{r_q}{r}\right)^{2b} + \cdots\right], \qquad e^{f(r)} = \frac{\sqrt{q_0}\, r}{b}\left[1 + \tilde{f}_2\left(\frac{r_q}{r}\right)^{2b} + \cdots\right],$$

$$h(r) = \left[\frac{L_0}{r}\right]^4\left[1 + \tilde{h}_2\left(\frac{r_q}{r}\right)^{2b} + \cdots\right], \qquad e^{\phi} = e^{\phi_0}\left(1 + \tilde{\phi}_2\left(\frac{r_q}{r}\right)^{2b} + \cdots\right), \quad (3.6.99)$$

where the coefficients $\tilde{g}_2$, $\tilde{f}_2$, $\tilde{h}_2$, and $\tilde{\phi}_2$ are related to the ones in (3.6.96) and (3.6.98) as:

$$\tilde{g}_2 = \frac{2b}{2b-1}\kappa^{2b}\, g_2, \qquad\qquad \tilde{f}_2 = \kappa^{2b}\left(f_2 + \frac{g_2}{2b-1}\right),$$

$$\tilde{h}_2 = \kappa^{2b}\left(h_2 - \frac{4g_2}{2b-1}\right), \qquad\qquad \tilde{\phi}_2 = \kappa^{2b}\,\phi_2. \quad (3.6.100)$$

Recalling (see (3.6.87)) that $r_q = 2\pi\, m_q$, it is clear from (3.6.99) that the deviation from
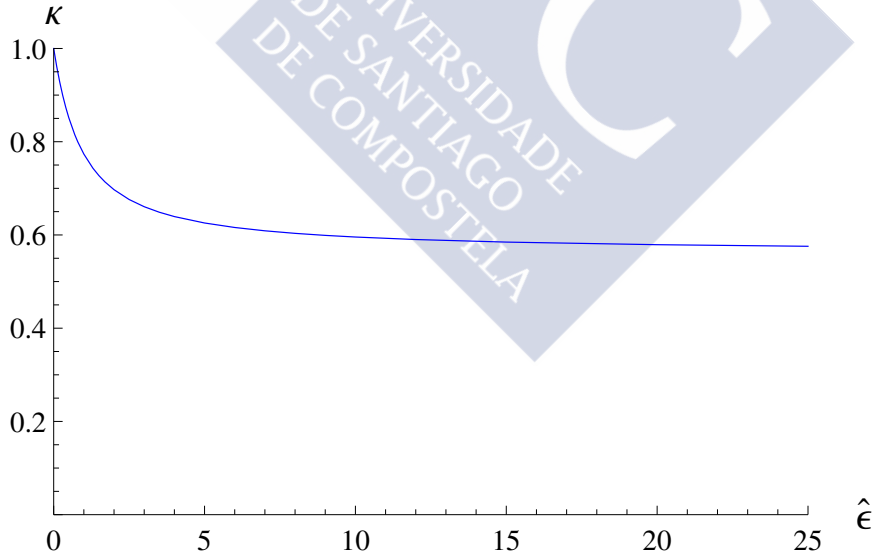
Figure 3.3: Plot of κ as a function of the deformation parameter $\hat{\epsilon}$. The κ asymptotes to some positive constant as $\hat{\epsilon} \to \infty$.

conformality is controlled by the quark mass and that the parameter b determines the power of the first mass corrections. In our holographic context this is quite natural if one takes into account that b determines the dimension Δ of the quark-antiquark bilinear operator in the

theory with dynamical quarks ($\Delta = 3 - b$, see [75, 136] and below). The coefficients of these mass corrections depend on the constants g_2, f_2, h_2, and ϕ_2 (whose analytic expressions we know from eqs. (3.6.96) and (3.6.98)), as well as on the constant κ, which must be determined numerically. κ as a function of the deformation parameter is plotted in Fig. 3.3. From this plot we notice that $\kappa(\hat{\epsilon})$ interpolates continuously between $\kappa = 1$ for $\hat{\epsilon} = 0$ and some positive constant value at large $\hat{\epsilon}$.

3.7 Holographic entanglement entropy

In a quantum theory the entanglement entropy S_A between a spatial region A and its complement is defined as the entropy seen by an observer in A which has no access to the degrees of freedom living in the complement of A. It can be computed as the von Neumann entropy for the reduced density matrix obtained by taking the trace over the degrees of freedom of the complement of A. For quantum field theories admitting a gravity dual, Ryu and Takayanagi proposed in [95] a simple prescription to compute S_A from the corresponding supergravity background. The holographic entanglement entropy between A and its complement in the proposal of [95] is obtained by finding the eight-dimensional spatial surface Σ whose boundary coincides with the boundary of A and is such that it minimizes the functional:

$$ S_A = \frac{1}{4\,G_{10}} \int_\Sigma d^8\xi \, e^{-2\phi} \, \sqrt{\det g_8} \, , \qquad (3.7.101) $$

where the ξ's are a system of eight coordinates of Σ, G_{10} is the ten-dimensional Newton constant ($G_{10} = 8\pi^6$ in our units) and g_8 is the induced metric on Σ in the string frame. The functional S_A evaluated on the minimal surface Σ is precisely the entanglement entropy between the region A and its complement.
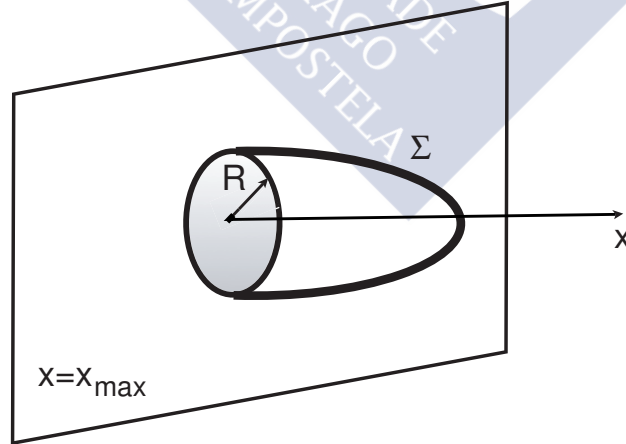
Figure 3.4: The surface Σ ends on the disk of radius R at the boundary $x = x_{max} \to \infty$.

In our case A is a region of the (x^1, x^2)-plane. In this section we will study in detail the case in which the region A is a disk with radius R as depicted in Fig. 3.4 (see appendix 3.A.3 for the analysis of the entanglement entropy of a strip in the (x^1, x^2)-plane). In order

to deal with the disk case it is convenient to choose a system of polar coordinates for the plane:

$$(dx^1)^2 + (dx^2)^2 = d\rho^2 + \rho^2 \, d\Omega_1^2 \ . \tag{3.7.102}$$

We will describe the eight-dimensional fixed time surface Σ by a function $\rho = \rho(x)$ with ρ being the radial coordinate of the boundary plane and x the holographic coordinate of the bulk. The eight-dimensional induced metric is:

$$ds_8^2 = h^{-\frac{1}{2}} \left[\rho'^2 + G(x) \right] dx^2 + h^{-\frac{1}{2}} \rho^2 \, d\Omega_1^2 + h^{\frac{1}{2}} \left[e^{2f} ds_{\mathbb{S}^4}^2 + e^{2g} \left(\left(E^1\right)^2 + \left(E^2\right)^2 \right) \right] , \tag{3.7.103}$$

where ρ' denotes the derivative with respect to the holographic coordinate x and the function $G(x)$ is defined as:

$$G(x) \equiv \frac{e^{2g} \, h}{x^2} \ . \tag{3.7.104}$$

Let us next define a new function $H(x)$ as:

$$H(x) \equiv h^2 \, e^{-4\phi} \, e^{8f+4g} \ . \tag{3.7.105}$$

Then, the entanglement entropy as a function of R is given by:

$$S(R) = \frac{2\pi \, V_6}{4G_{10}} \int_{x_*}^{\infty} dx \, \rho \, \sqrt{H(x)} \, \sqrt{\rho'^2 + G(x)} \ , \tag{3.7.106}$$

where $V_6 = 32\,\pi^3/3$ is the volume of the internal manifold and x_* is the x coordinate of the turning point of Σ. The Euler-Lagrange equation of motion derived from the entropy functional (3.7.106) is:

$$\frac{d}{dx} \left[\sqrt{H(x)} \, \frac{\rho \, \rho'}{\sqrt{\rho'^2 + G(x)}} \right] - \sqrt{H(x)} \, \sqrt{\rho'^2 + G(x)} = 0 \ . \tag{3.7.107}$$

Notice that the integrand in (3.7.106) depends on the independent variable x and we therefore cannot find a first-integral for the second-order differential equation (3.7.107). Thus, we have to deal directly with (3.7.107), which must be solved with the following boundary conditions at the tip of Σ:

$$\rho(x = x_*) = 0 \ , \qquad \rho'(x = x_*) = +\infty \ . \tag{3.7.108}$$

Notice also that the radius R of the disk at the boundary is just the UV limit of ρ:

$$\rho(x \to \infty) = R \ . \tag{3.7.109}$$

The integral (3.7.106) for $S(R)$ diverges due to the contribution of the UV region of large x. In order to characterize this divergence and to extract the finite part, let us study the behavior of the integrand in (3.7.106) as $x \to \infty$. From the definitions of the functions $H(x)$ and $G(x)$ and the UV behavior written in (3.6.95) and (3.6.97), it follows that H and G display a power-like behavior as $x \to \infty$,

$$H(x) \approx H_\infty \, x^{\frac{4}{b}} \ , \qquad G(x) \approx G_\infty \, x^{-2-\frac{2}{b}} \ , \qquad (x \to \infty) \ , \tag{3.7.110}$$

where the coefficients H_∞ and G_∞ are

$$H_\infty = \frac{L_0^8\, \kappa^4\, r_q^4\, q_0^4\, e^{-4\phi_0}}{b^{12}} \ , \qquad\qquad G_\infty = \frac{L_0^4}{b^2\, r_q^2\, \kappa^2} \ . \qquad (3.7.111)$$

By taking the $x \to \infty$ values of ρ and ρ' ($\rho = R$ and $\rho' = 0$) inside the integral in (3.7.106), as well as the asymptotic form of $H(x)$ and $G(x)$ (eq. (3.7.110)), we get:

$$S_{div}(R) = \frac{\pi\, V_6}{2G_{10}}\, R\, \sqrt{H_\infty\, G_\infty} \int^{x_{max}} x^{\frac{1}{b}-1}\, dx \ , \qquad (3.7.112)$$

where x_{max} is the maximum value of the holographic coordinate x (which acts as a UV regulator). After performing the integral, we obtain:

$$S_{div}(R) = \frac{\pi\, V_6}{2G_{10}}\, R\, b\, \sqrt{H_\infty\, G_\infty}\ x_{max}^{\frac{1}{b}} \ . \qquad (3.7.113)$$

Let us rewrite (3.7.113) in terms of physically relevant quantities. First of all, we notice that:

$$b\, \sqrt{H_\infty\, G_\infty} = \frac{L_0^6\, q_0^2\, e^{-2\phi_0}}{b^6}\, \kappa\, r_q = \frac{3\pi^2}{2}\, \frac{F_{UV}(\mathbb{S}^3)}{L_0^2}\, \kappa\, r_q \ , \qquad (3.7.114)$$

where $F_{UV}(\mathbb{S}^3)$ is the free energy[3] of the massless flavored theory on the three-sphere:

$$F_{UV}(\mathbb{S}^3) = \frac{2\pi}{3}\, \frac{N^2}{\sqrt{2\lambda}}\, \xi\!\left(\frac{N_f}{k}\right) \ , \qquad (3.7.117)$$

where the function $\xi\!\left(\frac{N_f}{k}\right)$ is given by:

$$\xi\!\left(\frac{N_f}{k}\right) \equiv \frac{1}{16}\, \frac{q_0^{\frac{5}{2}}\, (\eta_0 + q_0)^4}{(2 - q_0)^{\frac{1}{2}}\, (q_0 + \eta_0 q_0 - \eta_0)^{\frac{7}{2}}} \ . \qquad (3.7.118)$$

In (3.7.118) $\eta_0 = 1 + \hat{\epsilon}$ and q_0 is written in (3.6.83) in terms of the deformation parameter. For the unflavored ABJM theory the free energy is given by (3.7.117) with $\xi = 1$. This formula displays the famous $N^{\frac{3}{2}}$ behavior. The function $\xi(N_f/k)$ encodes the corrections to this behavior due to the smeared massless flavors. It was first computed in [75], where it was shown that it is remarkably close to the value found in [79] for localized embeddings.

---

[3]When the field theory is formulated on a three-sphere, its free energy is defined as:

$$F(\mathbb{S}^3) = -\log |Z_{\mathbb{S}^3}| \ , \qquad (3.7.115)$$

where $Z_{\mathbb{S}^3}$ is the Euclidean path integral. For a CFT whose gravity dual is of the form $AdS_4 \times \mathcal{M}_6$, the holographic calculation of $F(\mathbb{S}^3)$ gives [143]:

$$F(\mathbb{S}^3) = \frac{\pi L^2}{2G_N} \ , \qquad (3.7.116)$$

where L is the AdS_4 radius and G_N is the effective four-dimensional Newton's constant.

The function ξ is a monotonic function of the deformation parameter which grows as $\sqrt{\hat{\epsilon}}$ for large values of $\hat{\epsilon}$.

Using (3.7.114) and the fact that, in the deep UV region of large x, $r_{max} = \kappa\, r_q\, x_{max}^{\frac{1}{b}}$ (see (3.A.53)), we can rewrite $S_{div}(R)$ as:

$$S_{div}(R) \; = \; \frac{F_{UV}(\mathbb{S}^3)}{L_0^2}\, r_{max}\, R \; . \tag{3.7.119}$$

We notice in (3.7.119) that $S_{div}(R)$ diverges linearly with r_{max}. The coefficient of this divergent term is linear in the disk radius R and in $F_{UV}(\mathbb{S}^3)$. The latter is a measure of the effective number of degrees of freedom of the flavored theory in the high-energy UV limit in which the flavors can be considered to be massless. The appearance of $F_{UV}(\mathbb{S}^3)$ in (3.7.119) is thus quite natural.

The separation between the divergent and finite parts of $S(R)$ has ambiguities. In order to solve these ambiguities, Liu and Mezei proposed in [137] to consider the function $\mathcal{F}(R)$, defined as:

$$\mathcal{F}(R) \; \equiv \; R\, \frac{\partial S}{\partial R} \; - \; S \; . \tag{3.7.120}$$

It was argued in [137] that $\mathcal{F}(R)$ is finite and a monotonic function of R which provides a measure of the number of degrees of freedom of a system at a scale R.

In a 3d CFT the entanglement entropy for a disk of radius R has the form:

$$S_{CFT}(R) \; = \; \alpha\, R \; - \; \beta \; , \tag{3.7.121}$$

where α is a UV divergent non-universal part and β is finite and independent of R. It was shown in [144] that the finite part β is equal to the free energy of the theory on $\mathbb{S}^3$. Notice that $\mathcal{F} = \beta$ when S is of the form (3.7.121). Therefore, for a conformal fixed point the function $\mathcal{F}$ is constant and equal to the free energy on the three-sphere of the corresponding CFT. In the next subsection we will obtain the UV and IR values of $\mathcal{F}$ and we will show that they coincide with the free energies on $\mathbb{S}^3$ of the massless flavored theory and of the unflavored ABJM model, respectively.

It is interesting to point out that the entanglement entropy of a disk in a $(2+1)$-dimensional system at large R can also be written in the form (3.7.121), if one neglects terms which vanish in the $R \to \infty$ limit. In a gapped system, the R-independent part β of the right-hand side of (3.7.121) is the so-called topological entanglement entropy [145, 146] and serves to characterize topologically ordered many-body states which contain non-local entanglement due to non-local correlations (examples of such states are the Laughlin states of the fractional quantum Hall effect or the $\mathbb{Z}_2$ fractionalized states). The topological entanglement entropy β is related to the so-called total quantum dimension $\mathcal{D}$ of the system as $\beta = \log \mathcal{D}$. In general $\mathcal{D} > 1$ (or $\beta > 0$) signals a topological order (for example $\mathcal{D} = \sqrt{q}$ for the quantum Hall system with filling fraction $\nu = 1/q$, with q an odd integer).

For our system, we can obtain the embedding function $\rho(x)$ by numerical integration of the differential equation (3.7.107) and then we can get the functions $S(R)$ and $\mathcal{F}(R)$ by using (3.7.106) and the definition of $\mathcal{F}(R)$ in (3.7.120). The results for the latter are plotted as a function of $R\, r_q \propto R\, m_q$ in Fig. 3.5. We notice that $\mathcal{F}(R)$ is a monotonically
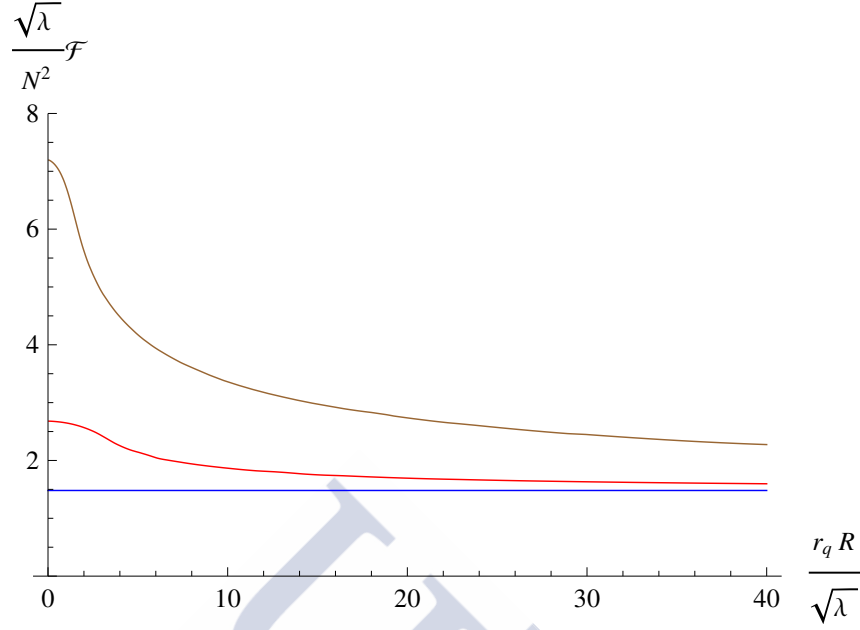
Figure 3.5: Plot of the running free energy $\mathcal{F}$ as a function of $r_q R$ for $\hat{\epsilon} = 0$ (bottom, blue), 1 (middle, red), and 9 (top, brown).

decreasing function that interpolates smoothly between the two limiting values at $R\, m_q = 0$ and $R\, m_q \to \infty$. The UV limit of $\mathcal{F}$ at small $R\, m_q$ equals the free energy (3.7.117) of the massless flavored theory, whereas for large $R\, m_q$ the function $\mathcal{F}$ approaches the free energy of the unflavored ABJM model (*i.e.*, the value in (3.7.117) with $\xi = 1$). This behavior is in agreement with the general expectation in [137, 139] and corresponds to a smooth decoupling of the massive flavors as their mass m_q is increased continuously.

We will study the UV and IR limits of $\mathcal{F}$ analytically in the next two subsections. Some details of these calculations are deferred to appendix 3.A.3, where we also study the entanglement entropy for the strip geometry.

3.7.1 UV limit

In order to study the UV limit of the disk entanglement entropy, let us write the Euler-Lagrange equation (3.7.107) when $H(x)$ and $G(x)$ are given by their asymptotic values (3.7.110):

$$\frac{d}{dx}\left[x^{\frac{2}{b}} \frac{\rho\,\rho'}{\sqrt{\rho'^2 + G_\infty\, x^{-2-\frac{2}{b}}}} \right] - x^{\frac{2}{b}} \sqrt{\rho'^2 + G_\infty\, x^{-2-\frac{2}{b}}} = 0 \ . \tag{3.7.122}$$

This equation can be solved exactly by the function:

$$\rho_{UV}(x) = \sqrt{R^2 - b^2\, G_\infty\, x^{-\frac{2}{b}}} \ , \tag{3.7.123}$$

which clearly satisfies the initial conditions (3.7.108), with the following value of the turning point coordinate x_*:

$$x_*^{2/b} = \frac{b^2 \, G_\infty}{R^2} \; . \tag{3.7.124}$$

Since $G_\infty \propto r_q^{-2}$, it follows from (3.7.124) that $x_*^{2/b} \propto (r_q \, R)^{-2}$. Therefore, the turning point coordinate x_* is large if r_q or R are small. In this case it would be justified to use the asymptotic UV values of the functions G and H, since the minimal surface Σ lies entirely in the large x region. Notice also that (3.7.123) can be written in terms of x_* as:

$$\rho_{UV} = R \sqrt{1 - \left(\frac{x_*}{x}\right)^{2/b}} \; . \tag{3.7.125}$$

In order to calculate the entropy in this UV limit it is very useful to use the following relation satisfied by the function $\rho_{UV}(x)$ written in (3.7.123):

$$\rho_{UV} \sqrt{\left(\rho'_{UV}\right)^2 + G_\infty \, x^{-2-\frac{2}{b}}} = R \sqrt{G_\infty} \, x^{-1-\frac{1}{b}} \; . \tag{3.7.126}$$

Making use of (3.7.126) in (3.7.106), we find the following expression for the entanglement entropy:

$$S_{UV}(R) = \frac{\pi \, V_6}{2 G_{10}} \, R \sqrt{H_\infty \, G_\infty} \int_{x_*}^{x_{max}} x^{\frac{1}{b}-1} \, dx \; . \tag{3.7.127}$$

The divergent part of this integral is due to its upper limit and is just given by (3.7.119). The finite part of S is:

$$S_{finite,UV} = -\frac{\pi \, V_6}{2 G_{10}} \, b \sqrt{H_\infty \, G_\infty} \, R \, x_*^{\frac{1}{b}} = -\frac{\pi \, V_6}{2 G_{10}} \, b^2 \, G_\infty \sqrt{H_\infty} \; , \tag{3.7.128}$$

where, in the second step, we used (3.7.124) to eliminate x_*. Notice that the right-hand side of (3.7.128) is independent of the disk radius R. Moreover, by using (3.7.111) and (3.7.114) we find that:

$$S_{finite,UV} = -F_{UV}(\mathbb{S}^3) \; . \tag{3.7.129}$$

Therefore, in this UV limit, the dependence on R of the entanglement entropy takes the form (3.7.121), where β is just the free energy of the massless flavored theory on the three-sphere. It follows trivially from this form of S_{UV} and the definition (3.7.120) that $\mathcal{F}_{UV} = \beta$ and therefore:

$$\mathcal{F}_{UV} \equiv \lim_{r_q R \to 0} \mathcal{F}(R) = F_{UV}(\mathbb{S}^3) \; . \tag{3.7.130}$$

It is also possible to compute analytically the first correction to (3.7.130) for small values of $r_q \, R$. The details of this calculation are given in appendix 3.A.3. Here we will just present the final result, which can be written as:

$$\mathcal{F}(R) = F_{UV}(\mathbb{S}^3) + c_{UV} \, (r_q \, R)^{2(3 - \Delta_{UV})} + \cdots \; , \tag{3.7.131}$$

where c_{UV} is a constant coefficient depending on the deformation parameter (see eq. (3.A.82)) and $\Delta_{UV} = 3 - b$ is the dimension of the quark-antiquark bilinear operator in the UV

flavored theory (this dimension was found in section 7.3 of [75] from the analysis of the fluctuations of the flavor branes, see also [136]). It is interesting to point out that (3.7.131) is the behavior expected [137] for a flow caused by a source deformation with a relevant operator of dimension Δ_{UV}. Moreover, one can verify that c_{UV} is negative for all values of the deformation parameter $\hat{\epsilon}$, which confirms that the UV fixed point is a local maximum of $\mathcal{F}$.

3.7.2 IR limit

Let us now analyze the IR limit of the entanglement entropy $S(R)$ and of the function $\mathcal{F}(R)$. This limit occurs when the 8d surface Σ penetrates deeply into the geometry and, therefore, when the coordinate x_* of the turning point is small ($x_* \ll 1$). This happens when either the disk radius R or the quark mass $m_q = r_q/2\pi$ are large. Looking at the embedding function $\rho(x)$ obtained by numerical integration of (3.7.107) one notices that, when x_* is small, the function $\rho(x)$ is approximately constant and equal to its asymptotic value $\rho = R$ in the region $x \geq 1$ (see Fig. 3.6). Therefore, the dependence of ρ on the holographic coordinate x is determined by the integral of (3.7.107) in the region $x \leq 1$, where the background is given by the unflavored running solution. Actually, when x_* is small it is a good approximation to consider (3.7.107) for the unflavored background, *i.e.*, when the constants $c, \gamma \to 0$, with γ/c fixed and given by $\gamma/c = r_q$. In this limit the different functions of the background are:

$$e^f \approx e^g \approx r_q\, x\,, \qquad\qquad h \approx \frac{1}{r_q^4}\, \frac{2\pi^2\, N}{k}\, \frac{1}{x^4}\,. \qquad (3.7.132)$$

It follows that $G(x)$ and $H(x)$, as defined in (3.7.104) and (3.7.105), are then given by:
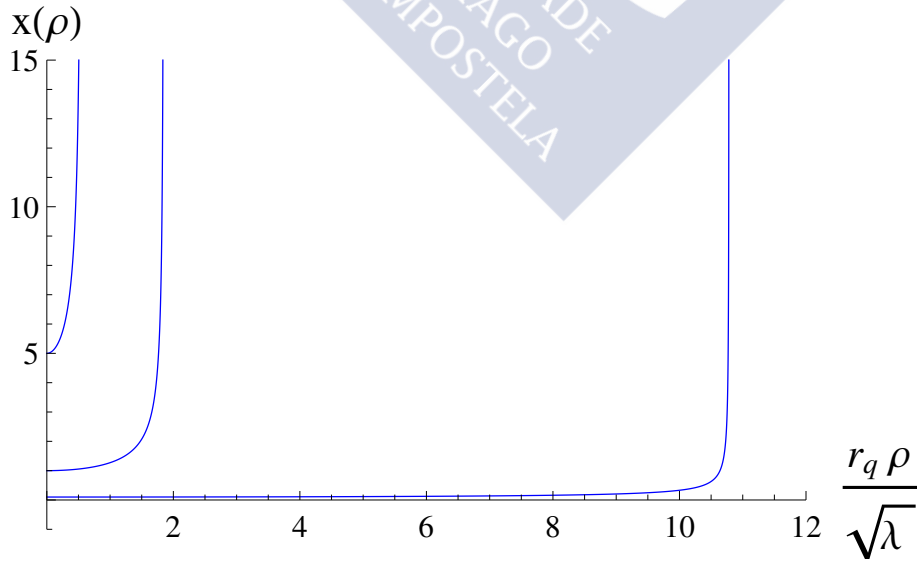
Figure 3.6: Representation of the embedding function $\rho(x)$ for different values of the turning point $x_* = 0.1, 1, 5$ and $\hat{\epsilon} = 9$.

$$G_{IR}(x) = \frac{1}{r_q^2} \frac{2\pi^2 N}{k} \frac{1}{x^4} = G_0\, x^{-4}\,, \qquad\qquad H_{IR}(x) = r_q^4\, \frac{4\pi^4\, N^2}{k^2}\, e^{-4\phi_{IR}}\, x^4 = H_0\, x^4\,,$$

$$(3.7.133)$$

where, in the last step, we have defined the constants G_0 and H_0, and ϕ_{IR} is the constant dilaton corresponding to the unflavored background,

$$e^{\phi_{IR}} = 2\sqrt{\pi}\left(\frac{2N}{k^5}\right)^{\frac{1}{4}}\,.$$

$$(3.7.134)$$

Let us now elaborate on the expression (3.7.106) for the entanglement entropy. We split the integration interval of the variable x as $[x_*, \infty] = [x_*, 1] \cup [1, \infty]$ and take into account that one can put $\rho = R = $ constant in the region $x \geq 1$. We get:

$$S_{IR}(R) = \frac{\pi\, V_6}{2G_{10}} \int_{x_*}^{1} dx\, \rho\, \sqrt{H_{IR}(x)}\, \sqrt{\rho'^2 + G_{IR}(x)} + \frac{\pi\, V_6}{2G_{10}}\, R \int_{1}^{x_{max}} \sqrt{H(x)\, G(x)}\,.$$

$$(3.7.135)$$

The second term in (3.7.135) is linear in R and will not contribute to $\mathcal{F}(R)$. To evaluate the first integral in (3.7.135) we must determine the embedding function $\rho(x)$ by integrating (3.7.107) when $G(x)$ and $H(x)$ are given by their IR values (3.7.133). The resulting equation is just the same as (3.7.122) with G_∞ and H_∞ substituted by G_0 and H_0 and $b = 1$. Then, the function $\rho(x)$ can be written as in (3.7.123),

$$\rho_{IR}(x) = \sqrt{\hat{R}^2 - G_0\, x^{-2}}\,,$$

$$(3.7.136)$$

where $\hat{R}$ is a constant. By requiring that $\rho_{IR}(x = 1) = R$, we get:

$$\hat{R}^2 = R^2 + G_0\,.$$

$$(3.7.137)$$

It follows from (3.7.136) that the coordinate x_* of the turning point is given by:

$$x_*^2 = \frac{G_0}{\hat{R}^2} = \frac{G_0}{G_0 + R^2}\,.$$

$$(3.7.138)$$

Notice that when $r_q \to \infty$ (and $G_0 \to 0$) or R is large one can neglect the G_0 in the denominator of (3.7.138) and then $x_*^2 \approx G_0\, R^{-2} \propto (r_q\, R)^{-2}$, which is a small number. Moreover, by using the explicit form (3.7.136) of $\rho(x)$ in this IR region, we get:

$$\rho_{IR}\, \sqrt{(\rho'_{IR})^2 + G_{IR}} = \hat{R}\, \sqrt{G_0}\, x^{-2}\,,$$

$$(3.7.139)$$

and the first integral in (3.7.135) can be explicitly evaluated:

$$\int_{x_*}^{1} dx\, \rho_{IR}\, \sqrt{H_{IR}(x)}\, \sqrt{(\rho'_{IR})^2 + G_{IR}(x)} = \hat{R}\, \sqrt{G_0\, H_0} - G_0\, \sqrt{H_0}\,.$$

$$(3.7.140)$$

Notice that, at leading order $\hat{R} \approx R$ and, thus, the first term in (3.7.140) does not contribute to $\mathcal{F}(R)$. Then, the IR limit of $\mathcal{F}$ is determined by the second contribution in (3.7.140) and given by:

$$\mathcal{F}_{IR} = \frac{\pi\, V_6}{2G_{10}}\, G_0\, \sqrt{H_0}\,.$$

$$(3.7.141)$$

Moreover, from the values of G_0 and H_0 written in (3.7.133) we get:

$$G_0\sqrt{H_0} \;=\; \frac{\pi^3}{\sqrt{2}}\,N^{\frac{3}{2}}\,k^{\frac{1}{2}} \;=\; \frac{3\pi^2}{2}\,F_{IR}(\mathbb{S}^3)\;, \qquad (3.7.142)$$

where $F_{IR}(\mathbb{S}^3)$ is the free energy on the three-sphere of the unflavored ABJM theory:

$$F_{IR}(\mathbb{S}^3) \;=\; \frac{\pi\sqrt{2}}{3}\,k^{\frac{1}{2}}\,N^{\frac{3}{2}}\;. \qquad (3.7.143)$$

It follows that the IR limit of the $\mathcal{F}$ function is:

$$\mathcal{F}_{IR} \;\equiv\; \lim_{r_q R\to\infty}\,\mathcal{F}(R) \;=\; F_{IR}(\mathbb{S}^3)\;, \qquad (3.7.144)$$

as expected in the deep IR limit in which the flavors become infinitely massive and can therefore be integrated out. The corrections to the result (3.7.144) near the IR fixed point could be obtained by applying the techniques recently introduced in [147]. We will not attempt to perform this calculation here.

3.8 Wilson loops and the quark-antiquark potential

In this section we evaluate the expectation values of the Wilson loop and the corresponding quark-antiquark potential for our model. We will employ the standard holographic prescription of refs. [131, 148], in which one considers a fundamental string hanging from the UV boundary. Then, one computes the regularized Nambu-Goto action for this configuration, from which the $q\bar{q}$ potential energy can be extracted. In a theory with dynamical flavors this potential energy contains information about the screening of external charges by the virtual quarks popping out from the vacuum. In our case we expect having a non-trivial flow connecting two conformal behaviors as we move from the UV regime of small $q\bar{q}$ separation (in units of the quark mass m_q) to the IR regime of large $q\bar{q}$ distance. We will verify below that this expectation is indeed fulfilled by our model.

Let us denote by (t, x^1, x^2) the Minkowski coordinates and consider a fundamental string for which we take (t, x^1) as its worldvolume coordinates. If the embedding is characterized by a function $x = x(x^1)$, with x being the holographic coordinate, the induced metric is:

$$ds_2^2 \;=\; -h^{-\frac{1}{2}}\,dt^2 \;+\; h^{\frac{1}{2}}\left[\frac{e^{2g}}{x^2}\,x'^2 \;+\; h^{-1}\right](dx^1)^2\;, \qquad (3.8.145)$$

where x' denotes the derivative of x with respect to x^1. The Nambu-Goto lagrangian density takes the form:

$$\mathcal{L}_{NG} \;=\; \frac{1}{2\pi}\,\sqrt{-\det g_2} \;=\; \frac{1}{2\pi}\,\sqrt{\frac{e^{2g}}{x^2}\,x'^2 \;+\; h^{-1}}\;. \qquad (3.8.146)$$

As $\mathcal{L}_{NG}$ does not depend on x^1, we have the following conservation law:

$$x'\,\frac{\partial\,\mathcal{L}_{NG}}{\partial x'} \;-\; \mathcal{L}_{NG} \;=\; \text{constant}\;. \qquad (3.8.147)$$

Therefore, if x_* denotes the turning point of the string, we have the first integral of the equations of motion:

$$\sqrt{1 + \frac{e^{2g}\, h}{x^2}\, x'^{\,2}} \; = \; \frac{\sqrt{h_*}}{\sqrt{h}} \; , \tag{3.8.148}$$

where $h_* \equiv h(x = x_*)$. Then x' is given by:

$$x' \; = \; \pm \frac{x\sqrt{h_* - h(x)}}{e^{g(x)}\, h(x)} \; , \tag{3.8.149}$$

where the two signs correspond to the two branches of the hanging string. The $q\bar{q}$ separation d in the x^1 direction is:

$$d \; = \; 2 \int_{x_*}^{\infty} \frac{e^{g(x)}\, h(x)}{x\,\sqrt{h_* - h(x)}} \; dx \; . \tag{3.8.150}$$

In order to compute the potential energy of the $q\bar{q}$ pair, let us evaluate the on-shell action. By using the first integral (3.8.148) it is straightforward to check that the on-shell value of the Nambu-Goto lagrangian density is:

$$\mathcal{L}_{NG}(\text{on} - \text{shell}) \; = \; \frac{1}{2\pi} \frac{\sqrt{h_*}}{h} \; . \tag{3.8.151}$$

Therefore, the on-shell action becomes:

$$S_{\text{on-shell}} \; = \; \frac{T}{\pi} \int_{x_*}^{\infty} \frac{e^{g(x)}}{x} \frac{\sqrt{h_*}}{\sqrt{h_* - h(x)}}\, dx \; , \tag{3.8.152}$$

where $T = \int dt$. The integral (3.8.152) is divergent and must be regularized as in [131, 148] by subtracting the action of two straight strings stretched between the origin and the UV boundary, which corresponds to subtracting the (infinite) quark masses in the static limit. After applying this procedure we arrive at the following expression for the regulated on-shell action:

$$S_{\text{on-shell}}^{\text{reg}} \; = \; S_{\text{on-shell}} - \frac{T}{\pi} \int_0^{\infty} \frac{e^{g(x)}}{x}\, dx \; , \tag{3.8.153}$$

from which we get the $q\bar{q}$ potential energy:

$$E_{q\bar{q}} \; = \; \frac{1}{\pi} \int_{x_*}^{\infty} \frac{e^{g(x)}}{x} \left[\frac{\sqrt{h_*}}{\sqrt{h_* - h(x)}} - 1 \right] dx - \frac{r_*}{\pi} \; , \tag{3.8.154}$$

where r_* is the r coordinate of the turning point:

$$r_* \; = \; \int_0^{x_*} \frac{e^{g(x)}}{x}\, dx \; . \tag{3.8.155}$$

From (3.8.150) and (3.8.154) we have computed numerically the potential energy $E_{q\bar{q}}$ as a function of the $q\bar{q}$ distance d. The result of this numerical calculation is shown in Fig. 3.7. As mentioned above, we expect to have a potential energy which interpolates between the two conformal behaviors with $E_{q\bar{q}} \propto 1/d$ at the UV and IR. Actually, in the limiting cases in
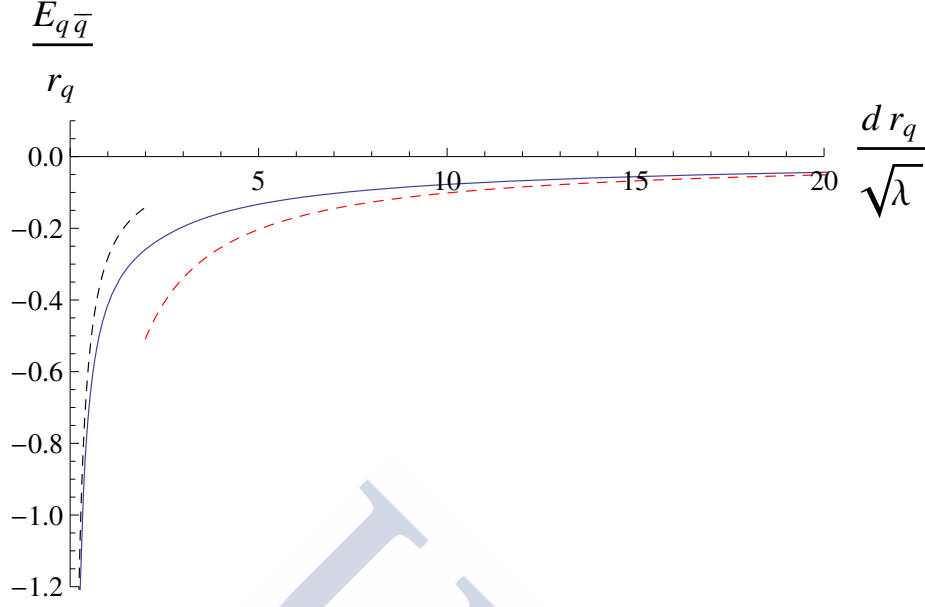
Figure 3.7: Plot of the $q\bar{q}$ potential energy for $\hat{\epsilon} = 9$. The numerical result is compared to the UV leading estimate (3.8.156) (black dashed curve on the left) and to the leading IR potential (red dashed curve on the right).

which $r_q d$ is small or large the function $E_{q\bar{q}}(d)$ can be calculated analytically (see appendix 3.A.4). In both cases $E_{q\bar{q}} \propto 1/d$, but with different coefficients. Indeed, in the UV limit $r_q d \to 0$, the $q\bar{q}$ potential can be approximated as:[4]

$$E_{q\bar{q}}^{UV} \approx -\frac{4\pi^3 \sqrt{2\lambda}}{\left[\Gamma\left(\frac{1}{4}\right)\right]^4} \, \sigma \, \frac{1}{d} , \qquad (r_q d \to 0) , \qquad (3.8.156)$$

where $\lambda = N/k$ is the 't Hooft coupling and σ is the so-called screening function:

$$\sigma = \sqrt{\frac{2 - q_0}{q_0(q_0 + \eta_0 q_0 - \eta_0)}} \qquad b^2 = \frac{1}{4} \frac{q_0^{\frac{3}{2}} (\eta_0 + q_0)^2 (2 - q_0)^{\frac{1}{2}}}{(q_0 + \eta_0 q_0 - \eta_0)^{\frac{5}{2}}} . \qquad (3.8.157)$$

Notice that σ encodes all the dependence of the right-hand side of (3.8.156) on the number of flavors. Actually, the potential (3.8.156) is just the one corresponding to having massless flavors (which was first computed for this model in [75]), as expected in the high-energy UV regime in which all masses can be effectively neglected. The function σ characterizes the corrections of the static $q\bar{q}$ potential due to the screening produced by the unquenched massless flavors ($\sigma \to 1$ for $N_f \to 0$, whereas σ decreases as $\sigma \propto \sqrt{k/N_f}$ for N_f large). In Fig. 3.7 we compare the leading UV result (3.8.156) with the numerical calculation in the small $r_q d$ region.

Similarly, one can compute analytically the $q\bar{q}$ potential in the region where $r_q d$ is large.

---

[4]Also, the first correction to the UV conformal behavior (3.8.156) is computed in appendix 3.A.4.

At leading order the result is (see appendix 3.A.4):

$$E_{q\bar{q}}^{IR} \approx -\frac{4\pi^3 \sqrt{2\lambda}}{\left[\Gamma\left(\frac{1}{4}\right)\right]^4} \frac{1}{d} \,, \qquad\qquad (r_q \, d \to \infty) \,. \qquad (3.8.158)$$

In Fig. 3.7 we compare the analytic expression (3.8.158) to the numerical result in the large distance region. Notice that the difference between (3.8.156) and (3.8.158) is that the screening function σ is absent in (3.8.158). Therefore, in the deep IR the flavor effects on the $q\bar{q}$ potential disappear, which is consistent with the intuition that massive flavors are integrated out at low energies.

3.9   Two-point functions of high dimension operators

In this section we study the two-point functions of bulk operators with high dimension. The form of these correlators can be obtained semiclassically by analyzing the geodesics of massive particles in the dual geometry [149, 150, 151],

$$\langle \mathcal{O}(x) \, \mathcal{O}(y) \rangle \sim e^{-m \, \mathcal{L}_r(x,y)} \,, \qquad\qquad (3.9.159)$$

where m is the mass of the bulk field dual to $\mathcal{O}$. We are assuming that m is large in order to apply a saddle point approximation in the calculation of the correlator. In (3.9.159) $\mathcal{L}_r(x,y)$ is a regularized length along a spacetime geodesic connecting the boundary points x and y. To find these geodesics, let us write the Einstein frame metric of our geometry as:

$$ds_{10}^2 = e^{-\frac{\phi}{2}} \, h^{-\frac{1}{2}} \, dx_{1,2}^2 + e^{-\frac{\phi}{2}} h^{\frac{1}{2}} \left[e^{2g} \frac{dx^2}{x^2} + e^{2f} \, ds_{\mathbb{S}^4}^2 + e^{2g} \left(\left(E^1\right)^2 + \left(E^2\right)^2 \right) \right] \,. \quad (3.9.160)$$

Then, the induced metric for a curve parametrized as $x = x(x^1)$ is:

$$ds_1^2 = e^{-\frac{\phi}{2}} \, h^{-\frac{1}{2}} \left(1 + G(x) \, x'^{\,2} \right) (dx^1)^2 \,, \qquad\qquad (3.9.161)$$

with $x' = dx/dx^1$ and $G(x)$ is the function defined in (3.7.104). Therefore, the action of a particle of mass m whose worldline is the curve $x = x(x^1)$ is:

$$S = m \int ds_1 = m \int e^{-\frac{\phi}{4}} \, h^{-\frac{1}{4}} \, \sqrt{1 + G(x) \, x'^{\,2}} \, dx^1 \,. \qquad\qquad (3.9.162)$$

The geodesics we are looking for are solutions of the Euler-Lagrange equation derived from the action (3.9.162). This equation has a first integral which is given by:

$$e^{\frac{\phi(x)}{4}} \left[h(x) \right]^{\frac{1}{4}} \sqrt{1 + G(x) \, x'^{\,2}} = e^{\frac{\phi_*}{4}} \, h_*^{\frac{1}{4}} \,, \qquad\qquad (3.9.163)$$

where $\phi_* \equiv \phi(x = x_*)$ and $h_* \equiv h(x = x_*)$, with x_* being the x coordinate of the turning point, i.e., the minimum value of x along the geodesic. It follows from (3.9.163) that:

$$x' = \pm \frac{1}{\sqrt{G(x)}} \sqrt{e^{\frac{1}{2}(\phi_* - \phi(x))} \left(\frac{h_*}{h(x)} \right)^{\frac{1}{2}} - 1} \,. \qquad\qquad (3.9.164)$$

The spatial separation l of the two points in the correlator can be obtained by integrating $1/x'$. We get:

$$l = 2 \int_{x_*}^{\infty} dx \frac{\sqrt{G(x)}}{\sqrt{e^{\frac{1}{2}(\phi_* - \phi(x))} \left(\frac{h_*}{h(x)}\right)^{\frac{1}{2}} - 1}} \ . \tag{3.9.165}$$

Moreover, the length of the geodesic can be obtained by integrating ds_1 over the worldline,

$$\mathcal{L} = 2 \int_{x_*}^{\infty} dx \frac{e^{-\frac{\phi(x)}{4}} \left[h(x)\right]^{-\frac{1}{4}} \sqrt{G(x)}}{\sqrt{1 - e^{\frac{1}{2}(\phi(x)) - \phi_*} \left(\frac{h(x)}{h_*}\right)^{\frac{1}{2}}}} \ . \tag{3.9.166}$$

This integral is divergent. In order to regularize it, let us study the UV behavior of the integrand. For large x, the functions $h(x)$ and $G(x)$ behave as in (3.6.97) and (3.7.110), respectively. Thus, at leading order for large x,

$$\left[h(x)\right]^{-\frac{1}{4}} \sqrt{G(x)} \approx \frac{L_0}{b} x^{-1} \ . \tag{3.9.167}$$

In the UV region $x \to \infty$, the integrand in $\mathcal{L}$ behaves approximately as $2\, b^{-1}\, L_0\, e^{-\phi_0/4}\, x^{-1}$, which produces a logarithmic UV divergence when it is integrated. In order to tackle this divergence, let us regulate the integral by extending it up to some cutoff $x_{\max}$ and renormalize the geodesic length by subtracting the divergent part. Accordingly, we define the renormalized geodesic length as:

$$\mathcal{L}_r = 2 \int_{x_*}^{x_{max}} dx \frac{e^{-\frac{\phi(x)}{4}} \left[h(x)\right]^{-\frac{1}{4}} \sqrt{G(x)}}{\sqrt{1 - e^{\frac{1}{2}(\phi(x)) - \phi_*} \left(\frac{h(x)}{h_*}\right)^{\frac{1}{2}}}} - \frac{2\, L_0\, e^{-\frac{\phi_0}{4}}}{b} \log(\mathcal{C}\, x_{max}) \,, \tag{3.9.168}$$

where $\mathcal{C}$ is a constant to be fixed by choosing a suitable normalization condition for the correlator.

Our background interpolates between two limiting AdS_4 geometries, at the UV and IR, with different radii. For an equal-time two-point function $\left\langle \mathcal{O}(t,l)\, \mathcal{O}(t,0) \right\rangle$ the UV and IR limits should correspond to the cases in which $r_q\, l$ is small or large, respectively. At the two endpoints of the flow, the theory is conformal invariant and the two-point correlator behaves as a power law in l. We can use this fact to fix the normalization constant $\mathcal{C}$ in (3.9.168). Actually, we will assume that the field $\mathcal{O}$ is canonically normalized in the short-distance $r_q\, l \to 0$ limit and, therefore, the UV limit of the two-point correlator is:

$$\left\langle \mathcal{O}(t,l)\, \mathcal{O}(t,0) \right\rangle_{UV} = \frac{1}{\left(r_q\, l/\sqrt{\lambda}\right)^{2\Delta_{UV}}} \,, \qquad (r_q\, l \to 0) \,, \tag{3.9.169}$$

where the $\sqrt{\lambda}$ and r_q factors have been introduced for convenience. In (3.9.169) Δ_{UV} is the conformal dimension of the operator $\mathcal{O}$ in the UV CFT, which for the dual of a bulk field of mass m is:

$$\Delta_{UV} = m\, L_0\, e^{-\frac{\phi_0}{4}} \,, \tag{3.9.170}$$

where we have taken into account that m is large and that $L_0\, e^{-\frac{\phi_0}{4}}$ is the AdS_4 radius of the UV massless flavored geometry in the Einstein frame. It is shown in appendix 3.A.5 that, indeed, the correlators derived from (3.9.168) display the canonical form (3.9.169) if the constant $\mathcal{C}$ is chosen appropriately (see (3.A.140)). In appendix 3.A.5 we have also computed the first deviation from the conformal UV behavior. In this case the numerator on the right-hand side of (3.9.169) is not one but a function $f_\Delta(r_q\, l/\sqrt{\lambda})$ such that $f_\Delta(r_q\, l/\sqrt{\lambda} = 0) = 1$. We show in appendix 3.A.5 that $f_\Delta(r_q\, l/\sqrt{\lambda}) - 1 \propto (r_q\, l/\sqrt{\lambda})^{2b}$ for small $r_q\, l$. The explicit form of the first correction to the non-conformal behavior can be computed analytically from the mass corrections of section 3.6.1 and appendix 3.A.2 (see eqs. (3.A.151)-(3.A.153)).
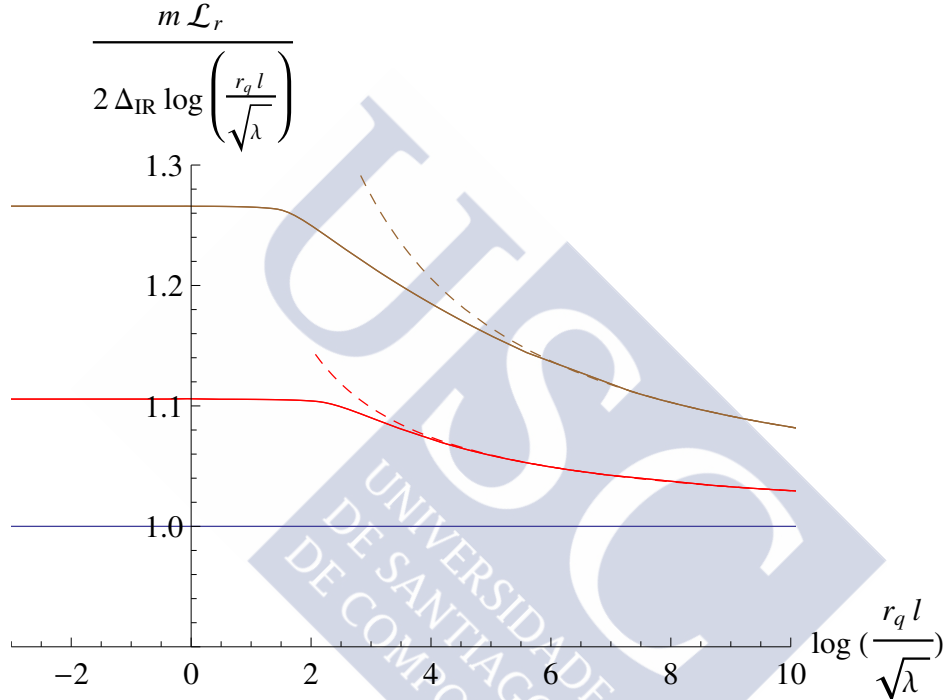
Figure 3.8: Plot of $m\,\mathcal{L}_r/\big(2\Delta_{IR}\log(r_q\, l/\sqrt{\lambda})\big)$ versus the logarithm of $r_q\, l/\sqrt{\lambda}$. Notice that, according to (3.9.159), $m\,\mathcal{L}_r = -\log\langle\mathcal{O}(t, l)\,\mathcal{O}(t, 0)\rangle$. The three curves correspond to $\hat{\epsilon} = 0$ (bottom, blue), $\hat{\epsilon} = 1$ (middle, red), and $\hat{\epsilon} = 9$ (top, brown). In the deep UV ($r_q\, l \to 0$) the curves approach the constant value Δ_{UV}/Δ_{IR}. The dashed curves correspond to the behavior (3.9.172), with the normalization constant $\mathcal{N}$ given in (3.A.167).

When the distance $r_q\, l$ is large the theory reaches a new conformal point. Accordingly, the two-point function should behave again as a power law. Notice, however, that the conformal dimension Δ_{IR} in the IR of an operator dual to a particle of mass m is different from the UV value (3.9.170). Indeed, in the IR the conformal dimension Δ_{IR} for an operator $\mathcal{O}$ of mass m is the one corresponding to the unflavored ABJM theory,

$$\Delta_{IR} = m\, L_{ABJM}\, e^{-\frac{\phi_{ABJM}}{4}} \,, \tag{3.9.171}$$

where L_{ABJM} and ϕ_{ABJM} are given, respectively, in (3.2.3) and (3.2.4). Actually, one can check that $\Delta_{UV} \geq \Delta_{IR}$ and that $\Delta_{UV}/\Delta_{IR} \propto \hat{\epsilon}^{\frac{1}{16}}$ for large values of the deformation param-

eter $\hat{\epsilon}$. The calculation of the two-point function in the IR limit of large $r_q\, l$ is performed in detail in appendix 3.A.5, with the result:

$$\left\langle \mathcal{O}(t,l)\,\mathcal{O}(t,0) \right\rangle_{IR} \;=\; \frac{\mathcal{N}}{\left(r_q\, l/\sqrt{\lambda}\right)^{2\Delta_{IR}}}\;, \qquad\qquad (r_q\, l \to \infty)\;, \qquad\qquad (3.9.172)$$

where $\mathcal{N}$ is a constant whose analytic expression is written in (3.A.167). Notice that $\mathcal{N} \neq 1$ due to our choice of the constant $\mathcal{C}$ in (3.9.168), which corresponds to imposing the canonical normalization (3.9.169) to the two-point function in the UV regime.

The results obtained by the numerical evaluation of the integral (3.9.168) interpolate smoothly between the conformal behaviors (3.9.169) and (3.9.172). This is shown in Fig. 3.8, where we plot $-\log\langle\mathcal{O}(t,l)\,\mathcal{O}(t,0)\rangle/(2\Delta_{IR}\log(r_q\, l/\sqrt{\lambda}))$ as a function of $\log(r_q\, l/\sqrt{\lambda})$. For small values of $r_q\, l/\sqrt{\lambda}$ the curve asymptotes to the ratio Δ_{UV}/Δ_{IR} of conformal dimensions, in agreement with (3.9.169), whereas for large $r_q\, l/\sqrt{\lambda}$ we recover the IR behavior (3.9.172).

3.10 Meson spectrum

Let us now test the flow encoded in our geometry by analyzing the mass spectrum of $q\bar{q}$ bound states. We will loosely refer to these bound states as mesons, although our background is not confining and quarkonia would be a more appropriate name for them. To carry out our analysis we will introduce additional external quarks, with a mass μ_q not necessarily equal to the mass m_q of the quarks which backreact on the geometry. To distinguish between the two types of flavors we will call valence quarks to the additional ones, whereas the unquenched N_f dynamical flavors of the geometry will be referred to as sea quarks. The ratio μ_q/m_q of the masses of the two types of quarks will be an important quantity in what follows. Indeed, μ_q/m_q is the natural parameter for the holographic renormalization group trajectory. When μ_q/m_q is large (small) we expect to reach a UV (IR) conformal fixed point, whereas for intermediate values of this mass ratio the theory should flow in such a way that the screening effects produced by the sea quarks decrease as we move towards the IR.

Within the context of the gauge/gravity duality, the valence quarks can be introduced by adding an additional flavor D6-brane, which will be treated as a probe in the backreacted geometry. The mesonic mass spectrum can be obtained from the normalizable fluctuations of the D6-brane probe. The way in which the D6-brane probe is embedded in the ten-dimensional geometry preserving the supersymmetry of the background can be determined by using kappa symmetry. For fixed values of the Minkowski and holographic coordinates, the D6-brane extends over a cycle inside the $\mathbb{CP}^3$ which has two directions along the $\mathbb{S}^4$ base and one direction along the $\mathbb{S}^2$ fiber. In order to specify further this configuration, let us parameterize the $SU(2)$ left invariant one-forms ω_i of the four-sphere metric (3.2.7) in terms of three angles $\hat{\theta}$, $\hat{\varphi}$ and $\hat{\psi}$,

$$
\begin{aligned}
\omega^1 &= \cos\hat{\psi}\, d\hat{\theta} + \sin\hat{\psi}\,\sin\hat{\theta}\, d\hat{\varphi}\;, \\
\omega^2 &= \sin\hat{\psi}\, d\hat{\theta} - \cos\hat{\psi}\,\sin\hat{\theta}\, d\hat{\varphi}\;, \\
\omega^3 &= d\hat{\psi} + \cos\hat{\theta}\, d\hat{\varphi}\;,
\end{aligned}
\qquad\qquad (3.10.173)
$$

with $0 \leq \hat{\theta} \leq \pi$, $0 \leq \hat{\varphi} < 2\pi$, $0 \leq \hat{\psi} \leq 4\pi$. Then, our D6-brane probe will be extended along the Minkowski directions and embedded in the geometry in such a way that the angles $\hat{\theta}$ and $\hat{\varphi}$ are constant and that the angle θ of the $\mathbb{S}^2$ fiber depends on the holographic variable x. The pullbacks (denoted by a hat) of the left-invariant $SU(2)$ one-forms (3.10.173) are $\hat{\omega}^1 = \hat{\omega}^2 = 0$ and $\hat{\omega}^3 = d\hat{\psi}$. The kappa symmetric configurations are those for which the function $\theta(x)$ satisfies the first order BPS equation [75]:

$$x \frac{d\theta}{dx} = \cot\theta , \tag{3.10.174}$$

which can be integrated as:

$$\cos\theta = \frac{x_*}{x} . \tag{3.10.175}$$

Here x_* is the minimum value of the variable x for the embedding, *i.e.*, the value of x for the tip of the brane. This minimum value of the coordinate x for the embedding is related to the mass μ_q of the valence quarks introduced by the flavor probe. Indeed, by computing the Nambu-Goto action of a fundamental string stretched in the holographic direction between $x = 0$ and $x = x_*$ we obtain μ_q as:

$$\mu_q = \frac{1}{2\pi\alpha'} \int_0^{x_*} \frac{e^{g(x)}}{x} dx . \tag{3.10.176}$$

In the following we will take the Regge slope $\alpha' = 1$. Moreover, to simplify the description of the embedding, let us introduce the angular coordinate α, defined as follows:

$$\xi = \tan\left(\frac{\alpha}{2}\right) , \tag{3.10.177}$$

and let us define new angles β and ψ as:

$$\beta = \frac{\hat{\psi}}{2} , \qquad \psi = \varphi - \frac{\hat{\psi}}{2} , \tag{3.10.178}$$

where φ is the angle in (3.2.9). One can check that the ranges of the new angular variables are $0 \leq \alpha < \pi$, $0 \leq \beta$, $\psi < 2\pi$. We will take the following set of worldvolume coordinates for the D6-brane:

$$\zeta^a = (x^\mu, x, \alpha, \beta, \psi) . \tag{3.10.179}$$

Then, it is straightforward to verify that the induced metric on the D6-brane worldvolume takes the form:

$$ds_7^2 = h^{-\frac{1}{2}} dx_{1,2}^2 + \frac{h^{\frac{1}{2}} e^{2g}}{x^2 - x_*^2} dx^2 + h^{\frac{1}{2}} e^{2f} \left[d\alpha^2 + \sin^2\alpha \, d\beta^2 \right] + (x^2 - x_*^2) \frac{h^{\frac{1}{2}} e^{2g}}{x^2} \left(d\psi + \cos\alpha \, d\beta \right)^2 . \tag{3.10.180}$$

We will restrict ourselves to study a particular set of fluctuations of the D6-brane probe, namely the fluctuations of the worldvolume gauge field A_a. The equation for these fluctuations is:

$$\partial_a \left[e^{-\phi} \sqrt{-\det g} \, g^{ac} g^{bd} F_{cd} \right] = 0 , \tag{3.10.181}$$

where g_{ab} is the induced metric (3.10.180). More concretely, we will study this equation for the following ansatz for A_a:

$$A_\mu = \xi_\mu e^{ik_\nu x^\nu} R(x) , \qquad (\mu = 0, 1, 2) , \qquad A_x = A_i = 0 , \qquad (3.10.182)$$

where ξ_μ is a constant polarization vector and A_i denote the components along the angular directions. These modes are dual to the vector mesons of the theory, with k_μ being the momentum of the meson ($\eta^{\mu\nu} k_\mu k_\nu = -m^2$, with m being the mass of the meson). The non-vanishing components of the field strength F_{ab} are:

$$F_{\mu\nu} = i(k_\mu \xi_\nu - k_\nu \xi_\mu) e^{ik_\nu x^\nu} R(x) , \qquad F_{x\mu} = \xi_\mu e^{ik_\nu x^\nu} R'(x) . \qquad (3.10.183)$$

The fluctuation equation (3.10.181) is trivially satisfied when $b = i$, whereas for $b = x$ it is satisfied if the polarization is transverse:

$$\eta^{\mu\nu} k_\mu \xi_\nu = 0 . \qquad (3.10.184)$$

Moreover, by taking $b = \mu$ in (3.10.181) we arrive at the following differential equation for the radial function R:

$$\partial_x \left[\frac{h^{\frac{1}{4}} e^{2f-\phi}}{x} (x^2 - x_*^2) \partial_x R \right] + m^2 \frac{h^{\frac{5}{4}} e^{2f+2g-\phi}}{x} R = 0 . \qquad (3.10.185)$$
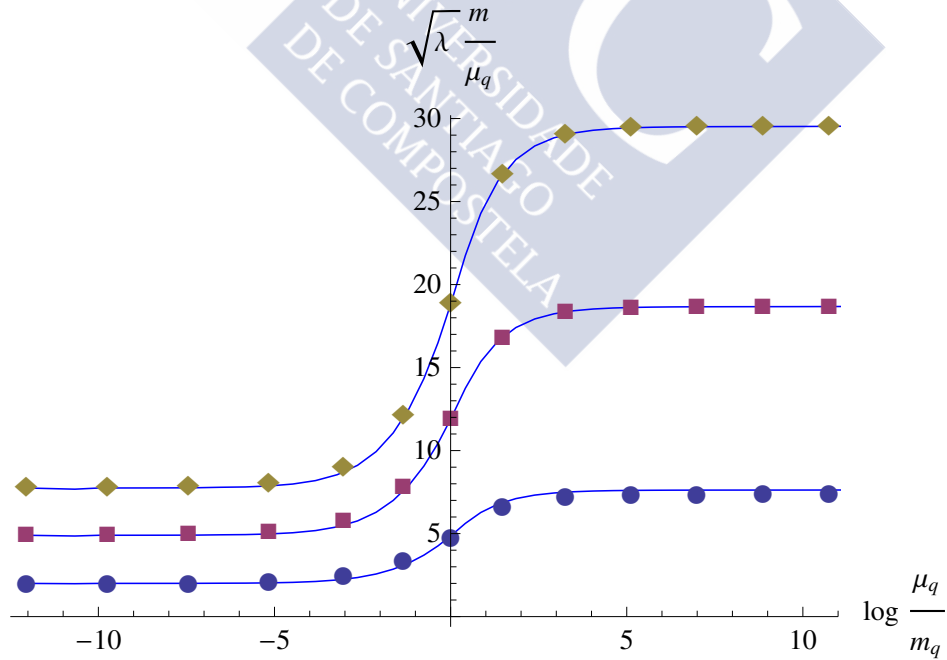
Figure 3.9: Numerical values of the meson masses for the first three levels ($n = 0, 1, 2$) as a function of the sea quark mass m_q for deformation parameter $\hat{\epsilon} = 9$. The solid curves depict the WKB estimate (3.10.186).

The mass levels correspond to the values of m for which there are normalizable solutions of (3.10.185). They can be obtained numerically by the shooting technique. One gets in this way a discrete spectrum depending on a quantization number n ($n \in \mathbb{Z}$, $n \geq 0$). The numerical results for the first three levels are shown in Fig. 3.9 as functions of the mass ratio μ_q/m_q. One notices in these results that the meson masses increase as we move from the IR ($\mu_q/m_q \to 0$) to the UV ($\mu_q/m_q \to \infty$). This non-trivial flow is due to the vacuum polarization effects of the sea quarks, which are enhanced as we move towards the UV and the sea quarks become effectively massless. This is the expected behavior of bound state masses for a theory in the Coulomb phase, since the screening effects reduce effectively the strength of the quark-antiquark force.

One can get a very accurate description of the flow by applying the WKB approximation. The detailed calculation is presented in appendix 3.A.6. The WKB formula for the mass spectrum is:

$$m_{WKB} = \frac{\pi}{\sqrt{2}\,\xi(x_*)} \sqrt{(n+1)(2n+1)} \,, \qquad (n = 0, 1, 2, \cdots) \,, \qquad (3.10.186)$$

where $\xi(x_*)$ is the following integral:

$$\xi(x_*) = \int_{x_*}^{\infty} dx\, \frac{e^{g(x)}\sqrt{h(x)}}{\sqrt{x^2 - x_*^2}} \,. \qquad (3.10.187)$$

The WKB mass levels (3.10.186) are compared with those obtained by the shooting technique in Fig. 3.9. We notice from these plots that the estimate (3.10.186) describes rather well the numerical results along the flow. Moreover, we can use the UV and IR limits of the functions g and h to obtain the asymptotic form of the WKB spectrum at the endpoints of the flow. This analysis is performed in detail in appendix 3.A.6 (see eqs. (3.A.182) and (3.A.188)). As expected, in the deep IR the mass levels coincide with those of the unflavored ABJM model. In this latter model the mass spectrum of vector mesons can be computed analytically since the fluctuation equation can be solved in terms of hypergeometric functions [152, 153]. When $\mu_q/m_q \to \infty$ the meson masses coincide with those obtained for the massless flavored model of [75].

We can use the WKB formulas (3.A.182) and (3.A.188) for the spectrum at the endpoints of the renormalization group flow to estimate the variation generated in the meson masses by changing the sea quark mass m_q and switching on and off gradually the screening effects. It is interesting to point out that, within the WKB approximation, the ratio of these masses only depends on the number of flavors, and is given by:

$$\frac{m_{WKB}^{(UV)}}{m_{WKB}^{(IR)}} = \frac{\sqrt{\pi}}{2}\, \frac{\Gamma\left(\frac{b+1}{2b}\right)}{\Gamma\left(\frac{2b+1}{2b}\right)}\, \frac{1}{\sigma} \,, \qquad (3.10.188)$$

where σ is the screening function defined in (3.8.157). As expected, when $N_f = 0$ the right-hand side of (3.10.188) is equal to one, $i.e.$, there is no variation of the masses along the flow. On the contrary, when $N_f > 0$ the UV/IR mass ratio in (3.10.188) is always greater than one, which means that the masses grow as we move towards the UV and the screening effects

become more important. In appendix 3.A.6 we have expanded (3.10.188) for low values of the deformation parameter $\hat{\epsilon}$ (see (3.A.189)). Moreover, for large $\hat{\epsilon}$ the UV/IR mass ratio grows as $\sqrt{\hat{\epsilon}}$ (see (3.A.190) for the explicit formula).

3.11 Discussion

In this chapter we obtained a holographic dual to Chern-Simons matter theory with un-quenched flavor in the strongly-coupled Veneziano limit. The flavor degrees of freedom were added by a set of D6-branes smeared along the internal directions, which backreacted on the geometry by squashing it, while preserving $\mathcal{N} = 1$ supersymmetry. We considered massive flavors and found a non-trivial holographic renormalization group flow connecting two scale-invariant fixed points: the unflavored ABJM theory at the IR and the massless flavored model at the UV.

The quark mass m_q played an important role as a control parameter of the solution. By increasing m_q our solutions became closer to the unflavored ABJM model and we smoothly connected the unquenched flavored model to the ABJM theory without fundamentals. After this soft introduction of flavor no pathological behavior was found. Indeed, our backgrounds had good IR and UV behaviors, contrary to what happens to other models with unquenched flavor [73]. This made the ABJM model especially adequate to analyze the effects of un-quenched fundamental matter in a holographic setup.

We analyzed different flavor effects in our model. In general, the screening effects due to loops of fundamentals were controlled by the relative value of the quark mass m_q with respect to the characteristic length scale l of the observable. If $m_q l$ was small, which corresponds to the UV regime, the flavor effects were important, whereas they were suppressed if $m_q l$ is large, *i.e.*, at the IR. Among the different observables that we analyzed, the holographic entanglement entropy for a disk was specially appropriate since it counts precisely the effective number of degrees of freedom which are relevant at the length scale given by the radius of the disk. By using the refined entanglement entropy $\mathcal{F}$ introduced in [137], we explicitly obtained the running of $\mathcal{F}$ and verified the reduction of the number of degrees at the IR that was mentioned above. The other observables studied also supported this picture.

The results obtained in this chapter can be generalized in several directions. One possible generalization could be the construction of a black hole for the unquenched massive flavor. Such a background could serve to study the meson melting phase transition which occurs when the tip of the brane approaches the horizon. This system was studied in [136], in the case in which the massive flavors are quenched and the corresponding flavor brane is a probe. Another possibility would be trying to find a gravity dual of a theory in which the sum of the two Chern-Simons levels is non-vanishing. According to [62] we should find a flavored solution of type IIA supergravity with non-zero Romans mass.

Moreover, to make contact with any condensed matter physics system, one is forced to consider non-vanishing components of the gauge field in the background or at the probe level. As an initial step in this direction, in chapter 4 we consider a probe D6-brane with electric field, magnetic field, charge density, currents and internal flux, in the ABJM background, and a gravity dual of a fractional quantum Hall system is constructed. Also, by adding

only charge density to the probe D6-brane worldvolume, quantum phase transitions are studied in chapter 5. A possible generalization of the studies performed in chapters 4 and 5 would be to consider the same probe D6-brane configuration with worldvolume gauge fields embedded in the background obtained in this chapter. A further generalization, and much more complicated, would be to consider the backreaction of the D6-branes with worldvolume gauge fields turned on.

3.A   Appendices

3.A.1   BPS equations

In this appendix we will derive the master equation (3.3.25), as well as the equations that allow to construct the metric and dilaton from the master function $W(x)$ (*i.e.*, (3.3.26), (3.3.27), and (3.3.28)).

Let us begin by writing the BPS equations that guarantee the preservation of $\mathcal{N} = 1$ SUSY. They can be written in terms of the function Λ introduced in [75], which is defined as the following combination of the dilaton and the warp factor:

$$e^{\Lambda} \equiv e^{\phi} \, h^{-\frac{1}{4}} \ . \tag{3.A.1}$$

Then, it was proved in [75] that $\Lambda(r)$, $f(r)$, and $g(r)$ are solutions to the following system of first-order differential equations:

$$\frac{d\Lambda}{dr} = k \, \eta \, e^{\Lambda - 2f} - \frac{k}{2} \, e^{\Lambda - 2g} \ ,$$

$$\frac{df}{dr} = \frac{k \, \eta}{4} \, e^{\Lambda - 2f} - \frac{k}{4} \, e^{\Lambda - 2g} + e^{-2f + g} \ ,$$

$$\frac{dg}{dr} = \frac{k \, \eta}{2} \, e^{\Lambda - 2f} + e^{-g} - e^{-2f + g} \ . \tag{3.A.2}$$

Moreover, the warp factor $h(r)$ can be recovered from Λ, f, and g through:

$$h(r) = e^{-\Lambda(r)} \left[\alpha - 3\pi^2 N \int^r e^{2\Lambda(z) - 4f(z) - 2g(z)} \, dz \right] \ , \tag{3.A.3}$$

where α is an integration constant. Given h and Λ, the dilaton ϕ is obtained from (3.A.1). The function K of the RR four-form can be related to the other functions of the background by using (3.3.21). Alternatively, K can be obtained from the BPS system as:

$$K = \frac{d}{dr} \left(e^{-\phi} \, h^{-\frac{3}{4}} \right) \ . \tag{3.A.4}$$

In terms of the x variable defined in (3.3.22), the BPS system (3.A.2) becomes:

$$x \frac{d\Lambda}{dx} = k\,\eta\,e^{\Lambda - 2f + g} - \frac{k}{2}\,e^{\Lambda - g} \ ,$$

$$x \frac{df}{dx} = \frac{k}{4}\,\eta\,e^{\Lambda - 2f + g} - \frac{k}{4}\,e^{\Lambda - g} + e^{-2f + 2g} \ ,$$

$$x \frac{dg}{dx} = \frac{k}{2}\,\eta\,e^{\Lambda - 2f + g} + 1 - e^{-2f + 2g} \ . \tag{3.A.5}$$

In order to reduce this system, let us define as in [75] the functions $\Sigma(x)$ and $\Delta(x)$,

$$\Sigma \equiv \Lambda - f \ , \qquad\qquad \Delta \equiv f - g \ . \tag{3.A.6}$$

Then, one can easily show that $\Sigma(x)$ and $\Delta(x)$ satisfy the system:

$$x \frac{d\Sigma}{dx} = \frac{k}{4}\,e^{\Sigma}\left(3\eta\,e^{-\Delta} - e^{\Delta}\right) - e^{-2\Delta} \ ,$$

$$x \frac{d\Delta}{dx} = -\frac{k}{4}\,e^{\Sigma}\left(\eta\,e^{-\Delta} + e^{\Delta}\right) - 1 + 2e^{-2\Delta} \ , \tag{3.A.7}$$

whereas g can be obtained from Σ and Δ by integrating the equation:

$$x \frac{dg}{dx} = \frac{k}{2}\,\eta\,e^{\Sigma - \Delta} + 1 - e^{-2\Delta} \ . \tag{3.A.8}$$

Let us next define the master function $W(x)$ as in (3.3.24). One immediately verifies that, in terms of the functions Δ and Σ, this definition is equivalent to

$$W(x) = \frac{4}{k}\,e^{\Delta - \Sigma}\,x \ . \tag{3.A.9}$$

By computing the derivative of (3.A.9) and using the BPS system (3.A.7), one can easily prove that:

$$\frac{dW}{dx} = \frac{12}{k}\,e^{-\Sigma - \Delta} - 4\eta \ . \tag{3.A.10}$$

From (3.A.10) one immediately finds:

$$e^{\Sigma + \Delta} = \frac{12}{k}\,\frac{1}{W' + 4\eta} \ , \tag{3.A.11}$$

where the prime denotes derivative with respect to x. Moreover, from the BPS system we can calculate the derivative of $\Sigma + \Delta$ and write the result as:

$$x \frac{d}{dx}\left(e^{\Sigma + \Delta}\right) = \frac{2x\,\eta\,e^{\Sigma + \Delta}}{W} - \left[\frac{k}{2}\,e^{\Sigma + \Delta} + 1\right]e^{\Sigma + \Delta} + \frac{4}{k}\frac{x}{W} \ . \tag{3.A.12}$$

Plugging (3.A.11) into (3.A.12), we arrive at the following second-order equation for $W(x)$:

$$x \frac{d}{dx}\left(\frac{1}{W' + 4\eta}\right) + \frac{W' + 4\eta + 6}{(W' + 4\eta)^2} - \frac{x}{3}\frac{W' + 10\eta}{W(W' + 4\eta)} = 0 \ , \tag{3.A.13}$$

which can be straightforwardly shown to be equivalent to the master equation (3.3.25).

Let us see now how one can reconstruct the full solution from the knowledge of the function $W(x)$. First of all, we notice that from the expression of W in (3.A.9), we get:

$$e^{\Sigma - \Delta} \;=\; \frac{4}{k}\,\frac{x}{W}\;. \tag{3.A.14}$$

By combining this expression with (3.A.11) we obtain Σ and Δ:

$$e^{2\Sigma} \;=\; \frac{48}{k^2}\,\frac{x}{W(W'+4\eta)}\;, \qquad\qquad e^{2\Delta} \;=\; \frac{3W}{x(W'+4\eta)}\;. \tag{3.A.15}$$

By noticing that $e^{2\Delta} = q$ we arrive at the representation of the squashing function q written in (3.3.29). Moreover, by using this result in (3.A.8), we obtain the differential equation satisfied by g:

$$\frac{dg}{dx} \;=\; \frac{2\eta}{3W} - \frac{W'}{3W} + \frac{1}{x}\;, \tag{3.A.16}$$

which allows to obtain $g(x)$ once $W(x)$ is known. The result of this integration is just the expression written in (3.3.26). Moreover, taking into account the expression of the squashing factor q we get precisely the expression of f written in (3.3.26).

Let us now compute Λ by using $\Lambda = \Sigma + \Delta + g$ and (3.A.11). We get:

$$e^{\Lambda} \;=\; \frac{12}{k}\,\frac{e^{g}}{W'+4\eta}\;, \tag{3.A.17}$$

and, after using (3.3.26), we arrive at:

$$e^{\Lambda} \;=\; \frac{12}{k}\,\frac{x}{W^{\frac{1}{3}}(W'+4\eta)}\,\exp\!\left[\frac{2}{3}\int^{x}\frac{\eta(\xi)d\xi}{W(\xi)}\right]\;. \tag{3.A.18}$$

By using this result and (3.3.26) in (3.A.3), we get that the warp factor can be written as in (3.3.27). The expression (3.3.28) for the dilaton is just a consequence of the definition of Λ in (3.A.1) and of (3.A.18).

Equations of motion

Let us now verify that the first-order BPS system (3.A.2) implies the second-order equations of motion for the different fields. Let us work in Einstein frame and write the total action as:

$$S \;=\; S_{IIA} + S_{\text{sources}}\;, \tag{3.A.19}$$

where the action of type IIA supergravity is given by:

$$S_{IIA} \;=\; \frac{1}{2\kappa_{10}^2}\left[\int\sqrt{-g}\left(R - \frac{1}{2}\,\partial_{\mu}\phi\,\partial^{\mu}\phi\right) - \frac{1}{2}\int\left[e^{\frac{3\phi}{2}}\,{}^*F_2\wedge F_2 + e^{\frac{\phi}{2}}\,{}^*F_4\wedge F_4\right]\right]\;, \tag{3.A.20}$$

and the source contribution is the DBI+WZ action for the set of smeared D6-branes. Let us write this last action as in [75]. First of all, we introduce a charge distribution three-form Ω. Then, the DBI+WZ action is given by:

$$S_{\text{sources}} = -T_{D6} \int \left(e^{\frac{3\phi}{4}} \mathcal{K} - C_7 \right) \wedge \Omega \, , \tag{3.A.21}$$

where the DBI term has been written in terms of the so-called calibration form (denoted by $\mathcal{K}$), whose pullback to the worldvolume is equal to the induced volume form for the supersymmetric embeddings. The expression of $\mathcal{K}$ has been written in [75]. Let us reproduce it here for completeness:

$$\mathcal{K} = -e^{012} \wedge \left(e^{3458} - e^{3469} + e^{3579} + e^{3678} + e^{4567} + e^{4789} + e^{5689} \right) \, , \tag{3.A.22}$$

where the e^i's are the one-forms of the basis corresponding to the forms (3.2.11) and (3.2.14) (see [75] for further details). Notice that the equation of motion for C_7 derived from (3.A.19) is just $dF_2 = 2\pi \, \Omega$. Therefore, the Ω for our ansatz can be read from the right-hand side of (3.3.20).

The Maxwell equations for the forms F_2 and F_4 derived from (3.A.19) are:

$$d\left(e^{\frac{3\phi}{2}} \, {}^*F_2 \right) = 0 \, , \qquad d\left(e^{\frac{\phi}{2}} \, {}^*F_4 \right) = 0 \, , \tag{3.A.23}$$

while the equation for the dilaton is:

$$d\,{}^*d\phi = \frac{3}{4} \, e^{\frac{3\phi}{2}} \, {}^*F_2 \wedge F_2 + \frac{1}{4} e^{\frac{\phi}{2}} \, {}^*F_4 \wedge F_4 + \frac{3}{2} \kappa_{10}^2 \, T_{D6} \, e^{\frac{3\phi}{4}} \mathcal{K} \wedge \Omega \, . \tag{3.A.24}$$

One can verify that, for our ansatz, (3.A.23) and (3.A.24) are a consequence of the BPS equations (3.A.2). To carry out this verification we need to know the radial derivatives of $h(r)$ and $\phi(r)$ (which are not written in (3.A.2)). The derivative of h can be related to the derivative of $\Lambda(r)$,

$$\frac{dh}{dr} = -h \, \frac{d\Lambda}{dr} - 3\pi^2 \, N \, e^{\Lambda - 4f - 2g} \, . \tag{3.A.25}$$

The radial derivative of the dilaton can be put in terms of the derivative of Λ and h by using (3.A.1):

$$\frac{d\phi}{dr} = \frac{d\Lambda}{dr} + \frac{1}{4h} \frac{dh}{dr} \, . \tag{3.A.26}$$

It remains to check Einstein equations, which read:

$$R_{\mu\nu} - \frac{1}{2} \, g_{\mu\nu} \, R = \frac{1}{2} \, \partial_\mu \phi \, \partial_\nu \phi - \frac{1}{4} \, g_{\mu\nu} \, \partial_\rho \phi \, \partial^\rho \phi + \frac{1}{4} e^{\frac{3\phi}{2}} \left[2 F^{(2)}_{\mu\rho} F^{(2)\,\rho}_\nu - \frac{1}{2} \, g_{\mu\nu} \, F_2^2 \right]$$

$$+ \frac{1}{48} e^{\frac{\phi}{2}} \left[4 F^{(4)}_{\mu\rho\sigma\lambda} F^{(4)\,\rho\sigma\lambda}_\nu - \frac{1}{2} \, g_{\mu\nu} \, F_4^2 \right] + T^{\text{sources}}_{\mu\nu} \, , \tag{3.A.27}$$

where $T^{\text{sources}}_{\mu\nu}$ is the stress-energy tensor for the flavor branes, which is defined as:

$$T^{\text{sources}}_{\mu\nu} = -\frac{2\kappa_{10}^2}{\sqrt{-g}} \frac{\delta S_{\text{sources}}}{\delta g^{\mu\nu}} \, . \tag{3.A.28}$$

In order to write the explicit expression for $T_{\mu\nu}^{\text{sources}}$ derived from the definition (3.A.28), let us introduce the following operation for any two p-forms $\omega_{(p)}$ and $\lambda_{(p)}$:

$$\omega_p \lrcorner \lambda_{(p)} = \frac{1}{p!} \omega^{\mu_1 \ldots \mu_p} \lambda_{\mu_1 \ldots \mu_p} \ . \tag{3.A.29}$$

Then, by computing explicitly the derivative of the action (3.A.21) with respect to the metric, one can check that:

$$T_{\mu\nu}^{\text{sources}} = \kappa_{10}^2 \, T_{D_6} \, e^{\frac{3\phi}{4}} \left[g_{\mu\nu} \, {}^*\mathcal{K} \lrcorner \Omega - \frac{1}{2} \Omega_\mu{}^{\rho\sigma} \left({}^*\mathcal{K} \right)_{\nu\rho\sigma} \right] \ . \tag{3.A.30}$$

It is now straightforward to compute explicitly the different components of this tensor. Written in flat components in the basis in which the calibration form has the form (3.A.22), we get:[5]

$$T_{00} = -T_{11} = -T_{22} = k \left(\eta - 1 + \frac{e^g}{2} \frac{d\eta}{dr} \right) e^{-2f - g + \frac{3\phi}{2}} \, h^{-\frac{3}{4}} \ ,$$

$$T_{33} = k(\eta - 1) \, e^{-2f - g + \frac{3\phi}{2}} \, h^{-\frac{3}{4}} \ ,$$

$$T_{ab} = -\frac{k}{2} \left(\eta - 1 + \frac{e^g}{2} \frac{d\eta}{dr} \right) e^{-2f - g + \frac{3\phi}{2}} \, h^{-\frac{3}{4}} \delta_{ab} \ , \qquad\qquad (a, b = 4, \ldots, 7) \ ,$$

$$T_{88} = T_{99} = -\frac{k}{2} \left(\eta - 1 + e^g \frac{d\eta}{dr} \right) e^{-2f - g + \frac{3\phi}{2}} \, h^{-\frac{3}{4}} \ . \tag{3.A.31}$$

By using these values one can verify that, the Einstein equations (3.A.27) are indeed satisfied as a consequence of the first-order system (3.A.2). Notice that, for the massive flavored background of section 3.6, $d\eta/dr$ (and, therefore, $T_{\mu\nu}$) has a finite discontinuity at $r = r_q$. It follows from (3.A.27) that the Ricci tensor $R_{\mu\nu}$ has also a finite jump at this point.

3.A.2   Mass corrections in the UV

In this appendix we show how to obtain the first corrections to the conformal behavior of the metric and the dilaton from the UV asymptotic expansion of the master function $W(x)$ written in (3.6.89). First we notice that the ratio η_0/A_0 can be written in terms of b as:

$$\frac{\eta_0}{A_0} = \frac{3}{2b} - 1 \ , \tag{3.A.32}$$

leading to a useful identity:

$$x^{\frac{1}{b} - \frac{2}{3}} \, \exp\left[-\frac{2}{3} \int_1^x \frac{\eta_0}{A_0} \frac{d\xi}{\xi} \right] = 1 \ . \tag{3.A.33}$$

Inserting the unit written in this way in the integral appearing in the expression of e^g in (3.5.78), we get:

$$\exp\left[\frac{2}{3} \int_1^x \frac{\eta(\xi) d\xi}{W(\xi)} \right] = x^{\frac{1}{b} - \frac{2}{3}} \, J \, \mathcal{G}(x) \ , \tag{3.A.34}$$

---

[5] As compared to the case studied in [75], now we have terms proportional to $d\eta/dr$ that were absent for massless flavors.

where J is the following constant integral (depending on $\hat{\epsilon}$):

$$J \equiv \exp\left[\frac{2}{3}\int_1^\infty \left[\frac{\eta(\xi)}{W(\xi)} - \frac{\eta_0}{A_0\,\xi}\right]d\xi\right] , \qquad (3.A.35)$$

and $\mathcal{G}(x)$ is the function

$$\mathcal{G}(x) \equiv \exp\left[\frac{2}{3}\int_\infty^x \left[\frac{\eta(\xi)}{W(\xi)} - \frac{\eta_0}{A_0\,\xi}\right]d\xi\right] . \qquad (3.A.36)$$

Using these results, we can immediately write:

$$e^g = r_q \left[\frac{(\hat{\gamma}+1)^2}{2\,\hat{\gamma}}\right]^{\frac{1}{3}} J\,x^{\frac{1}{b}} \left[\frac{x}{W(x)}\right]^{\frac{1}{3}} \mathcal{G}(x) . \qquad (3.A.37)$$

The function $\mathcal{G}(x)$ can be easily expanded for large x. At first non-trivial order we get:

$$\mathcal{G}(x) = 1 + \frac{1}{3A_0}\left[\eta_0 - 1 + A_2\,\frac{\eta_0}{A_0}\right]\frac{1}{x^2} + \cdots . \qquad (3.A.38)$$

Using that, for large x,

$$\left[\frac{x}{W(x)}\right]^{\frac{1}{3}} = \frac{1}{A_0^{\frac{1}{3}}}\left[1 - \frac{A_2}{3\,A_0}\frac{1}{x^2} + \cdots\right] , \qquad (3.A.39)$$

we easily arrive at the expansion of e^g written in (3.6.95). Let us next find the large x expansion for f, which can be obtained by using the expansion of g and q in the relation $e^f = \sqrt{q}\,e^g$. We get:

$$e^f = \sqrt{q_0}\,\frac{\kappa\,r_q}{b}\,J\,x^{\frac{1}{b}}\left[1 + \frac{f_2}{x^2} + \cdots\right] , \qquad (3.A.40)$$

where the coefficient f_2 is given by:

$$f_2 = g_2 + \frac{1}{2}\frac{q_2}{q_0} = g_2 + \frac{2-b}{2b}\,q_2 . \qquad (3.A.41)$$

It is straightforward to demonstrate that (3.A.41) coincides with the value of f_2 written in (3.6.96).

Let us now analyze the UV expansion of h. First, we evaluate the integral appearing in (3.3.27):

$$\int_x^\infty \frac{\xi\,e^{-3g(\xi)}}{W(\xi)^2}\,d\xi = \frac{2\hat{\gamma}\,b}{3\,(\hat{\gamma}+1)^2\,A_0\,(Jr_q)^3}\,x^{-\frac{3}{b}}\left[1 - \frac{3}{3+2b}\left(3g_2 + 2\frac{A_2}{A_0}\right)\frac{1}{x^2} + \cdots\right] . \qquad (3.A.42)$$

By combining this result with the expansions (3.6.95) and (3.6.91) we get:

$$h(x) = L_0^4\left[\frac{2\,\hat{\gamma}\,A_0}{(\hat{\gamma}+1)^2}\right]^{\frac{4}{3}}\frac{x^{-\frac{4}{b}}}{(J\,b\,r_q)^4}\left[1 + \frac{h_2}{x^2} + \cdots\right] , \qquad (3.A.43)$$

where L_0 is the UV AdS radius (3.3.54) and the coefficient h_2 is:

$$h_2 = -\frac{2(6+b)}{3+2b}\, g_2 - \left(\frac{6}{3+2b} + \frac{b}{3(2-b)}\right)\frac{A_2}{A_0} - \frac{2}{3}\frac{3-2b}{2-b}\frac{\eta_0-1}{\eta_0}\,. \tag{3.A.44}$$

One can readily check that the prefactor in (3.A.43) coincides with the one in (3.6.97) and that the coefficient h_2 written in (3.A.44) is the same as the one in (3.6.98).

Let us now obtain the UV expansion of the function $\Lambda(x)$, defined in (3.A.1), which can be written as:

$$e^{\Lambda(x)} = \frac{12\,r_q\,J}{k}\left[\frac{(\hat\gamma+1)^2}{2\,\hat\gamma}\right]^{\frac{1}{3}}\frac{x^{\frac{1}{b}}}{W'+4\eta}\left[\frac{x}{W(x)}\right]^{\frac{1}{3}}\mathcal{G}(x)\,. \tag{3.A.45}$$

The UV expansion of this expression is:

$$e^\Lambda = \frac{12\,r_q\,J}{k\,(A_0+4\eta_0)}\left[\frac{(\hat\gamma+1)^2}{2\,\hat\gamma\,A_0}\right]^{\frac{1}{3}}x^{\frac{1}{b}}\left(1+\frac{\Lambda_2}{x^2}+\cdots\right)\,, \tag{3.A.46}$$

where the coefficient Λ_2 can be written in terms of g_2 as:

$$\Lambda_2 = g_2 + \frac{A_2+4(\eta_0-1)}{A_0+4\eta_0} = g_2 + \frac{b}{3(2-b)}\left[\frac{2(3-2b)}{b}\frac{\eta_0-1}{\eta_0}+\frac{A_2}{A_0}\right]\,. \tag{3.A.47}$$

By using the value of g_2 in (3.6.96), we can find a more explicit expression for Λ_2:

$$\Lambda_2 = \frac{3-2b}{3}\left[\frac{1}{2b}+\frac{2}{2-b}\right]\frac{\eta_0-1}{\eta_0}+\frac{1}{3}\left[\frac{3-4b}{2b}+\frac{b}{2-b}\right]\frac{A_2}{A_0}\,. \tag{3.A.48}$$

Let us next obtain the expansion of e^ϕ by using $e^\phi = e^\Lambda h^{\frac{1}{4}}$. We get:

$$e^\phi = e^{\phi_0}\left(1+\frac{\phi_2}{x^2}+\cdots\right)\,, \tag{3.A.49}$$

where the prefactor is

$$e^{\phi_0} = \frac{12\,L_0}{k(A_0+4\eta_0)\,b}\,, \tag{3.A.50}$$

and can be shown to be the same as the asymptotic value of the dilaton written in (3.3.56). The coefficient ϕ_2 is:

$$\phi_2 = \Lambda_2 + \frac{1}{4}h_2\,, \tag{3.A.51}$$

which has been written more explicitly in (3.6.98).

Finally, let us write these results in terms of the r variable. At next-to-leading order, the relation between the coordinates x and r is obtained by integrating the differential equation:

$$\frac{dr}{dx} = \frac{e^g}{x} = \frac{\kappa\,r_q}{b}\left[x^{\frac{1}{b}-1}+g_2\,x^{\frac{1}{b}-3}+\cdots\right]\,. \tag{3.A.52}$$

We get:

$$r = \kappa\,r_q\left[x^{\frac{1}{b}}-\frac{g_2}{2b-1}x^{\frac{1}{b}-2}+\cdots\right]\,. \tag{3.A.53}$$

This relation can be inverted as:

$$x = \left(\frac{r}{\kappa\,r_q}\right)^b\left[1+\frac{b}{2b-1}g_2\left(\frac{\kappa\,r_q}{r}\right)^{2b}+\cdots\right]\,. \tag{3.A.54}$$

By plugging the expansion (3.A.54) into (3.6.95) and (3.6.97) one easily arrives at (3.6.99) and (3.6.100).

3.A.3 More on the entanglement entropy

Let us study analytically the entanglement entropy and the $\mathcal{F}$ function near the UV fixed point at $R = 0$. We shall represent $S(R)$ in terms of a local functional $\mathcal{L} = \mathcal{L}(H(x), G(x), \rho(x))$ as:

$$S(R) = \int_{x_*}^{\infty} \mathcal{L} \, dx \; . \tag{3.A.55}$$

We will use this representation to compute the first-order variation of S when the background functions H and G and the embedding function ρ are varied around their UV values:

$$H(x) = H_{UV}(x) + \delta H(x) \; , \qquad G(x) = G_{UV}(x) + \delta G(x) \; , \qquad \rho(x) = \rho_{UV}(x) + \delta \rho(x) \; , \tag{3.A.56}$$

where $H_{UV} = H_{\infty} \, x^{\frac{4}{b}}$, $G_{UV} = G_{\infty} \, x^{-2-\frac{2}{b}}$ and $\rho_{UV}(x)$ is the function written in (3.7.123). At first order the corrections $\delta H(x)$ and $\delta G(x)$ can be parameterized as:

$$\delta H(x) = H_{\infty} \, H_2 \, x^{\frac{4}{b}-2} \; , \qquad \delta G(x) = G_{\infty} \, G_2 \, x^{-4-\frac{2}{b}} \; . \tag{3.A.57}$$

The constants H_2 and G_2 in (3.A.57) can be related to the ones characterizing the behavior of the background at the UV:

$$H_2 = 2 \left(h_2 + 4 f_2 + 2 g_2 - 2 \phi_2 \right) \; , \qquad G_2 = h_2 + 2 g_2 \; . \tag{3.A.58}$$

It is useful to define the following combination of H_2 and G_2:

$$\mathcal{H}_2 = \frac{H_2}{2} + \frac{G_2}{2b + 1} \; . \tag{3.A.59}$$

The perturbation of the profile $\delta \rho(x)$ is the correction, at first-order, of the solution of (3.7.107) which satisfies $\delta \rho(x \to \infty) = 0$. By computing the first variation of (3.7.107) we find that $\delta \rho(x)$ is solution to the following second-order inhomogeneous differential equation:

$$\frac{d}{dx} \left[\frac{\sqrt{H_{UV}} \, \rho_{UV} \, \rho'_{UV}}{\sqrt{(\rho'_{UV})^2 + G_{UV}}} \left(\frac{\delta \rho'}{\rho'_{UV}} + \frac{\delta \rho}{\rho_{UV}} + \frac{\delta H}{2 H_{UV}} - \frac{1}{2} \frac{2 \rho'_{UV} \, \delta \rho' + \delta G}{(\rho'_{UV})^2 + G_{UV}} \right) \right]$$

$$- \sqrt{H_{UV}} \sqrt{(\rho'_{UV})^2 + G_{UV}} \left(\frac{\delta H}{2 \, H_{UV}} + \frac{1}{2} \frac{2 \rho'_{UV} \, \delta \rho' + \delta G}{(\rho'_{UV})^2 + G_{UV}} \right) = 0 \; . \tag{3.A.60}$$

More explicitly, after using the UV values of H, G, and ρ, the differential equation (3.A.60) can be written as:

$$\frac{d}{dx} \left[\frac{2 \, x^{\frac{3}{b}+1} \, \rho_{UV}^4}{R^2 \, G_{\infty}} \, \delta \rho' \; + \; 2b \, x^{\frac{1}{b}} \, \delta \rho \; + \; b \, H_2 \, x^{\frac{1}{b}-2} \, \rho_{UV} \; - \; \frac{b \, G_2}{R^2} \, x^{\frac{1}{b}-2} \, \rho_{UV}^3 \right]$$

$$- 2b \, x^{\frac{1}{b}} \, \delta \rho' \; - \; \frac{R^2 \, H_2 \, x^{\frac{1}{b}-3}}{\rho_{UV}} \; - \; G_2 \, x^{\frac{1}{b}-3} \, \rho_{UV} = 0 \; . \tag{3.A.61}$$

Let us next calculate the first-order variation of the entanglement entropy. From (3.A.55) we get:

$$\delta S \;=\; \int_{x_*}^{\infty} dx \left[\left. \frac{\partial \mathcal{L}}{\partial H} \right|_{UV} \delta H \;+\; \left. \frac{\partial \mathcal{L}}{\partial G} \right|_{UV} \delta G \right] \;+\; \Pi_{UV}(x)\, \delta\rho(x) \Bigg|_{x=x_*}^{x=\infty} , \qquad (3.A.62)$$

where $\Pi_{UV}(x)$ is defined as:

$$\Pi_{UV}(x) \equiv \left. \frac{\partial \mathcal{L}}{\partial \rho'} \right|_{UV} \;=\; \frac{2}{3\pi^2}\, \sqrt{H_{UV}(x)}\; \frac{\rho_{UV}\, \rho'_{UV}}{\sqrt{(\rho'_{UV})^2 + G_{UV}(x)}} \, . \qquad (3.A.63)$$

Using the explicit form of ρ_{UV} we get:

$$\Pi_{UV}(x) \;=\; \frac{2b}{3\pi^2}\, \sqrt{H_\infty\, G_\infty}\; x^{\frac{1}{b}} \sqrt{1 \,-\, \frac{b^2\, G_\infty}{R^2}\, x^{-\frac{2}{b}}} \, , \qquad (3.A.64)$$

and it follows that:

$$\Pi_{UV}(x = x_*) = 0 \, . \qquad (3.A.65)$$

Therefore, the lower limit contribution to the last term in (3.A.62) vanishes. Let us now study the contribution to this term of the $x \to \infty$ limit. We will now check that $\delta\rho(x)$ decreases as $x \to \infty$ in such a way that:

$$\lim_{x \to \infty} \Pi_{UV}(x)\, \delta\rho(x) \;=\; 0 \, . \qquad (3.A.66)$$

Thus, the upper limit of the last term in (3.A.62) also vanishes. To prove (3.A.66) we have to integrate the differential equation (3.A.61) and extract the large x behavior of the solution. Amazingly, (3.A.61) can be integrated analytically. Its general solution can be written as the sum of two terms:

$$\delta\rho \;=\; \delta\rho_P + \delta\rho_G \, , \qquad (3.A.67)$$

where $\delta\rho_P$ is a particular solution of the equation and $\delta\rho_G$ is a general solution of the homogeneous part of (3.A.61). We have found a particular solution $\delta\rho_P$, which can be written in terms of hypergeometric functions and is given by:

$$\delta\rho_P = \frac{R^{2b+2}\mathcal{H}_2}{2b(b-1)(2b-1)G_\infty\, \rho_{UV}} \;\times$$

$$\times \left[\left(Rx^{\frac{1}{b}} - b\,\sqrt{G_\infty} \right)^{2-2b} {}_2F_1\!\left(2b-2, 2b-2; 2b-1; \frac{b\,\sqrt{G_\infty}}{b\sqrt{G_\infty} - R\,x^{\frac{1}{b}}} \right) \right.$$

$$\left. + \left(R\,x^{\frac{1}{b}} + b\,\sqrt{G_\infty} \right)^{2-2b} {}_2F_1\!\left(2b-2, 2b-2; 2b-1; \frac{b\sqrt{G_\infty}}{b\sqrt{G_\infty} + R\,x^{\frac{1}{b}}} \right) \right]$$

$$- \left[\frac{b^2\, G_2\, G_\infty}{2\,(2b+1)}\, x^{-\frac{2}{b}} + \frac{R^2\, \mathcal{H}_2}{2b-1} + \frac{R^4\, \mathcal{H}_2}{b\,(b-1)\,(2b-1)\, G_\infty}\, x^{\frac{2}{b}} \right] \frac{1}{x^2\, \rho_{UV}} \, . \qquad (3.A.68)$$

We are only interested in the behavior of $\delta\rho_P$ for large x. It is straightforward to prove that, for large x, $\delta\rho_P$ can be approximated as:

$$\delta\rho_P \approx \frac{b^2\,G_\infty\left[bH_2 - (b-1)\,G_2\right]}{2\,(b+1)\,(2b-1)\,R}\,x^{-2-\frac{2}{b}}\,. \tag{3.A.69}$$

Thus, as $\Pi_{UV} \propto x^{\frac{1}{b}}$ for large x,

$$\lim_{x\to\infty}\,\Pi_{UV}(x)\,\delta\rho_P(x) = 0\,. \tag{3.A.70}$$

The general solution of the homogeneous differential equation which vanishes as $x \to \infty$ is:

$$\delta\rho_G = \frac{C}{x^{\frac{1}{b}}\,\rho_{UV}}\left[\frac{R\,x^{\frac{1}{b}}}{2b\,\sqrt{G_\infty}}\,\log\frac{R\,x^{\frac{1}{b}} + b\,\sqrt{G_\infty}}{R\,x^{\frac{1}{b}} - b\,\sqrt{G_\infty}} - 1\right]\,, \tag{3.A.71}$$

where C is an arbitrary constant. For large x the function in (3.A.71) behaves as:

$$\delta\rho_G \approx \frac{C\,b^2\,G_\infty}{3\,R^3}\,x^{-\frac{3}{b}}\,. \tag{3.A.72}$$

Therefore,

$$\lim_{x\to\infty}\,\Pi_{UV}(x)\,\delta\rho_G(x) = 0\,. \tag{3.A.73}$$

Then, eq. (3.A.66) holds and the last term in (3.A.62) does not contribute to δS, as claimed above. Let us now calculate the other two contributions. First of all, the term due to the variation of H is given by:

$$\int_{x_*}^{\infty} dx\,\frac{\partial\mathcal{L}}{\partial H}\bigg|_{UV}\,\delta H = \frac{1}{3\pi^2}\int_{x_*}^{\infty}dx\,\frac{\rho_{UV}\,\sqrt{(\rho'_{UV})^2 + G_{UV}(x)}}{\sqrt{H_{UV}(x)}}\,\delta H$$

$$= \frac{1}{3\pi^2}\,\frac{bH_2}{2b-1}\,\sqrt{H_\infty G_\infty}\,R\,x_*^{\frac{1}{b}-2}\,, \tag{3.A.74}$$

which, after using (3.7.124) to eliminate x_*, becomes:

$$\int_{x_*}^{\infty}dx\,\frac{\partial\mathcal{L}}{\partial H}\bigg|_{UV}\,\delta H = \frac{1}{3\pi^2}\,\frac{H_2\,b^{2-2b}}{2b-1}\,\sqrt{H_\infty}\,G_\infty^{1-b}\,R^{2b}\,. \tag{3.A.75}$$

Similarly,

$$\int_{x_*}^{\infty}dx\,\frac{\partial\mathcal{L}}{\partial G}\bigg|_{UV}\,\delta G = \frac{1}{3\pi^2}\int_{x_*}^{\infty}dx\,\frac{\sqrt{H_{UV}(x)}\,\rho_{UV}}{\sqrt{(\rho'_{UV})^2 + G_{UV}(x)}}\,\delta G$$

$$= \frac{2}{3\pi^2}\,\frac{b^2}{4b^2-1}\,\frac{G_2\,\sqrt{H_\infty}\,G_\infty}{x_*^2}\,, \tag{3.A.76}$$

which, after eliminating x_*, gives:

$$\int_{x_*}^{\infty}dx\,\frac{\partial\mathcal{L}}{\partial G}\bigg|_{UV}\,\delta G = \frac{2}{3\pi^2}\,\frac{G_2\,b^{2-2b}}{4b^2-1}\,\sqrt{H_\infty}\,G_\infty^{1-b}\,R^{2b}\,. \tag{3.A.77}$$

Thus, δS can be written as:

$$\delta S \;=\; \frac{2}{3\pi^2}\,\frac{b^{2-2b}}{2b-1}\,\sqrt{H_\infty}\,G_\infty^{1-b}\,\mathcal{H}_2\,R^{2b}\;, \qquad (3.A.78)$$

where $\mathcal{H}_2$ is the constant defined in (3.A.59). Using the definition (3.7.120), it follows that the change in the function $\mathcal{F}$ is:

$$\delta\mathcal{F} \;=\; \frac{2}{3\pi^2}\,b^{2-2b}\,\sqrt{H_\infty}\,G_\infty^{1-b}\,\mathcal{H}_2\,R^{2b}\;. \qquad (3.A.79)$$

Taking into account (3.7.111) and (3.7.114) this expression can be written as:

$$\delta\mathcal{F} \;=\; F_{UV}(\mathbb{S}^3)\,\mathcal{H}_2\left(\frac{\kappa}{L_0^2}\right)^{2b}(r_q\,R)^{2b} \;=\; F_{UV}(\mathbb{S}^3)\,\mathcal{H}_2\,x_*^{-2}\;. \qquad (3.A.80)$$

Therefore, we can write the $\mathcal{F}$ function near the UV fixed point as:

$$\mathcal{F} \;=\; F_{UV}(\mathbb{S}^3) \;+\; c_{UV}\,(r_q\,R)^{2b}\;, \qquad (3.A.81)$$

where the constant coefficient c_{UV} can be read from (3.A.80),

$$c_{UV} \;=\; \left(\frac{\kappa}{L_0^2}\right)^{2b}\,F_{UV}(\mathbb{S}^3)\mathcal{H}_2\;. \qquad (3.A.82)$$

Eq. (3.A.81) coincides with (3.7.131) when the former is written in terms of the dimension $\Delta_{UV} = 3 - b$ of the quark-antiquark bilinear operator in the massless flavored theory. Moreover, as $F_{UV}(\mathbb{S}^3)$ is always positive, the sign of c_{UV} depends on the sign of the coefficient $\mathcal{H}_2$. We have checked that $\mathcal{H}_2$ is negative for all values of the deformation parameter $\hat{\epsilon}$, in agreement with the expectation that $\mathcal{F}$ is maximized at the UV fixed point.

Entanglement entropy on the strip

Let us now evaluate the entanglement entropy in the case in which the region A is the strip $-\frac{l}{2} \le x^1 \le +\frac{l}{2}$ of width l in the (x^1, x^2)-plane (see Fig. 3.10). In this case we consider a constant time surface Σ, whose embedding in the ten-dimensional space is determined by a function $x = x(x^1)$. The induced metric on Σ is,

$$ds_8^2 \;=\; h^{-\frac{1}{2}}\left[\left(1 + G(x)\,x'^2\right)(dx^1)^2 + (dx^2)^2\right] + h^{\frac{1}{2}}\left[e^{2f}\,ds_{\mathbb{S}^4}^2 + e^{2g}\left(\left(E^1\right)^2 + \left(E^2\right)^2\right)\right]\;, \qquad (3.A.83)$$

where x' denotes the derivative of the holographic coordinate x with respect to the cartesian coordinate x^1 and the function $G(x)$ has been defined in (3.7.104). The entropy functional for the strip of width l is given by:

$$S(l) \;=\; \frac{V_6\,L_2}{4\,G_{10}}\int_{-\frac{l}{2}}^{+\frac{l}{2}}dx^1\,\sqrt{H(x)}\,\sqrt{1 + G(x)\,x'^2} \;\equiv\; \int_{-\frac{l}{2}}^{+\frac{l}{2}}dx^1\,\mathcal{L}_{strip}\;, \qquad (3.A.84)$$

where V_6 is the volume of the internal manifold, whose value was given after (3.7.106), $H(x)$ is the function defined in (3.7.105), and $L_2 = \int dx^2$ is the length of the strip. As the
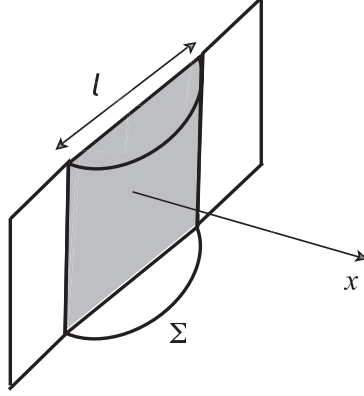
Figure 3.10: The surface Σ ends on a strip of length l at the boundary.

integrand in $S(l)$ does not depend on the coordinate x^1, the corresponding Euler-Lagrange equation admits the following first integral:

$$x' \frac{\mathcal{L}_{strip}}{\partial x'} - \mathcal{L}_{strip} = \text{constant} , \tag{3.A.85}$$

or, more explicitly,

$$\frac{\sqrt{H(x)}}{\sqrt{1 + G(x)\, x'^2}} = \sqrt{H_*} , \tag{3.A.86}$$

where $H_* = H(x = x_*)$ and x_* is the holographic coordinate of the turning point. It follows from this last expression that x' is given by:

$$x' = \pm \frac{1}{\sqrt{G(x)}} \sqrt{\frac{H(x)}{H_*} - 1} . \tag{3.A.87}$$

Therefore, the width of the strip is given by the integral:

$$l = 2\sqrt{H_*} \int_{x_*}^{\infty} dx \, \frac{\sqrt{G(x)}}{\sqrt{H(x) - H_*}} , \tag{3.A.88}$$

and the entropy $S(l)$ is:

$$S(l) = \frac{V_6 \, L_2}{2G_{10}} \int_{x_*}^{\infty} dx \, \frac{\sqrt{G(x)\, H(x)}}{\sqrt{H(x) - H_*}} . \tag{3.A.89}$$

The integral (3.A.89) for $S(l)$ is divergent in the UV. Indeed, from the behavior of the functions $H(x)$ and $G(x)$ at large x (eqs. (3.7.110) and (3.7.111)), it follows that, when $x \to \infty$, the integrand in (3.A.89) behaves as:

$$\frac{\sqrt{G(x)\, H(x)}}{\sqrt{H(x) - H_*}} \approx \sqrt{H_\infty \, G_\infty} \; x^{\frac{1}{b} - 1} , \tag{3.A.90}$$

and $S(l)$ therefore diverges as $x_{\max}^{\frac{1}{b}}$, where $x_{\max}$ is the upper limit of the integral, which can be regarded as a UV cutoff. More explicitly, one can rearrange the integral in (3.A.89) as:

$$\int_{x_*}^{x_{\max}} dx \, \frac{\sqrt{G(x)}\, H(x)}{\sqrt{H(x) - H_*}} = \int_{x_*}^{x_{\max}} dx \left[\frac{\sqrt{G(x)}\, H(x)}{\sqrt{H(x) - H_*}} - \sqrt{H_\infty\, G_\infty} \, x^{\frac{1}{b}-1} \right]$$
$$+ b \sqrt{H_\infty\, G_\infty} \left[x_{max}^{\frac{1}{b}} - x_*^{\frac{1}{b}} \right] , \quad (3.A.91)$$

where the divergent term is explicitly shown. We now define the rescaled functions $\hat{G}(x)$ and $\hat{H}(x)$ as:

$$\hat{G}(x) \equiv \frac{G(x)}{G_\infty} , \qquad \hat{H}(x) \equiv \frac{H(x)}{H_\infty} , \qquad \hat{H}_* \equiv \frac{H_*}{H_\infty} . \qquad (3.A.92)$$

Then, the finite term in $S(l)$ can be written as:

$$S_{finite}(l) = \frac{V_6\, L_2}{2 G_{10}} \sqrt{H_\infty\, G_\infty} \left[\int_{x_*}^{\infty} dx \left(\frac{\sqrt{\hat{G}(x)}\, \hat{H}(x)}{\sqrt{\hat{H}(x) - \hat{H}_*}} - x^{\frac{1}{b}-1} \right) - b\, x_*^{\frac{1}{b}} \right] , \qquad (3.A.93)$$

whereas the divergent term takes the form:

$$S_{div} = \frac{V_6\, L_2}{2 G_{10}} b \sqrt{H_\infty\, G_\infty} \, x_{max}^{\frac{1}{b}} . \qquad (3.A.94)$$

We have evaluated numerically the right-hand side of (3.A.93) as a function of the strip width l. The result is displayed in Fig. 3.11. One notices from these results that $S_{finite}(l)/L_2$ is negative and diverges as $-c/l$ for small l, where c is a constant. Actually, for small l the surface Σ is in the UV region of the geometry and one can evaluate the entropy analytically in this limit. This is the subject of the next subsection, where we show that the constant c is proportional to the free energy on the three-sphere of the massless flavored theory (see eq. (3.A.105) below). The analytical UV calculation is compared to the numerical results in Fig. 3.11.

UV limit

In order to study the UV limit it is convenient to change variables in the integrals (3.A.88) and (3.A.93). Let us introduce a new variable z, related to x as $x = x_*\, z$. Then, l can be represented as:

$$l = 2\, x_*^{\frac{2}{b}+1} \sqrt{G_\infty} \int_1^{\infty} dz \, \frac{\sqrt{\hat{G}(x_*\, z)}}{\sqrt{\hat{H}(x_*\, z) - x_*^{4/b}}} , \qquad (3.A.95)$$

while $S_{finite}(l)$ is given by:

$$S_{finite}(l) = -\frac{V_6\, L_2}{2\, G_{10}} \sqrt{H_\infty\, G_\infty} \, x_*^{\frac{1}{b}} \left[b - \int_1^{\infty} dz \left(x_*^{1-\frac{1}{b}} \frac{\sqrt{\hat{G}(x_*\, z)}\, \hat{H}(x_*\, z)}{\sqrt{\hat{H}(x_*\, z) - x_*^{4/b}}} - z^{\frac{1}{b}-1} \right) \right] .$$
$$(3.A.96)$$
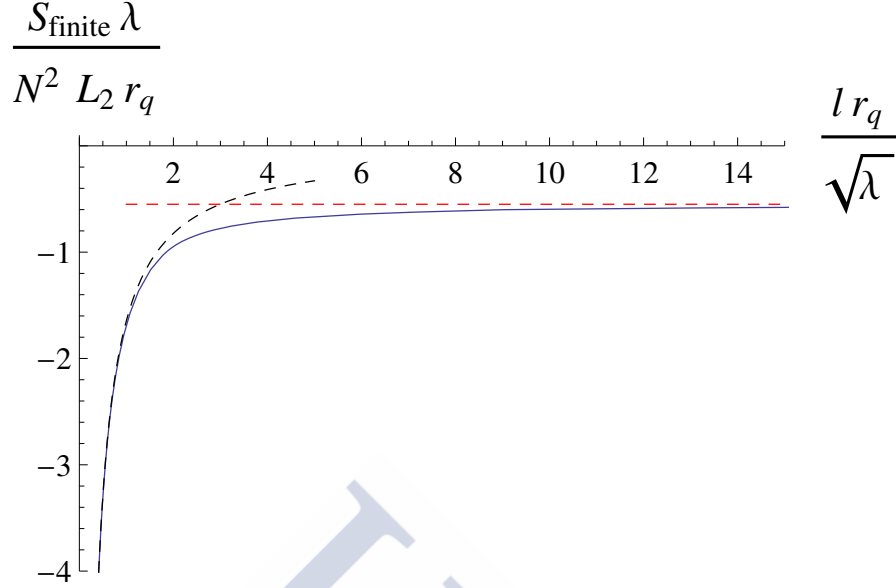
Figure 3.11: Plot of the entanglement entropy versus the width of the strip. The solid curve corresponds to the numerical results for $\hat{\epsilon} = 9$, while the the black dashed curve on the left is the analytic UV result (3.A.105) and the dashed red line on the right corresponds to the IR value (3.A.112).

Let us now obtain the expressions of l and $S_{finite}(l)$ in the limit in which $x_* \to \infty$. In this case the argument of the functions $\hat{G}$ and $\hat{H}$ in the integrals is always large and one can take $\hat{G}(x) \approx x^{-2-\frac{2}{b}}$, $\hat{H}(x) \approx x^{\frac{4}{b}}$. We get:

$$l \approx 2\, x_*^{-\frac{1}{b}} \sqrt{G_\infty}\, I_1 \,, \tag{3.A.97}$$

where I_1 is the following integral:

$$I_1 = \int_1^\infty \frac{dz}{z^{1+\frac{1}{b}} \sqrt{z^{\frac{4}{b}} - 1}} = \frac{b\sqrt{2}\,\pi^{\frac{3}{2}}}{\left[\Gamma\!\left(\frac{1}{4}\right)\right]^2} \,. \tag{3.A.98}$$

Using (3.A.98) in (3.A.97), we get:

$$l \approx \frac{b\sqrt{G_\infty}}{x_*^{\frac{1}{b}}} \frac{2\sqrt{2}\,\pi^{\frac{3}{2}}}{\left[\Gamma\!\left(\frac{1}{4}\right)\right]^2} \,. \tag{3.A.99}$$

Similarly, the finite part of the entropy is:

$$S_{finite}(l) \approx -\frac{V_6\, L_2}{2\, G_{10}} \sqrt{H_\infty\, G_\infty}\, x_*^{\frac{1}{b}} \left(b - I_2 \right) \,, \tag{3.A.100}$$

where I_2 is the integral:

$$I_2 = \int_1^\infty z^{\frac{1}{b}-1} \left[\frac{z^{\frac{2}{b}}}{\sqrt{z^{\frac{4}{b}} - 1}} - 1 \right] dz = b\left[1 - \frac{\sqrt{2}\,\pi^{\frac{3}{2}}}{\left[\Gamma\!\left(\frac{1}{4}\right)\right]^2} \right] \,. \tag{3.A.101}$$

Plugging (3.A.101) into (3.A.100), we arrive at:

$$S_{finite}(l) \approx -\frac{V_6\, L_2}{2\, G_{10}}\, b\, \sqrt{H_\infty\, G_\infty}\; x_*^{\frac{1}{b}}\, \frac{\sqrt{2}\,\pi^{\frac{3}{2}}}{\left[\Gamma\!\left(\frac{1}{4}\right)\right]^2}\; . \qquad (3.A.102)$$

Eliminating x_* in favor of l, we get:

$$S_{finite}(l) \approx -\frac{2\pi^3\, V_6\, L_2}{G_{10}}\, \frac{b^2\, G_\infty\, \sqrt{H_\infty}}{\left[\Gamma\!\left(\frac{1}{4}\right)\right]^4}\, \frac{1}{l}\; . \qquad (3.A.103)$$

However, from the definition of G_∞ and H_∞ in (3.7.111) it follows that:

$$b^2\, G_\infty\, \sqrt{H_\infty} = \frac{L_0^8\, q_0^2\, e^{-2\phi_0}}{b^6} = \frac{3\pi^2}{2} F_{UV}(\mathbb{S}^3)\; , \qquad (3.A.104)$$

where $F_{UV}(\mathbb{S}^3)$ is the free energy of the massless flavored theory on the three sphere (see (3.7.117)). It follows that:

$$\frac{S_{finite}(l)}{L_2} \approx -\frac{4\pi^2\, F_{UV}(\mathbb{S}^3)}{\left[\Gamma\!\left(\frac{1}{4}\right)\right]^4}\, \frac{1}{l}\; , \qquad (3.A.105)$$

which is the result we were looking for. From the comparison of Fig. 3.11 to the numerical results we conclude that (3.A.105) is a good description of the entropy in the small l region. Notice that the coefficient of $1/l$ on the right-hand side of (3.A.105) is determined by the free energy of the massless flavored theory. This is expected on general grounds in the UV region, since the masses of the quarks can be neglected in the high-energy regime.

IR limit

Let us now evaluate $S_{finite}(l)$ in the regime in which l is large. In this case the surface Σ penetrates deeply in the bulk and its tip is near the origin (*i.e.*, x_* is small). We will proceed as in section 3.7.2 and split the interval $[x_*,\infty]$ in the integrals (3.A.88) and (3.A.93) as $[x_*,\infty] = [x_*, x_a] \cup [x_a,\infty]$, where $x_a < 1$ is considered small enough so that one can use the unflavored background functions in the interval $[x_*, x_a]$. Moreover, when $x \in [x_a,\infty]$ with $x_a \gg x_*$, $H_* \propto x_*^4 \ll H(x) \propto x^4$ and one can neglect the terms containing H_* in the integrals. Then, the strip width l can be approximated as:

$$l \approx \frac{2c}{\gamma}\, \frac{L_{ABJM}^2}{x_*}\, \int_1^{\frac{x_a}{x_*}}\, \frac{dz}{z^2\, \sqrt{z^4-1}} + 2\sqrt{H_*}\, \int_{x_a}^\infty\, dx\, \frac{\sqrt{G(x)}}{\sqrt{H(x)}}\; . \qquad (3.A.106)$$

When, $x_a \gg x_*$ and $x_* \to 0$ we can extend the first integral in (3.A.106) up to ∞ and neglect the contribution of the second integral (which is proportional to $\sqrt{H_*} \propto x_*^2$). Then, l can be approximately written as:

$$l \approx \frac{c}{\gamma}\, L_{ABJM}^2\, \frac{2\sqrt{2}\,\pi^{\frac{3}{2}}}{\left[\Gamma\!\left(\frac{1}{4}\right)\right]^2}\, \frac{1}{x_*}\; , \qquad (3.A.107)$$

and, as expected, a small value of x_* leads to a large value of l. Similarly, we can perform the same type of manipulations in the expression (3.A.93) of S_{finite}. We find:

$$\frac{S_{finite}(l)}{L_2} \approx \frac{2}{3\pi^3} \frac{\gamma}{c} L_{ABJM}^6 e^{-2\phi_{ABJM}} x_* \int_1^{\frac{x_a}{x_*}} \frac{z^2 \, dz}{\sqrt{z^4 - 1}}$$

$$+ \frac{2}{3\pi^3} \sqrt{G_\infty H_\infty} \left[\int_{x_a}^\infty \left(\sqrt{\hat{G}(x) \hat{H}(x)} - x^{\frac{1}{b}-1} \right) dx - b \, x_a^{\frac{1}{b}} \right] . \quad (3.A.108)$$

Performing the first integral in (3.A.108) in the limit $x_* \to 0$ for fixed x_a, we arrive at:

$$\frac{S_{finite}(l)}{L_2} \approx -\frac{2\sqrt{2}}{3\pi^{\frac{3}{2}} \left[\Gamma\left(\frac{1}{4}\right) \right]^2} \frac{\gamma}{c} L_{ABJM}^6 e^{-2\phi_{ABJM}} x_* + \mathcal{S}_\infty , \quad (3.A.109)$$

where $\mathcal{S}_\infty$ is the constant:

$$\mathcal{S}_\infty = \frac{2}{3\pi^3} \sqrt{G_\infty H_\infty} \left[\int_{x_a}^\infty \left(\sqrt{\hat{G}(x)\hat{H}(x)} - x^{\frac{1}{b}-1} \right) dx - b x_a^{\frac{1}{b}} \right] + \frac{2}{3\pi^3} \frac{\gamma}{c} L_{ABJM}^6 e^{-2\phi_{ABJM}} x_a .$$
$$(3.A.110)$$

We can now eliminate in (3.A.109) the turning point x_* in favor of l by using (3.A.107). We find:

$$\frac{S_{finite}(l)}{L_2} \approx -\frac{4\pi^2 F_{IR}(\mathbb{S}^3)}{\left[\Gamma\left(\frac{1}{4}\right) \right]^4} \frac{1}{l} + \mathcal{S}_\infty , \quad (3.A.111)$$

where we have written the result in terms of $F_{IR}(\mathbb{S}^3)$. The first term in (3.A.111) is just the strip entanglement entropy for the unflavored theory. The constant $\mathcal{S}_\infty$ represents the asymptotic value of $S_{finite}(l)/L_2$ as $l \to \infty$. One can approximate this constant by taking $x_a \to 0$ in (3.A.110). After using (3.7.114) to relate G_∞ and H_∞ to $F_{UV}(\mathbb{S}^3)$, we arrive at:

$$\mathcal{S}_\infty \approx r_q \frac{\kappa F_{UV}(\mathbb{S}^3)}{\pi b L_0^2} \int_0^\infty \left(\sqrt{\hat{G}(x)\hat{H}(x)} - x^{\frac{1}{b}-1} \right) dx . \quad (3.A.112)$$

3.A.4   Asymptotic quark-antiquark potential

The purpose of this appendix is to obtain the analytic expressions for the $q\bar{q}$ potential energy in the UV and IR limit. We will start by calculating the leading and subleading UV potential.

UV potential

Let us find the approximate value of the $q\bar{q}$ potential in the case in which the distance d is small and the hanging string only explores the UV of the geometry. This is equivalent to considering the limit in which the turning point x_* is large. It is then more convenient to perform a change of variables in the integrals (3.8.150) and (3.8.154) and write d and $E_{q\bar{q}}$ as:

$$d = 2 \int_1^\infty \frac{e^{g(x_* z)} h(x_* z)}{z \sqrt{h_* - h(x_* z)}} \, dz ,$$

$$E_{q\bar{q}} = \frac{1}{\pi} \int_1^\infty \frac{e^{g(x_* z)}}{z} \left[\frac{\sqrt{h_*}}{\sqrt{h_* - h(x_* z)}} - 1 \right] dz - \frac{r_*}{\pi} . \quad (3.A.113)$$

We want to compute the leading value of $E_{q\bar{q}}$, as well as the first deviation from the conformal behavior. For this reason we will make use of the asymptotic expressions of the different functions of the metric derived in section 3.6.1.

Let us begin by computing the integrals in (3.A.113) in a power series expansion for large x_*. From (3.6.95) and (3.6.97) we get:

$$e^{g(x_* z)}\, h(x_* z) \;=\; \frac{L_0^4}{b\,\kappa^3\,r_q^3}\; x_*^{-\frac{3}{b}}\, z^{-\frac{3}{b}} \left(1 + \frac{h_2 + g_2}{x_*^2\, z^2} + \cdots \right),\qquad (3.A.114)$$

where g_2 and h_2 are given in (3.6.96) and (3.6.98) and κ has been defined in (3.6.94). Then, it follows that:

$$\frac{1}{\sqrt{h_* - h(x_* z)}} \;=\; \frac{\kappa^2\, r_q^2}{L_0^2}\; x_*^{\frac{2}{b}}\; \frac{z^{\frac{2}{b}}}{\sqrt{z^{\frac{4}{b}} - 1}} \left(1 - \frac{h_2}{2\, x_*^2}\, \frac{z^{\frac{4}{b}+2} - 1}{z^2\, (z^{\frac{4}{b}} - 1)} + \cdots \right).\qquad (3.A.115)$$

Using these results we obtain the following expansion of the $q\bar{q}$ separation d:

$$d \;=\; \frac{2\, L_0^2}{b\,\kappa\, r_q\, x_*^{\frac{1}{b}}} \left[I_1 + \frac{1}{x_*^2} \left((h_2 + g_2)\, I_3 - \frac{h_2}{2}\, I_4 \right) + \cdots \right],\qquad (3.A.116)$$

where I_1 is the integral (3.A.98), and I_3 and I_4 are:

$$I_3 \;=\; \int_1^\infty \frac{dz}{z^{3+\frac{1}{b}}\,\sqrt{z^{\frac{4}{b}} - 1}} \;=\; \frac{b\sqrt{\pi}}{4}\, G(b)\,,$$

$$I_4 \;=\; \int_1^\infty \frac{z^{\frac{4}{b}+2} - 1}{z^{3+\frac{1}{b}}\,(z^{\frac{4}{b}} - 1)^{\frac{3}{2}}}\, dz \;=\; \frac{b\sqrt{\pi}}{2} \left[\frac{3 + 2b}{4}\, G(b) - \frac{\sqrt{2}\,\pi}{[\Gamma(\frac{1}{4})]^2} \right],\qquad (3.A.117)$$

where $G(b)$ is the following ratio of Euler Gamma functions:

$$G(b) \equiv \frac{\Gamma\!\left(\frac{3+2b}{4}\right)}{\Gamma\!\left(\frac{5+2b}{4}\right)}.\qquad (3.A.118)$$

Using these results we arrive at:

$$d \approx \frac{2\, L_0^2}{\kappa\, r_q\, x_*^{\frac{1}{b}}} \left[\frac{\sqrt{2}\,\pi^{\frac{3}{2}}}{[\Gamma(\frac{1}{4})]^2} + \frac{\sqrt{\pi}}{4\, x_*^2} \left(g_2 + (1 - 2b)\, \frac{h_2}{4} \right) G(b) + \frac{\sqrt{2}\,\pi^{\frac{3}{2}}}{4\, x_*^2}\, \frac{h_2}{[\Gamma(\frac{1}{4})]^2} \right].\qquad (3.A.119)$$

Let us now compute the $q\bar{q}$ energy at leading and next-to-leading order in the UV (large x_* or small d). First, we need the expansion:

$$\frac{\sqrt{h_*}}{\sqrt{h_* - h(x_* z)}} \;=\; \frac{z^{\frac{2}{b}}}{\sqrt{z^{\frac{4}{b}} - 1}} + \frac{h_2}{2\, x_*^2}\, \frac{z^{\frac{2}{b}-2}\, (1 - z^2)}{(z^{\frac{4}{b}} - 1)^{\frac{3}{2}}} + \cdots.\qquad (3.A.120)$$

Then, it is easy to verify that $E_{q\bar{q}}$ can be expanded as:

$$E_{q\bar{q}} \approx \frac{\kappa\, r_q}{\pi\, b}\, x_*^{\frac{1}{b}} \left[I_2 + \frac{1}{x_*^2} \left(\frac{h_2}{2}\, I_5 + g_2\, I_6 \right) \right] - \frac{r_*}{\pi},\qquad (3.A.121)$$

where I_2 is the integral (3.A.101) and I_5 and I_6 are:

$$I_5 = \int_1^\infty \frac{z^{\frac{3}{b}-3}(1-z^2)}{(z^{\frac{4}{b}}-1)^{\frac{3}{2}}}\,dz = \frac{b\sqrt{\pi}}{2}\left[\frac{\sqrt{2}\,\pi}{\left[\Gamma\!\left(\frac{1}{4}\right)\right]^2} - \frac{2b+1}{4}\,G(b)\right],$$

$$I_6 = \int_1^\infty z^{\frac{1}{b}-3}\left[\frac{z^{\frac{2}{b}}}{\sqrt{z^{\frac{4}{b}}-1}} - 1\right]dz = \frac{b}{2b-1}\left[\frac{(2b+1)\sqrt{\pi}}{4}\,G(b) - 1\right]. \quad (3.A.122)$$

To compute $E_{q\bar{q}}$ we also need r_* as a function of x_*. It follows from (3.A.53) that:

$$r_* = \kappa\, r_q\, x_*^{\frac{1}{b}}\left[1 - \frac{g_2}{2b-1}\frac{1}{x_*^2} + \cdots\right]. \quad (3.A.123)$$

Then, one can check that:

$$E_{q\bar{q}} \approx \kappa\, r_q\, x_*^{\frac{1}{b}}\left[-\frac{\sqrt{2\pi}}{\left[\Gamma\!\left(\frac{1}{4}\right)\right]^2} + \frac{1}{x_*^2}\left(\frac{\sqrt{2\pi}}{\left[\Gamma\!\left(\frac{1}{4}\right)\right]^2}\frac{h_2}{4} + \frac{2b+1}{4\sqrt{\pi}(2b-1)}\left(g_2 + (1-2b)\frac{h_2}{4}\right)G(b)\right)\right]. \quad (3.A.124)$$

Let us write $E_{q\bar{q}}$ as a function of the $q\bar{q}$ separation d. For this purpose we have to eliminate x_* in favor of d. By inverting (3.A.119), we get:

$$\kappa\, r_q\, x_*^{\frac{1}{b}} \approx \frac{2\sqrt{2}\pi^{\frac{3}{2}}}{\left[\Gamma\!\left(\frac{1}{4}\right)\right]^2}\frac{L_0^2}{d} +$$

$$+ r_q\,\frac{\sqrt{\pi}}{2}\left[\frac{\kappa\left[\Gamma\!\left(\frac{1}{4}\right)\right]^2}{2\sqrt{2}\,\pi^{\frac{3}{2}}}\right]^{2b}\left(\frac{\sqrt{2}\,\pi}{\left[\Gamma\!\left(\frac{1}{4}\right)\right]^2}h_2 + \left(g_2 + (1-2b)\frac{h_2}{4}\right)G(b)\right)\left(\frac{r_q\,d}{L_0^2}\right)^{2b-1}. \quad (3.A.125)$$

Using this result, we get the following dependence of $E_{q\bar{q}}$ with the distance d

$$\frac{E_{q\bar{q}}}{r_q} \approx -\frac{4\pi^2}{\left[\Gamma\!\left(\frac{1}{4}\right)\right]^4}\frac{L_0^2}{r_q\,d} + \frac{\sqrt{2}\,\pi}{\left[\Gamma\!\left(\frac{1}{4}\right)\right]^2}\left[\frac{\kappa\left[\Gamma\!\left(\frac{1}{4}\right)\right]^2}{2\sqrt{2}\,\pi^{\frac{3}{2}}}\right]^{2b}\left(\frac{g_2}{2b-1} - \frac{h_2}{4}\right)G(b)\left(\frac{r_q\,d}{L_0^2}\right)^{2b-1}, \quad (3.A.126)$$

where we have represented this relation in terms of the rescaled quantities $E_{q\bar{q}}/r_q$ and $r_q\,d/L_0^2$. Notice that the leading term (the first term on the right-hand side of (3.A.126)) is given by the potential of the massless flavored background, as expected.

IR potential

We now estimate the $q\bar{q}$ potential for large separations. In this case we will content ourselves to compute the leading order contribution. For large $q\bar{q}$ separations the hanging fundamental string penetrates deeply in the geometry, which is equivalent to saying that x_* is small. We will follow an approach similar to the one in sections 3.7.2 and 3.A.3 and we will split the $[x_*, \infty]$ interval of the integrals (3.8.150) and (3.8.154) as $[x_*, \infty] = [x_*, x_a] \cup [x_a, \infty]$ with $x_a < 1$ being small. We will assume that x_a is small enough so that the background functions

are well approximated by (3.7.132) in the interval $[x_*, x_a]$. Then, we can estimate the integral (3.8.150) for d as:

$$d \approx \frac{2\,L_{ABJM}^2\,x_*^2}{r_q} \int_{x_*}^{x_a} \frac{dx}{x^2\,\sqrt{x^4 - x_*^4}} + \frac{2}{\sqrt{h_*}} \int_{x_a}^{\infty} \frac{e^g\,h}{x}\,dx \ , \qquad (3.A.127)$$

where L_{ABJM} is the unflavored AdS radius (3.2.3) and we have used the fact that for $x_* \ll 1$ we have that $h_* \gg h(x)$ when $x \in [x_a, \infty]$ and, therefore, in this interval we can neglect $h(x)$ in the square root of the denominator of the integrand in (3.8.150). The first integral in (3.A.127) can be done analytically, yielding the result:

$$d \approx \frac{2\,L_{ABJM}^2}{x_*\,r_q} \left[\frac{\sqrt{2}\,\pi^{\frac{3}{2}}}{\left[\Gamma\!\left(\frac{1}{4}\right)\right]^2} - \frac{1}{3}\left(\frac{x_*}{x_a}\right)^3 {}_2F_1\!\left(\frac{1}{2}, \frac{3}{4}; \frac{7}{4}; \left(\frac{x_*}{x_a}\right)^4\right) \right] + \frac{2\,x_*^2\,r_q^2}{L_{ABJM}^2} \int_{x_a}^{\infty} \frac{e^g\,h}{x}\,dx \ . $$
$$(3.A.128)$$

For small x_*, at leading order, we get from (3.A.128):

$$d \approx \frac{L_{ABJM}^2}{x_*\,r_q}\,\frac{2\sqrt{2}\,\pi^{\frac{3}{2}}}{\left[\Gamma\!\left(\frac{1}{4}\right)\right]^2} \ , \qquad (3.A.129)$$

which confirms that $r_q\,d$ is large when x_* is small. We can make similar approximations in the integral (3.8.154) with the result:

$$E_{q\bar{q}} \approx \frac{r_q}{\pi} \left[\int_{x_*}^{x_a} \left[\frac{x^2}{\sqrt{x^4 - x_*^4}} - 1 \right] dx - x_* \right] . \qquad (3.A.130)$$

Performing explicitly the integral, we get:

$$E_{q\bar{q}} \approx -\frac{x_*\,r_q}{\pi} \left[\frac{\sqrt{2}\,\pi^{\frac{3}{2}}}{\left[\Gamma\!\left(\frac{1}{4}\right)\right]^2} + \frac{x_a}{x_*} - \frac{x_a}{x_*}\,{}_2F_1\!\left(-\frac{1}{4}, \frac{1}{2}; \frac{3}{4}; \left(\frac{x_*}{x_a}\right)^4\right) \right] , \qquad (3.A.131)$$

which, at leading order, becomes:

$$E_{q\bar{q}} \approx -\frac{\sqrt{2\pi}}{\left[\Gamma\!\left(\frac{1}{4}\right)\right]^2}\,x_*\,r_q \ . \qquad (3.A.132)$$

Eliminating x_* by using (3.A.129) we arrive at the estimate (3.8.158).

3.A.5   Asymptotics of the two-point functions

In this appendix we study the renormalized geodesic distance, and the corresponding two-point function of bulk operators with large conformal dimensions, in the UV limit of small separation l and in the IR regime in which $r_q\,l \to \infty$. In the former case, our study will serve to fix the normalization constant $\mathcal{C}$ of (3.9.168), as well as the analytic form of the correlator near the UV fixed point. This is the case we analyze first in the next subsection.

UV behavior

We will now obtain the form of the correlator in the UV limit in which the turning point x_* is large and the geodesic does not penetrate much into the bulk of the geometry. In order to study this limiting case, it is convenient to perform a change of variables in the integral (3.9.165) and write it as:

$$l = 2\,x_* \int_1^\infty dz \frac{\sqrt{G(x_*\,z)}}{\sqrt{e^{\frac{1}{2}\,(\phi_* - \phi(x_*\,z))}\left(\frac{h_*}{h(x_*\,z)}\right)^{\frac{1}{2}} - 1}} \,. \tag{3.A.133}$$

Similarly, the renormalized geodesic length can be represented as:

$$\mathcal{L}_r = 2\,x_* \int_1^{z_{max}} dz \frac{e^{-\frac{\phi(x_*\,z)}{4}}\left[h(x_*\,z)\right]^{-\frac{1}{4}}\sqrt{G(x_*\,z)}}{\sqrt{1 - e^{\frac{1}{2}\,(\phi(x_*\,z)) - \phi_*}\left(\frac{h(x_*\,z)}{h_*}\right)^{\frac{1}{2}}}} - \frac{2\,L_0\,e^{-\frac{\phi_0}{4}}}{b}\,\log(\mathcal{C}\,x_*\,z_{max})\,, \tag{3.A.134}$$

where $z_{max} = x_{max}/x_*$. When x_* is large the argument of the functions in the integrals (3.A.133) and (3.A.134) is large and one can use the UV asymptotic expressions (3.6.97) and (3.7.110). Therefore, we can approximate l as:

$$l \approx 2\sqrt{G_\infty}\,x_*^{-\frac{1}{b}} \int_1^\infty \frac{dz}{z^{1+\frac{1}{b}}\sqrt{z^{\frac{2}{b}} - 1}}\,. \tag{3.A.135}$$

The integral in (3.A.135) just gives b and, thus, we have:

$$l \approx 2\,b\,\sqrt{G_\infty}\,x_*^{-\frac{1}{b}} = \frac{2}{\kappa}\frac{L_0^2}{r_q\,x_*^{\frac{1}{b}}}\,. \tag{3.A.136}$$

It follows that, when x_* is large $r_q\,l$ is small. Thus the UV limit we are studying corresponds to $r_q\,l \to 0$. Similarly, the UV limit of $\mathcal{L}_r$ is:

$$\mathcal{L}_r \approx \frac{2\,L_0\,e^{-\frac{\phi_0}{4}}}{b}\left[\int_1^\infty \frac{dz}{z}\left[\frac{z^{\frac{1}{b}}}{\sqrt{z^{\frac{2}{b}} - 1}} - 1\right] - \log(\mathcal{C}\,x_*)\right]\,. \tag{3.A.137}$$

The integral in this last equation is:

$$\int_1^\infty \frac{dz}{z}\left[\frac{z^{\frac{1}{b}}}{\sqrt{z^{\frac{2}{b}} - 1}} - 1\right] = b\,\log 2\,. \tag{3.A.138}$$

On the other hand, the UV conformal dimension Δ_{UV} of a bulk field of mass m has been written in (3.9.170). Taking these facts into account, we can write:

$$e^{-m\,\mathcal{L}_r} \approx \frac{\left(b\,\sqrt{G_\infty}\,\mathcal{C}^{\frac{1}{b}}\right)^{2\Delta_{UV}}}{l^{2\Delta_{UV}}}\,. \tag{3.A.139}$$

If the operator $\mathcal{O}$ is canonically normalized in the short-distance $r_q\,l \to 0$ limit, the coefficient in the numerator of (3.A.139) should be chosen to be one as in (3.9.169). Therefore, it follows that the constant $\mathcal{C}$ is fixed to

$$\mathcal{C}^{\frac{1}{b}} = \frac{\sqrt{\lambda}}{r_q\,b\,\sqrt{G_\infty}} = \frac{\kappa\sqrt{\lambda}}{L_0^2} \ . \tag{3.A.140}$$

Let us now evaluate the first correction of the two-point correlator around the UV fixed point. Let us expand the function $G(x)$ for large x as in (3.A.56) and (3.A.57). Then, for large x_* we get:

$$\sqrt{G(x_*\,z)} \approx \sqrt{G_\infty}\,x_*^{-1-\frac{1}{b}}\,z^{-1-\frac{1}{b}}\left[1 + \frac{G_2}{2}\,x_*^{-2}\,z^{-2}\right] , \tag{3.A.141}$$

where $G_2 = h_2 + 2g_2$. Similarly:

$$\sqrt{e^{\frac{1}{2}\,(\phi_*-\phi(x_*\,z))}\left(\frac{h_*}{h(x_*\,z)}\right)^{\frac{1}{2}} - 1} \approx \sqrt{z^{\frac{2}{b}} - 1}\left[1 + \frac{\phi_2 + h_2}{4x_*^2}\,\frac{z^{\frac{2}{b}-2}\,(z^2-1)}{z^{\frac{2}{b}} - 1}\right] . \tag{3.A.142}$$

It follows that the separation l of the two points of the correlator can be written as:

$$l \approx 2\,b\,\sqrt{G_\infty}\,x_*^{-\frac{1}{b}}\left[1 + \frac{1}{2x_*^2}\left(G_2\,J_1 - \frac{\phi_2 + h_2}{2}\,J_2\right)\right] , \tag{3.A.143}$$

where J_1 and J_2 are the following integrals:

$$J_1 \equiv \frac{1}{b}\int_1^\infty \frac{dz}{z^{3+\frac{1}{b}}\,\sqrt{z^{\frac{2}{b}} - 1}} = \frac{\sqrt{\pi}}{2}\,\frac{\Gamma\left(1+b\right)}{\Gamma\left(\frac{3}{2} + b\right)} ,$$

$$J_2 \equiv \frac{1}{b}\int_1^\infty \frac{z^2-1}{z^{3-\frac{1}{b}}\left(z^{\frac{2}{b}} - 1\right)^{\frac{3}{2}}}\,dz = \sqrt{\pi}\,\frac{\Gamma\left(1+b\right)}{\Gamma\left(\frac{1}{2} + b\right)} - 1 \ . \tag{3.A.144}$$

Let us invert the relation (3.A.143) at first order and write x_* as a function of l. We get:

$$x_* \approx \left[\frac{2\sqrt{G_\infty}\,b}{l}\right]^b\left[1 + c_{x_*}\,l^{2b}\right] , \tag{3.A.145}$$

where c_{x_*} is a constant given by:

$$c_{x_*} = \frac{b}{\left(2\sqrt{G_\infty}\,b\right)^{2b}}\left[\left(\frac{g_2}{2b+1} - \frac{2b-1}{2b+1}\,\frac{h_2}{4} - \frac{\phi_2}{4}\right)\frac{\sqrt{\pi}\,\Gamma\left(1+b\right)}{\Gamma\left(\frac{1}{2} + b\right)} + \frac{\phi_2 + h_2}{4}\right] . \tag{3.A.146}$$

Moreover, the renormalized geodesic length at first order takes the form:

$$\mathcal{L}_r \approx 2\,L_0\,e^{-\frac{\phi_0}{4}}\left[\log\left(\frac{2b\,r_q\,\sqrt{G_\infty}}{x_*^{\frac{1}{b}}\,\sqrt{\lambda}}\right) + \frac{1}{x_*^2}\left[\left(g_2 - \frac{\phi_2}{4} + \frac{h_2}{4}\right)J_3 - \frac{\phi_2 + h_2}{4}\,J_2\right]\right] , \tag{3.A.147}$$

where J_2 is the integral defined in (3.A.144) and J_3 is:

$$J_3 \equiv \frac{1}{b} \int_1^\infty \frac{dz}{z^{3-\frac{1}{b}} \sqrt{z^{\frac{2}{b}} - 1}} = \frac{\sqrt{\pi}}{2} \frac{\Gamma(b)}{\Gamma\left(\frac{1}{2} + b\right)} \ . \tag{3.A.148}$$

Let us now write $\mathcal{L}_r$ in terms of l. By using (3.A.145) to eliminate x_* in terms of l we arrive at:

$$\mathcal{L}_r \approx 2 L_0 \, e^{-\frac{\phi_0}{4}} \left[\log\left(\frac{r_q \, l}{\sqrt{\lambda}}\right) + c_{\mathcal{L}} \left(\frac{r_q \, l}{\sqrt{\lambda}}\right)^{2b} \right] , \tag{3.A.149}$$

where the coefficient $c_{\mathcal{L}}$ is given by:

$$c_{\mathcal{L}} = \left(\frac{\sqrt{\lambda}}{2b \, r_q \, \sqrt{G_\infty}}\right)^{2b} \frac{\sqrt{\pi}\, \Gamma(b)}{\Gamma\left(\frac{1}{2} + b\right)} \left[\frac{g_2}{2(2b+1)} - \frac{\phi_2}{8} - \frac{1}{8} \frac{2b-1}{2b+1} h_2 \right] . \tag{3.A.150}$$

Therefore, the two-point correlator near the UV fixed point can be written as:

$$\left\langle \mathcal{O}(t,l)\, \mathcal{O}(t,0) \right\rangle = \frac{f_\Delta(r_q \, l/\sqrt{\lambda})}{(r_q \, l/\sqrt{\lambda})^{2\Delta_{UV}}} \ , \tag{3.A.151}$$

where the function f_Δ parameterizes the deviation from the conformal behavior near the UV fixed point and is given, at first order, by

$$f_\Delta(r_q \, l/\sqrt{\lambda}) \approx 1 + c_\Delta \left(\frac{r_q \, l}{\sqrt{\lambda}}\right)^{2b} , \tag{3.A.152}$$

where the new constant c_Δ is just:

$$c_\Delta = -\frac{\Delta_{UV}}{4} \frac{\sqrt{\pi}\, \Gamma(b)}{\Gamma\left(\frac{1}{2} + b\right)} \left(\frac{\kappa}{2\sqrt{2}\,\pi\,\sigma}\right)^{2b} \left[\frac{4}{2b+1} g_2 - \frac{2b-1}{2b+1} h_2 - \phi_2 \right] . \tag{3.A.153}$$

IR behavior

Let us now analyze the two-point functions in the IR limit, which corresponds to taking $x_* \to 0$. In this case the geodesic penetrates deeply in the bulk. We will proceed similarly to what we did in section 3.A.4 for the $q\bar{q}$ potential in the IR. Accordingly, we split the interval $[x_*, x_{max}]$ as $[x_*, x_{max}] = [x_*, x_a] \cup [x_a, x_{max}]$ for some $x_a < 1$ small. Near the turning point, i.e., when $x_* \le x \le x_a$, we can approximate the functions $h(x)$ and $g(x)$ as:

$$h(x) \approx \left(\frac{c\, L_{IR}}{\gamma}\right)^4 \frac{1}{x^4} \ , \qquad e^g \approx \frac{\gamma}{c}\, x \ , \tag{3.A.154}$$

where $L_{IR} = L_{ABJM}$ is the AdS radius of the unflavored ABJM solution and γ and c are the parameters of the unflavored running solution. It follows that, in this IR region, the function $G(x)$ behaves as:

$$G(x) \approx \frac{c^2}{\gamma^2} \frac{L_{IR}^4}{x^4} \ . \tag{3.A.155}$$

Moreover, the dilaton ϕ_{IR} is constant and given by the ABJM value ϕ_{ABJM} written in (3.2.4).

Suppose that we have chosen some $x_a \gg x_*$. Let us then split the integral (3.9.165) for l as:

$$l = 2 \left[\int_{x_*}^{x_a} dx + \int_{x_a}^{x_{max}} dx \right] \frac{\sqrt{G(x)}}{\sqrt{e^{\frac{1}{2}(\phi_* - \phi(x))} \left(\frac{h_*}{h(x)} \right)^{\frac{1}{2}} - 1}} \equiv l_{IR} + l_{UV} , \qquad (3.A.156)$$

where x_{max} should be sent to $+\infty$ at the end of the calculation. Let us approximate the first integral in (3.A.156) by taking the functions in the deep IR, as in (3.A.154). We obtain:

$$l_{IR} \approx \frac{2c}{\gamma} L_{IR}^2 \int_{x_*}^{x_a} \frac{dx}{x^2 \sqrt{\frac{x^2}{x_*^2} - 1}} = \frac{2c}{\gamma} \frac{L_{IR}^2}{x_*} \sqrt{1 - \frac{x_*^2}{x_a^2}} . \qquad (3.A.157)$$

For small x_*/x_a we can approximate this integral as:

$$l_{IR} \approx \frac{2c}{\gamma} \frac{L_{IR}^2}{x_*} . \qquad (3.A.158)$$

To evaluate l_{UV} approximately we notice that $h_* \propto x_*^{-4}$ and, therefore, it is large for $x_* \to 0$. Then, we can neglect the one inside the square root and approximate l_{UV} as:

$$l_{UV} \approx x_* \frac{\gamma \, e^{-\frac{\phi_{IR}}{4}}}{c \, L_{IR}} \int_{x_a}^{\infty} dx \, e^{\frac{\phi(x)}{4}} \left[h(x) \right]^{\frac{1}{4}} \sqrt{G(x)} . \qquad (3.A.159)$$

Since the integral in (3.A.159) converges and is independent of x_*, it follows that $l_{UV} \sim x_*$ and, therefore, it can be neglected with respect to the large value of $l_{IR} \sim 1/x_*$. Thus, we take

$$l \approx \frac{\hat{\gamma} - 1}{\gamma} \frac{L_{IR}^2}{r_q \, x_*} . \qquad (3.A.160)$$

Notice that it follows from this equation that $r_q \, l$ is large if x_* is small, as it should be in the IR regime. Let us next perform a similar analysis for the renormalized geodesic length $\mathcal{L}_r$. First, we consider the IR integral:

$$\int_{x_*}^{x_a} dx \frac{e^{-\frac{\phi(x)}{4}} \left[h(x) \right]^{-\frac{1}{4}} \sqrt{G(x)}}{\sqrt{1 - e^{\frac{1}{2}(\phi(x)) - \phi_*} \left(\frac{h(x)}{h_*} \right)^{\frac{1}{2}}}} \approx e^{-\frac{\phi_{IR}}{4}} L_{IR} \int_{x_*}^{x_a} \frac{dx}{x \sqrt{1 - \frac{x_*^2}{x^2}}} =$$

$$= e^{-\frac{\phi_{IR}}{4}} L_{IR} \log \left(\frac{x_a + \sqrt{x_a^2 - x_*^2}}{x_*} \right) \approx e^{-\frac{\phi_{IR}}{4}} L_{IR} \log \left(\frac{2x_a}{x_*} \right) . \qquad (3.A.161)$$

To evaluate the UV integral we proceed similarly to what we did for the integral for l and, in this case, we only keep the one inside the square root. Then:

$$\int_{x_a}^{x_{max}} dx \frac{e^{-\frac{\phi(x)}{4}} \left[h(x) \right]^{-\frac{1}{4}} \sqrt{G(x)}}{\sqrt{1 - e^{\frac{1}{2}(\phi(x)) - \phi_*} \left(\frac{h(x)}{h_*} \right)^{\frac{1}{2}}}} \approx \int_{x_a}^{x_{max}} dx \, e^{-\frac{\phi(x)}{4}} \left[h(x) \right]^{-\frac{1}{4}} \sqrt{G(x)} . \qquad (3.A.162)$$

Therefore:

$$m\,\mathcal{L}_r \approx 2\,\Delta_{IR}\log\left(\frac{2x_a}{x_*}\right) + 2m\int_{x_a}^{x_{max}} dx\; e^{-\frac{\phi(x)}{4}}\left[h(x)\right]^{-\frac{1}{4}}\sqrt{G(x)} - 2\,\Delta_{UV}\log\left(\frac{\kappa\sqrt{\lambda}\,x_{max}^{\frac{1}{b}}}{L_0^2}\right),$$
(3.A.163)

where Δ_{IR} is the conformal dimension of the operator $\mathcal{O}$ in the IR conformal point, given by:

$$\Delta_{IR} = m\,L_{IR}\,e^{-\frac{\phi_{IR}}{4}}\,,$$
(3.A.164)

which is just (3.9.171). Let us next define the following quantities:

$$\mathcal{I}_{IR} \equiv -2m\int_{x_a}^{1} dx\, e^{-\frac{\phi(x)}{4}}\left[h(x)\right]^{-\frac{1}{4}}\sqrt{G(x)} \;-\; 2\,\Delta_{IR}\log x_a\,,$$

$$\mathcal{I}_{UV} \equiv -2m\int_{1}^{x_{max}} dx\, e^{-\frac{\phi(x)}{4}}\left[h(x)\right]^{-\frac{1}{4}}\sqrt{G(x)} \;+\; \frac{2\,\Delta_{UV}}{b}\log x_{max}\,.$$
(3.A.165)

Then, after using the relation (3.A.160) to eliminate x_* in favor of l, we get:

$$m\,\mathcal{L}_r \approx \log(r_q\,l/\sqrt{\lambda})^{2\Delta_{IR}} + \log\left[\left(\frac{2\gamma}{\hat{\gamma}-1}\frac{\sqrt{\lambda}}{L_{IR}^2}\right)^{2\Delta_{IR}}\left(\frac{\kappa}{L_0^2}\right)^{-2\Delta_{UV}}\right] - \mathcal{I}_{IR} - \mathcal{I}_{UV}\,.$$
(3.A.166)

Then, it follows that the IR limit $r_q\,l \to \infty$ of the two-point correlator is as in (3.9.172), where $\mathcal{N}$ is the normalization constant given by:

$$\mathcal{N} = \frac{\left(\frac{\kappa\sqrt{\lambda}}{L_0^2}\right)^{2\Delta_{UV}}}{\left(\frac{2\gamma}{\hat{\gamma}-1}\frac{\sqrt{\lambda}}{L_{IR}^2}\right)^{2\Delta_{IR}}}\exp\left[\mathcal{I}_{IR} + \mathcal{I}_{UV}\right]\,.$$
(3.A.167)

It turns out that, in the expression of the integrals in (3.A.165) we can take the limits $x_a \to 0$ (in $\mathcal{I}_{IR}$) and $x_{max} \to \infty$ (in $\mathcal{I}_{UV}$). Actually, it can be easily proved that, after taking these limits, $\mathcal{I}_{IR}$ and $\mathcal{I}_{UV}$ can be recast as:

$$\mathcal{I}_{IR} = 2\Delta_{IR}\int_{0}^{1}\frac{dx}{x}\left[1 - e^{\frac{\phi_{IR}-\phi(x)}{4}}\left[\frac{h_{IR}(x)}{h(x)}\right]^{\frac{1}{4}}\sqrt{\frac{G(x)}{G_{IR}(x)}}\right],$$

$$\mathcal{I}_{UV} = \frac{2\Delta_{UV}}{b}\int_{1}^{\infty}\frac{dx}{x}\left[1 - e^{\frac{\phi_0-\phi(x)}{4}}\left[\frac{h_{UV}(x)}{h(x)}\right]^{\frac{1}{4}}\sqrt{\frac{G(x)}{G_{UV}(x)}}\right].$$
(3.A.168)

Notice that the form of the correlator is consistent with the fact that the conformal symmetry is recovered in the IR limit $r_q\,l \to \infty$. The non-canonical normalization factor $\mathcal{N}$ is due to the fact that we chose to renormalize $\mathcal{L}$ in such a way that the correlator is canonically normalized in the opposite UV limit $r_q\,l \to 0$.

3.A.6   WKB mass levels

Consider the following differential equation for the function $R(x)$:

$$\partial_x \left[P(x)\, \partial_x R \right] + m^2\, Q(x)\, R = 0 \ , \tag{3.A.169}$$

where x takes values in the range $x_* \le x \le \infty$, m is the mass parameter and $P(x)$ and $Q(x)$ are two arbitrary functions that are independent of m. We will assume that near $x \approx x_*, \infty$ these functions behave as:

$$P \approx P_1 (x - x_*)^{s_1} \ , \qquad Q \approx Q_1 (x - x_*)^{s_2} \ , \qquad \text{as } x \to x_* \ ,$$

$$P \approx P_2\, x^{r_1} \ , \qquad\qquad Q \approx Q_2\, x^{r_2} \ , \qquad \text{as } x \to \infty \ , \tag{3.A.170}$$

where P_i, Q_i, s_i, and r_i are constants. By a of suitable change of variables, the differential equation (3.A.169) can be converted into a Schrödinger equation, which only admits a discrete set of normalizable solutions for a set of values of m parameterized by a quantum number $n \ge 0$. The mass levels for large values of n can be evaluated in the WKB approximation [154], with the result:

$$m_{WKB} = \frac{\pi}{\xi} \sqrt{(n+1)\left(n + \frac{|s_1 - 1|}{s_2 - s_1 + 2} + \frac{|r_1 - 1|}{r_1 - r_2 - 2} \right)} \ , \tag{3.A.171}$$

where $\xi = \xi(x_*)$ is the integral:

$$\xi = \int_{x_*}^{\infty} dx \sqrt{\frac{Q(x)}{P(x)}} \ . \tag{3.A.172}$$

In our case, the functions $P(x)$ and $Q(x)$ which correspond to the fluctuation equation (3.10.185) are:

$$P(x) = \frac{h^{\frac{1}{4}}\, e^{2f-\phi}}{x}\, (x^2 - x_*^2) \ , \qquad Q(x) = \frac{h^{\frac{5}{4}}\, e^{2f+2g-\phi}}{x} \ , \tag{3.A.173}$$

and it is immediate to extract the exponents s_1, s_2, r_1, and r_2:

$$s_1 = 1 \ , \qquad s_2 = 0 \ , \qquad r_1 = 1 + \frac{1}{b} \ , \qquad r_2 = -1 - \frac{1}{b} \ . \tag{3.A.174}$$

Using these values one immediately finds that the WKB mass levels are given by (3.10.186).

Asymptotic spectra

Let us now evaluate analytically the meson spectrum in the two limiting cases in which the sea quark mass $m_q = r_q/2\pi$ is small or large compared to the valence quark mass μ_q. Notice that $e^g \propto m_q$ (see eqs. (3.5.77) and (3.5.78)). Therefore, (3.10.176) can be regarded as giving the relation μ_q/m_q as a function of x_*.

Let us consider first the case in which m_q is small. Clearly, when $m_q \to 0$ for fixed μ_q one necessarily must have x_* large. Actually, integrating (3.10.176) by using the asymptotic expression of g written in (3.6.95) at leading order, we get:

$$\mu_q \approx \kappa\, m_q\, x_*^{\frac{1}{b}}\ , \tag{3.A.175}$$

where the constant κ has been defined in (3.6.94). Thus, when $m_q \to 0$ for fixed μ_q the x coordinate of the tip of the flavor brane increases as:

$$x_* \sim m_q^{-b}\ , \qquad (m_q \to 0)\ . \tag{3.A.176}$$

Let us now evaluate $\xi(x_*)$ when x_* is large. First of all we perform a change of variables in the integral (3.10.187) and rewrite $\xi(x_*)$ as:

$$\xi(x_*) = \int_1^\infty dz\, \frac{e^{g(x_*\, z)}\sqrt{h(x_*\, z)}}{\sqrt{z^2 - 1}}\ . \tag{3.A.177}$$

If x_* is large, the argument of the functions g and h in (3.A.177) is large and we can use their UV asymptotic expressions (3.6.95) and (3.6.97) to evaluate them. At leading order, we get:

$$e^{g(x_*\, z)} \approx \frac{r_*}{b}\, z^{\frac{1}{b}}\ , \qquad\qquad h(x_*\, z) \approx \frac{L_0^4}{r_*^4}\, z^{-\frac{4}{b}}\ , \tag{3.A.178}$$

where r_* is the value of the r coordinate corresponding to $x = x_*$. Therefore, for $m_q \to 0$ for fixed μ_q the ξ is approximately

$$\xi \approx \frac{L_0^2}{b\, r_*} \int_1^\infty \frac{dz}{z^{\frac{1}{b}}\sqrt{z^2 - 1}} = \frac{L_0^2}{r_*}\sqrt{\pi}\, \frac{\Gamma\!\left(\frac{2b+1}{2b}\right)}{\Gamma\!\left(\frac{b+1}{2b}\right)}\ . \tag{3.A.179}$$

Using this result in (3.10.186) we get the following mass spectrum in the UV limit:

$$m_{WKB}^{(UV)} = \frac{\sqrt{\pi}}{\sqrt{2}}\, \frac{r_*}{L_0^2}\, \frac{\Gamma\!\left(\frac{b+1}{2b}\right)}{\Gamma\!\left(\frac{2b+1}{2b}\right)}\, \sqrt{(n+1)(2n+1)}\ , \qquad (\mu_q/m_q \to \infty)\ . \tag{3.A.180}$$

Let us write this result in terms of physical quantities. Recall that L_0 and r_* are related to the 't Hooft coupling λ and to the valence quark mass μ_q as:

$$L_0^2 = \pi\sqrt{2\lambda}\,\sigma\ , \qquad\qquad r_* = 2\pi\alpha'\,\mu_q\ , \tag{3.A.181}$$

where σ is the screening function written in (3.8.157). Then, for large μ_q/m_q, we have:

$$m_{WKB}^{(UV)} = \frac{\sqrt{\pi}\,\mu_q}{\sigma\sqrt{\lambda}}\, \frac{\Gamma\!\left(\frac{b+1}{2b}\right)}{\Gamma\!\left(\frac{2b+1}{2b}\right)}\, \sqrt{(n+1)(2n+1)}\ , \qquad (\mu_q/m_q \to \infty)\ , \tag{3.A.182}$$

where we have taken $\alpha' = 1$. Eq. (3.A.182) is exactly the WKB mass spectrum one gets for vector mesons in the massless flavored background of ref. [75].

Let us next consider the limit in which μ_q/m_q is small. Since $e^g \sim m_q$, it follows from (3.10.176) that x_* must be small. Actually, we can estimate the relation between μ_q/m_q and x_* by extracting from (3.4.66) and (3.5.77) the approximate expression of e^g near $x = 0$. We get:

$$e^g \approx \frac{\gamma}{c} x \approx \pi \left(\hat{\gamma} + 1 \right) m_q x \ . \tag{3.A.183}$$

Then, we have:

$$\mu_q \approx \frac{\hat{\gamma} + 1}{2} m_q x_* \ , \tag{3.A.184}$$

and it follows that, for fixed μ_q and large m_q, the coordinate of the tip of the flavor brane behaves as:

$$x_* \sim \frac{1}{m_q} \ , \qquad (m_q \to \infty) \ . \tag{3.A.185}$$

Thus, for large sea quark mass $x_* \to 0$ and thus the dynamics of the fluctuating flavor brane is dominated by the IR, where the solution corresponds to the running solution of the unflavored system. In this case, we have at leading order near $x \sim 0$:

$$e^{g(x)} \approx \frac{\gamma}{c} x \approx r_* \frac{x}{x_*} \ , \qquad h(x) \approx \frac{2\pi^2 N}{k} \frac{c^4}{\gamma^4} \frac{1}{x^4} \approx \frac{2\pi^2 N}{k} \frac{1}{r_*^4} \left(\frac{x_*}{x} \right)^4 \ , \tag{3.A.186}$$

where, in the last step, we used that $c/\gamma \approx x_*/r_*$. Thus,

$$e^{g(x_* z)} \sqrt{h(x_* z)} \approx \frac{\sqrt{2\pi^2 \lambda}}{r_*} \frac{1}{z} \ , \tag{3.A.187}$$

and, after evaluating the integral (3.A.177) and writing the result in terms of the 't Hooft coupling λ and the valence quark mass μ_q , we have:

$$m_{WKB}^{(IR)} = \frac{2\mu_q}{\sqrt{\lambda}} \sqrt{(n+1)(2n+1)} \ , \qquad (\mu_q/m_q \to 0) \ , \tag{3.A.188}$$

which is exactly the mass spectrum of vector mesons in the unflavored ABJM model [153]. By combining (3.A.182) and (3.A.188) we obtain the UV/IR mass relation written in (3.10.188). It is now straightforward to obtain this ratio for small and large values of the deformation parameter. Indeed, for small $\hat{\epsilon}$ one can expand $m_{WKB}^{(UV)}/m_{WKB}^{(IR)}$ as:

$$\frac{m_{WKB}^{(UV)}}{m_{WKB}^{(IR)}} = 1 + \frac{3 - \log 2}{4} \hat{\epsilon} + \frac{1}{384} \left[12 \left(\log 2 \left(\log 2 + 3 \right) - 3 \right) - \pi^2 \right] \hat{\epsilon}^2 + \cdots \ . \tag{3.A.189}$$

Moreover, in the opposite limit in which $\hat{\epsilon}$ is very large, we have:

$$\frac{m_{WKB}^{(UV)}}{m_{WKB}^{(IR)}} \approx \frac{8\sqrt{2\pi}}{5\sqrt{15}} \frac{\Gamma\left(\frac{9}{10} \right)}{\Gamma\left(\frac{7}{5} \right)} \sqrt{\hat{\epsilon}} \ . \tag{3.A.190}$$

3.A.7 Analytical expansion in flavor

In this appendix we will construct an analytic solution to (3.3.25) in a power series expansion in the flavor deformation parameter $\hat{\epsilon}$. We start by writing an ansatz for $W(x)$ as:

$$W(x) = \sum_{n=0} W_n(x)\hat{\epsilon}^n = 2x + W_1(x)\hat{\epsilon} + W_2(x)\hat{\epsilon}^2 + W_3(x)\hat{\epsilon}^3 + \mathcal{O}(\hat{\epsilon}^4) \ , \qquad (3.A.191)$$

where we cut the series at level $\mathcal{O}(\hat{\epsilon}^3)$ up to which point we will write down explicit results in the following. In (3.A.191), we chose $W_0(x) = 2x$, such that for $\hat{\epsilon} = 0$ we recover the ABJM theory by construction. Expanding the master equation (3.3.25) in $\hat{\epsilon}$ yields, at first order,

$$36x^2 - 84x^4 + 36x^3 W_1(x) - 12x^4 W_1'(x) - 6x^5 W_1''(x) = 0 \qquad (3.A.192)$$

A general solution is:

$$W_1(x) = \frac{7x^2 - 2}{2x} + a_1 x^2 + \frac{b_1}{x^3} \ , \qquad (3.A.193)$$

where a_1 and b_1 are integration constants. We wish to match with massless flavored ABJM in the UV, so we set $a_1 = 0$, because the leading term in the UV should go as x. The second constant b_1 is fixed by demanding continuity at the boundary of the cavity, that is, at $x = 1$. For that purpose, we will consider the running solution (3.4.70) inside the cavity and expand it in $\hat{\epsilon}$. Recall that γ depends on $\hat{\epsilon}$, for which we write an expansion:

$$\gamma = \gamma_1 \hat{\epsilon} + \gamma_2 \hat{\epsilon}^2 + \gamma_3 \hat{\epsilon}^3 + \dots \ . \qquad (3.A.194)$$

By expanding (3.4.70) we find

$$W_{running}(x) = 2x \left\{ 1 + 3\gamma_1 x\hat{\epsilon} + (3\gamma_2 x - 2\gamma_1^2 x^2)\hat{\epsilon}^2 + (3\gamma_3 x - 4\gamma_1\gamma_2 x^2 + 3\gamma_1^3 x^3)\hat{\epsilon}^3 \right\} + \dots \ . \qquad (3.A.195)$$

Now, imposing continuity of $W_1(x)$ and its first derivative at $x = 1$, we obtain:

$$\gamma_1 = \frac{2}{5} \quad , \quad b_1 = -\frac{1}{10} \ . \qquad (3.A.196)$$

Thus, the exact solution to the master equation at first order in $\hat{\epsilon}$ reads:

$$W_1(x) = \begin{cases} \frac{12}{5}x^2 \ , & x \leq 1 \\[2mm] \frac{7x^2 - 2}{2x} - \frac{1}{10x^3} \ , & x \geq 1 \ . \end{cases} \qquad (3.A.197)$$

It is straightforward to repeat the iterative procedure for higher $\hat{\epsilon}$ orders. The expression for $W_2(x)$ reads:

$$W_2(x) = \begin{cases} -\frac{8x^2}{875}(70x - 171) \ , & x \leq 1 \\[2mm] \frac{13125x^8 + 3500x^6 - 3962x^4 - 3360x^4 \log x + 300x^2 - 35}{14000x^7} \ , & x \geq 1 \ , \end{cases} \qquad (3.A.198)$$

and that for $W_3(x)$:

$$W_3(x) = \begin{cases} \dfrac{16x^2(135135x(35x-76)+2356888)}{197071875} \,, & x \leq 1 \\[2em] -\dfrac{23}{208000x^{11}} + \dfrac{89}{184800x^9} - \dfrac{302}{39375x^7} + \dfrac{8293}{98000x^5} - \dfrac{2120717}{8400000x^3} \\[1.5em] \quad -\dfrac{\log(x)\left(10703x^4+20160x^4\log(x)-3600x^2+840\right)}{70000x^7} - \dfrac{15x}{32} + \dfrac{37}{96x} \,, & x \geq 1 \,. \end{cases} \tag{3.A.199}$$

The constants γ, κ and b read:

$$\gamma = \frac{2\hat{\epsilon}}{5} + \frac{228\hat{\epsilon}^2}{875} + \mathcal{O}(\hat{\epsilon}^3) \,, \tag{3.A.200}$$

$$\kappa = 1 - \frac{33\hat{\epsilon}}{80} + \frac{128881\hat{\epsilon}^2}{448000} + \mathcal{O}(\hat{\epsilon}^3) \,, \tag{3.A.201}$$

$$b = 1 + \frac{\hat{\epsilon}}{4} - \frac{7\hat{\epsilon}^2}{42} + \mathcal{O}(\hat{\epsilon}^3) \,. \tag{3.A.202}$$

The metric functions can then be explicitly solved for. We will write them down in the second order of the expansion parameter $\hat{\epsilon}$. The constants are fixed to make the functions continuous across the boundary of the cavity $x = x_q = 1$ corresponding to $r = r_q$. We only present the solutions in terms of x-variable, the transformation to the original coordinate is readily obtained through the relationship $x \leftrightarrow r$ below (3.A.213).

The squashing functions read:

$$\frac{e^f}{r_q} - x = \begin{cases} \hat{\epsilon}\left(\dfrac{2x}{5} - \dfrac{3x^2}{5}\right) + \hat{\epsilon}^2 \dfrac{1085x^3-1104x^2+176x}{1750} + \mathcal{O}(\hat{\epsilon}^3) \,, & x \leq 1 \\[2em] \hat{\epsilon}\dfrac{-33x^4-20x^4\log(x)+20x^2-3}{80x^3} \\[1.5em] \quad +\hat{\epsilon}^2\dfrac{142881x^8-130200x^6+34426x^4-6600x^2+280x^4\log x\left(615x^4+50x^4\log x-100x^2-129\right)-315}{448000x^7} \\[1.5em] \quad +\mathcal{O}(\hat{\epsilon}^3) \,, & x \geq 1 \,. \end{cases} \tag{3.A.203}$$

and

$$\frac{e^g}{r_q} - x = \begin{cases} \hat{\epsilon}\left(\dfrac{2x}{5} - \dfrac{4x^2}{5}\right) + \hat{\epsilon}^2 \dfrac{8}{875}\left(105x^3 - 92x^2 + 11x\right) + \mathcal{O}(\hat{\epsilon}^3) \,, & x \leq 1 \\[2em] \hat{\epsilon}\dfrac{-53x^4-20x^4\log x+20x^2+1}{80x^3} \\[1.5em] \quad +\hat{\epsilon}^2\dfrac{903243x^8-754600x^6+133854x^4+11400x^2+840x^4\log x\left(715x^4+50x^4\log x-100x^2+43\right)+1015}{1344000x^7} \\[1.5em] \quad +\mathcal{O}(\hat{\epsilon}^3) \,, & x \geq 1 \,. \end{cases} \tag{3.A.204}$$

The relative squashing between the spheres reads:

$$q - 1 = \begin{cases} \hat{\epsilon}\frac{2x}{5} + \hat{\epsilon}^2 \frac{4}{875}x(57 - 70x) + \mathcal{O}(\hat{\epsilon}^3) \,, & x \leq 1 \\[3mm] \hat{\epsilon}\left(\frac{1}{2} - \frac{1}{10x^4}\right) + \hat{\epsilon}^2 \frac{-13125x^8 + 17500x^6 - 6006x^4 - 10080x^4 \log(x) - 900x^2 + 35}{42000x^8} + \mathcal{O}(\hat{\epsilon}^3) \,, & x \geq 1 \,. \end{cases}$$
$$(3.A.205)$$

In order to compute $h(x)$ outside the cavity we use expression (3.3.27), and β is fixed to zero. Furthermore, to match it with the corresponding function inside the cavity (3.4.68), we impose the matching condition (3.5.79) . This condition fixes α to be:

$$\alpha = \frac{25}{14\hat{\epsilon}^2} - \frac{4646}{539\hat{\epsilon}} + \mathcal{O}(\hat{\epsilon}^0) \,, \qquad (3.A.206)$$

and the function $h(x)$ is:

$$\frac{kr_q^4}{4\pi^2 N}h - \frac{1}{2x^4} \qquad (3.A.207)$$

$$= \begin{cases} \hat{\epsilon}\frac{2\left(x^3 + 14x - 14\right)}{35x^4} + \hat{\epsilon}^2 \frac{2\left(440x^4 - 1230x^3 + 1155x^2 - 3652x + 2882\right)}{9625x^4} + \mathcal{O}(\hat{\epsilon}^3) \,, & x \leq 1 \\[3mm] \hat{\epsilon}\frac{91x^4 + 140x^4 \log x - 84x^2 + 9}{280x^8} \\[2mm] + \hat{\epsilon}^2 \frac{1320x^4 \log x\left(-665x^4 + 700x^4 \log x - 840x^2 + 306\right) + 11\left(-58659x^6 + 14560x^4 + 20424x^2 - 5280\right)x^2 + 7465}{3696000x^{12}} \\[2mm] + \mathcal{O}(\hat{\epsilon}^3) \,, & x \geq 1 \,. \end{cases}$$
$$(3.A.208)$$

The dilaton reads:

$$\left(\frac{k^5}{2\pi^2 N}\right)^{1/4} xe^\phi - 2x \qquad (3.A.209)$$

$$= \begin{cases} \hat{\epsilon}\frac{2}{35}\left(x^2 - 14\right)x^2 + \hat{\epsilon}^2 \frac{\left(165x^5 + 1540x^3 + 11060x^2 - 70070x + 35112\right)x^2}{67375} + \mathcal{O}(\hat{\epsilon}^3) \,, & x \leq 1 \\[3mm] -\hat{\epsilon}\frac{245x^4 - 84x^2 + 3}{70x^3} \\[2mm] + \hat{\epsilon}^2 \frac{5322625x^8 - 4117960x^6 + 765534x^4 - 110880x^4 \log x - 27720x^2 - 575}{1078000x^7} \\[2mm] + \mathcal{O}(\hat{\epsilon}^3) \,, & x \geq 1 \,. \end{cases}$$
$$(3.A.210)$$

and the expression for the function $e^\Lambda = e^\phi h^{-1/4}$ is:

$$\frac{k e^\Lambda}{r_q} - 2x$$

$$(3.A.211)$$

$$= \begin{cases} \hat\epsilon \frac{4}{5} x(1 - 4x) + \hat\epsilon^2 \frac{16}{875} x \left(280 x^2 - 184 x + 11\right) + \mathcal{O}(\hat\epsilon^3) \,, & x \leq 1 \\[2em] -\hat\epsilon \frac{153 x^4 + 20 x^4 \log x - 60 x^2 + 3}{40 x^3} \\[1em] +\hat\epsilon^2 \frac{3906243 x^8 - 3243800 x^6 + 692958 x^4 - 40200 x^2 + 840 x^4 \log x \left(1215 x^4 + 50 x^4 \log x - 300 x^2 - 129\right) - 385}{672000 x^7} \\[1em] +\mathcal{O}(\hat\epsilon^3) \,, & x \geq 1 \,. \end{cases}$$

$$(3.A.212)$$

In order to transform the above formulas to the canonical radial coordinate r, let us write down the relation to x. Integrating equation (3.3.22) by using (3.A.204) and fixing the integration constant by imposing the condition $r(x = 1) = r_q$, the relation between the holographic coordinates r and x outside the cavity can be computed. Expanding expression (3.4.65) in $\hat\epsilon$ we obtain the corresponding relation inside the cavity:

$$\frac{r}{r_q} - x = \begin{cases} -\hat\epsilon \frac{2}{5} x(x - 1) + \hat\epsilon^2 \frac{8}{875} x \left(35 x^2 - 46 x + 11\right) + \mathcal{O}(\hat\epsilon^3) \,, & x \leq 1 \\[2em] +\hat\epsilon \left[\frac{2}{3} + \frac{-99 x^4 - 60 x^4 \log x - 60 x^2 - 1}{240 x^3} \right] \\[1em] +\hat\epsilon^2 \frac{1159929 x^8 + 2515800 x^6 - 145894 x^4 - 6840 x^2 + 840 x^4 \log x \left(1845 x^4 + 150 x^4 \log x + 300 x^2 - 43\right) - 435}{4032000 x^7} \\[1em] +\mathcal{O}(\hat\epsilon^3) \,, & x \geq 1 \,. \end{cases}$$

$$(3.A.213)$$

Finally, introducing (3.6.81) in expression (3.3.19) we obtain the expansion for the F_2 form, and using (3.3.21) and (3.3.22) in expression (3.3.18), and expanding to second order in $\hat\epsilon$, we obtain the expression for the F_4 form.

Chapter 4

Holographic fractional Hall effect

4.1   Introduction

Since its discovery more than thirty years ago, the QHE has been the subject of intense research. Nevertheless, some aspects of the FQHE involve strongly-coupled dynamics and are still not fully understood. The holographic AdS/CFT duality has proven to be a powerful tool in the study of quantum matter in the strongly-coupled regime, since it provides answers to difficult field theory questions by using classical gravitational theories in higher dimensions. Therefore, it is quite natural to explore the possibility of constructing holographic models of the (F)QHE and to extract properties that are very difficult to obtain via weakly-coupled many-body field theory.

In recent years, two types of holographic models of the QHE have been proposed. The first class consists of bottom-up models in Einstein-Maxwell-axio-dilaton theories [155, 156, 157, 158, 159]. These models are endowed with an $SL(2, \mathbb{Z})$ duality and, as a consequence, they capture some observed features of QH physics. However, it is very difficult to engineer these types of models to have a mass gap; [160] is so far the only example of a gapped model in this class.

The second approach to holographically realize the QHE makes use of top-down D-brane constructions [161, 162, 163], in which a (2+1)-dimensional gauge theory with fermions in the fundamental representation is modeled by a suitable Dp-Dq brane intersection. The limit in which the Dq-brane is treated as a probe in the Dp-brane background corresponds in the field theory dual to the so-called quenched approximation in which loops of fundamental fermions are neglected. In this approach, the worldvolume theory of the probe brane encodes the physics of the fermions. Generically, the probe brane crosses the horizon, yielding a black hole embedding, which is dual to a gapless metallic state. The quantum Hall state is realized holographically as a Minkowski embedding, in which the brane ends smoothly above the black hole horizon. The distance from the horizon at which the probe caps off determines the mass gap.

In this chapter, we want to engineer quantum Hall states in the flavored ABJM theory. Such Hall states are only possible if parity is broken, which can be accomplished by turning on an appropriate internal flux on the D6-brane worldvolume. However, treating the backre-

action of this internal flux is quite challenging. For now, we will start with a single quenched massive quark in the background of N_f unquenched massless quarks, a system analyzed in [164, 136]. We then will turn on a parity-breaking internal flux on the worldvolume of this probe D6-brane.

In the presence of this internal flux, the Wess-Zumino term of the probe action contains the term $\int \hat{C}_1 \wedge F^3$, where $\hat{C}_1$ is the pullback of the RR potential one-form. In the ABJM background C_1 has only internal components. Therefore, after integrating over the internal directions, we are left with an axionic term $F \wedge F$ along AdS_4, which indeed breaks parity and corresponds to a Chern-Simons term on the boundary.

Even in the probe limit, choosing a consistent ansatz for this internal flux, which must also be quantized appropriately, is not obvious. We can, however, take a cue from the ABJ model [61], *i.e.*, the $U(N+M)_k \times U(N)_{-k}$ Chern-Simons matter theory, which can be engineered in string theory by adding fractional D2-branes to the ABJM setup. The corresponding gravity dual can be obtained from the ABJM solution by turning on a flat Neveu-Schwarz B_2 field proportional to the Kähler form of $\mathbb{CP}^3$. The pullback of this parity-breaking B_2 on a probe D6-brane can alternately be viewed as a worldvolume gauge field flux. Inspired by this example, we will generalize this ABJ solution into an ansatz for the case with no background B_2 field and only a probe worldvolume flux, but with backreacted massless flavors.

Equipped with this ansatz for the internal gauge flux, we will show that, indeed, there are quantum Hall states in this setup. From the QH perspective, one can regard the effects of the massless, backreacted quarks as representing intrinsic disorder due to the quantum fluctuations of the massive quark. We compute the contribution of these fluctuations to the conductivities in the form of an integral extended in the holographic direction, from the tip of the brane to the AdS boundary.

Surprisingly, we will find a very special family of explicit, supersymmetric, gapped QH solutions at zero temperature. These BPS solutions have nonzero charge density and equal electric and magnetic fields, and we can compute the Hall conductivity, including the effects of quark loops, analytically.

The rest of this chapter is organized as follows. In section 4.2 we review the ABJM background with flavor at finite temperature. Then, in section 4.3, we consider the embedding of a probe D6-brane with internal flux. We first present in section 4.3.1 the ansatz for the internal components of the worldvolume gauge field that will be used throughout the chapter and discuss the corresponding flux quantization condition. In section 4.3.2 we generalize these results to nonvanishing background electric and magnetic fields, as well as to nonzero charge density and currents. We compute the corresponding longitudinal and transverse conductivities in section 4.4. In section 4.5 we analyze the residual $SO_+(1,1)$ boost invariance of our system at zero temperature. An analytic supersymmetric solution of the equations of motion at zero temperature is presented in section 4.6. Section 4.7 is devoted to the analysis of quark-antiquark bound states, *i.e.*, mesons. In particular, we study the effect of the broken parity on the mass spectrum. In section 4.8 we discuss our results.

The chapter is completed with several appendices 4.A where we provide details of our background geometry and discuss the quantization condition of the worldvolume flux ob-

tained by comparison with the ABJ solution. We also include a detailed analysis of the equations of motion of the probe and kappa symmetry. Besides, we include the equations governing the fluctuations of the probe , where we also estimate the meson masses using a WKB approximation.

4.2 The flavored ABJM black hole

In this section we will review, following [75, 164, 136], the background geometry corresponding to the ABJM model with unquenched massless flavors in the smeared approximation at finite temperature. Additional details of this supergravity solution are given in appendix 4.A.1. The ten-dimensional metric, in string frame, has the form

$$ds^2 = L^2 \, ds^2_{BH_4} + ds^2_6 \, , \tag{4.2.1}$$

where L is the radius of curvature, $ds^2_{BH_4}$ is the metric of a planar black hole in the four-dimensional Anti-de Sitter space, given by

$$ds^2_{BH_4} = -r^2 h(r) dt^2 + \frac{dr^2}{r^2 h(r)} + r^2 \big[dx^2 + dy^2 \big] \, , \tag{4.2.2}$$

and ds^2_6 is the metric of the compact internal six-dimensional manifold. The blackening factor $h(r)$ is given by

$$h(r) = 1 - \frac{r_h^3}{r^3} \, , \tag{4.2.3}$$

where the horizon radius r_h is related to the temperature T by $T = \frac{3 r_h}{4\pi}$. The internal metric ds^2_6 in (4.2.1) is a deformation of the Fubini-Study metric of $\mathbb{CP}^3$, realized as an $\mathbb{S}^2$-bundle over $\mathbb{S}^4$. Let $ds^2_{\mathbb{S}^4}$ be the standard metric for the unit round four-sphere and let z^i $(i = 1, 2, 3)$ be three Cartesian coordinates parameterizing the unit two-sphere $(\sum_i (z^i)^2 = 1)$. Then, ds^2_6 can be written as:

$$ds^2_6 = \frac{L^2}{b^2} \left[q \, ds^2_{\mathbb{S}^4} + \big(dz^i + \epsilon^{ijk} A^j z^k \big)^2 \right] \, , \tag{4.2.4}$$

where A^i are the components of the non-abelian one-form connection corresponding to an $SU(2)$ instanton. In appendix 4.A.1 we give a more explicit representation of the ds^2_6 line element in terms of alternative coordinates.

The parameters b and q in (4.2.4) are constant squashing factors which encode the effect of the massless flavors in the backreacted metric. Indeed, when $q = b = 1$ the metric (4.2.4) is just the canonical Fubini-Study metric of the $\mathbb{CP}^3$ manifold with radius $2L$ in the so-called twistor representation. In this case (4.2.1) is the metric of the unflavored ABJM model at nonzero temperature. When the effect of the delocalized D6-brane sources is taken into account, the resulting metric is deformed as in (4.2.4). It was shown in [75] that at zero temperature the particular deformation written in (4.2.4) preserves $\mathcal{N} = 1$ SUSY.

The parameter b in (4.2.4) represents the relative squashing of the $\mathbb{CP}^3$ part of the metric with respect to the AdS_4 part due to the flavor, while q parameterizes an internal deformation

which preserves the $\mathbb{S}^4$-$\mathbb{S}^2$ split of the twistor representation of $\mathbb{CP}^3$. The explicit expressions for the coefficients q and b found in [75] are given in (3.6.83) and (3.3.48) respectively, where we drop the subindex 0 for simplicity in the rest of the thesis. Recall that $\hat{\epsilon}$ is given by (3.6.80) and η is given by (3.6.82). As functions of $\hat{\epsilon}$, the squashing parameters q and b are monotonically increasing functions, which approach the values $q \approx 5/3$ and $b \approx 5/4$ as $\hat{\epsilon} \to \infty$. Recall that another way to encode the loop effects of the massless sea quarks is the screening factor σ, defined in (3.8.157). Without flavors, $\sigma = 1$, and as $\hat{\epsilon} \to \infty$, $\sigma \to 0$. The *AdS* radius L can then expressed in terms of λ and the screening factor:

$$L^2 = \pi\sqrt{2\lambda}\,\sigma \ . \tag{4.2.5}$$

The complete solution of type IIA supergravity with sources is endowed with RR two- and four-forms F_2 and F_4, as well as with a constant dilaton ϕ (whose value depends on N, N_f, and k). Their explicit expressions are given in the appendix 4.A.1.

4.3 D6-brane probes with flux

We are interested in the dynamics of a massive quark holographically dual to a probe D6-brane with internal flux in the flavored ABJM background. The D6-brane extends along r and the three Minkowski directions and, wraps on the internal manifold a three-cycle topologically equivalent to $\mathbb{RP}^3 = \mathbb{S}^3/\mathbb{Z}_2$. This three-cycle will be parameterized by three angles α, β, and ψ, and will be characterized by an embedding function $\theta(r)$. With this embedding, the D6-brane then has an induced metric given by (for details see appendix 4.A.1):

$$\frac{ds_7^2}{L^2} = r^2 \left[-h(r)\,dt^2 + dx^2 + dy^2\right] + \frac{1}{r^2}\left(\frac{1}{h(r)} + \frac{r^2\,\theta'^{\,2}}{b^2}\right)dr^2$$

$$+ \frac{1}{b^2}\left[q\,d\alpha^2 + q\sin^2\alpha\,d\beta^2 + \sin^2\theta\,(d\psi + \cos\alpha\,d\beta\,)^2\right] , \tag{4.3.6}$$

where $0 \leq \alpha < \pi$, $0 \leq \beta, \psi < 2\pi$, and $\theta = \theta(r)$ determines the profile of the probe brane. Notice that the second line in (4.3.6) is the line element of a squashed $\mathbb{RP}^3$.

For a supersymmetric configuration at zero temperature, it is possible to use kappa symmetry to find an explicit solution for $\theta(r)$ (see the analysis in [75] and in appendix 4.A.3). But, in general we will have to numerically solve the equations of motion to find $\theta(r)$.

The thermodynamic properties of D6-branes embedded in this way were studied in detail in [136]. Here we will generalize some of these results by including worldvolume gauge fields. In particular, we will turn on a nontrivial flux on the internal cycle. In the rest of this section we will determine the form of this internal worldvolume flux which gives rise to a consistent solution of the brane equations of motion.

4.3.1 Internal flux

Since we are primarily interested in gapped, QH states, let us focus on Minkowski (MN) embeddings of the probe, in which the brane ends smoothly at a radial position r_* above the

horizon, *i.e.*, $r_* > r_h$. The D6-brane can cap off smoothly if, at the tip of the brane $r = r_*$, the angle θ reaches its minimal value $\theta = 0$ where an $\mathbb{S}^1 \subset \mathbb{RP}^3$ shrinks to zero. At the tip, the last term of (4.3.6) vanishes and the induced metric takes the form:

$$\frac{ds_7^2}{L^2}\bigg|_{r=r_*} = r^2 \left[-h_* dt^2 + dx^2 + dy^2 \right] + \frac{q}{b^2} \left[d\alpha^2 + \sin^2\alpha \, d\beta^2 \right] , \qquad (4.3.7)$$

where $h_* = h(r = r_*)$. From (4.3.7), we see that at the tip of the brane the coordinates α and β span a non-collapsing $\mathbb{S}^2_*$. As in other probe-brane QH models [161, 162], we want to turn on a flux of the worldvolume gauge field F on this non-shrinking sphere.

Of course, this flux must be quantized appropriately. We will adopt the following quantization condition:

$$\frac{1}{2\pi\alpha'} \int_{\mathbb{S}^2_*} F = \frac{2\pi M}{k} , \qquad M \in \mathbb{Z} . \qquad (4.3.8)$$

Notice that, compared with the ordinary flux quantization condition of the worldvolume gauge field, we are considering in (4.3.8) M/k fractional units of flux. In appendix 4.A.1 we verify that (4.3.8) is the correct prescription for the flux quantization by studying the background without massless flavors, *i.e.*, $N_f = 0$. In this case one can induce an internal F flux through $\mathbb{S}^2_*$ by switching on a flat Neveu-Schwarz B_2 field proportional to the Kähler form of $\mathbb{CP}^3$. Then, the quantization condition (4.3.8) follows from the fractional holonomy of B_2 along the $\mathbb{CP}^1$ cycle of $\mathbb{CP}^3$. In this setup the integer M is the number of fractional D2-branes and this configuration is dual to the ABJ model [61] with gauge group $U(N+M)_k \times U(N)_{-k}$. We also check in appendix 4.A.1 that M can be identified with the Page charge for fractional D2-branes.

Let us now write a concrete ansatz for the internal gauge field F. We will represent F in terms of a potential one-form A given by:

$$A = L^2 a(r) \left(d\psi + \cos\alpha \, d\beta \right) , \qquad (4.3.9)$$

where the L^2 factor is introduced for convenience and $a = a(r)$ is a function of the radial coordinate which determines the varying flux on the (α, β) two-sphere. The field strength $F = dA$ corresponding to (4.3.9) is simply:

$$F = L^2 \left[a'(r) \, dr \wedge \left(d\psi + \cos\alpha d\beta \right) - a(r) \sin\alpha \, d\alpha \wedge d\beta \right] , \qquad (4.3.10)$$

which restricted to $\mathbb{S}^2_*$ becomes:

$$F\big|_{\mathbb{S}^2_*} = -L^2 a_* \sin\alpha \, d\alpha \wedge d\beta , \qquad (4.3.11)$$

where $a_* \equiv a(r = r_*)$ is the value of the flux function at the tip. It follows that

$$\int_{\mathbb{S}^2_*} F = -4\pi L^2 a_* , \qquad (4.3.12)$$

and the condition (4.3.8) quantizes the values of a_* in the following way:

$$a_* = -\frac{\pi M}{kL^2} , \qquad M \in \mathbb{Z} . \qquad (4.3.13)$$

Let us denote the value of the flux function at the tip as:

$$a_* = -Q \ . \tag{4.3.14}$$

To write the quantization condition (4.3.13) in terms of physical quantities, recall that the *AdS* radius L can be written as in (4.2.5). Plugging this into (4.3.13), we find the following quantization condition for Q:

$$Q = \frac{\sqrt{\lambda}}{\sqrt{2}\,\sigma} \frac{M}{N} \ , \qquad M \in \mathbb{Z} \ . \tag{4.3.15}$$

Using the ansatz (4.3.10) for the internal flux, we can try to find a solution for a MN embedding of the probe D6-brane. In appendix 4.A.2 we check that (4.3.10), together with embedding ansatz corresponding to the induced metric (4.3.6), is a consistent truncation of the equations of motion of the probe.

At zero temperature, we have found an analytic solution for $\theta(r)$ and the flux function $a = a(r)$ which preserves two of the four supercharges of the $\mathcal{N} = 1$ superconformal background. The explicit calculations are performed in appendix 4.A.3 with the use of kappa symmetry. Here we just quote the result for $\theta(r)$ and $a(r)$:

$$\cos\theta(r) = \left(\frac{r_*}{r}\right)^b \tag{4.3.16}$$

$$a(r) = -Q\,(\cos\theta(r))^{\frac{1}{q}} = -Q\left(\frac{r_*}{r}\right)^{\frac{b}{q}}. \tag{4.3.17}$$

However, to realize the quantum Hall states we are interested in, we need to generalize our ansatz for the gauge field to include electric and magnetic fields, as well as the components dual to the charge density and current. We analyze this more general set up in the next subsection.

4.3.2   Background fields and currents

If we want a more general ansatz that includes background electric and magnetic fields and the associated charged current, we need to consider other components of the worldvolume gauge field. In the standard way, a magnetic field B and an electric field E are added by turning on the radial zero modes of F_{xy} and F_{0x}. The charge density is holographically related to F_{r0}, the longitudinal and Hall currents come from F_{rx} and F_{ry}. We therefore take the worldvolume gauge field to have the form:

$$A = L^2 \left[a_0(r)\,dt + (Et + a_x(r))\,dx + (B\,x + a_y(r))\,dy + a(r)\,(d\psi + \cos\alpha\,d\beta) \right] . \tag{4.3.18}$$

We can continue to use the induced metric ansatz given by (4.3.6), characterized by the embedding function $\theta = \theta(r)$.

Interestingly, due to our choice in (4.3.18) of the internal components of the gauge field, the dependence of the action on the internal angles of the $\mathbb{RP}^3$ cycle factorizes and consequently, we can consistently take the functions θ, a, a_0, a_x, and a_y to depend only on the

radial variable. After integrating over the internal angles α, β, and ψ, the DBI action of the D6-brane for our ansatz can be written as:

$$S_{DBI} = \int d^3x\, dt\, \mathcal{L}_{DBI} \,, \tag{4.3.19}$$

where the DBI lagrangian density $\mathcal{L}_{DBI}$ can be compactly written as:

$$\mathcal{L}_{DBI} = -\frac{8\pi^2\, L^7\, T_{D6}\, e^{-\phi}}{b^4} \frac{\sqrt{(B^2 + r^4)h - E^2}\,\sqrt{q^2 + b^4\, a^2}}{\sqrt{h}} \sqrt{\Delta} \,, \tag{4.3.20}$$

where T_{D6} is the D6-brane tension and the quantity Δ is defined to be

$$\Delta \;=\; b^4 r^2 h a'^2 \,+\, \sin^2\theta \left[b^2 + r^2 h\, \theta'^2 \right.$$
$$\left. +\frac{b^2 h}{E^2 - (B^2 + r^4)h}\left[(Ba_0' + Ea_y')^2 \,+\, r^4(a_0'^2 - ha_x'^2 + ha_y'^2) \right] \right] \,. \tag{4.3.21}$$

The Wess-Zumino term of the action is:

$$S_{WZ} = T_{D6} \int_{\mathcal{M}_7} \left(\hat{C}_7 \,+\, \hat{C}_5 \wedge F \,+\, \frac{1}{2}\hat{C}_3 \wedge F \wedge F \,+\, \frac{1}{6}\hat{C}_1 \wedge F \wedge F \wedge F \right) \,, \tag{4.3.22}$$

where, $\hat{C}_7$, $\hat{C}_5$, $\hat{C}_3$, and $\hat{C}_1$ are the pullbacks to the D6-brane of the RR gauge fields. All of these terms, except for $\hat{C}_5 \wedge F$, give non-vanishing contributions to the equations of motion.[1]

In the holographic setup, the charge density is encoded in the bulk by the radial electric displacement field $\tilde{D}(r)$, which is given by the derivative of the DBI lagrangian density with respect to the radial component of the physical electric field. From the ansatz (4.3.18), and taking into account the physical gauge field $A_{phys} = A/(2\pi\alpha')$, we find:

$$\tilde{D} = \frac{\partial \mathcal{L}_{DBI}}{\partial A'_{0,phys}} = \frac{2\pi\alpha'}{L^2}\frac{\partial \mathcal{L}_{DBI}}{\partial a_0'} \,. \tag{4.3.23}$$

We will set $\alpha' = 1$ from now on. In order to write $\tilde{D}(r)$ in a compact fashion, let us define a function $g(r)$ as:

$$g(r) = \frac{q + \eta}{2b(2 - q)} \frac{r^4\, h^{\frac{3}{2}}\, \sin^2\theta\, \sqrt{q^2 + b^4\, a^2}}{\sqrt{(B^2 + r^4)\, h - E^2}\,\sqrt{\Delta}} \,. \tag{4.3.24}$$

Then, one can show that:

$$\tilde{D}(r) = \frac{N\sigma^2}{4\pi} \tilde{d}(r) \,, \tag{4.3.25}$$

---

[1]One subtlety is that when the backreaction of the flavors is included, the RR field strength F_2 is not closed, implying that there is no well-defined RR potential C_1. However, the equations of motion derived from (3.17) only contain F_2 and therefore can be generalized to the unquenched case; see appendix 4.A.2 for details.

where σ is the screening factor defined in (3.8.157) and $\tilde{d}(r)$ is the function:

$$\tilde{d}(r) \equiv \frac{g}{h}\left[\left(1+\frac{B^2}{r^4}\right)a_0' + \frac{BE}{r^4}a_y'\right] . \tag{4.3.26}$$

The total charge density is obtained by taking the boundary value of $\tilde{D}(r)$, which is proportional to:

$$d = \lim_{r\to\infty} \tilde{d}(r) . \tag{4.3.27}$$

Similarly, the physical currents along the x and y directions are given by:

$$J_x = \frac{2\pi\alpha'}{L^2}\frac{\partial\mathcal{L}_{DBI}}{\partial a_x'} , \qquad \tilde{J}_y = \frac{2\pi\alpha'}{L^2}\frac{\partial\mathcal{L}_{DBI}}{\partial a_y'} . \tag{4.3.28}$$

One can readily prove that:

$$J_x = \frac{N\sigma^2}{4\pi}j_x , \qquad \tilde{J}_y = \frac{N\sigma^2}{4\pi}\tilde{j}_y , \tag{4.3.29}$$

where j_x turns out to be:

$$j_x = -g\,a_x' , \tag{4.3.30}$$

and $\tilde{j}_y(r)$ is:

$$\tilde{j}_y(r) \equiv g\left[-\left(1-\frac{E^2}{r^4 h}\right)a_y' + \frac{BE}{r^4 h}a_0'\right] . \tag{4.3.31}$$

The equations of motion for the probe are worked out in detail in appendix 4.A.2. In particular, J_x is constant in r (see (4.A.56)) and represents the longitudinal current parallel to the electric field. On the other hand, $\tilde{J}_y(r)$ depends on the holographic variable. The transverse current J_y is obtained as the value of $\tilde{J}_y(r)$ at the UV boundary $r\to\infty$ which, according to (4.3.28), is determined from the limit:

$$j_y = \lim_{r\to\infty} \tilde{j}_y(r) . \tag{4.3.32}$$

The radial dependence of $\tilde{d}$ and $\tilde{j}_y$ is determined by the a_0 and a_y equations of motion, (4.A.55) and (4.A.57). With the definitions introduced above, they can be simply written as:

$$\partial_r\,\tilde{d} = B(\eta\cos\theta\,a' - a\sin\theta\,\theta') , \tag{4.3.33}$$
$$\partial_r\,\tilde{j}_y = E(\eta\cos\theta\,a' - a\sin\theta\,\theta') . \tag{4.3.34}$$

In the unflavored case $\eta = 1$, these two equations (4.3.33) and (4.3.34) can be integrated once because their right-hand side is proportional to $\partial_r(a\cos\theta)$. Indeed, for the unflavored background $a_0(r)$ and $a_y(r)$ are cyclic and can be eliminated by performing the appropriate Legendre transformation.

This is not the case, however, when $\eta \neq 1$. We can formally integrate (4.3.33) and (4.3.34), defining the integral $I(r)$ as:

$$I(r) \equiv \int_r^\infty \left(\eta \cos\theta(\bar{r})\, a'(\bar{r}) - a(\bar{r}) \sin\theta(\bar{r})\, \theta'(\bar{r}) \right) d\bar{r} \tag{4.3.35}$$

$$= -\cos\theta(r)\, a(r) + (\eta - 1) \int_r^\infty \cos\theta(\bar{r})\, a'(\bar{r})\, d\bar{r} , \tag{4.3.36}$$

where we have integrated by parts to obtain the second line. Clearly,

$$\lim_{r \to \infty} I(r) = 0 , \tag{4.3.37}$$

and equations (4.3.33) and (4.3.34) can be written as

$$\tilde{d}(r) = d - B\, I(r) , \qquad \tilde{j}_y(r) = j_y - E\, I(r) . \tag{4.3.38}$$

Since a_0 and a_y are no longer cyclic, we need a new strategy to solve the equations of motion. Interestingly, there is still one conserved quantity associated with the equations of motion for A_0 and A_y. Eq. (4.A.60) can be recast as the radial independence of the quantity:

$$\Pi \equiv E\, \tilde{d}(r) - B\, \tilde{j}_y(r) . \tag{4.3.39}$$

Indeed, the equation $\partial_r \Pi = 0$ follows immediately from (4.3.33) and (4.3.34). This implies that Π can be written in terms of quantities evaluated at the boundary:

$$\Pi = E\, d - B\, j_y . \tag{4.3.40}$$

One can now try to write a_0', a_y', and a_x' in terms of the embedding function $\theta(r)$ and the flux function $a(r)$. Let us work this out in detail. First, we notice that one can invert Eqs. (4.3.26) and (4.3.31) and write a_0' and a_y' in terms of $\tilde{d}$ and $\tilde{j}_y$:

$$a_0' = \frac{h\left(1 - \frac{E^2}{r^4 h}\right) \tilde{d} + \frac{EB}{r^4} \tilde{j}_y}{g\left(1 + \frac{B^2}{r^4} - \frac{E^2}{r^4 h}\right)} , \qquad a_y' = \frac{\frac{EB}{r^4} \tilde{d} - \left(1 + \frac{B^2}{r^4}\right) \tilde{j}_y}{g\left(1 + \frac{B^2}{r^4} - \frac{E^2}{r^4 h}\right)} . \tag{4.3.41}$$

Notice that (4.3.41) are not actually solutions for a_0' and a_y' since g on the right-hand side is written in terms of these same fields. However, one can write an expression of g in terms of θ and a. Let us define X as:

$$X \equiv h\left(1 + \frac{B^2}{r^4} - \frac{E^2}{r^4 h}\right) \left[\left(\frac{q+\eta}{2b^2(2-q)}\right)^2 r^4 h(q^2 + b^4\, a^2) \sin^2\theta + h\tilde{d}^2 - j_x^2 - \tilde{j}_y^2 \right] - \frac{\left(hB\tilde{d} - E\tilde{j}_y\right)^2}{r^4} . \tag{4.3.42}$$

Then, after some calculation, we obtain:

$$g = \frac{\sin\theta\, \sqrt{X}}{\left(1 + \frac{B^2}{r^4} - \frac{E^2}{r^4 h}\right) \sqrt{b^2\, r^2\, h\, a'^2 + \sin^2\theta\, (1 + \frac{r^2}{b^2} h\, \theta'^2)}} . \tag{4.3.43}$$

Therefore, we have for a'_0, a'_x, and a'_y:

$$a'_0 = \frac{\sqrt{b^2\, r^2\, h\, a'^2 + \sin^2\theta\,(1 + \frac{r^2}{b^2}\, h\, \theta'^2)}}{\sin\theta\sqrt{X}}\left[h\left(1 - \frac{E^2}{r^4\, h}\right)\tilde{d} + \frac{EB}{r^4}\,\tilde{j}_y\right],$$

$$a'_x = -\frac{\sqrt{b^2\, r^2\, h\, a'^2 + \sin^2\theta\,(1 + \frac{r^2}{b^2}\, h\, \theta'^2)}}{\sin\theta\sqrt{X}}\left(1 + \frac{B^2}{r^4} - \frac{E^2}{r^4\, h}\right)j_x,$$

$$a'_y = \frac{\sqrt{b^2\, r^2\, h\, a'^2 + \sin^2\theta\,(1 + \frac{r^2}{b^2}\, h\, \theta'^2)}}{\sin\theta\sqrt{X}}\left[\frac{EB}{r^4}\,\tilde{d} - \left(1 + \frac{B^2}{r^4}\right)\tilde{j}_y\right]. \qquad (4.3.44)$$

The right-hand sides of (4.3.44) contain the radial functions $\tilde{d}$ and $\tilde{j}_y$, which in turn can be written as in (4.3.38) in terms of the constants d and j_y, and the integral $I(r)$ defined in (4.3.35).

In principle, we could use (4.3.44) to eliminate a'_0, a'_x, and a'_y from the equations of motion and to reduce the system to an effective problem for the functions $\theta(r)$ and $a(r)$. However, when $\eta \neq 1$, the functions $\tilde{d}(r)$ and $\tilde{j}_y$ depend non-locally on $\theta(r)$ and $a(r)$ and the corresponding reduced equations of motion would be a system of integro-differential equations for $\theta(r)$ and $a(r)$, which does not seem to be very easy to solve in practice. In the case in which there are no flavors backreacting on the geometry, *i.e.*, when $\eta = q = b = 1$, the integral $I(r)$ is just $I = -\cos\theta\, a$ and we can write $\tilde{d}$ and $\tilde{j}_y$ simply as $\tilde{d} = d + B\cos\theta\, a$ and $\tilde{j}_y = j_y + E\cos\theta\, a$. Thus, in this quenched case one can eliminate the gauge fields a_0, a_x, and a_y and reduce the problem to a system of two coupled, second-order differential equations for $\theta(r)$ and $a(r)$.

4.3.3 Minkowski embeddings

Having obtained the equations of motion for the D6-brane probe, the next step is to try to solve them. Although, as we will discuss in section 4.6, there are special analytic BPS solutions, in general we will have to resort to numerics.

Probe brane solutions are categorized into two classes by their IR behavior. The generic solution is a black hole embedding, in which the brane falls into the horizon; these correspond holographically to gapless, compressible states. In certain special circumstances, the brane can end smoothly at some $r = r_*$ when a wrapped cycle shrinks to zero size; these are Minkowski (MN) embeddings. MN solutions with broken parity correspond to gapped, quantum Hall states.

As discussed above in section 4.3.1, for a D6-brane probe in the flavored ABJM background, MN embeddings occur when $\theta(r_*) = 0$ for some r_*. In order to have a physical, finite-energy solution, the embedding $\theta(r)$ and the worldvolume gauge field F must be regular at the tip; that is, the induced metric (4.3.6) must be smooth, and a', a'_0, a'_x, a'_y must all be finite. Given that the function g (4.3.43) vanishes at the tip of the brane, the regularity of a'_0 and a'_y at the tip, combined with (4.3.26) and (4.3.31), implies that

$$\tilde{d}(r_*) = j_x = \tilde{j}_y(r_*) = 0 . \qquad (4.3.45)$$

We can interpret this condition to mean that there are no sources at the tip, which is physically sensible as the D6-brane could not support such a source. Suppose that $\tilde{d}(r_*) \neq 0$; this radial displacement field would have to be sourced, for example, by fundamental strings stretching from the horizon. Due to the shrinking cycle, the effective radial tension of the D6-brane vanishes at the tip, so these strings would then pull the D6-brane into the horizon, resulting in a black hole embedding.

The filling fraction ν is defined by

$$\nu \;=\; 2\pi\,\frac{D_{phys}}{B_{phys}}\;, \tag{4.3.46}$$

where the physical magnetic field B_{phys} is related to B by

$$B_{phys} \;=\; \frac{L^2}{2\pi}\,B \;=\; \sqrt{\frac{\lambda}{2}}\,\sigma\,B\;. \tag{4.3.47}$$

Combining (4.3.45) with (4.3.38) gives $d = BI(r_*)$, and the filling fraction for MN solutions is therefore

$$\nu \;=\; \frac{N\sigma}{\sqrt{2\lambda}}\,\frac{d}{B} \;=\; \frac{N\sigma}{\sqrt{2\lambda}}\,I(r_*)\;, \tag{4.3.48}$$

or, more explicitly using (4.3.36),

$$\nu \;=\; \frac{M}{2}\left[1 + (\eta - 1)\int_{r_*}^{\infty}\cos\theta(r)\,\frac{a'(r)}{Q}\,dr\right], \tag{4.3.49}$$

where M is the quantization integer and Q is minus the flow function at the tip (see (4.3.14)). Note that, (4.3.49) shows explicitly that, for a QH state with nonzero charge density, a nonzero flux is required. Moreover, ν is the sum of two contributions. The first term in (4.3.49) is proportional to the flux at the tip. The second term is only nonzero in the unquenched case $\eta \neq 1$ and contains an integral from the tip to the boundary. In terms of N_f and k, ν takes the form:

$$\nu \;=\; \frac{M}{2}\left[1 + \frac{3N_f}{4k}\int_{r_*}^{\infty}\cos\theta(r)\,\frac{a'(r)}{Q}\,dr\right]. \tag{4.3.50}$$

It follows that ν is a half-integer in the quenched case but gets corrections due to the massless sea quark loops in the unquenched Veneziano limit.

Numerically integrating the equations of motion, we have verified that there are MN solutions obeying the tip regularity conditions (4.3.45). At this point, we will be content with evidence for MN solutions with nonzero charge density d and magnetic field B. We will defer a more thorough study of the possible MN solutions to the future.

4.4 Conductivities

We are interested in analyzing the longitudinal and transverse conductivity of our configurations. In order to relate these quantities with the variables we have employed, let us point

out that the physical electric field E_{phys} is related to the quantity E used above as:

$$E_{phys} = \frac{L^2}{2\pi} E = \sqrt{\frac{\lambda}{2}} \sigma E .$$
(4.4.51)

The longitudinal and transverse conductivities σ_{xx} and σ_{xy} are defined in terms of J_x, $J_y \equiv \tilde{J}_y(r \to \infty)$ and E_{phys} as:

$$\sigma_{xx} = \frac{J_x}{E_{phys}} , \qquad \sigma_{xy} = \frac{J_y}{E_{phys}} .$$
(4.4.52)

The conductivities can be written as

$$\sigma_{xx} = \frac{N\sigma}{2\pi\sqrt{2\lambda}} \frac{j_x}{E} , \qquad \sigma_{xy} = \frac{N\sigma}{2\pi\sqrt{2\lambda}} \frac{j_y}{E} .$$
(4.4.53)

In the next two subsections we obtain formulas for σ_{xx} and σ_{xy} for the two types of embeddings (Minkowski and black hole) of the D6-brane probe.

4.4.1 Quantum Hall states

Let us now suppose that we have a Minkowski (MN) embedding. To compute the conductivities, we will adapt the method of [161, 162] but with some new twists. In particular, we use the invariance of Π under the the holographic flow. The conductivity comes directly from the condition (4.3.45) that there are no charge sources at the tip $r = r_*$. Since j_x in (4.3.30) must be equal to zero,

$$\sigma_{xx} = 0 .$$
(4.4.54)

Furthermore, (4.3.45) implies that Π vanishes at $r = r_*$ and, since it is radially invariant, $\Pi = 0$ at all values of r. From (4.3.40), we see that this is equivalent to $E\,d = B\,j_y$; the Hall conductivity is then:

$$\sigma_{xy} = \frac{N\sigma}{2\pi\sqrt{2\lambda}} \frac{j_y}{E} = \frac{N\sigma}{2\pi\sqrt{2\lambda}} \frac{d}{B} .$$
(4.4.55)

From (4.3.48), we find that

$$\sigma_{xy} = \frac{\nu}{2\pi} ,$$
(4.4.56)

which is exactly what one would expect for a QH state.

4.4.2 Gapless states

Let us now consider black hole embeddings, in which the D6-brane crosses the horizon at $r = r_h$. These embeddings correspond to gapless states. To compute the conductivity, we employ the pseudohorizon argument of [165] to Eq. (4.3.44). Let $r = r_p$ be the position of

the pseudohorizon, which is determined by the conditions:

$$h_p\left(r_p^4 + B^2\right) = E^2 ,$$

$$j_x^2 + \tilde{j}_y^2(r_p) = \left(\frac{q+\eta}{2b^2(2-q)}\right)^2 h_p\, r_p^4\, \sin^2\theta_p\,\left(q^2 + b^4\, a_p^2\right) + h_p\,\tilde{d}(r_p)^2 ,$$

$$E\,\tilde{j}_y(r_p) = B\,h_p\,\tilde{d}(r_p) , \tag{4.4.57}$$

where $h_p \equiv h(r_p)$, $\theta_p \equiv \theta(r_p)$, and $a_p \equiv a(r_p)$. It follows that the currents in x- and y-directions are given by:

$$j_x = \sqrt{h_p}\left[\left(1 - \frac{B^2 h_p}{E^2}\right)\tilde{d}^2(r_p) + \left(\frac{q+\eta}{2b^2(2-q)}\right)^2 r_p^4\,(q^2 + b^4\,a_p^2)\,\sin^2\theta_p\right]^{\frac{1}{2}} ,$$

$$j_y = \frac{B\,h_p}{E}\,d + E\left[1 - \frac{B^2 h_p}{E^2}\right]I(r_p) . \tag{4.4.58}$$

Notice that the previous expression involves the value of the integral I extended between the r_p and the boundary. Therefore, the conductivities are:

$$\sigma_{xx} = \frac{N\sigma}{2\pi\sqrt{2\lambda}}\frac{\sqrt{h_p}}{E}\left[\left(1 - \frac{B^2 h_p}{E^2}\right)\tilde{d}^2(r_p) + \left(\frac{q+\eta}{2b^2(2-q)}\right)^2 r_p^4\,(q^2 + b^4\,a_p^2)\,\sin^2\theta_p\right]^{\frac{1}{2}} ,$$

$$\sigma_{xy} = \frac{N\sigma}{2\pi\sqrt{2\lambda}}\left[\frac{B\,h_p}{E^2}\,d + \left[1 - \frac{B^2 h_p}{E^2}\right]I(r_p)\right] . \tag{4.4.59}$$

For small electric field, r_p is close to the horizon radius r_h. At first order in E^2 we can estimate r_p as:

$$r_p \approx r_h\left(1 + \frac{E^2}{3(r_h^4 + B^2)}\right) . \tag{4.4.60}$$

With this result we can write h_p approximately as:

$$h_p \approx \frac{E^2}{r_h^4 + B^2} . \tag{4.4.61}$$

Applying these results to (4.4.59), we obtain the linear conductivities:

$$\sigma_{xx} \approx \frac{N\sigma}{2\pi\sqrt{2\lambda}}\frac{r_h^2}{r_h^4 + B^2}\left[\tilde{d}_h^2 + \left(\frac{q+\eta}{2b^2(2-q)}\right)^2 (r_h^4 + B^2)\,(q^2 + b^4\,a_h^2)\,\sin^2\theta_h\right]^{\frac{1}{2}} , \tag{4.4.62}$$

$$\sigma_{xy} \approx \frac{N\sigma}{2\pi\sqrt{2\lambda}}\left[\frac{B\,\tilde{d}_h}{r_h^4 + B^2} + I_h\right] , \tag{4.4.63}$$

where $I_h \equiv I(r_h)$ is defined in (4.3.36).

These conductivities are analogous to the conductivities found in the metallic phases of other similar probe brane models, for example [166, 161, 162]. One important difference is that here, the unquenched sea quarks reduce the conductivity by the screening factor σ.

The longitudinal conductivity (4.4.62) receives contributions from two sources: the first term under the square root is due to the charge density at the horizon $\tilde{d}_h$, and the other term can be interpreted as being due to thermal pair production. At vanishing magnetic field and nonzero charge density, σ_{xx} diverges as r_h^{-2}. Charge carriers can only scatter off the thermal bath, and at zero temperature, momentum conservation implies an infinite DC conductivity. For nonzero B, σ_{xx} vanishes in the zero-temperature limit, as implied by Lorentz invariance.

The Hall conductivity (4.4.63) is the sum of two terms, which appear to correspond to the contributions of two types of charge carriers: the charges at the horizon $\tilde{d}_h$, which are sensitive to the heat bath and contribute to σ_{xx}, and the charges $BI_h = d - \tilde{d}_h$, which are smeared radially along the D6-brane and do not interact with the dissipative heat bath at all. In the limit where $d/B \to I_h$, i.e., $\tilde{d} \to 0$, the Hall conductivity smoothly approach the results found above for the MN embedding (4.4.56). Varying the d/B from zero to I_h and plotting the conductivity on the $(\sigma_{xy}, \sigma_{xx})$-plane is expected to reproduce the behavior, seen also in [162], qualitatively similar to the semi-circle law experimentally observed in QH systems [167].

4.5   Boost invariance at zero temperature

At zero temperature and before adding an electric field, the system is Lorentz invariant. In probe brane constructions, the zero-temperature limit of a black hole embedding is often problematic. However, Minkowski embeddings are perfectly well defined in the zero-temperature limit since the brane never reaches the black hole horizon. One important feature of this model and others in its class [161, 162, 163], is that MN embeddings can occur at nonzero charge density.

Turning on an electric field in the x-direction breaks rotation invariance, and the full Lorentz symmetry is reduced to a (1+1)-dimensional subgroup: boosts in the y-direction form a set of $SO_+(1,1)$ transformations which rotate the electromagnetic field and the currents. When $h = 1$, the equations of motion studied in section 4.3.2 and appendix 4.A.2 are not modified under these transformations.

In terms of the boundary variables, a boost with rapidity γ acts as

$$\begin{pmatrix} E \\ B \end{pmatrix} \to \mathcal{M}_\gamma \begin{pmatrix} E \\ B \end{pmatrix}, \qquad \begin{pmatrix} d \\ j_y \end{pmatrix} \to \mathcal{M}_\gamma \begin{pmatrix} d \\ j_y \end{pmatrix}. \qquad (4.5.64)$$

where $\mathcal{M}_\gamma$ is the symmetric matrix:

$$\mathcal{M}_\gamma \equiv \begin{pmatrix} \cosh\gamma & \sinh\gamma \\ \sinh\gamma & \cosh\gamma \end{pmatrix}. \qquad (4.5.65)$$

The transverse conductivity σ_{xy} is invariant under the boost because it is determined only by the flux (4.4.56).

The boundary electromagnetic fields and currents are packaged holographically in the bulk worldvolume field strength F. From the transformation properties of F due to a boost in the bulk, one can reproduce the transformation (4.5.64) of E and B and see that the radial components of F transform as

$$\begin{pmatrix} F_{r0} \\ F_{ry} \end{pmatrix} = \begin{pmatrix} a'_0 \\ a'_y \end{pmatrix} \rightarrow \mathcal{M}_{-\gamma} \begin{pmatrix} a'_0 \\ a'_y \end{pmatrix} ; \tag{4.5.66}$$

therefore, the symmetry acts contravariantly on (a'_0, a'_y). Using Eqs. (4.3.26) and (4.3.31), one can demonstrate that the functions $\tilde{d}$ and $\tilde{j}_y$ also rotate via $\mathcal{M}_\gamma$, namely:

$$\begin{pmatrix} \tilde{d} \\ \tilde{j}_y \end{pmatrix} \rightarrow \mathcal{M}_\gamma \begin{pmatrix} \tilde{d} \\ \tilde{j}_y \end{pmatrix} , \tag{4.5.67}$$

which matches, for $r = \infty$, the transformation (4.5.64) of d and j_y. One can also check that the quantity Π defined in (4.3.39) is invariant.

Apart from the boosts, the equations of motion are also invariant under the two types of discrete operations, which are the elements of $O(1,1)$ not connected to the identity. The first of these operations is the electric field inversion $\mathcal{P}_E$, which acts as:

$$\mathcal{P}_E : \begin{pmatrix} E \\ B \end{pmatrix} \rightarrow \begin{pmatrix} -E \\ B \end{pmatrix} , \quad \begin{pmatrix} a'_0 \\ a'_y \end{pmatrix} \rightarrow \begin{pmatrix} a'_0 \\ -a'_y \end{pmatrix} , \quad \begin{pmatrix} \tilde{d} \\ \tilde{j}_y \end{pmatrix} \rightarrow \begin{pmatrix} \tilde{d} \\ -\tilde{j}_y \end{pmatrix} . \tag{4.5.68}$$

Under $\mathcal{P}_E$, the function Π changes its sign, *i.e.*, Π behaves as a pseudoscalar. However, the conductivity σ_{xy} is left invariant. Similarly, the equations of motion are invariant under a magnetic field inversion $\mathcal{P}_B$, defined as:

$$\mathcal{P}_B : \begin{pmatrix} E \\ B \end{pmatrix} \rightarrow \begin{pmatrix} E \\ -B \end{pmatrix} , \quad \begin{pmatrix} a'_0 \\ a'_y \end{pmatrix} \rightarrow \begin{pmatrix} -a'_0 \\ a'_y \end{pmatrix} , \quad \begin{pmatrix} \tilde{d} \\ \tilde{j}_y \end{pmatrix} \rightarrow \begin{pmatrix} -\tilde{d} \\ \tilde{j}_y \end{pmatrix} . \tag{4.5.69}$$

Under this transformation, Π again changes its sign and σ_{xy} is again invariant.

We can use the $O(1,1)$ symmetry to classify the different configurations in terms of the sign of the following quadratic forms

$$\mathcal{Q}_1 \equiv E^2 - B^2 , \qquad \mathcal{Q}_2 \equiv d^2 - j_y^2 , \qquad \mathcal{Q}_3 \equiv B\,d - E\,j_y , \tag{4.5.70}$$

which are left invariant by the $O(1,1)$ transformations. We will call solutions with $\mathcal{Q}_1 > 0$ "electric-like" , and those with $\mathcal{Q}_1 < 0$ "magnetic-like". We can also have solutions with $\mathcal{Q}_1 = 0$, which we call "null" solutions. Notice that an electric-like (magnetic-like) solution can be connected continuously to a solution with $B = 0$ ($E = 0$) and, an electric-like solution cannot be transformed into a magnetic-like one. We could similarly classify the solutions according to the sign of $\mathcal{Q}_2$ and $\mathcal{Q}_3$.

For MN embeddings, however, $\mathcal{Q}_2$ and $\mathcal{Q}_3$ are not independent but are rather proportional to $\mathcal{Q}_1$. The regularity at the tip (4.3.45) implies $d/B = j_y/E = I(r_*)$. From these relations, we find

$$\mathcal{Q}_2 = \mathcal{Q}_3 I(r_*) = -\mathcal{Q}_1 I(r_*)^2 . \tag{4.5.71}$$

In the next section we will find an analytic solution to the equations of motion for which the three $\mathcal{Q}_i$ invariants vanish. Intuitively, one would think that these null solutions have a large degree of symmetry. In particular, they are related to the $E = B = a_0' = a_y' = 0$ solution by the infinite boost $\mathcal{M}_{-\infty}$. Indeed, we will prove that these are BPS solutions preserving a fraction of the supersymmetry of the background.

4.6 The BPS solution

In this section we find a simple, exact MN solution of the zero-temperature equations of motion (4.A.55)-(4.A.59). This solution preserves one supercharge, or one quarter of the supersymmetry of the background. Accordingly, we will refer to this solution as the BPS solution.

Let us first consider the probe D6-brane in the absence of electric and magnetic fields and with $a_0' = a_y' = 0$. At zero temperature, we found a SUSY solution in section 4.3.1 for which the embedding function $\theta(r)$ and the flux function $a(r)$ satisfy the system of first-order BPS equations (4.A.76) and (4.A.84) derived in appendix 4.A.3:

$$r\,\theta' = b\cot\theta \,, \qquad\qquad \frac{a'}{a} = -\frac{b}{q\,r} \,. \tag{4.6.72}$$

We now generalize this supersymmetric solution to include electric and magnetic fields, as well as charge density and current, provided they satisfy a BPS condition:

$$E = B \,, \qquad\qquad a_0' = -a_y' \,. \tag{4.6.73}$$

In addition, we take $a_x' = 0$. Notice that, since $h = 1$, (4.6.73) implies (4.A.60) is trivially satisfied with the constant on the right-hand side equal to zero. Moreover, the equations of motion for a_0 (4.A.55) and a_y (4.A.57) become equivalent. The quantity Δ defined in (4.3.21) greatly simplifies and satisfies:

$$\left.\frac{\sqrt{q^2 + b^4\,a^2}}{\sqrt{\Delta}}\right|_{BPS} = \frac{q}{b} \,. \tag{4.6.74}$$

As we saw in section 4.4.1, for MN embeddings $\Pi = 0$. Combining this fact with (4.6.73), yields $\tilde{d}(r) = \tilde{j}_y(r)$, and in particular, $d = j_y$.

Using these results it is straightforward to verify that the equations (4.A.59) and (4.A.58) for $\theta(r)$ and $a(r)$ become:

$$\partial_r\left[r^4\,\sin^2\theta\,\theta'\right] - b^2\,r^2\left(1 + \frac{b^4}{q^2}a^2 - b^2r^2a'^2\right)\cot\theta - (3 - 2b)\,b\,r^2\sin\theta\cos\theta = 0 \,,$$

$$\partial_r\left[r^4\,a'\right] + \frac{b}{q}\left(3 - \frac{b}{q}\right)r^2\,a = 0 \,. \tag{4.6.75}$$

Note that these equations are just the same as in the $E = B = a_0' = a_y' = 0$ case. One can also check that the second-order equations (4.6.75) are satisfied if the first-order ones

in (4.6.72) are fulfilled. So, the solutions for $\theta(r)$ and $a(r)$ are just as in section 4.3.1 (see (4.3.16) and (4.3.17)):

$$\cos\theta = \left(\frac{r_*}{r}\right)^b , \tag{4.6.76}$$

$$a = -Q\left(\frac{r_*}{r}\right)^{\frac{b}{q}} = -Q\left(\cos\theta\right)^{\frac{1}{q}} . \tag{4.6.77}$$

It remains to solve for a_0. Its equation of motion (4.A.55) simplifies to:

$$\partial_r\left[r^2 \sin^2\theta\, a_0'\right] = -2B\frac{(2-q)\,b^3}{q^2}\frac{a\cos\theta}{r} . \tag{4.6.78}$$

Plugging in the solutions (4.6.76) for $\theta(r)$ and (4.6.77) for $a(r)$, it is now straightforward to integrate (4.6.78). Using the relation $q = b/(2-b)$, we get:

$$a_0' = \frac{1}{r^2}\frac{1}{1-\left(\frac{r_*}{r}\right)^{2b}}\left[\frac{2b^2(2-q)}{q(q+\eta)}d - (4-3b)(2-b)b\,Q\,B\left(\frac{r_*}{r}\right)^2\right] , \tag{4.6.79}$$

The regularity condition of a_0' at the tip of the brane fixes a relation between d, Q, and B:

$$d = \frac{(q+\eta)(2-b)}{2}Q\,B . \tag{4.6.80}$$

From the first equality of (4.3.48), the filling fraction ν for this SUSY solution is then:

$$\nu = \frac{N\sigma}{\sqrt{2\lambda}}\frac{d}{B} = (q+\eta)(2-b)\frac{M}{4} . \tag{4.6.81}$$

As we found in (4.3.49) for general MN solutions, the filling fraction is proportional to the internal flux. In addition, (4.6.81) can be rewritten as

$$\nu = \left[1 + \frac{3N_f}{8k}\left(1-\gamma_m\right)\right]\frac{M}{2} , \tag{4.6.82}$$

where $\gamma_m = b-1$ is anomalous dimension of the quark mass (see [75, 164]). Notice that γ_m depends on N_f/k and controls the coefficient of the contribution of the quarks loops to ν.

For the BPS solution, the integral $I(r)$ can be explicitly performed using the expressions (4.6.76) and (4.6.77) for $\theta(r)$ and $a(r)$. In particular,

$$I(r_*) = Q + (\eta-1)\int_{r_*}^{\infty}\cos\theta a'\, dr = \frac{q+\eta}{q+1}Q . \tag{4.6.83}$$

As a cross-check, we can compute the filling fraction using the second equality in (4.3.48):

$$\nu = \frac{N\sigma}{\sqrt{2\lambda}}I(r_*) = \frac{q+\eta}{q+1}\frac{M}{2} , \tag{4.6.84}$$

which using the relation $q = b/(2-b)$ (see (3.3.48)) matches (4.6.81).

We can also use the integrated formula for $I(r)$ to write explicit expressions for $\tilde{d}$ and $\tilde{j}_y$:

$$\tilde{d}(r) = \tilde{j}_y(r) = d - \frac{(q+\eta)(2-b)}{2} Q B \left(\frac{r_*}{r}\right)^2 . \tag{4.6.85}$$

Note that, in particular, $d = j_y$. Notice that the non-constant terms in $\tilde{d}$ and $\tilde{j}_y$ behave as r^{-2}, with no flavor corrections, which is probably a consequence of the non-anomalous dimensions of these currents.

4.6.1   Nonzero temperature generalization

Let us now consider the system at $T > 0$ (*i.e.*, when $h \neq 1$). It is possible to find a truncation of the general system of equations which defines a solution that can be regarded as the $T > 0$ generalization of the BPS system studied above. This truncation occurs when the following relations are satisfied:

$$E = B , \qquad\qquad a_0' = -h\, a_y' . \tag{4.6.86}$$

Notice that Eq. (4.A.60) continues to be trivially satisfied. Moreover, Eqs. (4.A.55) and (4.A.57) still reduce to a single equation which is now:

$$\frac{q+\eta}{2b(2-q)} \partial_r \left[\frac{\sqrt{q^2 + b^4\, a^2}\sqrt{\left(1 - \frac{1}{h}\right)B^2 + r^4}}{\sqrt{\Delta}} \sin^2\theta\, a_0' \right] - B(\eta \cos\theta\, a' - a \sin\theta\, \theta') = 0 , \tag{4.6.87}$$

and where Δ takes the value:

$$\Delta = b^4 r^2 h a'^2 + \sin^2\theta \left[b^2 + r^2 h\, \theta'^2 + b^2 \left(\frac{1}{h} - 1\right) a_0'^2 \right] . \tag{4.6.88}$$

The equations for the flux function $a(r)$ and the embedding function $\theta(r)$ can likewise be straightforwardly derived from the probe action.

4.7   Spectrum of mesons

The addition of flux in the internal directions induces the breaking of parity symmetry in the Minkowski worldvolume directions. In this section we explore the effect of this parity violation on the mass spectrum of quark-antiquark bound states which, in an abuse of language, we will refer to as mesons. The standard method to find the meson spectrum in the holographic correspondence is to analyze the normalizable fluctuations of the worldvolume gauge and scalar fields of the flavor brane.[2] Here we will restrict ourselves to analyzing the fluctuations of the gauge field A around the zero-temperature supersymmetric configuration with only the internal components of A are switched on. Accordingly, let us take the worldvolume gauge field as:

$$A = A^{(0)} + \delta A , \tag{4.7.89}$$

---

[2]See [152, 153, 168] for the calculation of the meson spectrum in the unflavored ABJM model.

where δA is assumed to be small and the unperturbed gauge potential is given by:

$$A^{(0)} = L^2 a(r) (d\psi + \cos\alpha \, d\beta) , \qquad (4.7.90)$$

with $a(r)$ being the flux function for the SUSY embedding (4.6.77). We will also assume that the embedding function $\theta(r)$ does not fluctuate and is given by (4.6.76). We will denote by f the first-order correction to the worldvolume field strength (*i.e.*, $f = d\delta A$). We will assume that f has only components along the AdS directions. Its components are:

$$f_{mn} = \partial_m \delta A_n - \partial_n \delta A_m , \qquad (4.7.91)$$

where the indices m and n run over the AdS directions. One can verify that these modes are a consistent truncation of the full set of fluctuations of the probe. In appendix 4.A.4 we obtain the equations of motion for δA by computing the first variation of the equations of motion for the probe. These equations can be written as the Euler-Lagrange equations for the following second-order effective lagrangian density:

$$\mathcal{L}^{(2)} = -\frac{1}{4} \frac{r^2}{(2-b)b^2} \left(1 + (2-b)^2 b^2 Q^2 (\cos\theta)^{\frac{2}{q}}\right) f^{mn} f_{mn} - \frac{Q}{4b \, L^4} (4 - 3b) \left(\cos\theta\right)^{\frac{2}{b}} \tilde{f}^{mn} f_{mn} , \qquad (4.7.92)$$

where the indices in f^{mn} are raised with the inverse of the open string metric $\mathcal{G}^{mn}$:

$$\mathcal{G}^{x^\mu x^\nu} = \frac{\eta^{\mu\nu}}{r^2 \, L^2} , \qquad \mathcal{G}^{rr} = \frac{r^2}{L^2} \frac{\sin^2\theta}{1 + (2-b)^2 \, b^2 \, Q^2 \, (\cos\theta)^{\frac{2}{q}}} , \qquad (4.7.93)$$

and the dual field $\tilde{f}^{mn}$ is defined as:

$$\tilde{f}^{mn} = \frac{1}{2} \epsilon^{mnpq} f_{pq} . \qquad (4.7.94)$$

Notice that the lagrangian density (4.7.92) is that of axion electrodynamics in AdS_4, with the axion depending on the holographic direction, showing explicitly the breaking of parity in AdS when the flux is turned on. The equation of motion derived from $\mathcal{L}^{(2)}$ is:

$$\partial_m \left[r^2 \left(1 + (2-b)^2 b^2 Q^2 (\cos\theta)^{\frac{2}{q}}\right) \mathcal{G}^{mp} \mathcal{G}^{nq} f_{pq} \right] - \frac{\Lambda}{L^4} \tilde{f}^{rn} = 0 , \qquad (4.7.95)$$

where $\Lambda = \Lambda(r)$ is the function written in (4.A.102). To solve (4.7.95) let us first choose the gauge in which $\delta A_r = 0$, and let us separate variables in the remaining components of δA as follows:

$$\delta A_\mu = \xi_\mu \, e^{ik_\nu x^\nu} \, R(r) , \qquad (\mu = 0, 1, 2) , \qquad (4.7.96)$$

where ξ_μ is a constant polarization vector. The gauge condition $\delta A_r = 0$, together with (4.7.95), imposes the following transversality condition on ξ_μ:

$$k \cdot \xi = \eta^{\mu\nu} k_\mu \xi_\nu = 0 . \qquad (4.7.97)$$

When they are normalizable, these fluctuations are dual to vector mesons, whose mass m is given by:

$$m^2 = -\eta^{\mu\nu} k_\mu k_\nu . \qquad (4.7.98)$$

In order to find the equation for $R(r)$, let us choose, without loss of generality, the Minkowski momentun k^μ as:

$$k^\mu = (\omega, k, 0) , \tag{4.7.99}$$

i.e., we choose our coordinates in such a way that the momentum is oriented along the x-direction. Notice that the mass is just $m = \sqrt{\omega^2 - k^2}$. The polarization transverse to (4.7.99) is:

$$\xi_\mu = \left(-\frac{k}{\omega} \xi_1 , \xi_1 , \xi_2 \right) , \tag{4.7.100}$$

where ξ_1 and ξ_2 are undetermined. Let us next consider the following complex combinations of ξ_1 and ξ_2:

$$\chi_\pm = \sqrt{1 - \frac{k^2}{\omega^2}} \xi_1 \pm i\xi_2 . \tag{4.7.101}$$

Then, as shown in appendix 4.A.4, we can solve the fluctuation equation (4.7.95) by taking $\chi_+ \neq 0$, $\chi_- = 0$ or $\chi_+ = 0$, $\chi_- \neq 0$ provided the radial function in the ansatz (4.7.96) satisfies the following ordinary differential equation:

$$\mathcal{O} R_\pm \pm m \Lambda R_\pm = 0 , \tag{4.7.102}$$

where $\mathcal{O}$ is the second-order differential operator defined in (4.A.102) and $R_+ = R_+(r)$ ($R_- = R_-(r)$) is the radial function for the solution with $\chi_+ \neq 0$ ($\chi_- \neq 0$). Notice that the χ_+ and χ_- modes are two helicity states which correspond to two different circular polarizations of the vector meson in the $x - y$ plane. They are exchanged by the parity transformation $\xi_2 \to -\xi_2$, as is obvious from their definition (4.7.101).

To find the mass spectrum of the mesons we must determine the values of m for which there exists a normalizable solution to (4.7.102). In general this must be done numerically by using the shooting technique, although we can make analytic estimates using the WKB approximation, which we describe in detail in appendix 4.A.4. The result is a tower of solutions with increasing masses which depend on the flux. These masses depend on the location of the tip r_*, which can be related to the mass of the quarks m_q as:

$$m_q = \sqrt{\frac{\lambda}{2}} \, \sigma \, r_* . \tag{4.7.103}$$

In Fig. 4.1 we illustrate the dependence on the flux of the mass of the lightest state, for the quenched background with $N_f = 0$. The spectra of the two helicity states are different. The mass splitting obviously vanishes at $Q = 0$ and changes with the amount of flux.

For $N_f = 0$ it is possible to compute analytically the meson mass splitting at first order in Q. Indeed, the fluctuation equation at first order in Q for the unflavored background is:

$$\partial_r \left[(r^2 - r_*^2)\partial_r R_\pm \right] + \frac{m^2}{r^2} R_\pm \pm 2mQ \frac{r_*^2}{r^3} R_\pm = 0. \tag{4.7.104}$$

For $Q = 0$, Eq. (4.7.104) can be solved analytically in terms of hypergeometric functions. Let $R_n(r)$ be the normalizable regular solutions of (4.7.104) for $Q = 0$; they are given by:

$$R_n(r) = \left(\frac{r_*}{r} \right)^{2n+1} F\left(-n - \frac{1}{2}, -n; 1; 1 - \frac{r^2}{r_*^2} \right) , \qquad n = 0, 1, \dots . \tag{4.7.105}$$
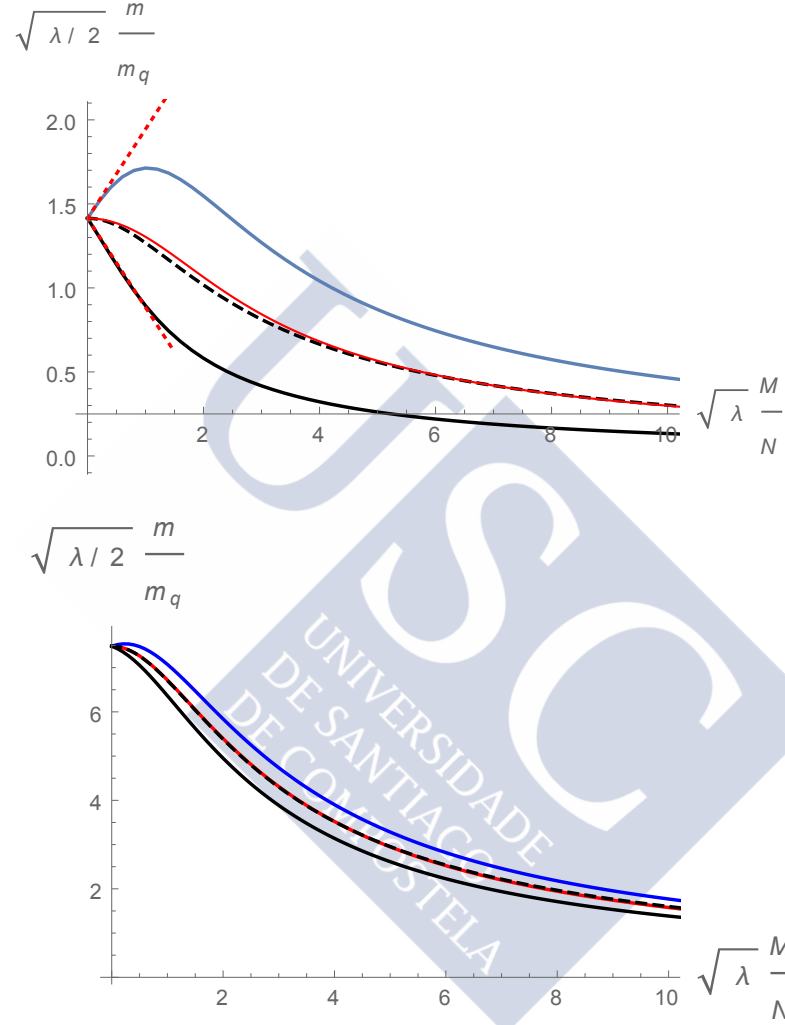
Figure 4.1: Meson masses in the quenched background as a function of the flux integer M for the lightest meson with excitation integer $n = 0$ (up) and for $n = 3$ (down). The upper blue (lower black) curves corresponds to the mode χ_- (χ_+). The intermediate red curve is the average of the two curves, and the dashed black curve is the WKB estimate (4.7.112). The two straight lines on the left panel are the first-order results written in (4.7.109).

The corresponding mass levels are:

$$\frac{m_n}{r_*} = \sqrt{2(n+1)(2n+1)} \, , \qquad\qquad n = 0, 1, \dots \, . \qquad (4.7.106)$$

Let us now solve (4.7.104) at first order in Q. We write:

$$R_{\pm,n}(r) = R_n(r) \pm Q \, \delta R_n(r) + \mathcal{O}(Q^2) \, , \qquad (4.7.107)$$

where the two signs are in correspondence with the ones in (4.7.104). The mass levels associated to $R_{\pm,n}$ will be denoted by $m_{\pm,n}$. The lightest regular normalizable modes at first order in Q are given by:

$$R_{\pm,0}(r) = \frac{r_*}{r} \pm Q \left[\frac{c}{r} + \frac{1}{\sqrt{2}} \left(\frac{r_*}{r}\right)^2 \left(1 - \frac{r}{r_*} \log\left(1 + \frac{r_*}{r}\right)\right) \right] + \mathcal{O}(Q^2) \, , \qquad (4.7.108)$$

with c being an integration constant. The masses for these modes are:

$$\frac{m_{\pm,0}}{r_*} = \sqrt{2} \mp \frac{3}{4} Q + \mathcal{O}(Q^2) \, . \qquad (4.7.109)$$

In Fig. 4.1 we plot these first-order results and we compare them with the numerical calculations. The first-order correction in the flux can similarly be obtained for the modes with $n \geq 1$, and the general form for the mass splitting is:

$$\frac{m_{-,n} - m_{+,n}}{r_*} = \frac{(2n+1)(3+4n)}{2(n+1)\pi} \left[\frac{\Gamma\left(n + \frac{1}{2}\right)}{\Gamma\left(n+1\right)} \right]^2 Q + \mathcal{O}(Q^2) \, . \qquad (4.7.110)$$

It follows from this expression that the first-order mass splitting becomes $4Q/\pi + \mathcal{O}(Q^2)$ as $n \to \infty$.

As shown in Fig. 4.1, the mass averaged over the two helicities is well approximated by the WKB method:

$$\frac{m_{+,n} + m_{-,n}}{2} \approx m_{WKB} \, . \qquad (4.7.111)$$

Let us write the WKB estimate of this helicity average in the unflavored background. By using the values of the WKB masses written in appendix 4.A.4, we have:

$$\frac{m_{+,n} + m_{-,n}}{2} \approx \frac{r_*}{F\left(-\frac{1}{2}, \frac{1}{2}; 1; -Q^2\right)} \sqrt{2(n+1)(2n+1)} \, . \qquad (4.7.112)$$

4.8   Discussion

In this chapter, we initiated a study of D6-brane probes with parity-breaking flux in the ABJM background with unquenched massless flavors. Minkowski embeddings of these probe branes holographically described massive fermions in quantum Hall states. The filling fraction was a half-integer in the quenched case, but received corrections when the dynamics of

the sea of massless flavors is included. The conductivities, both in the gapped Minkowski embeddings and in the metallic black hole ones, depended on the parity-breaking flux but also contained a contribution from the dynamical flavors. This was interpreted as an effect of the intrinsic disorder due to quantum fluctuations of the fundamental degrees of freedom.

Despite the complexity of the equations of motion we managed to obtain an explicit, analytic family of supersymmetric solutions with nonzero charge density, electric, and magnetic fields. For these gapped QH solutions, we obtained an analytic expression for the Hall conductivity, which includes the effects of quark loops. We also analyzed the residual $SO_+(1,1)$ boost invariance of the system at zero temperature; this is a powerful tool for generating non-supersymmetric solutions with general electric and magnetic fields starting from solutions with either $E{=}0$ or $B{=}0$. We also explored the effect of the parity violation on the computation of the meson spectrum. We restricted our analysis to the fluctuations of the gauge field around the zero-temperature supersymmetric configuration in which only the internal gauge field components were switched on.

There remain many open topics for further investigation. Although, we presented here a set of analytic, BPS solutions for a very specific set of parameters, more general solutions with nonzero temperature and arbitrary d, Q, E, and B still need to be studied, probably numerically. A thorough analysis of the thermodynamics and phase structure is needed to provide a complete understanding of this model. For example, we anticipate a phase transition as the temperature is increased from the MN to the black hole embeddings.[3]

The effects of internal flux and the sea of massless quarks are particularly interesting. And, we would also like to understand how the BPS solutions fit in to the complete picture.

Because there are so many possible parameters to vary, it makes sense to start by isolating one or two. A good first step could be to analyze, along the lines of [136], the thermodynamics of the D6-brane probe with only the internal flux, presented in section 4.3.2. In the absence of massless flavors, this system is essentially a probe D6-brane in the ABJ background, but with zero worldvolume gauge field. This is another system which deserves a detailed thermodynamic study.

Another interesting open problem is the study of flavor branes with internal flux in the ABJM background with unquenched massive quarks presented in chapter 3. Recall that the geometry found in chapter 3 is a running solution flowing between two AdS spaces, in which the control parameter is the mass of the sea quarks. One expects to find conductivities depending on the mass of the dynamical quarks, which interpolate between the values found here (for massless sea quarks) and the unflavored values (for infinitely massive quarks).

In this chapter we considered brane probes with electric and magnetic fields in their worldvolume and we have neglected the backreaction of these electromagnetic fields. Computing this backreaction is a very complicated task. One possible intermediate step could be considering the geometry dual to the non-commutative ABJM model, which was found in [175] by applying a TsT duality transformation. By adding internal flux to the probe branes we should be able to find Hall states similar to those found here [176].

We initiated a very limited fluctuation analysis in section 4.7, and a more thorough study

---

[3]For a massless probe brane embedding, this phase transition is related to the breaking of chiral symmetry. See *e.g.* [169, 170, 171, 172] for the holographic realization of (inverse) magnetic catalysis and [173, 174, 164] for the study of the effect of the dynamical flavors on magnetic catalysis.

is needed. One goal would be to compute the full meson dispersion about the BPS solution of section 4.6. The lightest neutral excitations of QH fluids are magneto-rotons, collective excitations whose minimum energy is at nonzero momentum. They have been detected in experiments, for example [177], and they have also been found in other holographic probe-brane QH models [178, 179]. Naturally, we would like to know if the spectrum of the model presented here also includes rotons.

Homogeneity-breaking instabilities seem to be a general feature of black hole embeddings in related brane models [180, 181, 182, 183], which are examples of the general type of instability described in [184]. In some cases, examples of spatially-modulated ground states have been found explicitly; for example, see [185, 186, 187, 188]. A thorough analysis of the quasi-normal mode spectrum is needed to determine whether such instabilities exists in this model. If so, the ABJM system, due to its symmetries and other special properties, might afford an ideal laboratory to study inhomogeneous phases.

Another interesting area to explore is alternative quantization of the D6-brane worldvolume gauge field. In a four-dimensional bulk, the gauge field can take Dirichlet, Neumann, or mixed boundary conditions in the UV, and these choices correspond to different boundary CFTs dual to strongly coupled anyon fluids in dynamical gauge fields. In particular, by changing the quantization as in [189, 190, 191], this ABJM system could be turned from a quantum Hall fluid into an anyon superfluid.

In the next chapter, we will focus on a D6-brane probe with density turned on, and all the rest of worldvolume gauge fields turned off. Of course, the equations of motion are a particular case of those presented in this chapter, but we will give a detailed analysis of the solutions. Besides, we give a detailed study of the fluctuations. The main feature that we have found is the interesting behavior of the quantum phase transitions involved.

4.A   Appendices

4.A.1   Details of the background geometry

In this appendix we specify the coordinate system we employ to represent the metric and forms of the background. Let us begin with the four-sphere part of the internal metric (4.2.4). Most of the following expressions are basically the ones presented in section (3.2) where we rewrite ξ in terms of a new angle α related by $\frac{2\xi}{1+\xi^2} = \sin \alpha$. Let ω^i ($i = 1, 2, 3$) be the $SU(2)$ left-invariant one-forms which satisfy $d\omega^i = \frac{1}{2}\,\epsilon_{ijk}\,\omega^j \wedge \omega^k$. Together with a new coordinate α, the ω^i's can be used to parameterize the metric of the four-sphere $\mathbb{S}^4$ as:

$$ds^2_{\mathbb{S}^4} \,=\, d\alpha^2 \,+\, \frac{\sin^2 \alpha}{4}\left[(\omega^1)^2 + (\omega^2)^2 + (\omega^3)^2\right]\,, \qquad (4.A.1)$$

where $0 \le \alpha < \pi$. The $SU(2)$ instanton one-forms A^i which fiber the $\mathbb{S}^2$ over the $\mathbb{S}^4$ in (4.2.4) can be written in these coordinates as:

$$A^i \,=\, -\sin^2\left(\frac{\alpha}{2}\right)\,\omega^i\,. \qquad (4.A.2)$$

Let us next parametrize the z^i coordinates of the $\mathbb{S}^2$ by means of two angles θ and φ ($0 \le \theta < \pi$, $0 \le \varphi < 2\pi$), namely:

$$z^1 = \sin\theta\,\cos\varphi\,, \qquad z^2 = \sin\theta\,\sin\varphi\,, \qquad z^3 = \cos\theta\,. \qquad (4.A.3)$$

Then, one can easily prove that the $\mathbb{S}^2$ part of the metric (4.2.4) can be written as:

$$\left(dx^i + \epsilon^{ijk}\,A^j\,z^k\right)^2 = (E^1)^2 + (E^2)^2\,, \qquad (4.A.4)$$

where E^1 and E^2 are the following one-forms:

$$
\begin{aligned}
E^1 &= d\theta + \sin^2\left(\frac{\alpha}{2}\right)\left[\sin\varphi\,\omega^1 - \cos\varphi\,\omega^2\right]\,, \\[2mm]
E^2 &= \sin\theta\left[d\varphi - \sin^2\left(\frac{\alpha}{2}\right)\omega^3\right] + \sin^2\left(\frac{\alpha}{2}\right)\cos\theta\left[\cos\varphi\,\omega^1 + \sin\varphi\,\omega^2\right]\,. \qquad (4.A.5)
\end{aligned}
$$

In order to write the explicit expression for F_2, we first define three new one-forms S^i ($i = 1, 2, 3$) as the following rotated version of the ω^i's:

$$
\begin{aligned}
S^1 &= \sin\varphi\,\omega^1 - \cos\varphi\,\omega^2\,, \\[2mm]
S^2 &= \sin\theta\,\omega^3 - \cos\theta\left(\cos\varphi\,\omega^1 + \sin\varphi\,\omega^2\right)\,, \\[2mm]
S^3 &= -\cos\theta\,\omega^3 - \sin\theta\left(\cos\varphi\,\omega^1 + \sin\varphi\,\omega^2\right)\,. \qquad (4.A.6)
\end{aligned}
$$

Next, we define the one-forms $\mathcal{S}^\alpha$ and $\mathcal{S}^i$ as:

$$\mathcal{S}^\alpha = d\alpha\,, \qquad \mathcal{S}^i = \frac{\sin\alpha}{2}\,S^i\,, \qquad (i = 1, 2, 3)\,, \qquad (4.A.7)$$

in terms of which the metric of the four-sphere is just $ds_{\mathbb{S}^4}^2 = (\mathcal{S}^\alpha)^2 + \sum_i(\mathcal{S}^i)^2$.

With these definitions, the ansatz for the RR two-form F_2 for the flavored background is

$$F_2 = \frac{k}{2}\left[E^1 \wedge E^2 - \eta\left(\mathcal{S}^\alpha \wedge \mathcal{S}^3 + \mathcal{S}^1 \wedge \mathcal{S}^2\right)\right]\,. \qquad (4.A.8)$$

Note that the two-form F_2 is not closed when $\eta \ne 1$; dF_2 is proportional to the charge distribution three-form of the flavor D6-branes. The RR four-form F_4 is:

$$F_4 = \frac{3k}{4}\,\frac{(\eta + q)b}{2 - q}\,L^2\,\Omega_{BH_4}\,, \qquad (4.A.9)$$

where Ω_{BH_4} is the volume-form of the four-dimensional black hole (4.2.2). The solution is completed by a constant dilaton ϕ given by

$$e^{-\phi} = \frac{b}{4}\,\frac{\eta + q}{2 - q}\,\frac{k}{L}\,. \qquad (4.A.10)$$

Let us now spell out the embedding of the D6-brane probe in the background geometry. We first represent the $SU(2)$ left-invariant one-forms ω^i in terms of three angles $\hat{\theta}$, $\hat{\varphi}$, and $\hat{\psi}$ as:

$$
\begin{aligned}
\omega^1 &= \cos\hat{\psi}\, d\hat{\theta} + \sin\hat{\psi}\, \sin\hat{\theta}\, d\hat{\varphi} \ , \\
\omega^2 &= \sin\hat{\psi}\, d\hat{\theta} - \cos\hat{\psi}\, \sin\hat{\theta}\, d\hat{\varphi} \ , \\
\omega^3 &= d\hat{\psi} + \cos\hat{\theta}\, d\hat{\varphi} \ .
\end{aligned}
\tag{4.A.11}
$$

In these coordinates our embedding is defined by the conditions:

$$
\hat{\theta}\,, \ \hat{\varphi} = \text{constant} \ ,
\tag{4.A.12}
$$

with the coordinate θ defined in (4.A.3) being a function of the radial coordinate r. The relation of the coordinates defined here with those used in (4.3.6) to write the internal part of the induced metric is as follows: The angle α here is equal to the one introduced in (4.A.1), while β and ψ are given by

$$
\beta = \frac{\hat{\psi}}{2} \ , \qquad\qquad \psi = \varphi - \frac{\hat{\psi}}{2} \ .
\tag{4.A.13}
$$

It is now easy to check that the pullback of the metric (4.2.1) to the worldvolume is, indeed, the line element written in (4.3.6).

Matching the unflavored ABJ model

Let us now explore our prescription (4.3.8) in the case of the unflavored model. The main point is that, when $N_f = 0$, the worldvolume gauge field for the supersymmetric configurations can be understood as induced by a flat NSNS B_2 field of the bulk, which is proportional to the Kähler form J of $\mathbb{CP}^3$. When the coefficient multiplying J is appropriately quantized, the corresponding supergravity solution is the dual of the ABJ theory with gauge group $U(N+M)_k \times U(N)_{-k}$. We will see that the rank difference M can be identified with the quantization integer in (4.3.8).

Let us begin our analysis by writing the Kähler form of $\mathbb{CP}^3$ in our variables:

$$
J = \frac{1}{4}\left(E^1 \wedge E^2 - \left(\mathcal{S}^\alpha \wedge \mathcal{S}^3 + \mathcal{S}^1 \wedge \mathcal{S}^2\right)\right) \ .
\tag{4.A.14}
$$

The pullback of J to the probe brane worldvolume is:

$$
\hat{J} = \frac{\theta' \sin\theta}{4}\, dr \wedge \left[d\psi + \cos\alpha\, d\beta \right] + \frac{\cos\theta \sin\alpha}{4}\, d\alpha \wedge d\beta \ ,
\tag{4.A.15}
$$

and, as claimed, it has the form written in (4.3.10) if we identify the flux function $a(r)$ with:

$$
a(r) = -Q\,\cos\theta(r) \ ,
\tag{4.A.16}
$$

where Q is a constant. Actually, one can check that the worldvolume gauge field F (4.3.10) for this unflavored case can be written in terms of the pullback of J as:

$$
F = 4\,L^2\,Q\,\hat{J} \ .
\tag{4.A.17}
$$

We will see below in appendix 4.A.3 that the relation (4.A.16) between the flux and embedding functions is dictated by supersymmetry when $N_f = 0$. Notice also that the flux function at the tip is just Q, as in (4.3.14).

In the DBI+WZ action for D-branes, the worldvolume gauge field F is always combined additively with the pullback of B_2. It follows that, in this case, the worldvolume flux can alternatively be thought of as induced by the following NSNS B_2 field:

$$B_2 = 4 Q L^2 J . \tag{4.A.18}$$

Notice that B_2 is a closed two-form, and it has the same form as in the proposed gravity dual of the ABJ model [61] with gauge group $U(N + M)_k \times U(N)_{-k}$, where Q is related to M. Actually, the integer M is determined by the discrete holonomy of B_2 on the $\mathbb{CP}^1$ cycle of the $\mathbb{CP}^3$ space, which is inherited from the holonomy of the three-dimensional three-form potential of the eleven-dimensional supergravity along the torsion cycle of the $\mathbb{S}^7/\mathbb{Z}_k$. Let us compute explicitly the integral of the two-form (4.A.18) along the $\mathbb{CP}^1$. In our coordinates (see [75]) the $\mathbb{CP}^1$ is obtained by keeping the coordinates of the $\mathbb{S}^4$ cycle fixed. Therefore, the pullback of J is just:

$$J_{|\mathbb{CP}^1} = \frac{1}{4} \sin \theta \, d\theta \wedge d\varphi , \tag{4.A.19}$$

and thus the integral of J along the $\mathbb{CP}^1$ is:

$$\int_{\mathbb{CP}^1} J = \pi . \tag{4.A.20}$$

It follows from (4.A.18) that:

$$\int_{\mathbb{CP}^1} B_2 = 4\pi L^2 Q . \tag{4.A.21}$$

Let us now use our quantization condition (4.3.13) and the identification (4.3.14) to write the period of B_2 in terms of k and the quantization integer M. We get:

$$\int_{\mathbb{CP}^1} B_2 = (2\pi)^2 \frac{M}{k} , \tag{4.A.22}$$

which is the fractional holonomy proposed in [61] for the gravity dual of the $U(N + M)_k \times U(N)_{-k}$ theory.

The coefficient Q can also be fixed by looking at the Page charge Q_4 for fractional D2-branes (D4-branes wrapped on a $\mathbb{CP}^1$ two-cycle), which is given by the following integral over the $\mathbb{CP}^2$ dual to the $\mathbb{CP}^1$ where the D4-branes are wrapped:

$$Q_4 = \frac{1}{(2\pi)^3} \int_{\mathbb{CP}^2} \left[F_4 + B_2 \wedge F_2 \right] . \tag{4.A.23}$$

We require that Q_4 is equal to our quantization integer M, which can then be interpreted as the number of fractional D2-branes. Taking into account (4.A.18) and that $F_2 = 2k J$ for this unflavored case, we get:

$$Q_4 = \frac{k L^2 Q}{\pi^3} \int_{\mathbb{CP}^2} J \wedge J . \tag{4.A.24}$$

To compute this integral we use the fact that the equation of the $\mathbb{CP}^2$ cycle in our coordinates is $\varphi = \theta = \pi/2$ (see appendix A in [75]), which implies:

$$J \wedge J_{|_{\mathbb{CP}^2}} = \frac{1}{16} \sin^2 \frac{\alpha}{2} \sin \alpha \, d\alpha \wedge \omega^1 \wedge \omega^2 \wedge \omega^3 \ . \tag{4.A.25}$$

Then, it follows that:

$$\int_{\mathbb{CP}^2} J \wedge J = \pi^2 \ . \tag{4.A.26}$$

Therefore,

$$Q_4 = \frac{k \, L^2 \, Q}{\pi} \ , \tag{4.A.27}$$

and the quantization condition $Q_4 = M$ coincides with the one obtained in (4.3.13) for $a_* = -Q$.

4.A.2   Probe brane equation of motion

Let us consider a Dp-brane probe propagating in a background of type II supergravity. Let g_{ij} denote the components of the induced metric on the worldvolume:

$$g_{ij} = g_{mn} \, \partial_i X^m \, \partial_j X^n \ , \tag{4.A.28}$$

where the X^n are coordinates of the ten-dimensional space and g_{mn} is the target space metric of the background. In what follows $m, n, \ldots$ will denote indices of the target space, whereas $i, j, \ldots$ will represent worldvolume indices. Let us denote by M the following matrix:

$$M = g + F \ , \tag{4.A.29}$$

where $F = dA$ is the worldvolume gauge field. Then, the action of a Dp-brane probe can be written as:

$$S_{D_p} = S_{DBI} + S_{WZ} \ , \tag{4.A.30}$$

where the DBI and WZ terms are:

$$S_{DBI} = -T_{Dp} \int_{\mathcal{M}_{p+1}} d^{p+1}\xi \, e^{-\phi} \sqrt{-\det M} \ , \qquad S_{WZ} = T_{Dp} \int_{\mathcal{M}_{p+1}} e^F \wedge C \ , \tag{4.A.31}$$

with T_{Dp} being the Dp-brane tension (from now on in this appendix we will take $T_{Dp} = 1$) and $C = \sum_r C_r$ is the sum of RR potentials. In order to write the equations of motion derived from this action following the analysis of section 2 of [192], let us consider the inverse $M^{-1} = [M^{ij}]$ of the matrix $M = [M_{ij}]$ and let us decompose M^{-1} in its symmetric and antisymmetric parts as:

$$M^{-1} = \mathcal{G}^{-1} + \mathcal{J} \ , \tag{4.A.32}$$

where $\mathcal{J} = [\mathcal{J}^{ij}]$ is the antisymmetric component of M^{-1} and $\mathcal{G}^{-1} = [\mathcal{G}^{ij}]$ is the inverse open string metric. Then, the equation of motion of the gauge field component A_j is [192]:

$$\partial_j \Big(e^{-\phi} \sqrt{-\det M} \, \mathcal{J}^{ji} \Big) = j^i \ , \tag{4.A.33}$$

where the source current for the gauge field j^i is given by:

$$j^i \equiv \frac{\delta S_{WZ}}{\delta A_i} \ . \tag{4.A.34}$$

Moreover, the equation for the scalar field X^m becomes [192]:

$$-\partial_i \Big(e^{-\phi} \sqrt{-\det M} \, \mathcal{G}^{ij} \, \partial_j \, X^n \, g_{nm} \Big)$$

$$+\sqrt{-\det M} \left(\frac{e^{-\phi}}{2} \mathcal{G}^{ji} \, \partial_i \, X^n \, \partial_j \, X^p \, g_{np,m} - e^{-\phi} \, \partial_m \phi \right) = j_m \ , \tag{4.A.35}$$

where the source for the scalar X^m is:

$$j_m \equiv \frac{\delta S_{WZ}}{\delta X^m} \ . \tag{4.A.36}$$

Currents for the D6-brane

Let us write the form of the currents for the case of a D6-brane probe. In this case, the WZ term of the action is:

$$S_{WZ} = \int_{\mathcal{M}_7} \left(\hat{C}_7 + \hat{C}_5 \wedge F + \frac{1}{2} \hat{C}_3 \wedge F \wedge F + \frac{1}{6} \hat{C}_1 \wedge F \wedge F \wedge F \right) \ . \tag{4.A.37}$$

Let us perform a general variation of the worldvolume gauge field $F \to F + d(\delta A)$, under which S_{WZ} varies as:

$$\delta S_{WZ} = \int_{\mathcal{M}_7} \left(\hat{C}_5 + \hat{C}_3 \wedge F + \frac{1}{2} \hat{C}_1 \wedge F \wedge F \right) \wedge d(\delta A) \ . \tag{4.A.38}$$

In order to compute the current associated to the worldvolume gauge field, we use the fact that, for any odd-dimensional form $\mathcal{O}$, one has

$$\mathcal{O} \wedge d(\delta A) = d\mathcal{O} \wedge \delta A - d(\mathcal{O} \wedge \delta A) \ . \tag{4.A.39}$$

The total derivative generates a boundary term which vanishes since we are assuming that A is fixed at the boundary in the variational process.[4] Taking into account that, with our notation $F_4 = -dC_3$, we get:

$$\delta S_{WZ} = \int_{\mathcal{M}_7} \left(\hat{F}_6 - \hat{F}_4 \wedge F + \frac{1}{2} \hat{F}_2 \wedge F \wedge F \right) \wedge \delta A \ . \tag{4.A.40}$$

Then, the gauge current along the worldvolume direction i is given by the expression:

$$j^i \, d^7\xi = \left(\hat{F}_6 - \hat{F}_4 \wedge F + \frac{1}{2} \hat{F}_2 \wedge F \wedge F \right) \wedge d\xi^i \ . \tag{4.A.41}$$

---

[4]Note that, although we have chosen Dirichlet boundary conditions for A here, A can, in fact, have arbitrary mixed boundary conditions, corresponding to alternative quantization, as discussed in [189].

In order to compute the source current j_m for X^m, we should vary in (4.A.37) the scalars which enter the pullback of the RR potentials. It turns out that the final expression can be written in a rather simple form, which we will now spell out. Let $V = V^m \frac{\partial}{\partial X^m}$ be any vector field in target space. The interior product of V with a p-form ω is a $(p-1)$-form $\iota_V \omega$ defined as follows. Let ω be:

$$\omega = \frac{1}{p!} \omega_{n_1,\dots,n_p} \, dX^{n_1} \wedge \cdots \wedge dX^{n_p} \ . \tag{4.A.42}$$

Then, $\iota_V \omega$ is given by:

$$\iota_V \omega = \frac{1}{(p-1)!} V^m \, \omega_{m,m_1,\dots,m_{p-1}} \, dX^{m_1} \wedge \cdots \wedge dX^{m_{p-1}} \ . \tag{4.A.43}$$

Let $\iota_m \omega$ denote the interior product of ω and the vector $\partial / \partial X^m$:

$$\iota_m \omega \equiv \iota_{\frac{\partial}{\partial X^m}} \omega \ . \tag{4.A.44}$$

Then, the current j_m, corresponding to the scalar X^m, can be written as:

$$j_m \, d^7\xi = \widehat{\iota_m F_8} + \widehat{\iota_m F_6} \wedge F - \frac{1}{2} \widehat{\iota_m F_4} \wedge F \wedge F + \frac{1}{6} \widehat{\iota_m F_2} \wedge F \wedge F \wedge F \ , \tag{4.A.45}$$

where the hat denotes the pullback of the different $\iota_m F_r$ to the worldvolume. In (4.A.45) F_8 and F_6 are defined as Hodge duals of F_2 and F_4, respectively, i.e., $F_8 = - * F_2$ and $F_6 = - * F_4$.

Notice that we have derived the expressions of j^i and j_m from the action (4.A.37), where we have assumed the existence of the RR potentials C_r. In the case of backreacting flavor some Bianchi identities are violated and, as a consequence, some of the RR potentials do not exist. However, the currents j^i and j_m (and the corresponding equations of motion) only depend on the RR field strengths and their pullbacks, and then they can be generalized to the case in which we include the backreaction. This is the point of view we will adopt in what follows.

The equations of motion for our ansatz

We now write explicitly the equations of motion for the D6-brane with a gauge potential A as the one written in (4.3.18). We will also assume that the embedding is defined by the conditions (4.A.12) with $\theta = \theta(r)$ being a function of r to be determined. The set of worldvolume coordinates we will employ is:

$$\xi^i = (t, x, y, r, \alpha, \beta, \psi) \ , \tag{4.A.46}$$

where α, β, and ψ are the angles defined in (4.A.1) and (4.A.13). First of all, let us write the non-zero components of the worldvolume gauge field strength F corresponding to the potential (4.3.18):

$$F_{tx} = L^2 E \ , \qquad F_{xy} = L^2 B \ ,$$

$$F_{rt} = L^2 a_0' \ , \qquad F_{rx} = L^2 a_x' \ , \qquad F_{ry} = L^2 a_y' \ ,$$

$$F_{r\psi} = L^2 a' \ , \qquad F_{r\beta} = L^2 a' \cos\alpha \ , \qquad F_{\alpha\beta} = -L^2 a \sin\alpha \ , \tag{4.A.47}$$

where the prime denotes the derivative with respect to the radial variable. Notice that, in our ansatz, isotropy in the $x - y$ plane is explicitly broken by the electric field in the x-direction.

We will start by computing the different components of the currents appearing in (4.A.33) and (4.A.35). It is straightforward to prove that $\hat{F}_6 = 0$, and it therefore does not contribute to j^i and j_m. The non-vanishing components of the gauge current j^i are:

$$j^t = \frac{kL^4}{2} B \sin\alpha \, (\eta \cos\theta \, a' - a \sin\theta \, \theta') \, ,$$

$$j^y = \frac{kL^4}{2} E \sin\alpha \, (\eta \cos\theta \, a' - a \sin\theta \, \theta') \, ,$$

$$j^\psi = \frac{kL^4}{2} \sin\alpha \left(\frac{3b}{2} \frac{\eta + q}{2 - q} r^2 a - \eta \, (B \, a_0' + E \, a_y') \cos\theta \right) . \tag{4.A.48}$$

We now work out the current for the three transverse scalars. First we compute the interior products of F_8 with the tangent vectors along the three scalar directions $m = \theta, \hat{\theta}, \hat{\varphi}$. We find:

$$\widehat{\iota_\theta F_8} = -\frac{(3 - 2b)(q + \eta)q}{8b^3(2 - q)} kL^6 \sin\alpha \, r^2 \sin(2\theta) \, d^7\xi \, . \tag{4.A.49}$$

Moreover, the product of F_8 with the other two tangent vectors gives a result proportional to $\widehat{\iota_\theta F_8}$:

$$\widehat{\iota_{\hat{\theta}} F_8} = -\sin^2\left(\frac{\alpha}{2}\right) \sin(\beta - \psi) \widehat{\iota_\theta F_8} \, , \qquad \widehat{\iota_{\hat{\varphi}} F_8} = \sin\hat{\theta} \sin^2\left(\frac{\alpha}{2}\right) \cos(\beta - \psi) \widehat{\iota_\theta F_8} \, . \tag{4.A.50}$$

We already mentioned that F_6 does not contribute since its pullback is zero. It is also immediate to check that F_4 does not have components along the transverse scalars and will not contribute to j_m. The contribution of F_2 to j_θ is determined by:

$$\frac{1}{6} \widehat{\iota_\theta F_2} \wedge F \wedge F \wedge F = \frac{kL^6}{2} \sin\alpha \, a \sin\theta \, (B \, a_0' + E \, a_y') \, d^7\xi \, , \tag{4.A.51}$$

while the result for the other scalars are:

$$\widehat{\iota_{\hat{\theta}} F_2} \wedge F \wedge F \wedge F = -\sin^2\left(\frac{\alpha}{2}\right) \sin(\beta - \psi) \widehat{\iota_\theta F_2} \wedge F \wedge F \wedge F \, ,$$

$$\widehat{\iota_{\hat{\varphi}} F_2} \wedge F \wedge F \wedge F = \sin\hat{\theta} \sin^2\left(\frac{\alpha}{2}\right) \cos(\beta - \psi) \widehat{\iota_\theta F_2} \wedge F \wedge F \wedge F \, . \tag{4.A.52}$$

Notice that the proportionality factors in (4.A.50) and (4.A.52) are the same. Thus, the current for the scalar θ becomes:

$$j_\theta = -\frac{kL^6}{2} \sin\alpha \sin\theta \left(\frac{(3 - 2b)(q + \eta)q}{2 \, b^3(2 - q)} r^2 \cos\theta - a \, (B \, a_0' + E \, a_y') \right) . \tag{4.A.53}$$

Moreover, the other two components of j_m are:

$$j_{\hat{\theta}} = -\sin^2\left(\frac{\alpha}{2}\right) \sin(\beta - \psi) \, j_\theta \, , \qquad j_{\hat{\varphi}} = \sin\hat{\theta} \sin^2\left(\frac{\alpha}{2}\right) \cos(\beta - \psi) \, j_\theta \, . \tag{4.A.54}$$

Let us now finally write the equations of motion for the different gauge field components and scalars. We have to compute the different components of the antisymmetric tensor $\mathcal{J}^{ij}$, as well as the elements of the inverse open string metric $\mathcal{G}^{ij}$. This calculation is straightforward (although rather tedious in some cases) and we limit ourselves to give the final result for the equations. The equation of A_t is:

$$\frac{q+\eta}{2b(2-q)}\,\partial_r\left[\frac{\sqrt{h}\,\sqrt{q^2+b^4\,a^2}}{\sqrt{\Delta}\sqrt{(B^2+r^4)h-E^2}}\,\sin^2\theta\left[B(B\,a_0'\,+\,E\,a_y')\,+\,r^4\,a_0'\right]\right]$$

$$-B(\eta\,\cos\theta\,a'\,-\,a\,\sin\theta\,\theta')\,=\,0\ ,\tag{4.A.55}$$

where Δ is the quantity defined in (4.3.21). The equation for A_x can be integrated once (a_x is a cyclic variable) to give the following equation for a_x':

$$r^4\,h^{\frac{3}{2}}\,\sin^2\theta\,\frac{\sqrt{q^2+b^4\,a^2}\,a_x'}{\sqrt{\Delta}\,\sqrt{(B^2+r^4)h-E^2}}\,=\,\text{constant}\ .\tag{4.A.56}$$

The equation for A_y is also non-trivial and given by:

$$\frac{q+\eta}{2b(2-q)}\,\partial_r\left[\frac{\sqrt{h}\,\sqrt{q^2+b^4\,a^2}}{\sqrt{\Delta}\sqrt{(B^2+r^4)h-E^2}}\,\sin^2\theta\left[E(B\,a_0'\,+\,E\,a_y')\,-\,r^4\,h\,a_y'\right]\right]$$

$$-E(\eta\,\cos\theta\,a'\,-\,a\,\sin\theta\,\theta')\,=\,0\ .\tag{4.A.57}$$

It is easy to demonstrate that the equations for A_r, A_α, and A_β are trivially satisfied by our ansatz. The only non-trivial equation for the gauge field that remains to write is the one corresponding to A_ψ, which is:

$$\partial_r\left[\frac{r^2\,\sqrt{h}\,\sqrt{q^2+b^4\,a^2}\,\sqrt{(B^2+r^4)h-E^2}}{\sqrt{\Delta}}\,a'\right]-\frac{\sqrt{\Delta}\,\sqrt{(B^2+r^4)h-E^2}}{\sqrt{h}\,\sqrt{q^2+b^4\,a^2}}\,a$$

$$+3r^2a\,-\,\frac{2(2-q)\,\eta}{b(q+\eta)}\,(B\,a_0'\,+\,E\,a_y')\cos\theta=0\ .\tag{4.A.58}$$

Finally, one can prove that the three equations for the transverse scalars θ, $\hat{\theta}$, and $\hat{\varphi}$ are the same, namely:

$$\partial_r\left[\frac{r^2\,\sin^2\theta\,\sqrt{h}\,\sqrt{q^2+b^4\,a^2}\,\sqrt{(B^2+r^4)h-E^2}}{\sqrt{\Delta}}\,\theta'\right]$$

$$-\frac{\sqrt{q^2+b^4\,a^2}\,\sqrt{(B^2+r^4)h-E^2}}{\sqrt{h}\,\sqrt{\Delta}}\left[\Delta\,-\,b^4\,r^2\,h\,a'^2\right]\cot\theta$$

$$-(3-2b)\,q\,r^2\,\sin\theta\cos\theta\,+\,\frac{2b^3(2-q)}{q+\eta}\,a\,\sin\theta\,(B\,a_0'\,+\,E\,a_y')\,=\,0\ .\tag{4.A.59}$$

Eq. (4.A.56) allows us to eliminate a'_x, after which we have four second-order, coupled differential equations (4.A.55)-(4.A.59) for four radial functions of a_0, a_y, a, and θ. Solving this system in general is a quite formidable task. For this reason it is worth to look for simplifications and partial integrations. Notice that (4.A.55) and (4.A.57) present some electric-magnetic symmetry. Actually, by combining these equations one easily finds the following constant of motion:

$$\frac{r^4\,\sqrt{h}\,\sqrt{q^2+b^4\,a^2}}{\sqrt{\Delta}\,\sqrt{(B^2+r^4)h-E^2}}\,\sin^2\theta\,\left[E\,a'_0+h\,B\,a'_y\right]\;=\;\text{constant}\,,\qquad(4.A.60)$$

which could be used to eliminate a'_0 or a'_y from the system of equations. Moreover, in the unflavored case ($\eta=b=q=1$), the last two terms in (4.A.55) and (4.A.57) can be combined to construct the radial derivative of $a\cos\theta$, which leads to two constants of motion. In this unflavored case, a_0 and a_y are cyclic variables and can be eliminated.

4.A.3 Kappa symmetry analysis

The kappa symmetry matrix for a Dp-brane in the type IIA theory is given by:

$$d^{p+1}\,\zeta\,\Gamma_\kappa\;=\;\frac{1}{\sqrt{-\det(g+F)}}\,e^F\wedge X\,,\qquad(4.A.61)$$

where g is the induced metric, ζ^α ($\alpha=0,\ldots,p$) are a set of worldvolume coordinates and X is the polyform matrix:

$$X\;=\;\sum_n\,\gamma_{2n+1}\left(\Gamma_{11}\right)^{n+1}\,,\qquad(4.A.62)$$

with γ_{2n+1} being the $(2n+1)$-form whose components are the antisymmetrized products of the induced Dirac matrices γ_μ:

$$\gamma_{2n+1}\;=\;\frac{1}{(2n+1)!}\,\gamma_{\mu_1\cdots\mu_{2n+1}}\,d\zeta^{\mu_1}\wedge\cdots\wedge d\zeta^{\mu_{2n+1}}\,.\qquad(4.A.63)$$

In particular, we are interested in the case of a D6-brane with a flux across a (non-compact) four-cycle. The corresponding kappa symmetry matrix takes the form:

$$d^7\,\zeta\,\Gamma_\kappa\;=\;\frac{1}{\sqrt{-\det(g+F)}}\left[\gamma_{(7)}+F\wedge\gamma_{(5)}\,\Gamma_{11}+\frac{1}{2}\,F\wedge F\wedge\gamma_{(3)}+\frac{1}{6}\,F\wedge F\wedge F\wedge\gamma_{(1)}\,\Gamma_{11}\right]\,.$$
$$(4.A.64)$$

Let us now study the conditions imposed by kappa symmetry in the case in which the embedding is determined by the conditions (4.A.12), the worldvolume gauge field takes the form (4.3.18) with $a_x=0$, and the background is the zero-temperature supergravity solution of [75]. We begin by computing the pullbacks of the left-invariant $SU(2)$ one-forms ω^i of (4.A.11) in the α, β, and ψ variables:

$$\hat{\omega}^1=\hat{\omega}^2=0\,,\qquad\qquad\hat{\omega}^3=2d\beta\,,\qquad(4.A.65)$$

whereas those of $\mathcal{S}^i$ and E^i are:

$$\hat{\mathcal{S}}^\alpha = d\alpha \,, \qquad \hat{\mathcal{S}}^1 = 0 \,, \qquad \hat{\mathcal{S}}^2 = \sin\alpha \sin\theta \, d\beta \,, \qquad \hat{\mathcal{S}}^3 = -\sin\alpha \cos\theta \, d\beta \,,$$

$$\hat{E}^1 = \theta' \, dr \,, \qquad\qquad \hat{E}^2 = \sin\theta \, (d\psi + \cos\alpha \, d\beta) \,. \tag{4.A.66}$$

The pullbacks of the frame one-forms used in appendix B of [75] are:

$$\hat{e}^\mu = L\,r\,dx^\mu \,, \qquad\qquad \hat{e}^3 = \frac{L}{r}\,dr \,, \qquad\qquad \hat{e}^4 = \frac{\sqrt{q}}{b}\,L\,d\alpha \,,$$

$$\hat{e}^5 = 0 \,, \qquad \hat{e}^6 = L\,\frac{\sqrt{q}}{b}\,\sin\alpha \sin\theta \, d\beta \,, \qquad\qquad \hat{e}^7 = -L\,\frac{\sqrt{q}}{b}\,\sin\alpha \cos\theta \, d\beta \,,$$

$$\hat{e}^8 = \frac{L}{b}\,\theta' \, dr \,, \qquad \hat{e}^9 = \frac{L}{b}\,\sin\theta \, (d\psi + \cos\alpha \, d\beta) \,. \tag{4.A.67}$$

The corresponding induced gamma matrices become:

$$\gamma_{x^\mu} = L\,r\,\Gamma_\mu \,, \qquad\qquad \gamma_r = \frac{L}{r}\left(\Gamma_3 + \frac{r}{b}\theta'\Gamma_8\right) \,, \qquad\qquad \gamma_\alpha = L\,\frac{\sqrt{q}}{b}\,\Gamma_4 \,,$$

$$\gamma_\beta = L\,\frac{\sqrt{q}}{b}\,\sin\alpha \sin\theta \left[\Gamma_6 - \cot\theta\,\Gamma_7 + \frac{\cot\alpha}{\sqrt{q}}\,\Gamma_9\right] \,, \qquad\qquad \gamma_\psi = \frac{L\sin\theta}{b}\,\Gamma_9 \,. \tag{4.A.68}$$

Let us next compute the different contributions on the right-hand side of (4.A.64). First of all we notice that:

$$\gamma_{(7)} = d^7 \zeta \, \gamma_* \,, \tag{4.A.69}$$

where γ_* is the antisymmetrized product of all induced gamma matrices, namely:

$$\gamma_* = \gamma_{txyr\alpha\beta\psi} \,. \tag{4.A.70}$$

In terms of flat 10d matrices, γ_* can be written as:

$$\gamma_* = \frac{q}{b^3}\,L^7\,r^2\,\sin\alpha\,\sin^2\theta\,\Gamma_{012}\left(\Gamma_3 + \frac{r\,\theta'}{b}\Gamma_8\right)\Gamma_4\left(\Gamma_6 - \cot\theta\,\Gamma_7\right)\Gamma_9 \,. \tag{4.A.71}$$

With our notation, the supersymmetric embeddings are those that satisfy $\Gamma_\kappa \epsilon = -\epsilon$, where ϵ is a Killing spinor of the background. To implement this relation we impose that ϵ satisfies the projection corresponding to a D2-brane, *i.e.*,

$$\Gamma_{012}\,\epsilon = -\epsilon \,. \tag{4.A.72}$$

We also impose that ϵ satisfies the generic projections found in appendix B of [75] for a generic ABJM-like geometry (Eqs. (B.4) and (B.14) in [75]):

$$\Gamma_{47}\,\epsilon = \Gamma_{56}\,\epsilon = \Gamma_{89}\,\epsilon \,, \qquad\qquad \Gamma_{3458}\,\epsilon = -\epsilon \,. \tag{4.A.73}$$

From these projections it follows that:

$$\Gamma_{3469}\,\epsilon \;=\; -\Gamma_{8479}\,\epsilon \;=\; \epsilon \;, \qquad\qquad \Gamma_{3479}\,\epsilon \;=\; \Gamma_{8469}\epsilon \;=\; -\Gamma_{38}\,\epsilon\;. \tag{4.A.74}$$

Using (4.A.72) and (4.A.73), $\gamma_*\,\epsilon$ reduces to:

$$\gamma_*\,\epsilon \;=\; -\frac{q}{b^3}\,L^7\,r^2\,\sin\alpha\,\sin^2\theta\,\left[\,1\;+\;\frac{r\,\theta'}{b}\,\cot\theta\;+\;\left(\cot\theta\;-\;\frac{r\,\theta'}{b}\right)\Gamma_{38}\,\right]\epsilon\;. \tag{4.A.75}$$

From the condition that γ_* acts diagonally on ϵ (*i.e.*, γ_* acts on ϵ as a matrix proportional to the unit matrix), we get the following equation for the embedding angle:

$$r\,\theta' \;=\; b\,\cot\theta\;. \tag{4.A.76}$$

Moreover, when (4.A.76) and the projections (4.A.72) and (4.A.73) hold, $\gamma_{(7)}$ acts on ϵ as:

$$\gamma_{(7)}\,\epsilon \;=\; -d^7\,\zeta\,\frac{q}{b^3}\,L^7\,r^2\,\sin\alpha\,\epsilon\;. \tag{4.A.77}$$

Let us now study the terms in (4.A.64) that are linear in the worldvolume gauge field F. Let us write these terms as:

$$F \wedge \gamma_{(5)}\Gamma_{11} \;=\; d^7\zeta\,\left[\,\Gamma^{flux} + \Gamma^{Min}\,\right]\;, \tag{4.A.78}$$

where Γ^{flux} contains the contributions of the components of F along the internal directions and Γ^{Min} is the contribution of the components of F with legs along the Minkowski spacetime. It is readily verified that:

$$\Gamma^{flux} \;=\; \gamma_{txy}\,\Gamma_{11}\,\left[\,\gamma_{\alpha\beta}\,F_{r\,\psi}\;-\;\gamma_{\alpha\psi}\,F_{r\,\beta}\;+\;\gamma_{r\psi}\,F_{\alpha\beta}\,\right]\;. \tag{4.A.79}$$

The antisymmetric products of induced gamma matrices appearing on (4.A.79) can be straightforwardly computed from (4.A.68):

$$\gamma_{\alpha\beta} \;=\; \frac{q}{b^2}\,L^2\,\sin\alpha\,\sin\theta\,\left[\,\Gamma_{46}\;-\;\cot\theta\,\Gamma_{47}\;+\;\frac{\cot\alpha}{\sqrt{q}}\,\Gamma_{49}\,\right]\;,$$

$$\gamma_{\alpha\psi} \;=\; \frac{\sqrt{q}}{b^2}\,L^2\,\sin\theta\,\Gamma_{49}\;,$$

$$\gamma_{r\psi} \;=\; \frac{L^2}{b}\,\frac{\sin\theta}{r}\,\left[\,\Gamma_{39}\;+\;\frac{r\,\theta'}{b}\,\Gamma_{89}\,\right]\;, \tag{4.A.80}$$

On the other hand, Γ^{Min} is given by:

$$\Gamma^{Min} \;=\; L^2\left(E\,\gamma_{yr}\;-\;a_0'\,\gamma_{xy}\;+\;B\,\gamma_{tr}\;-\;a_y'\,\gamma_{tx}\right)\gamma_{\alpha\beta\psi}\,\Gamma_{11}\;. \tag{4.A.81}$$

The products of the induced Dirac matrices needed to compute Γ^{Min} are:

$$\gamma_{yr} \;=\; L^2\,\left[\,\Gamma_{23}\;+\;\frac{r}{b}\,\theta'\,\Gamma_{28}\,\right]\;, \qquad\qquad \gamma_{xy} \;=\; L^2\,r^2\,\Gamma_{12}\;,$$

$$\gamma_{tr} \;=\; L^2\,\left[\,\Gamma_{03}\;+\;\frac{r}{b}\,\theta'\,\Gamma_{08}\,\right]\;, \qquad\qquad \gamma_{tx} \;=\; L^2\,r^2\,\Gamma_{01}\;,$$

$$\gamma_{\alpha\beta\gamma} \;=\; L^3\,\frac{q}{b^3}\,\sin\alpha\,\sin^2\theta\,\left(\,\Gamma_{469}\;-\;\cot\theta\,\Gamma_{479}\,\right)\;. \tag{4.A.82}$$

A quick inspection of the different terms appearing in $\Gamma^{flux}\epsilon$ and $\Gamma^{Min}\epsilon$ reveals that, after using the projections (4.A.72) and (4.A.73), all terms contain products of Γ matrices and there are no terms containing the unit matrix. Therefore, to implement the condition $\Gamma_\kappa \epsilon = -\epsilon$ we should require that $\Gamma^{flux}\epsilon = \Gamma^{Min}\epsilon = 0$. By combining (4.A.79) and (4.A.80) we find that the product of Γ's contained in $\Gamma^{flux}\epsilon$ is:

$$\frac{1}{L^4}\left[\gamma_{\alpha\beta}\,F_{r\psi} - \gamma_{\alpha\psi}\,F_{r\beta} + \gamma_{r\psi}\,F_{\alpha\beta}\right]\epsilon = \frac{\sin\alpha\,\sin\theta}{b}\left(\frac{q}{b}\,a' + \frac{a}{r}\right)\Gamma_{46}\,\epsilon$$

$$-\frac{\sin\alpha}{b^2}\left(q\cos\theta\,a' + \sin\theta\,\theta'\,a\right)\Gamma_{47}\,\epsilon\;. \qquad (4.A.83)$$

After using the equation (4.A.76) satisfied by the angle $\theta(r)$, we find that $\Gamma^{flux}\epsilon = 0$ if the flux function $a(r)$ satisfies the following first-order equation:

$$\frac{a'}{a} = -\frac{b}{q\,r}\;. \qquad (4.A.84)$$

When $E = B = 0$ and $a'_0 = a'_y = 0$, Eqs. (4.A.76) and (4.A.84) guarantee that the embedding preserves two of the four supersymmetries of the background. If this is not the case, we should continue analyzing the remaining terms in Γ_κ. From (4.A.81) and (4.A.82) we get:

$$\frac{1}{L^7}\Gamma^{Min}\,\epsilon = \frac{q}{b^3}\sin\alpha\,\sin^2\theta\left[E\left(\Gamma_{23} + \frac{r}{b}\theta'\Gamma_{28}\right) + B\left(\Gamma_{03} + \frac{r}{b}\theta'\Gamma_{08}\right) - r^2\,a'_0\,\Gamma_{12} - r^2\,a'_y\,\Gamma_{01}\right]$$

$$\times\left(\Gamma_{469} - \cot\theta\,\Gamma_{479}\right)\Gamma_{11}\,\epsilon\;. \qquad (4.A.85)$$

After using the projections (4.A.73) we can write the action of Γ^{Min} on the Killing spinor ϵ as:

$$\frac{1}{L^7}\Gamma^{Min}\,\epsilon = \frac{q}{b^3}\sin\alpha\,\sin^2\theta\left[(E\Gamma_2 + B\Gamma_0)\left[1 + \frac{r\theta'}{b}\cot\theta + \left(\cot\theta - \frac{r\theta'}{b}\right)\Gamma_{38}\right]\Gamma_{11}\right.$$

$$\left. +\left(a'_0\,\Gamma_2 - a'_y\,\Gamma_0\right)r^2\,(1 + \cot\theta\,\Gamma_{38})\,\Gamma_{13}\,\Gamma_{11}\right]\epsilon\;. \qquad (4.A.86)$$

Using the BPS equation for θ (4.A.76), we can rewrite this last expression as:

$$\frac{1}{L^7}\Gamma^{Min}\,\epsilon = \frac{q}{b^3}\sin\alpha\left[(E\Gamma_2 + B\Gamma_0)\Gamma_{11} + \left(a'_0\Gamma_2 - a'_y\Gamma_0\right)r^2\sin^2\theta(1 + \cot\theta\,\Gamma_{38})\,\Gamma_{13}\Gamma_{11}\right]\epsilon\;. \qquad (4.A.87)$$

To ensure that $\Gamma^{Min}\,\epsilon = 0$ we first impose one of the following two extra projections on ϵ:

$$\Gamma_{02}\,\epsilon = \pm\epsilon\;. \qquad (4.A.88)$$

Notice that the conditions (4.A.88) are compatible with the projections (4.A.72) and (4.A.73) that we have imposed so far. We get

$$\frac{1}{L^7}\Gamma^{Min}\,\epsilon = \frac{q}{b^3}\sin\alpha\left[(E \mp B)\Gamma_2\Gamma_{11} + \left(a'_0 \pm a'_y\right)r^2\sin^2\theta(1 + \cot\theta\Gamma_{38})\,\Gamma_{213}\Gamma_{11}\right]\epsilon\;, \qquad (4.A.89)$$

and we have that $\Gamma^{Min} \epsilon = 0$ if E, B, a_0', and a_y' satisfy the following conditions:

$$E = \pm B , \qquad\qquad a_0' = \mp a_y' . \tag{4.A.90}$$

The two signs correspond to the two projections in (4.A.88) (in section 4.6 we have chosen the upper signs). Therefore, after imposing these conditions, we have

$$F \wedge \gamma_{(5)} \, \epsilon = 0 . \tag{4.A.91}$$

Notice that the extra projection (4.A.88) is only needed if the worldvolume gauge field has components along the Minkowski directions. Furthermore, one can check that the BPS equations (4.A.76), (4.A.84), and (4.A.90) and the projections (4.A.72), (4.A.73), and (4.A.88) imply that the remaning terms in Γ_κ act on ϵ as:

$$\frac{1}{2} F \wedge F \wedge \gamma_{(3)} \, \epsilon = -d^7 \, \zeta \, \frac{b \, L^7}{q} \, r^2 \, a^2 \, \sin\alpha \, \epsilon ,$$

$$\frac{1}{6} F \wedge F \wedge F \wedge \gamma_{(1)} \, \Gamma_{11} \, \epsilon = 0 . \tag{4.A.92}$$

It follows that:

$$d^7 \, \zeta \, \Gamma_\kappa \, \epsilon_{|BPS} = -\frac{d^7 \, \zeta}{\sqrt{-\det(g+F)}|_{BPS}} \, \frac{b \, L^7}{q} \, r^2 \left(\frac{q^2}{b^4} + a^2 \right) \sin\alpha \, \epsilon_{|BPS} , \tag{4.A.93}$$

and one can verify by computing the DBI determinant for the BPS configuration that, indeed, $\Gamma_\kappa \, \epsilon_{|BPS} = -\epsilon_{|BPS}$.

4.A.4 Fluctuations

To find the equations satisfied by the fluctuations at first order, we just compute the variation of the gauge field equations (4.A.33). One can check that the variation of $\det M$ is zero at first order and, as a consequence, the equations for the fluctuations are:

$$\partial_j \left(e^{-\phi} \sqrt{-\det M} \, \delta\mathcal{J}^{ji} \right) = \delta j^i . \tag{4.A.94}$$

We will restrict our attention to the case in which the only non-zero components of δA are those along the Minkowski directions,

$$\delta A = c_\mu(x^\nu, r) \, dx^\mu . \tag{4.A.95}$$

Notice that in (4.A.95) we are assuming that the c_μ's do not depend on the internal angles. It is then easy to verify that, when the index i corresponds to one of those internal directions, the equation of motion (4.A.94) is satisfied automatically by the ansatz (4.A.95). Moreover, when $i = r$ this equation reduces to the following Lorentz condition:

$$- \partial_0 c_0 + \partial_1 c_1 + \partial_2 c_2 = 0 . \tag{4.A.96}$$

Finally, when $i = \mu = 0, 1, 2$, Eq. (4.A.94) becomes:

$$\frac{b}{q} \, \partial_r \left(\frac{r^2 \sin^2 \theta \, \sqrt{q^2 + b^4 a^2}}{\sqrt{b^2 \sin^2 \theta + r^2(b^4 \, a'^2 \, + \, \sin^2 \theta \, \theta'^{\, 2})}} \partial_r \, c^\mu \right)$$

$$+ \frac{1}{bq} \frac{\sqrt{q^2 + b^4 a^2}}{r^2} \sqrt{b^2 \sin^2 \theta + r^2(b^4 \, a'^2 \, + \, \sin^2 \theta \, \theta'^{\, 2})} \, \partial^\nu \partial_\nu \, c^\mu$$

$$+ \frac{2b^2}{q} \frac{2 - q}{\eta + q} \left(\eta \cos \theta \, a' \, - \, a \sin \theta \theta' \right) \epsilon^{\mu \alpha \beta} \, \partial_\alpha \, c_\beta \, = \, 0 \, , \qquad (4.A.97)$$

where $c^\mu \, = \, \eta^{\mu\nu} \, c_\nu$ and, in our conventions, $\epsilon^{012} = 1$. To solve these equations, let us separate variables in $c_\mu(x^\nu, r)$ as:

$$c_\mu(x^\nu, r) \, = \, \xi_\mu \, e^{i k_\nu \, x^\nu} \, R(r) \, , \qquad (\mu = 0, 1, 2) \, , \qquad (4.A.98)$$

where ξ_μ is a constant polarization vector. It follows immediately from (4.A.96) that this vector satisfies the transversality condition (4.7.97).

In order to write the fluctuation equation for the radial function R in a compact form, let us define the differential operator $\mathcal{O}$, which acts on any function of the radial coordinate $R(r)$ as:

$$\mathcal{O} \, R \, \equiv \, \frac{b}{q} \, \partial_r \left[\frac{r^2 \sin^2 \theta \, \sqrt{q^2 + b^4 a^2}}{\sqrt{b^2 \sin^2 \theta + r^2(b^4 \, a'^2 \, + \, \sin^2 \theta \, \theta'^{\, 2})}} \partial_r \, R \right]$$

$$+ \frac{m^2}{bq} \frac{\sqrt{q^2 + b^4 a^2}}{r^2} \sqrt{b^2 \sin^2 \theta + r^2(b^4 \, a'^2 \, + \, \sin^2 \theta \, \theta'^{\, 2})} \, R \, , \quad (4.A.99)$$

where m is the mass of the dual meson (see (4.7.98)). We also define the function $\Lambda(r)$ as:

$$\Lambda(r) \, \equiv \, \frac{2b^2}{q} \frac{2 - q}{\eta + q} \left(\eta \cos \theta \, a' \, - \, a \sin \theta \theta' \right) . \qquad (4.A.100)$$

Then, the fluctuation equation can be written as:

$$\xi^\mu \, \mathcal{O} \, R \, + \, i \epsilon^{\mu \alpha \beta} \, k_\alpha \, \xi_\beta \, \Lambda R \, = \, 0 \, . \qquad (4.A.101)$$

Moreover, by substituting the values of the functions $\theta(r)$ and $a(r)$ which correspond to a SUSY embedding (4.6.76) and (4.6.77), we can greatly simplify the operator $\mathcal{O}$ and the function Λ. We get:

$$\mathcal{O} \, R \, = \, \partial_r \left[r^{2-2b} \left(r^{2b} - r_*^{2b} \right) \partial_r \, R \right] \, + \, \frac{m^2}{r^{2(3-b)}} \left(r^{2(2-b)} + (2-b)^2 \, b^2 \, Q^2 \, r_*^{2(2-b)} \right) R \, ,$$

$$\Lambda \, = \, 2b \, (2 - b) \, (4 - 3b) \, Q \, \frac{r_*^2}{r^3} \, . \qquad (4.A.102)$$

The three equations in (4.A.101) are coupled to each other. Let us see how they can be decoupled and reduced to a single ordinary differential equation. First of all, without loss of

generality we pick the Minkowski momentum as $k^\mu = (\omega, k, 0)$ with the meson mass being $m = \sqrt{\omega^2 - k^2}$. The transverse polarization has been written in (4.7.100) in terms of two unknown constants ξ_1 and ξ_2. For this parametrization of ξ_μ one can show that the equations for $\mu = 0$ and $\mu = 1$ in (4.A.101) are equivalent and that the remaining two equations are just:

$$\xi_1 \, \mathcal{O} \, R \, + \, i\omega \xi_2 \, \Lambda R \, = \, 0 \,,$$

$$\xi_2 \, \mathcal{O} \, R \, - \, i\omega \left[1 - \frac{k^2}{\omega^2} \right] \xi_1 \, \Lambda R \, = \, 0 \,. \tag{4.A.103}$$

To decouple these equations, let us consider the complex combinations $\chi_\pm$ defined in (4.7.101). Then, one can straightforwardly show that the system (4.A.101) can be reduced to the equations:

$$\chi_+ \left(\mathcal{O} \, R + m \, \Lambda \, R \right) \, = \, 0 \,, \qquad\qquad \chi_- \left(\mathcal{O} \, R - m \, \Lambda \, R \right) \, = \, 0 \,. \tag{4.A.104}$$

Obviously, $\chi_\pm$ can be eliminated from (4.A.104) when they are non-vanishing and the system can be reduced to two ordinary differential equations for the radial functions $R_\pm$, which can be written as:

$$\partial_r \left[r^{2-2b} (r^{2b} - r_*^{2b}) \partial_r R_\pm \right] + \left[\frac{m^2}{r^{2(3-b)}} \left(r^{2(2-b)} + (2-b)^2 \, b^2 \, Q^2 \, r_*^{2(2-b)} \right) \pm m \, \Lambda(r) \right] R_\pm = 0 \,. \tag{4.A.105}$$

To find the mass spectrum we must compute the values of m leading to a normalizable solution. This can be done numerically by the shooting technique. We present these numerical results for the two types of modes in Figs. 4.1 and 4.2.

WKB mass spectrum

When the mass m is large we can neglect the term containing the function Λ in the fluctuation equation (4.A.105), and we can estimate the mass levels by using the WKB method developed in [154]. Indeed, let us consider a differential equation of the form

$$\partial_r \left(f(r) \, \partial_r \, R \right) + m^2 \, h(r) \, R = 0 \,, \tag{4.A.106}$$

where m is the mass parameter and $f(r)$ and $h(r)$ are two arbitrary functions that are independent of m. We will assume that near $r \approx r_*$ and $r \approx \infty$ these functions behave as:

$$f \approx f_1 (r - r_*)^{s_1} \,, \qquad h \approx h_1 (r - r_*)^{s_2} \,, \qquad \text{as } r \to r_* \,,$$

$$f \approx f_2 \, r^{r_1} \,, \qquad h \approx h_2 \, r^{r_2} \,, \qquad \text{as } r \to \infty \,, \tag{4.A.107}$$

where f_i, h_i, s_i, and r_i are constants. Then, the mass levels for large quantum number n can be approximately written in terms of these constants as [154]:

$$m_{WKB}^2 = \frac{\pi^2}{\xi^2} (n+1) \left(n + \frac{|s_1 - 1|}{s_2 - s_1 + 2} + \frac{|r_1 - 1|}{r_1 - r_2 - 2} \right) \,, \qquad (n \geq 0) \,, \tag{4.A.108}$$
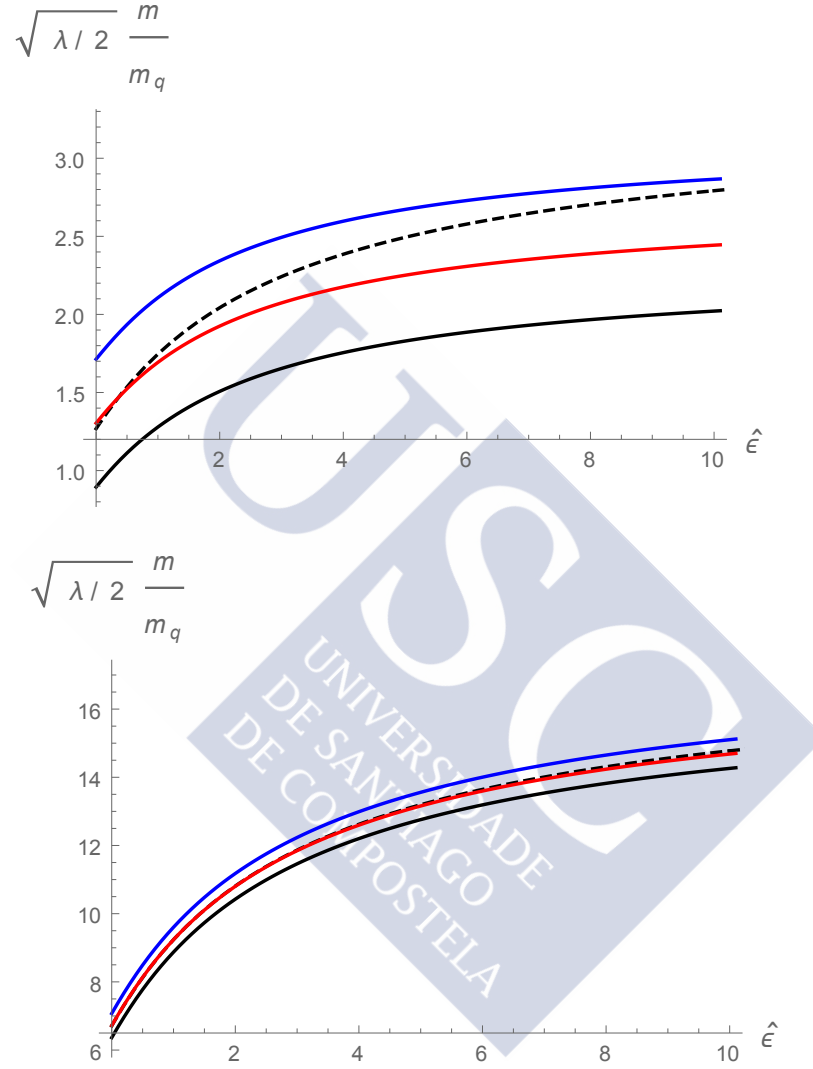
Figure 4.2: Meson masses in the unquenched background as a function of the flavor deformation parameter $\hat{\epsilon}$ for $\sqrt{\lambda}M/N = 1$ and two values of the excitation integer: $n = 0$ (left) and $n = 3$ (right). The upper blue (lower black) curve corresponds to the mode χ_- (χ_+). The intermediate red curve is the average of the two curves and the dashed black curve is the WKB estimate (4.A.113).

where ξ is the following integral:

$$\xi = \int_{r_*}^{\infty} dr \sqrt{\frac{h(r)}{f(r)}} . \tag{4.A.109}$$

In our case f and h are the functions:

$$f(r) = r^{2-2b}(r^{2b} - r_*^{2b}) ,$$

$$h(r) = \frac{1}{r^{2(3-b)}} \left(r^{2(2-b)} + (2-b)^2 b^2 Q^2 r_*^{2(2-b)} \right) . \tag{4.A.110}$$

The behavior of these functions at $r = r_*$ is characterized by the following values of the coefficients and exponents defined in (4.A.107):

$$f_1 = 2 b r_* , \qquad\qquad s_1 = 1 ,$$

$$h_1 = \frac{1 + (2-b)^2 b^2 Q^2}{r_*^2} , \qquad\qquad s_2 = 0 . \tag{4.A.111}$$

Similarly, for the behavior at large r we obtain:

$$f_2 = 1 , \qquad\qquad r_1 = 2 ,$$

$$h_2 = 1 , \qquad\qquad r_2 = -2 . \tag{4.A.112}$$

Therefore, the WKB mass spectrum is:

$$m_{WKB} = \frac{\pi}{\sqrt{2}\,\xi(b,Q)} \sqrt{(n+1)(2n+1)} , \tag{4.A.113}$$

where $\xi(b,Q)$ is the following integral:

$$\xi(b,Q) \equiv \frac{1}{r_*} \int_1^{\infty} \frac{dz}{z^{2(2-b)}} \frac{\sqrt{z^{2(2-b)} + (2-b)^2 b^2 Q^2}}{\sqrt{z^{2b} - 1}} . \tag{4.A.114}$$

By expanding in series the square root in the numerator and integrating term by term, we can express $\xi(b,Q)$ as the following series:

$$\xi(b,Q) = -\frac{1}{4 b r_*} \sum_{p=0}^{\infty} (-1)^p \left[(2-b)\, b\, Q \right]^{2p} \frac{\Gamma\left(p - \frac{1}{2}\right)}{p!} \frac{\Gamma\left(\frac{1+2p(2-b)}{2b}\right)}{\Gamma\left(\frac{1+2p(2-b)}{2b} + \frac{1}{2}\right)} . \tag{4.A.115}$$

Some particular values of the integral $\xi(b,Q)$ are:

$$\xi(b=1,Q) = \frac{\pi}{2r_*} F\left(-\frac{1}{2}, \frac{1}{2}; 1; -Q^2 \right) ,$$

$$\xi(b,Q=0) = \frac{\sqrt{\pi}}{r_*} \frac{\Gamma\left(\frac{2b+1}{2b}\right)}{\Gamma\left(\frac{b+1}{2b}\right)} . \tag{4.A.116}$$

Interestingly, for $b = 1$ and $Q = 0$ (the unflavored model without internal flux) the WKB formula for the mass levels is exact. Moreover, for large Q we can approximate $\xi(b, Q)$ as:

$$\xi(b, Q) \approx \frac{(2 - b)\, b\, Q}{r_*} \int_1^\infty \frac{dz}{z^{2(2-b)}\sqrt{z^{2b} - 1}} = \frac{\sqrt{\pi}\, Q}{r_*} \frac{(2 - b)\, b}{3 - b} \frac{\Gamma\left(\frac{3+b}{2b}\right)}{\Gamma\left(\frac{3}{2b}\right)} \, . \qquad (4.\text{A}.117)$$

It follows that, for fixed quantum number n, the WKB mass levels for large Q decrease as $1/Q$ according to the equation:

$$m_{WKB} \approx \frac{\sqrt{\pi}\, r_*}{\sqrt{2}\, Q} \frac{3 - b}{(2 - b)\, b} \frac{\Gamma\left(\frac{3}{2b}\right)}{\Gamma\left(\frac{3+b}{2b}\right)} \sqrt{(n + 1)(2n + 1)} \, . \qquad (4.\text{A}.118)$$

In Fig. 4.2 we compare the WKB estimates using (4.A.113) and the numerical results. The WKB method, however, is not valid at large values of Q, as it falls off the validity regime of [154]. Our numerical studies verified this expectation.
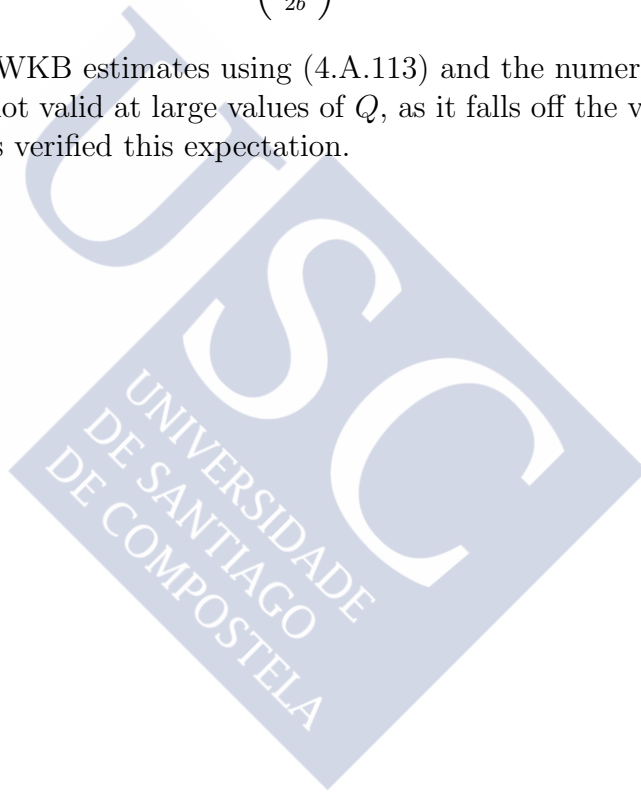
Chapter 5

Quantum phase transitions in the ABJM model

5.1 Introduction

Quantum phase transitions are transitions that happen at zero temperature and that are induced by quantum fluctuations. They occur when some control parameters are varied and tuned to critical values, at which the ground state of the system undergoes a macroscopic rearrangement and the energy levels develop a non-analytic behavior on these parameters. Although, the quantum phase transitions occur at zero temperature, they determine the behavior of the system at low temperature in the so-called quantum critical regime, which is a region of the phase diagram surrounding the quantum critical point (see, for example [193] [194] for reviews).

Strong coupling is a natal environment, where one expects quantum phase transitions. Therefore, a natural question is whether holography could be useful to search and characterize new types of quantum critical matter. Indeed, it is extremely important to develop new theoretical models which could shed light on the nature of quantum criticality and could serve to establish new paradigms to describe these phenomena.

In the recent years different holographic models displaying quantum phase transitions have been studied in the literature (see, for example [195, 196, 197, 198, 199, 200, 201, 202]). We are especially interested in top-down models, for which the field theory dual is clearly identified. In particular, we will deal with probe flavor D-branes in a gravitational background, that corresponds, in the field theory side, to adding fields on the fundamental representation of the gauge group which act as charge carriers. When N_f flavor D-branes are added to a geometry generated by N_c color branes with $N_f \ll N_c$, we can use the probe approximation and neglect the backreaction of the flavor branes on the geometry. This precludes the fundamentals being dynamical and they are treated as quenched in the field theory.

The worldvolume dynamics of the flavor branes is governed by an action which has two pieces. The first one is the standard Dirac-Born-Infeld (DBI) action, which contains a gauge field. The other one is the Wess-Zumino (WZ) action which couples the brane to the Ramond-Ramond potentials of the background. The effects from the latter typically

lead to far reaching consequences. In this probe brane setup it is rather simple to generate a configuration dual to a compressible state with non-zero charge density [203, 204, 205, 206, 207]. Indeed, the charge density is dual to a radial electric field on the worldvolume. When the density is non-vanishing all consistent embeddings reach the horizon, *i.e.* are black hole embeddings, whereas at zero density there could also be Minkowski embeddings which always stay outside the horizon.[1] It was shown in [195] for the D3-D7 and D3-D5 systems that a quantum phase transition takes place at zero temperature at the point where the charge density vanishes, which corresponds to the chemical potential being equal to the quark mass. This phase transition is of second order and is realized in the holographic dual as a topology change of the embedding (from the black hole to Minkowski). In [208] the critical exponents of the transition were found, corresponding to a non-relativistic scale invariant field theory with hyperscaling violation. These results were generalized in [209] to generic Dp-D$(p+4)$ and Dp-D$(p+2)$ intersections.

The aim of this chapter is to study the quantum phase transitions of brane probes in the gravity dual of the ABJM Chern-Simons matter theory, especially in the Veneziano limit. Recall that the ABJM theory (explained in detail in section 1.3.1) is an $U(N) \times U(N)$ Chern-Simons gauge theory in $2+1$ dimensions with levels $(k, -k)$ and bifundamental fields transforming in the $(N, \bar{N})$ and $(\bar{N}, N)$ representations of the gauge group. When N and k are large the theory admits a supergravity description in the ten-dimensional type IIA theory. The corresponding geometry is of the form $AdS_4 \times \mathbb{CP}^3$ with fluxes.

The flavors in the ABJM theory are fields transforming in the fundamental representations $(N, 1)$ and $(1, N)$ of the gauge group. In the holographic dual these flavors are introduced by means of D6-branes extended in AdS_4 and wrapping an $\mathbb{RP}^3$ cycle inside the $\mathbb{CP}^3$ internal manifold. In the probe approximation these holographic quarks have been reviewed in section 1.4.2. Moreover, by using the smearing technique (reviewed in section 1.4.1), when N_f is large, one can obtain simple analytic geometries encoding the effects of dynamical quarks in holography. The geometry generated by the backreaction of massless flavors in ABJM has been obtained in [75] at zero temperature and generalized in [136] to non-vanishing temperature. A detailed review on this solution was given in section 4.2, together with some details in appendix 4.A. The backreaction affects the ABJM geometry rather mildly since the metric differs from the unflavored one by constant squashing factors which depend on N_f. For massive quarks this construction was carried out in chapter 3.

In this chapter we probe the ABJM background (with and without massless dynamical quarks included) with a flavor D6-brane corresponding to a massive quark. We study the dynamics of this probe at zero temperature and non-vanishing charge density. This dynamics is governed by the DBI action, with the WZ term playing a fundamental role. We are interested in the phase structure of the system as the charge density is varied and, in particular, in analyzing the phase transition that occurs when the charge density is small.

The D6-brane embedding ansatz is a particular case of the one studied in section 4.3. Consequently, the equations of motion obtained in this chapter are a particular case of the ones of section 4.3. In chapter 4 we only solve the equations for a concrete case. In this chapter, we solve the equations of motion for a different particular case.

We first study the probe in the unflavored ABJM background. Working at zero tem-

---

[1]Suitable WZ terms would allow regular Minkowski embeddings even at non-zero charge density [161, 162].

perature, we find a continuous quantum phase transition at the point where the charge density vanishes. This transition is similar to the one that happens in the Dp-Dq systems in [208, 209] and corresponds to passing from a black hole to a Minkowski embedding. However, the scaling behavior of the probe near the critical point differs from the ones found in [208, 209]. Indeed, we find that the corresponding critical exponents are different and, in addition, our system displays multiplicative logarithmic corrections to the scaling behavior.
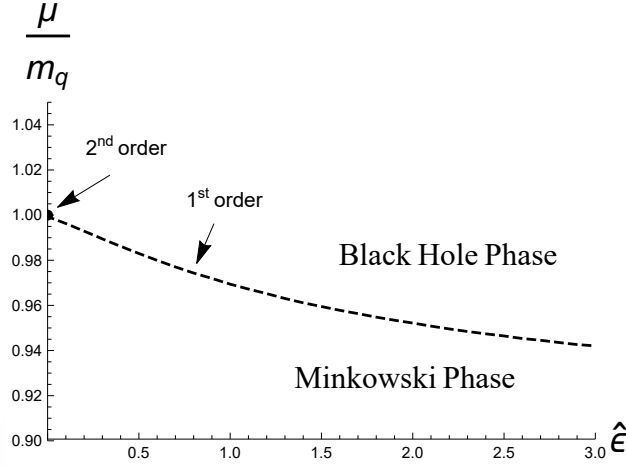
Figure 5.1: The phase diagram of the unquenched ABJM model at zero temperature separates two different domains. At high enough chemical potential to quark mass ratios, the system is in the so-called black hole phase, which corresponds to a metallic behavior. The lower domain stands for Minkowski phase, where the system is gapped to charged excitations and resembles an insulating phase. The two domains are separated by a curve of first order phase transitions, whose location depends on the amount of flavor in the background $\hat{\epsilon} \propto N_f$ (see (3.6.80)) for a given chemical potential. The curve ends at the second order critical point in the quenched limit $N_f \to 0$. Interestingly, the corresponding critical exponents characterizing the continuous phase transition exhibit multiplicative logarithmic corrections.

We also study the effects due to the presence of unquenched dynamical quarks in the background. In general, the inclusion of the flavor backreaction in holography is quite challenging. However, in the ABJM model the deformation of the geometry due to massless flavors seems quite mild and this gives us a unique opportunity to explore the different flavor effects. What we found below is that the influence on the phase transition of the unquenched case is not so moderate as their effects of the geometry could suggest. Indeed, we show below that the flavored black hole to Minkowski phase transition occurs at non-zero density and, moreover, it is of first order. We have been able to compute several quantities characterizing this discontinuous transition, such as its latent heat and the speed of sound close to the transition point.

The rest of this chapter is organized as follows. In section 5.2 we study the embeddings of flavor D6-branes in the unquenched massless flavored ABJM background, both at zero and non-zero temperature. Section 5.3 is devoted to the analysis of the zero temperature thermodynamics and to explore the quantum phase transitions in the unflavored and flavored

cases. In section 5.4 we determine the charge susceptibility and diffusion constants at non-zero temperature. In section 5.5 we analyze the fluctuations of the probe and, in particular, we calculate the speed of its zero sound mode. In section 5.6 we summarize our results and discuss possible future research directions. The chapter is completed with appendix 5.A.1 in which we carry out in detail the analysis of the fluctuations of the D6-brane.

5.2   Probes on the flavored ABJM

We are interested in analyzing the behavior of a flavor D6-brane probe in the background described in section 4.2 of chapter 4 (for details see also appendix 4.A). This flavor brane is extended along the AdS_4 coordinates (x^μ, r) and wraps a compact three-dimensional sub-manifold of the internal space. Let us recall the expression (4.3.6) of the induced metric on the worldvolume of the flavor D6-brane:

$$\frac{ds_7^2}{L^2} = r^2 \left[-h(r)\, dt^2 + dx^2 + dy^2 \right] + \frac{1}{r^2} \left(\frac{1}{h(r)} + \frac{r^2\, \theta'^2}{b^2} \right) dr^2$$

$$+ \frac{1}{b^2} \left[q\, d\alpha^2 + q\, \sin^2\alpha\, d\beta^2 + \sin^2\theta\, (\, d\psi\, +\, \cos\alpha\, d\beta\,)^2 \right], \qquad (5.2.1)$$

where α, β, and ψ are angles taking values in the range $0 \leq \alpha < \pi$, $0 \leq \beta, \psi < 2\pi$, and $\theta = \theta(r)$ is an angle which determines the profile of the probe brane. We want to deal with a system with non-zero baryonic charge density. Therefore, we should have a non-zero value of the tr component of the worldvolume gauge field strength $F = dA$. Accordingly, we will adopt the following ansatz:

$$\theta = \theta(r)\,, \qquad\qquad A = L^2\, A_t(r)\, dt\,. \qquad\qquad (5.2.2)$$

Recall that the D6-brane probe is governed by the standard DBI+WZ action:

$$S = S_{DBI} + S_{WZ}\,, \qquad\qquad (5.2.3)$$

where S_{DBI} and S_{WZ} are given by:

$$S_{DBI} = -T_{D6} \int_{\mathcal{M}_7} d^7\zeta\, e^{-\phi}\, \sqrt{-\det(g+F)}\,,$$

$$S_{WZ} = T_{D6} \int_{\mathcal{M}_7} \left(\hat{C}_7 + \hat{C}_5 \wedge F + \frac{1}{2}\hat{C}_3 \wedge F \wedge F + \frac{1}{6}\hat{C}_1 \wedge F \wedge F \wedge F \right). \quad (5.2.4)$$

In (5.2.4) g is the induced metric on the worldvolume and the $\hat{C}_p$'s are the pullbacks of the different RR potentials of the background. In the flavored ABJM background $dF_2 \neq 0$ and, therefore, the RR potential C_1 is not well-defined. In this unquenched case one should work directly with the equations of motion of the probe derived from S, which contain the RR field strengths F_p and do not contain the potentials (see appendix 4.A.2). Nevertheless, to determine the embedding corresponding to the ansatz (5.2.2), only the term with C_7 in (5.2.4) is relevant (the explicit expression of C_7 can be found in [75, 136]).

We will use the following system of worldvolume coordinates $\zeta^a = (x^\mu, r, \alpha, \beta, \psi)$. After integrating over the internal coordinates, we can write the action in the form:

$$S = \int d^3x\, dr\, \mathcal{L} , \tag{5.2.5}$$

where $\mathcal{L}$ is the lagrangian density of the probe, given by:

$$\mathcal{L} = -\mathcal{N}\, r^2\, \sin\theta \left[\sqrt{b^2(1 - A_t'^2) + r^2\, h\, \theta'^2} - b\sin\theta - r\cos\theta\, \theta' \right] . \tag{5.2.6}$$

Here and in the following, the prime denotes differentiation with respect to r. In (5.2.6) $\mathcal{N}$ is a constant given by:

$$\mathcal{N} = \frac{8\pi^2\, L^7\, T_{D6}\, e^{-\phi}}{b^4}\, q . \tag{5.2.7}$$

Notice that the ansatz 5.2.2 is a particular case of the ansatz for the embedding of the D6-brane considered in section 4.3 of chapter 4, for $E = B = a_x(r) = a_y(r) = a(r) = 0$. Consequently, the equations of motion obtained from the lagrangian 5.2.6 are a particular case of the equations of motion in section 4.3.

In the lagrangian (5.2.6) the variable A_t is cyclic and its equation of motion can be integrated once as:

$$r^2\, \sin\theta\, \frac{A_t'}{\sqrt{1 - A_t'^2 + \frac{r^2}{b^2}\, h\, \theta'^2}} = d , \tag{5.2.8}$$

where d is a constant, which is proportional to the charge density. This equation can be inverted to give:

$$A_t' = \frac{d}{b}\, \frac{\sqrt{b^2 + r^2\, h\, \theta'^2}}{\sqrt{d^2 + r^4 \sin^2\theta}} . \tag{5.2.9}$$

According to the standard AdS/CFT dictionary the chemical potential μ is identified with the value of A_t at the UV:

$$\mu = A_t(r \to \infty) . \tag{5.2.10}$$

For a black hole embedding one can write an expression for A_t as an integral over the radial variable r. Indeed, in this case we integrate (5.2.9) with the condition $A_t(r = r_h) = 0$, namely:

$$A_t(r) = \frac{d}{b} \int_{r_h}^r \frac{\sqrt{b^2 + \tilde{r}^2\, h\, \theta'^2}}{\sqrt{d^2 + \tilde{r}^4 \sin^2\theta}}\, d\tilde{r} . \tag{5.2.11}$$

Then, it follows that the chemical potential μ for a black hole embedding is:

$$\mu = \frac{d}{b} \int_{r_h}^\infty \frac{\sqrt{b^2 + r^2\, h\, \theta'^2}}{\sqrt{d^2 + r^4 \sin^2\theta}}\, dr . \tag{5.2.12}$$

Let us now write the equation of motion for $\theta(r)$:

$$\partial_r \left[\frac{r^4\, h\, \sin\theta}{\sqrt{1 - A_t'^2 + \frac{r^2}{b^2}\, h\, \theta'^2}}\, \theta' \right] - b\, r^2\, \cos\theta \left[(3 - 2b)\sin\theta + b\, \sqrt{1 - A_t'^2 + \frac{r^2}{b^2}\, h\, \theta'^2} \right] = 0 . \tag{5.2.13}$$

Using (5.2.9) to eliminate A_t', we can rewrite (5.2.13) as:

$$\partial_r \left[\frac{r^2\, h\, \sqrt{d^2 + r^4 \sin^2\theta}}{\sqrt{b^2 + r^2\, h\, \theta'^2}}\, \theta' \right] - r^2 \cos\theta \sin\theta \left[3 - 2b + \frac{r^2\, \sqrt{b^2 + r^2\, h\, \theta'^2}}{\sqrt{d^2 + r^4 \sin^2\theta}} \right] = 0 \ . \qquad (5.2.14)$$

Eq. (5.2.14) must be solved numerically, except in the case of vanishing temperature and density, where an analytic supersymmetric solution is available [75]. All solutions of (5.2.14) reach the UV with an angle which approaches asymptotically the value $\theta = \pi/2$. Actually, for large r the deviation of θ with respect to this asymptotic value can be represented as:

$$\frac{\pi}{2} - \theta(r) \sim \frac{m}{r^b} + \frac{c}{r^{3-b}} + \cdots \ , \qquad (5.2.15)$$

where b is the constant (depending of the flavor deformation parameter $\hat\epsilon$) defined in (3.3.48) and m and c are constants related to the quark mass and the condensate, respectively. The precise holographic dictionary for our probes has been worked out in [136]. For our purposes it is sufficient to recall that the physical quark mass m_q is proportional to $m^{\frac{1}{b}}$. This non-trivial exponent is related to the anomalous mass dimension $\gamma_m = b - 1$, which enters in the (holographic) Callan-Zymanzik equation [164].
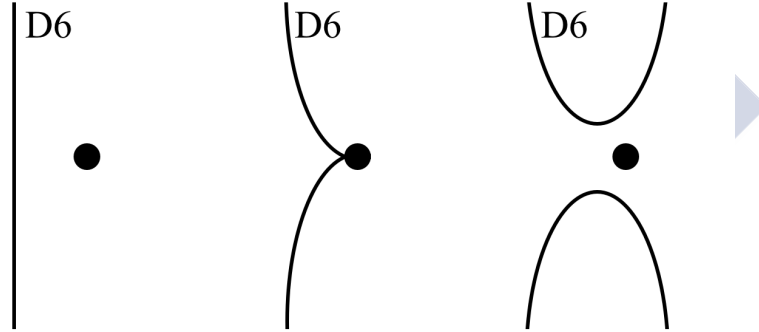

Figure 5.2: We sketch the three possible embeddings available in the model at non-zero chemical potentials at non-vanishing mass parameter at zero temperature. The left-most profile corresponds to Minkowski embeddings, where the D6-brane does not enter the Poincaré horizon, displayed as the black dot. The middle profile corresponds to that of a black hole embedding penetrating the horizon, while the right-most profile stands for D6-anti-D6-brane embeddings. This figure is adapted from the one in [195], in the context of a D3-D7 model, where a clean flat space interpretation can be given.

The different solutions of (5.2.14) are obtained by imposing suitable boundary conditions at the IR. We will study them in the next two subsections, starting with the embeddings at zero temperature. There are three different kinds of embeddings, sketched in Fig. 5.2. They are introduced one-by-one in the following subsection.
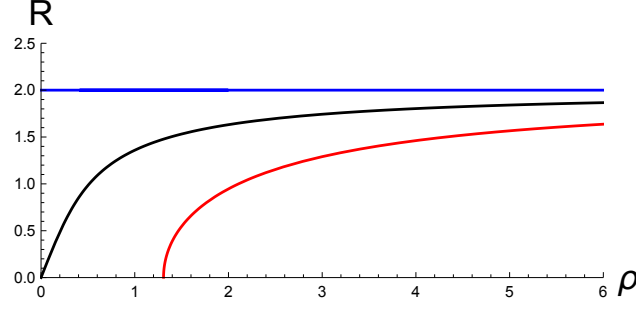
Figure 5.3: We depict the profiles of the three possible types of embeddings in the (ρ, R) coordinates defined in (5.2.18) at zero temperature. The top-most curve corresponds to the Minkowski embedding, while the middle curve entering in the Poincaré horizon corresponds to the black hole embedding. The bottom curve stands for one of branches of the brane-antibrane embeddings.
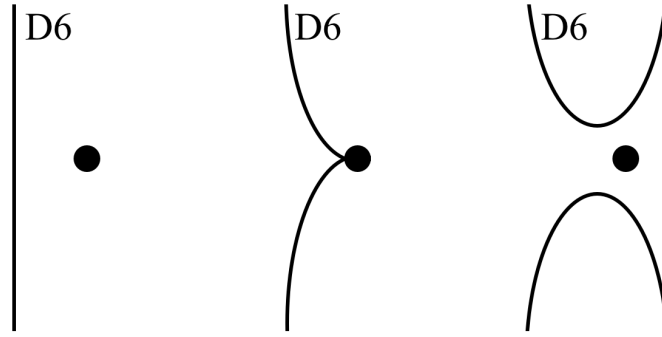

Figure 5.4: hola

5.2.1 Embeddings at zero temperature

Let us now consider eq. (5.2.14) for $T = 0$ (*i.e.* for $h = 1$). One can verify by numerical integration that (5.2.14) admits a family of solutions in which the embeddings reach the origin $r = 0$ at any given value of $\theta_0 = \theta(r = 0)$, quantities which we shall denote as initial angles. These solutions are called black hole embeddings as they are continuously connected with their $T \neq 0$ counterparts. Actually, one can solve (5.2.14) for $h = 1$ in a power series expansion near $r = 0$ as:

$$\theta(r) = \theta_0 + b(3 - 2b) \frac{\sin \theta_0 \cos \theta_0}{6d} r^2 + \cdots .\qquad(5.2.16)$$

These solutions can be found numerically by imposing the initial conditions $\theta(r = 0) = \theta_0$ and $\theta'(r = 0) = 0$. The mass parameter m of the embedding (determined by the value of $r^b \cos \theta$ at $r \to \infty$) is related to the initial angle θ_0. Given the embedding, the chemical potential can be obtained by evaluating the integral (5.2.12). When $\theta_0 \to \pi/2$ the mass approaches zero. In fact, the whole embedding becomes trivial with constant angle. When $\theta_0 \to 0$, on the other hand, the embedding becomes increasingly spiky and the corresponding

chemical potential approaches the value:

$$\lim_{\theta_0 \to 0} \mu = m^{\frac{1}{b}} \ . \tag{5.2.17}$$
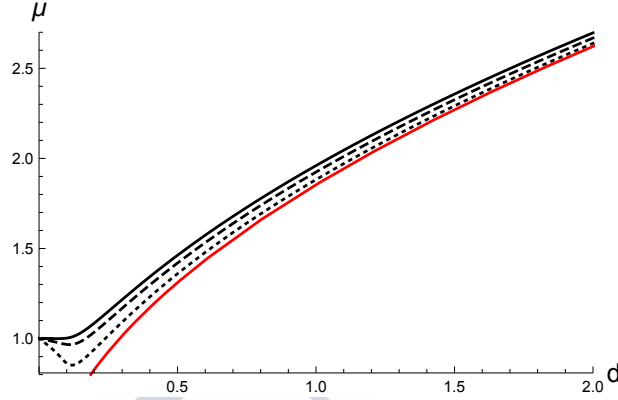

Figure 5.5: We plot the chemical potential μ as a function of the density d for fixed quark mass. The continuous black curve corresponds to the unflavored case ($b = 1$), the dashed curve is for $b = 1.1$, while the dotted curve is for $b = 1.25$ (corresponding to $\hat{\epsilon} \to \infty$). All curves are for $m = 1$. The continuous red curve corresponds to the conformal D3-D5 system with massless quarks, for which $\mu = \gamma \, d^{\frac{1}{2}}$, with $\gamma = \frac{1}{4\sqrt{\pi}} \Gamma(1/4)^2$.

We have verified (5.2.17) numerically. This result can also be easily demonstrated analytically as follows. Let us first introduce the Cartesian-like coordinates (ρ, R), related to (θ, r) as:

$$R = r^b \cos\theta \ , \qquad \rho = r^b \sin\theta \ . \tag{5.2.18}$$

In these coordinates the black hole embeddings start in the IR at the origin $R = \rho = 0$ with a certain angle θ_0 with respect to the R-axis and they end at the UV at $R = m$ with $\rho \to \infty$ (see Fig. 5.3). If the initial angle θ_0 is very small, the embeddings are very spiky and approach the maximal value $R = m$ very fast for very small values of the coordinate ρ. Instead of parameterizing the embedding as $\theta = \theta(r)$, it is more convenient in this situation to represent it as $\rho = \rho(R)$. It is then straightforward to demonstrate that μ is given by the integral:

$$\mu = \frac{d}{b} \int_0^m \frac{\sqrt{1 + (\frac{d\rho}{dR})^2}}{\sqrt{d^2(\rho^2 + R^2)^{1-\frac{1}{b}} + \rho^2(\rho^2 + R^2)^{\frac{1}{b}}}} \ dR \ . \tag{5.2.19}$$

For $\theta_0 \to 0$ the coordinate ρ is very close to zero except when $R \approx m$ and we can approximate the integral (5.2.19) by taking $\rho \approx 0$ in the integrand. We get:

$$\mu \approx \frac{1}{b} \int_0^m R^{\frac{1}{b}-1} \ dR = m^{\frac{1}{b}} \ , \tag{5.2.20}$$

in agreement with (5.2.17). For a fixed value of the mass parameter m, the limiting value (5.2.17) corresponds to sending $d \to 0$. Actually, the dependence of μ on d for fixed m can

be obtained numerically by performing the integral (5.2.12). The result is shown in Fig. 5.5, where we notice an important difference between the unflavored and flavored cases. Indeed, when $N_f = 0$ the chemical potential μ grows monotonically with d, starting from its minimal value $\mu = m$ at $d = 0$. When d is large the chemical potential grows as $\mu \propto d^{\frac{1}{2}}$, which is the behavior expected in a conformal theory in 2+1 dimensions. On the contrary, when the backreaction of the flavors is added, μ decreases for small values of d until it reaches a minimum at a non-zero value of d and then it grows and converges eventually to the unflavored case. The presence of minimum in the $\mu = \mu(d)$ curve means that the charge susceptibility $\chi = \partial d / \partial \mu$ diverges at $d \neq 0$, signaling a discontinuous phase transition at a non-zero density. We will confirm this fact below.

The black hole embeddings considered above are not the only possible ones. Indeed, there are also two other configurations in which the brane does not reach the $r = 0$ origin. The so-called brane-antibrane embeddings are characterized by the initial boundary conditions:

$$\theta(r_0) = \frac{\pi}{2} , \qquad \theta'(r_0) = \infty , \qquad (5.2.21)$$

where r_0 is the minimal value of r. In terms of the (ρ, R) variables the brane is orthogonal to the ρ-axis in the IR (at $\rho = \rho_0 = r_0^b$, $R = 0$) and becomes parallel to the ρ-axis as ρ becomes large (see Fig. 5.3). Notice that $dR/d\rho$ diverges at $\rho = \rho_0$, which indicates that the brane has a turn-around point where the brane jumps to a second branch.

A third class of configurations are the so-called Minkowski embeddings, in which the brane reaches the R-axis at some non-zero value of R, as shown in Fig. 5.3. Due to charge conservation these embeddings are only consistent if the density d is zero. When this is the case there are analytic solutions which preserve some amount of supersymmetry [75]. In terms of the (r, θ) variables, these embedding are:

$$\cos \theta(r) = \frac{m}{r^b} , \qquad (d = 0) . \qquad (5.2.22)$$

Equivalently $R = m$. Notice that in this case the minimal value of r is $r_0 = m^{\frac{1}{b}}$. Moreover, when d vanishes it follows from (5.2.9) that $A_t' = 0$ and, therefore, the gauge field A_t is an arbitrary constant, which equals the chemical potential μ. Thus, the SUSY embeddings (5.2.22) correspond to $d = 0$, with μ being a free parameter.

Notice that, in this zero temperature case, the mass parameter m can be scaled out by a suitable change of the radial variable followed by some redefinitions. Indeed, from (5.2.15) we conclude that m can be taken to be one if one changes variables from r to $\tilde{r} = r/m^{\frac{1}{b}}$. Then, it follows from (5.2.12) that m can be eliminated from this last equation if d and μ are written in terms of the rescaled quantities $\tilde{d}$ and $\tilde{\mu}$, defined as $\tilde{d} = d/m^{\frac{2}{b}}$ and $\tilde{\mu} = \mu/m^{\frac{1}{b}}$.

In section 5.3 we will determine which of these three types of embeddings at zero temperature is thermodynamically favored. We will carry out this analysis by comparing their thermodynamic potentials Ω in the grand canonical ensemble.

5.2.2 Embeddings at finite temperature

As will become clear later, we need to extend some of our analysis to small and non-zero temperature. All three types of embeddings, as discussed in the preceding section, extend

continuously to $T \neq 0$. However, as our main motivation in this work are the quantum critical phenomena, we will restrict our attention in the black hole phase. Let us thus only consider the black hole embeddings at non-zero temperature. These embeddings reach the horizon $r = r_h$ with some angle $\theta = \theta_0$. Near $r = r_h$ we can solve (5.2.14) in powers of $r - r_h$. The first two terms in this expansion are:

$$\theta(r) \; = \; \theta_0 \, + \, \theta_1 \, (r - r_h) \, + \, \cdots \; , \tag{5.2.23}$$

where the constant θ_1 is given by:

$$\theta_1 \; = \; b \, \frac{\cos\theta_0 \, \sin\theta_0 \left[b \, r_h^2 \, + \, (3 - 2b) \, \sqrt{d^2 + r_h^4 \, \sin^2\theta_0} \right]}{3(d^2 \, + \, r_h^4 \, \sin^2\theta_0)} \; r_h \; . \tag{5.2.24}$$

To get the full $\theta(r)$ function we need to integrate numerically (5.2.14) with the initial condition at $r = r_h$ given by (5.2.24). Notice that (5.2.14) depends explicitly on r_h through the blackening factor h. It turns out that the horizon radius r_h can be scaled out by an appropriate change of variables followed by a redefinition of the density d. Indeed, let us define the reduced variable $\hat{r}$ and density $\hat{d}$ as:

$$\hat{r} \; = \; \frac{r}{r_h} \, , \qquad\qquad \hat{d} \; = \; \frac{d}{r_h^2} \; . \tag{5.2.25}$$

Then, it is readily verified that the embedding equation in terms of $\hat{r}$ is just (5.2.14) with $r_h = 1$ and d substituted by $\hat{d}$. Other quantities can be similarly rescaled. Indeed, let us define $\hat{\mu}$ and $\hat{m}$ as:

$$\hat{\mu} \; = \; \frac{\mu}{r_h} \, , \qquad\qquad \hat{m} \; = \; \frac{m}{r_h^b} \; . \tag{5.2.26}$$

It is straightforward to find an expression of $\hat{\mu}$ in terms of the rescaled quantities:

$$\hat{\mu} \; = \; \frac{\hat{d}}{b} \int_1^\infty \frac{\sqrt{b^2 + \hat{r}^2 \, h(\hat{r}) \left(\frac{d\theta}{d\hat{r}} \right)^2}}{\sqrt{\hat{d}^2 + \hat{r}^4 \, \sin^2\theta}} \, d\hat{r} \; . \tag{5.2.27}$$

Notice also that the ratio $\hat{m}^{\frac{1}{b}}/\hat{\mu}$ does not depend on r_h:

$$\frac{\hat{m}^{\frac{1}{b}}}{\hat{\mu}} \; = \; \frac{m^{\frac{1}{b}}}{\mu} \; . \tag{5.2.28}$$

5.3   Zero temperature thermodynamics

The zero-temperature grand canonical potential Ω is given by minus the on-shell action of the probe brane:

$$\Omega \; = \; -S_{on-shell} \; . \tag{5.3.29}$$

Notice that, as pointed out in [136], the on-shell action of our ABJM system is finite and does not need to be regulated. Indeed, the WZ term of the action serves as a regulator of

the DBI term, giving rise to consistent thermodynamics. The explicit expression of Ω at zero temperature is given by:

$$\Omega = \mathcal{N} \int_{r_0}^{\infty} r^2 \sin\theta \left[\frac{r^2 \sin\theta \sqrt{b^2 + r^2\,\theta'^2}}{\sqrt{d^2 + r^4 \sin^2\theta}} - b\sin\theta - r\cos\theta\,\theta' \right] dr \ . \tag{5.3.30}$$

Other thermodynamic properties at $T = 0$ can be obtained from (5.3.30). For example, the pressure P is just:

$$P = -\Omega \ . \tag{5.3.31}$$

Moreover, we can evaluate Ω for the different embeddings and determine the one that is favored at different values of the chemical potential. One can verify by plugging (5.2.22) in (5.3.30) that $\Omega = 0$ for the SUSY embeddings (5.2.22) which have zero density d and arbitrary μ. In the case of the black hole embeddings the situation varies greatly when the backreaction is included. Indeed, for the unflavored background with $b = 1$ the grand canonical potential of the black hole embeddings is always negative and grows monotonically as μ decreases towards its minimal value $\mu \searrow m$, where $\Omega = 0$ and $d = 0$ (see Fig. 5.6, left). On the contrary, in the flavored backgrounds with $b > 1$, the grand canonical potential is negative for large values of μ and vanishes for some $\mu = \mu_c$ which corresponds to a non-zero density $d = d_c$ (see Fig. 5.6, right). From this point on, $\Omega \geq 0$, reaching a maximum positive value, which corresponds to the minimum value of the chemical potential μ. It is at this point where the black hole embedding ceases to exist as it annihilates with another (unstable) black hole embedding. This latter black hole branch is the one which connects with the Minkowski embeddings at larger mu, *i.e.* until the grand potential reaches the value $\Omega = 0$ when $\mu = m^{\frac{1}{b}}$ and $d = 0$. The grand canonical potential for the brane-antibrane embeddings is always non-negative and decreases monotonically as μ grows ($\mu \leq m^{\frac{1}{b}}$ for these embeddings). This structure in the (μ, Ω) plane is the well-known swallow-tail shape, typical of first-order phase transitions.
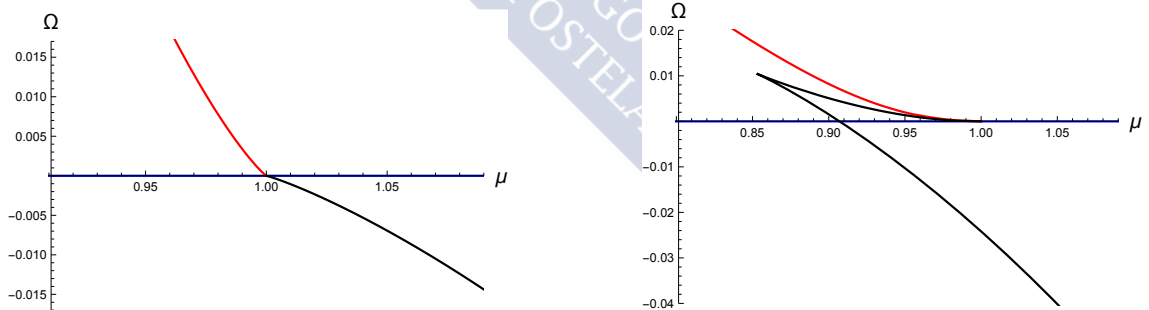

Figure 5.6: We plot the grand canonical potential Ω as a function of the chemical potential μ for the unflavored (left) and flavored (right) models. The black (red) curve corresponds to the black hole (brane-antibrane) embedding. The supersymmetric Minkowski embeddings $\Omega(\mu) = 0$ we have represented with a blue curve on the horizontal axis. The curves for the flavored model on the right have been obtained for $b = 1.25$. All curves are with $m = 1$.

From the numerical results displayed in Fig. 5.6 it is clear that the black hole embeddings are thermodynamically preferred for values of μ such that their grand canonical potential

Ω_{bh} is negative. Moreover, when μ is such that $\Omega_{bh} > 0$, the Minkowski embeddings (with $d = \Omega = 0$) are preferred. Notice also that the brane-antibrane configurations are always thermodynamically disfavored. Therefore, at $\mu = \mu_c$ such that $\Omega_{bh}(\mu_c) = 0$ there is a black hole-Minkowski embedding phase transition. In Fig. 5.6 we see that the nature of this quantum phase transition for the unflavored model is very different from that of the backreacted background. Indeed, in the quenched unflavored case we have a continuous second order phase transition in which the density d vanishes in both phases at the transition point $\mu_c = m$. In section 5.3.1 we will study in detail this quantum critical point and we will characterize the scaling of the different physical quantities near the transition.

In the unquenched flavored model the phase transition at $\mu = \mu_c$ is discontinuous since d jumps from a non-zero value in the black hole phase to $d = 0$ in the Minkowski phase. Therefore, we have a first-order phase transition, for which we will determine the latent heat and other quantities in section 5.3.2.
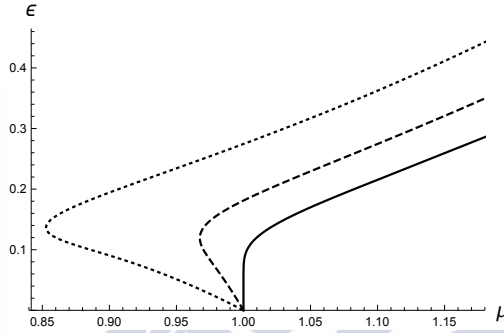

Figure 5.7: We depict the internal energy ϵ as a function of the chemical potential μ for the unflavored model (continuous curve) and for the flavored model with $b = 1.1$ (dashed curve) and $b = 1.25$ (dotted curve). In all the cases we have used $m = 1$.

Once the grand canonical potential Ω is known, we can determine other thermodynamic functions. Indeed, the charge density ρ_{ch} is given by:

$$\rho_{ch} = -\frac{\partial \Omega}{\partial \mu} . \tag{5.3.32}$$

By computing numerically the derivative in (5.3.32) at fixed mass m, we have checked that ρ_{ch} is related to d as:

$$\rho_{ch} = \mathcal{N} b d , \tag{5.3.33}$$

where $\mathcal{N}$ is the normalization constant (5.2.7). Eq. (5.3.33) confirms our identification of the constant d. The energy density ϵ can be obtained as:

$$\epsilon = \Omega + \mu \rho_{ch} . \tag{5.3.34}$$

More explicitly, after using (5.3.30), (5.2.12), and (5.3.33), we have the following integral expression for ϵ,

$$\epsilon = \mathcal{N} \int_{r_0}^{\infty} \left[\sqrt{b^2 + r^2 \theta'^2} \sqrt{d^2 + r^4 \sin^2 \theta} - b r^2 \sin^2 \theta - r^3 \sin \theta \cos \theta \, \theta' \right] dr , \tag{5.3.35}$$

where r_0 is the minimal value of r for the embedding. In Fig. 5.7 we plot ϵ for black hole embeddings as a function of μ, both for the quenched and unquenched model. We notice that the energy density in the quenched theory grows monotonically with the chemical potential, starting from the value $\epsilon = 0$ at the transition point at $\mu = m$. On the contrary, when dynamical quarks are added to the background, the function ϵ_{bh} is not monotonic and becomes double-valued, with a point where $\partial\epsilon/\partial\mu = \mu\partial\rho_{ch}/\partial\mu$ blows up. This is, of course, consistent with the results plotted in Fig. 5.5.

The speed of the first sound is defined as:

$$u_s^2 = \frac{\partial P}{\partial \epsilon} \ . \tag{5.3.36}$$

We evaluated numerically the derivative in (5.3.36) for black hole embeddings by using (5.3.31) and (5.3.30). The results are represented in Fig. 5.8, both for the quenched and unquenched cases. Again, they are very different in these two cases. In the quenched model u_s^2 is always non-negative and decreases monotonically when m/μ varies in the physical interval $[0, 1]$. In Fig. 5.8 (left) we compare u_s^2 for our quenched system with the corresponding values for the D3-D5 model [208, 209]. In the unquenched case u_s^2 is not monotonic and becomes negative for small μ, which again signals a discontinuous phase transition.
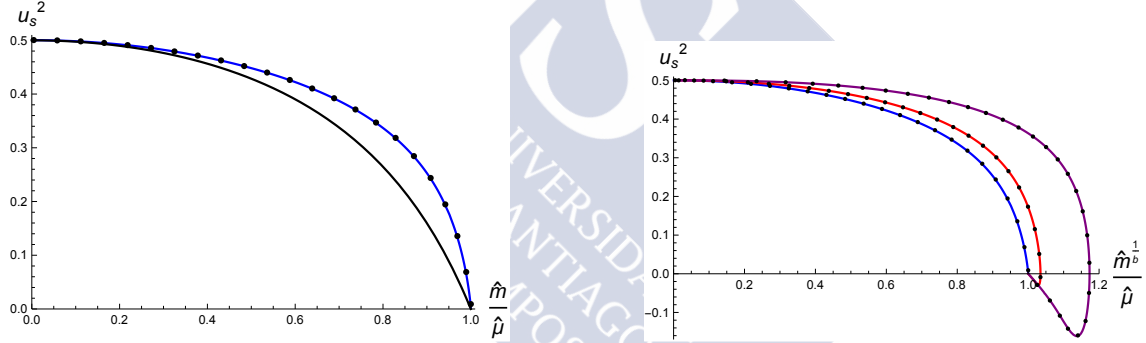

Figure 5.8: Left: We plot u_s^2 as a function of m/μ for the unflavored background (blue curve). We compare with the same quantity for the D3-D5 model (black curve). Right: We plot u_s^2 for different numbers of flavors: $b = 1$ (blue), $b = 1.1$ (red), and $b = 1.25$ (purple). In both plots the points are the values of the square of the speed of zero sound obtained by integrating the fluctuation equations of section 5.5; we conclude that the speeds of first and zero sounds agree in this model.

5.3.1 The unflavored transition

We have shown above that the unflavored system experiences a continuous phase transition at $\mu = m$ and $T = 0$. In this section we look in more detail the behavior of the system near this quantum critical point. Accordingly, let us define $\bar{\mu}$ as:

$$\bar{\mu} = \mu - m \ . \tag{5.3.37}$$

Clearly $\bar{\mu} = 0$ is the location of the phase transition. Therefore, we expect that the grand canonical potential Ω behaves in a non-analytic form near $\bar{\mu} = 0$. We assume that the system displays a scaling behavior near the critical point. The goal of this section is to characterize this behavior in terms of a set of critical exponents.

Let us consider a system with hyperscaling violation exponent θ and dynamical exponent z in n spatial dimensions ($n = 2$ in our case). Recall that in such a system $n - \theta$ is the effective number of spatial dimensions near the critical point and z is the effective dimension of the energy. Therefore $[\bar{\mu}] = z$ and the energy densities (such as our grand canonical potential Ω) should have a dimension equal to $n - \theta + z$. These dimension assignments allow us to write Ω near $\bar{\mu} = 0$ as:

$$\Omega \approx -C\,\bar{\mu}^{\frac{n+z-\theta}{z}} \left(\left|\log \frac{\bar{\mu}}{m}\right|\right)^{-\zeta}, \tag{5.3.38}$$

where $C > 0$ is a constant. Eq. (5.3.38) is a generalization of the expression written in [208] by including a logarithmic multiplicative term with some new exponent ζ. We show below that ζ cannot be zero in our ABJM case. This is to be compared with the Dp-Dq systems studied in [208, 209], where $\zeta = 0$. Similar multiplicative logarithmic corrections to the scaling has been studied in general in [210] for thermal phase transitions.

The charge density $\rho_{ch} = \mathcal{N}\,d$ is obtained by computing the derivative of Ω with respect to $\bar{\mu}$. We get:

$$\mathcal{N}\,d \approx C\,\bar{\mu}^{\frac{n-\theta}{z}} \left(\left|\log \frac{\bar{\mu}}{m}\right|\right)^{-\zeta} \left[1 + \frac{n-\theta}{z} + \frac{\zeta}{\left|\log \frac{\bar{\mu}}{m}\right|}\right]. \tag{5.3.39}$$

Let us next consider, following [208], the non-relativistic energy density e, defined as:

$$e = \epsilon - \rho_{ch}\,m = \Omega + \rho_{ch}\,\bar{\mu}. \tag{5.3.40}$$

Near the critical point, e behaves as:

$$e \approx C\,\bar{\mu}^{\frac{n+z-\theta}{z}} \left(\left|\log \frac{\bar{\mu}}{m}\right|\right)^{-\zeta} \left[\frac{n-\theta}{z} + \frac{\zeta}{\left|\log \frac{\bar{\mu}}{m}\right|}\right], \tag{5.3.41}$$

and it is very convenient to consider the ratio e/P, which is given by:

$$\frac{e}{P} \approx \frac{n-\theta}{z} + \frac{\zeta}{\left|\log \frac{\bar{\mu}}{m}\right|}. \tag{5.3.42}$$

If $\theta \neq n$ the ratio e/P reaches a constant non-vanishing value as $\bar{\mu} \to 0$. This is clearly not the case for our system, as illustrated in Fig. 5.9. Therefore, our system should have $\theta = 2$. Moreover, the logarithmic exponent ζ should be non-zero and positive.[2] Therefore we get the following leading behavior for our system:

$$\rho_{ch} = \mathcal{N}\,d \approx \frac{C}{\left(\left|\log \frac{\bar{\mu}}{m}\right|\right)^{\zeta}}, \qquad\qquad \frac{e}{P} \approx \frac{\zeta}{\left|\log \frac{\bar{\mu}}{m}\right|}. \tag{5.3.43}$$

---

[2]Indeed, if we had $\theta = 2$ and $\zeta = 0$ the charge density d in (5.3.39) would be non-zero at the critical point, which is not the case for our ABJM system.

We can also compute the speed of sound u_s near the critical point by using (5.3.36), with the result:

$$u_s^2 \approx \frac{1}{\zeta} \frac{\bar{\mu} \left| \log \frac{\bar{\mu}}{m} \right|}{m + \bar{\mu}} \left[1 - \frac{1}{1 + \zeta + \left| \log \frac{\bar{\mu}}{m} \right|} \right] , \tag{5.3.44}$$

which, at leading order for $\bar{\mu} \to 0$ becomes simply:

$$u_s^2 \approx \frac{1}{\zeta} \frac{\bar{\mu}}{m} \left| \log \frac{\bar{\mu}}{m} \right| . \tag{5.3.45}$$
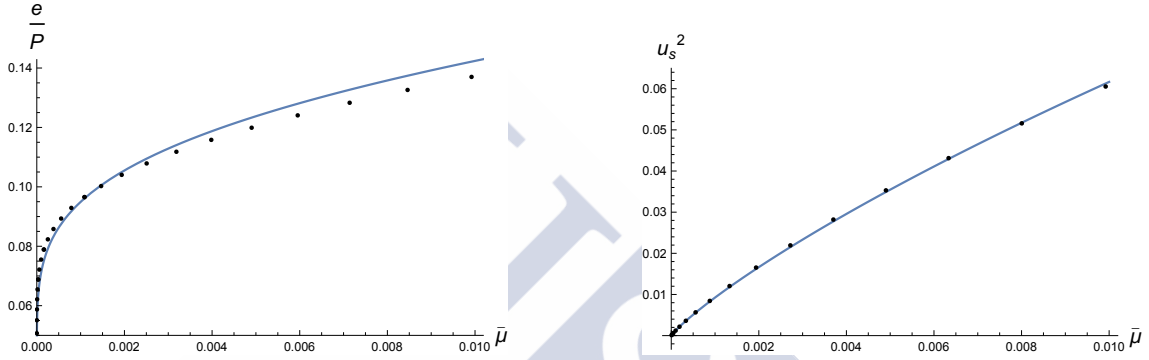

Figure 5.9: On the left we plot the numerical values of the ratio e/P as a function of $\bar{\mu}$. The continuous line is a fit to the expression written in (5.3.43). The value of ζ obtained in this fit is $\zeta = 0.65575$. On the right we plot the values of u_s^2, together with the scaling expression (5.3.45) for $\zeta = 0.74689$.

To determine the value of the exponent ζ we can fit the numerical values of e/P and u_s^2 near $\bar{\mu} = 0$ to our scaling expressions (5.3.43) and (5.3.45). Due to the logarithmic behavior of these quantities we must explore very small values of $\bar{\mu}$. The results of these fits is shown in Fig. 5.9. The values of ζ obtained are in the range $\zeta = 0.65 - 0.75$.

Let us determine, following the reasoning in [208], the dynamical critical exponent z by dimensional analysis of the dispersion relation of the sound mode, which is of the form $\omega = u_s k$, where u_s is given by (5.3.45) near the critical point $\bar{\mu} = 0$. Actually, we will see that the speed of the zero sound, obtained by numerical integration of the fluctuation equations of the probe brane, is exactly the same as the one determined by (5.3.36). Near $\bar{\mu} = 0$ eq. (5.3.45) tells us that $u_s \sim \sqrt{\bar{\mu}}$ (times a logarithmic correction) and, since $[\omega] = [\bar{\mu}] = z$ and $[k] = 1$, the dimensional consistency of the dispersion relation $\omega = u_s k$ implies that $z = 2$. Therefore, the values of θ and z for our system are:

$$\theta = 2 , \qquad z = 2 . \tag{5.3.46}$$

Notice that the value of θ just found differs from the value $\theta = 1$ obtained in [208] for the conformal systems D3-D7 and D3-D5.

Let us now consider the system at small non-zero temperature $T \ll \bar{\mu}$. We can evaluate the free energy f at first order in T by using the results of [211]. Notice that at $T = 0$,

$f = \epsilon$. Indeed, according to the analysis of [211], when T is small the free energy density can be approximated as:

$$f(\mu, m, T) = f(\mu, m, T = 0) + \pi \rho_{ch} T + \mathcal{O}(T^2) . \tag{5.3.47}$$

Then, the non-relativistic free energy density is given by:

$$f_{non-rel}(\mu, m, T) = f(\mu, m, T) - \rho_{ch} m = e + \pi \rho_{ch} T + \mathcal{O}(T^2) . \tag{5.3.48}$$

Evaluating the right-hand side of (5.3.48) for our system, we get the following expression of $f_{non-rel}$ for small $\bar{\mu}$ and $T/\bar{\mu}$:

$$f_{non-rel}(\mu, m, T) = C \frac{\bar{\mu}}{\left(\left|\log \frac{\bar{\mu}}{m}\right|\right)^{\zeta+1}} \left[\zeta + \pi \left|\log \frac{\bar{\mu}}{m}\right| \frac{T}{\bar{\mu}} + \cdots\right] . \tag{5.3.49}$$

On general grounds, near a quantum phase transition the free energy density should behave as a homogeneous function when the control parameter $\bar{\mu}$ and the temperature T are scaled as $\bar{\mu} \to \Lambda^{\frac{1}{\nu}} \bar{\mu}$, $T \to \Lambda^z T$, where ν is the critical exponent that characterizes the divergence of the correlation length $\xi \sim (T - 0)^{-\nu}$ [194]. Eq. (5.3.49) is the first order term of a Taylor expansion of the scaling function of $f_{non-rel}$. If we disregard the logarithmic terms in (5.3.49) (which give rise to subleading terms when $\bar{\mu} \to 0$), it follows that T and $\bar{\mu}$ should be scaled by the same power of the scale factor Λ. Since $z = 2$ for our system, we must have $\nu = 1/2$. Eq. (5.3.49) also determines the value of the exponent α which characterizes the scaling of the heat capacity $c_V \sim (T - 0)^{-\alpha}$. Indeed, according to the analysis of [208] the global power of $\bar{\mu}$ in $f_{non-rel}(\mu, m, T)$ should be $2 - \alpha$. If we ignore again the logarithmic correction, this prescription gives $\alpha = 1$. Therefore, we have obtained that the critical exponents α and ν are given by

$$\alpha = 1 , \qquad \nu = \frac{1}{2} . \tag{5.3.50}$$

Notice that the values of θ, z, α, and ν listed in (5.3.46) and (5.3.50) satisfy the hyperscaling relation

$$(n + z - \theta)\nu = 2 - \alpha , \tag{5.3.51}$$

with $n = 2$.

5.3.2 The flavored transition

We already pointed out above that the black hole-Minkowski phase transition with dynamical quarks in the background is of first order. At the transition point the density jumps from being $d = d_c \neq 0$ in the black hole phase to $d = 0$ in the Minkowski phase. We have investigated numerically the dependence of d_c on $\hat{\epsilon}$ and m and we found that, with big accuracy, this dependence can be written as:

$$d_c(\hat{\epsilon}, m) = \tilde{d}_c(\hat{\epsilon}) \, m^{\frac{2}{b}} = \tilde{d}_c(\hat{\epsilon}) \, m_q^2 , \tag{5.3.52}$$

where $m_q = m^{\frac{1}{b}}$ is proportional to the physical mass of the quarks. Notice that the dependence on m written in (5.3.52) is the one expected by the rescaling argument given at the end of section 5.2.1.

The flavor dependent coefficient of the quadratic law (5.3.52) grows monotonically with $\hat{\epsilon}$, as shown in Fig. 5.10 (left). For small $\hat{\epsilon}$ this growth is very fast and saturates very quickly for larger values of the deformation parameter.
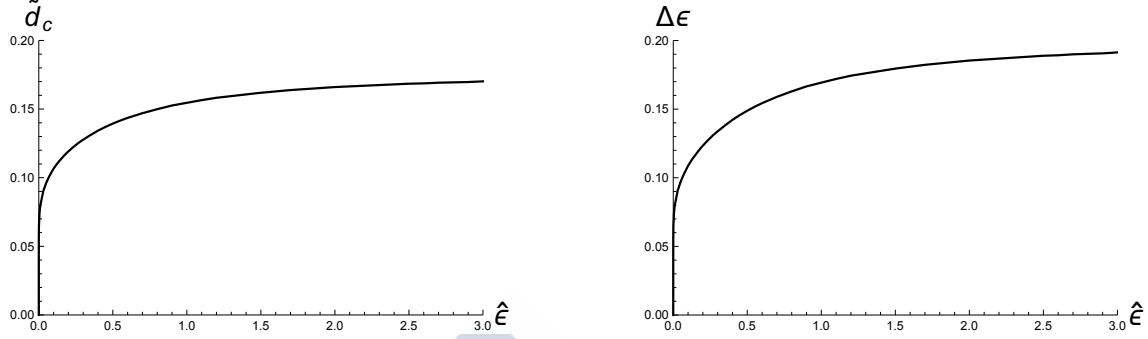

Figure 5.10: Left: We plot the function $\tilde{d}_c(\hat{\epsilon})$ introduced in (5.3.52) at $m = 1$. Right: We depict the latent heat $\Delta\epsilon$ for $m = 1$ as a function of $\hat{\epsilon}$.

The phase transition occurs at a critical chemical potential $\mu_c < m^{\frac{1}{b}} = m_q$. Actually, the ratio μ_c/m_q is a decreasing function of $\hat{\epsilon}$ which approaches the value $\mu_c/m_q \approx 0.9$ when $\hat{\epsilon} \to \infty$. It is also interesting to point out that the value of μ where the speed of sound vanishes (see Fig. 5.8)) corresponds to the turning point of Ω as a function of μ for a black hole embedding, *i.e.* to the minimum value of μ for such embeddings. The phase transition occurs for a value of μ close to its lowest value where u_s^2 is still positive. Moreover, it follows from the above discussion that $\mu_c \sim d_c^{\frac{1}{2}}$.

We also studied the latent heat of the phase transition, *i.e.* the difference $\Delta\epsilon$ of the internal energy of the two phases. Notice that, as $\Omega = 0$ in both phases at the transition point and $\rho_{ch} = 0$ in the Minkowski phase, $\Delta\epsilon$ is simply obtained by evaluating $\mu\,\rho_{ch}$ at the black hole side of the transition:

$$\Delta\epsilon = (\mu\,\rho_{ch})_{bh} \,. \tag{5.3.53}$$

The behavior of this quantity with the number of flavors when $m = 1$ is displayed in Fig. 5.10 (right). We notice that the latent heat resembles the behavior of the critical density. We have also verified that $\Delta\epsilon$ grows with the quark mass as $\Delta\epsilon \sim m_q^3 = m^{\frac{3}{b}}$.

Most of the figures that we have presented above have been produced using $m = 1$. It is however simple to obtain the results for any value of m by using the rescaling argument presented above. Indeed, one can readily show that the different quantities scale with $m_q = m^{\frac{1}{b}}$ as:

$$\epsilon \sim \Omega \sim m_q^3 \,, \ \mu \sim m_q \,, \ d \sim m_q^2 \,. \tag{5.3.54}$$

We have checked that this behavior is confirmed by our numerical results.

5.4   Charge susceptibility and diffusion constant

Let us now consider the system at non-zero temperature and compute the charge suscepti-
bility, which is defined as:

$$\chi = \frac{\partial \rho_{ch}}{\partial \mu} \ . \tag{5.4.55}$$

Taking into account that the charge density ρ_{ch} is related to d as $\rho_{ch} = \mathcal{N} \, b \, d$ (5.3.33), we
can rewrite this last expression as:

$$\chi^{-1} = \frac{1}{\mathcal{N} \, b} \frac{\partial \mu}{\partial d} \ . \tag{5.4.56}$$

We now evaluate explicitly the derivative in (5.4.56) as:

$$\frac{\partial \mu}{\partial d} = \int_{r_h}^{\infty} \frac{\partial A'_t}{\partial d} \, dr \ . \tag{5.4.57}$$

The derivative inside the integral in (5.4.57) can be computed directly. We get:

$$\frac{\partial A'_t}{\partial d} = \frac{\sqrt{\Delta}}{b} \frac{r^2 \sin \theta}{d^2 + r^4 \sin^2 \theta} \left[1 - d \left(\cot \theta \frac{\partial \theta}{\partial d} - \frac{r^2 \, h \, \theta'}{\Delta} \frac{\partial \theta'}{\partial d} \right) \right] \ . \tag{5.4.58}$$

where Δ is defined as:

$$\Delta \equiv b^2 (1 - A'^2_t) + r^2 \, h \, \theta'^2 = \frac{r^4 \sin^2 \theta (b^2 + r^2 \, h \, \theta'^2)}{d^2 + r^4 \sin^2 \theta} \ . \tag{5.4.59}$$

Thus, the charge susceptibility can be written in the form:

$$\chi^{-1} = \frac{1}{\mathcal{N}} \int_{r_h}^{\infty} dr \frac{\sqrt{\Delta}}{b^2} \frac{r^2 \sin \theta}{d^2 + r^4 \sin^2 \theta} \left[1 - d \left(\cot \theta \frac{\partial \theta}{\partial d} - \frac{r^2 \, h \, \theta'}{\Delta} \frac{\partial \theta'}{\partial d} \right) \right] \ . \tag{5.4.60}$$

The charge diffusion constant D can be related to the charge susceptibility and to the
DC conductivity σ by the Einstein relation:

$$D = \sigma \chi^{-1} \ . \tag{5.4.61}$$

The value of σ can be obtained from the two-point correlators of the transverse currents. This
calculation is performed in detail in appendix 5.A.1. Alternatively, σ can be computed by
employing the Karch-O'Bannon method [165], as was done for the ABJM model in chapter
4. The result obtained by these two methods agree and is given by:

$$\sigma = \mathcal{N} \frac{b}{r_h^2} \sqrt{d^2 + r_h^4 \sin^2 \theta_h} \ . \tag{5.4.62}$$

We can now plug (5.4.60) and (5.4.62) into the right-hand side of (5.4.61) to get the diffusion
constant D. The final result is:

$$D = \frac{\sqrt{d^2 + r_h^4 \sin^2 \theta_h}}{b \, r_h^2} \int_{r_h}^{\infty} dr \frac{r^2 \sin \theta \sqrt{\Delta}}{d^2 + r^4 \sin^2 \theta} \left[1 - d \left(\cot \theta \frac{\partial \theta}{\partial d} - \frac{r^2 \, h \, \theta'}{\Delta} \frac{\partial \theta'}{\partial d} \right) \right] \ . \tag{5.4.63}$$
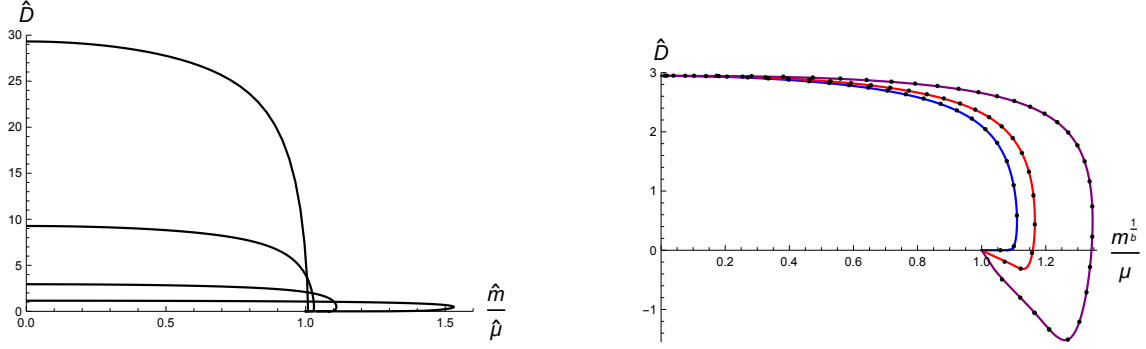
Figure 5.11: We plot the rescaled diffusion constant $\hat{D} = r_h\,D$ as a function of the ratio of the mass and the chemical potential. Left: We plot the values of $\hat{D}$ for the unflavored theory for different values of the rescaled density $\hat{d} = d/r_h^2$. The values of $\hat{d}$ in this plot are $\hat{d} = 1, 10, 100, 1000$ (bottom-up). Right: We plot the values of $\hat{D}$ for $\hat{d} = 10$ and for different number of flavors: $b = 1$ (blue), $b = 1.1$ (red), and $b = 1.25$ (purple), inside-out. The continuous curves are obtained by the Einstein relation and the points correspond to the diffusive fluctuation modes of the probe.

In the case of massless quarks, the embedding is just $\theta = \text{constant} = \pi/2$ and the integral (5.4.63) can be evaluated in analytic form. We get:

$$D_{m=0} = \frac{\sqrt{d^2 + r_h^4}}{r_h^3}\, F\!\left(\frac{3}{2}, \frac{1}{2}; \frac{5}{4}; -\frac{d^2}{r_h^4}\right)\,. \tag{5.4.64}$$

In the general case of massive quarks we have evaluated (5.4.63) numerically for the un-flavored and flavored backgrounds as a function of the chemical potential. The results of these calculations are displayed in Fig. 5.11. In the unflavored background D is always non-negative and vanishes when $\mu = m$ (see Fig. 5.11, left). On the contrary, when $N_f \neq 0$ the diffusion constant is maximal for large chemical potential (and given by the massless value (5.4.64)) and becomes negative after μ reaches its minimal value, which means that the system becomes unstable and that the first-order phase transition at $T = 0$ survives at non-zero temperature. In the next section we obtain the diffusion constant by looking at the fluctuation modes of the probe in the hydrodynamical regime. The corresponding values of D are also plotted in Fig. 5.11, where we notice that they agree perfectly with the values found above by using Einstein relation.

5.5 Fluctuations

We now want to carry out a dynamic (*i.e.* time-dependent) study of our system, to complement the static analysis performed so far. Accordingly, let us consider the generic $T \neq 0$ background and let us allow the probe brane to fluctuate around the black hole embeddings described in section 5.2. In general, the equations of motion of these fluctuations are very complicated since the different fluctuation modes are coupled. However, there are certain modes that can be decoupled from the rest and, therefore, they constitute a consistent truncation of the general system of equations. In this section we will study one of these restricted

sets of fluctuations, which involves the gauge field A and the transverse scalar θ. These fields take the form:

$$A = L^2 \left[A_t(r) \, dt + a_t(t,x,r) \, dt + a_x(t,x,r) \, dx + a_r(t,x,r) \, dr \right] , \quad \theta = \theta(r) + \lambda(t,x,r) , \tag{5.5.65}$$

where a_t, a_x, a_r, and λ are the first-order perturbations. One can check that the ansatz (5.5.65) is indeed a consistent truncation of the equations of motion. These truncated equations can be derived from a second order lagrangian density $\mathcal{L}^{(2)}$, which is derived in detail in appendix 5.A.1. The expression for $\mathcal{L}^{(2)}$ is:

$$\mathcal{L}^{(2)} = -\mathcal{N} \, r^2 \, \sin\theta \sqrt{\Delta} \left[\frac{1}{4} \, \mathcal{G}^{nm} \, \mathcal{G}^{pq} \, f_{mq} \, f_{np} + \frac{L^2}{2b^2} \left(1 - \frac{r^2 \, h \, \theta'^2}{\Delta} \right) \mathcal{G}^{mn} \partial_m \lambda \, \partial_n \lambda \right.$$

$$+ \left(\left(b - \frac{3}{2} \right) \frac{\sin\theta}{\sqrt{\Delta}} + \frac{r^2 \, h \, \theta'^2 - \Delta}{2 \sin^2\theta \Delta} \right) \lambda^2 - \frac{d^2 \theta'^2}{2 \, b^2 \, r^4 \sin^2\theta \Delta} \, (\partial_t \lambda)^2$$

$$\left. + \frac{d\theta'}{br^2 \sin\theta \sqrt{\Delta}} \, \mathcal{G}^{mn} \partial_m \lambda \, f_{nt} + \frac{b \, d \cot\theta}{L^2 r^2 \sin\theta \sqrt{\Delta}} \, \lambda f_{tr} \right] , \tag{5.5.66}$$

where $\mathcal{G}^{mn}$ is the open string metric defined in (5.A.3), f_{mn} is the field strength for a_m ($f = L^2 da$) and Δ is given by (5.4.59). Let us now write the different equations of motion which can be derived from the total lagrangian (5.5.66). The non-zero values of $\mathcal{G}^{mn}$ are written in (5.A.5). First of all, we write the equation of motion for a_r (in the $a_r = 0$ gauge):

$$\frac{b^2 + r^2 \, h \, \theta'^2}{h \, \Delta} \, \partial_t a_t' - \partial_x a_x' - \frac{d}{b \sin\theta \sqrt{\Delta}} \left(\theta' \, \partial_t \lambda' - \frac{\Delta}{r^2 \, h} \cot\theta \, \partial_t \lambda \right) = 0 . \tag{5.5.67}$$

The equation of motion for a_t is:

$$\partial_r \left[\frac{b^2 \, r^2 \, \sin\theta}{\Delta^{\frac{3}{2}}} \, (b^2 + r^2 \, h \, \theta'^2) \, a_t' + d \, b \left(\cot\theta \, \lambda - \frac{r^2 \, h \, \theta'}{\Delta} \, \lambda' \right) \right]$$

$$+ \frac{\sin\theta (b^2 + r^2 \, h \, \theta'^2)}{r^2 \, h \, \sqrt{\Delta}} \, \partial_x (\partial_x a_t - \partial_t a_x) - \frac{d \, \theta'}{b \, r^2} \, \partial_x^2 \lambda = 0 , \tag{5.5.68}$$

while the equation of motion for a_x becomes:

$$\partial_r \left(\frac{b^2 \, r^2 \, h \, \sin\theta}{\sqrt{\Delta}} \, a_x' \right) + \frac{\sin\theta (b^2 + r^2 \, h \, \theta'^2)}{r^2 \, h \, \sqrt{\Delta}} \, \partial_t (\partial_x a_t - \partial_t a_x) - \frac{d \, \theta'}{b \, r^2} \, \partial_t \partial_x \lambda = 0 . \tag{5.5.69}$$

Finally, the equation of motion for the scalar λ is:

$$\partial_r \left[\frac{r^2 \sin\theta h}{\sqrt{\Delta}} \left[r^2 \left(1 - \frac{r^2 \, h \, \theta'^2}{\Delta} \right) \lambda' + \frac{b \, d \theta'}{\sin\theta \sqrt{\Delta}} \, a_t' \right] \right] \tag{5.5.70}$$

$$+ b \, d \cot\theta \, a_t' + \frac{d\theta'}{b \, r^2} \, \partial_x (\partial_x a_t - \partial_t a_x) + r^2 \sin\theta \sqrt{\Delta} \left[(3 - 2b) \frac{\sin\theta}{\sqrt{\Delta}} + \frac{\Delta - r^2 \, h \, \theta'^2}{\sin^2\theta \Delta} \right] \lambda$$

$$+ \frac{\sin\theta}{b^2 \sqrt{\Delta}} \left[\frac{(b^2 + r^2 \, h \, \theta'^2)(r^2 \, h \, \theta'^2 - \Delta)}{h \, \Delta} - \frac{d^2 \, \theta'^2}{r^2 \sin^2\theta} \right] \partial_t^2 \lambda + \frac{\sin\theta \sqrt{\Delta}}{b^2} \left(1 - \frac{r^2 \, h \, \theta'^2}{\Delta} \right) \partial_x^2 \lambda = 0 .$$

Let us next Fourier transform the gauge field and the scalar to momentum space as:

$$a_\nu(r, t, x) = \int \frac{d\omega\, dk}{(2\pi)^2}\, a_\nu(r, \omega, k)\, e^{-i\omega t + ikx} \,,$$

$$\lambda(r, t, x) = \int \frac{d\omega\, dk}{(2\pi)^2}\, \lambda(r, \omega, k)\, e^{-i\omega t + ikx} \,, \tag{5.5.71}$$

and define the electric field E as the following gauge-invariant combination:

$$E = k\, a_t + \omega\, a_x \,. \tag{5.5.72}$$

Then, the equation of motion for a_r in momentum space is:

$$\frac{b^2 + r^2\, h\, \theta'^2}{h\, \Delta}\, \omega\, a'_t + k\, a'_x - \frac{\omega\, d}{b \sin\theta \sqrt{\Delta}} \left(\theta'\, \lambda' - \frac{\Delta}{r^2\, h} \cot\theta\, \lambda \right) = 0 \,. \tag{5.5.73}$$

We now combine this last equation with the definition of E. We get a'_t and a'_x as functions of E and λ:

$$a'_t = \frac{k\, h\, \Delta}{\Delta h k^2 - (b^2 + r^2 h\theta'^2)\omega^2}\, E' - \frac{\omega^2\, h\, d\, \sqrt{\Delta}}{b\left[\Delta h k^2 - (b^2 + r^2 h\theta'^2)\omega^2\right] \sin\theta} \left(\theta'\lambda' - \frac{\Delta}{r^2 h} \cot\theta\lambda \right) ,$$

$$a'_x = \frac{-(b^2 + r^2 h\theta'^2)\omega}{\Delta h k^2 - (b^2 + r^2 h\theta'^2)\omega^2}\, E' + \frac{\omega\, k\, h\, d\, \sqrt{\Delta}}{b\left[\Delta h k^2 - (b^2 + r^2 h\theta'^2)\omega^2\right] \sin\theta} \left(\theta'\lambda' - \frac{\Delta}{r^2 h} \cot\theta\lambda \right) . \tag{5.5.74}$$

After using these equations, it is easy to check that (5.5.68) and (5.5.69) become equivalent and equal to the following differential equation for the electric field E:

$$\partial_r \left[\frac{b^2\, r^2\, h}{(b^2 + r^2\, h\, \theta'^2)\omega^2 - \Delta\, h\, k^2} \left(\frac{\sin\theta}{\sqrt{\Delta}}(b^2 + r^2\, h\, \theta'^2)\, E' - \frac{k\, d\, h}{b} \left(\theta'\, \lambda' - \frac{\Delta}{r^2\, h} \cot\theta\lambda \right) \right) \right]$$

$$+ \frac{\sin\theta(b^2 + r^2\, h\, \theta'^2)}{r^2\, h\, \sqrt{\Delta}}\, E - \frac{d\theta'}{b\, r^2}\, k\, \lambda = 0 \,. \tag{5.5.75}$$

Let us now write the equation of motion for the scalar field λ in momentum space as:

$$0 = \partial_r \left[\frac{r^2 \sin\theta h}{\sqrt{\Delta}} \left[r^2 \left(1 - \frac{r^2\, h\, \theta'^2}{\Delta} \right)\lambda' + \frac{b\, d\, \theta'}{\sin\theta\sqrt{\Delta}}\, a'_t \right] \right] \tag{5.5.76}$$

$$+ b\, d \cot\theta\, a'_t - k\, \frac{d\theta'}{b\, r^2}\, E + r^2 \sin\theta\, \sqrt{\Delta} \left[(3 - 2b)\frac{\sin\theta}{\sqrt{\Delta}} + \frac{\Delta - r^2\, h\, \theta'^2}{\sin^2\theta\Delta} \right] \lambda$$

$$- \omega^2\, \frac{\sin\theta}{b^2\sqrt{\Delta}} \left[\frac{(b^2 + r^2\, h\, \theta'^2)(r^2\, h\, \theta'^2 - \Delta)}{h\, \Delta} - \frac{d^2\, \theta'^2}{r^2 \sin^2\theta} \right] \lambda - k^2\, \frac{\sin\theta\sqrt{\Delta}}{b^2} \left(1 - \frac{r^2\, h\, \theta'^2}{\Delta} \right)\lambda \,,$$

where it should be understood that a'_t is given by the first equation in (5.5.74). The fluctuation equations (5.5.75) and (5.5.76) depend explicitly on the horizon radius r_h through the blackening factor h. This dependence can be eliminated by performing the familiar rescaling

of the radial variable and of the different quantities appearing in the equations. Indeed, let us rescale the radial variable r and the density d as in (5.2.25). Moreover, we also define the rescaled frequency and momentum as:

$$\hat{\omega} = \frac{\omega}{r_h} \, , \qquad \hat{k} = \frac{k}{r_h} \, . \tag{5.5.77}$$

Then, one can easily verify that the resulting equations of motion are independent of r_h if the fields E and λ are rescaled appropriately. Actually, since only the relative power of r_h in these two fields matters, we can decide not to rescale the electric field E. The rescaling of the scalar λ that allows to eliminate r_h is:

$$\hat{\lambda} = r_h^2 \lambda \, . \tag{5.5.78}$$

The resulting equations of motion are just (5.5.75) and (5.5.76) with $r_h = 1$ and with all quantities replaced by their hatted counterparts.

The collective excitations of the brane system are dual to the quasinormal modes of the probe. The latter can be obtained by solving (5.5.75) and (5.5.76) for low ω and k by imposing infalling boundary conditions at the horizon and the vanishing of the source terms at the UV. At low temperature, in the so-called collisionless quantum regime, the dominant excitation is the holographic zero sound [212, 213, 181] (see also [182, 183, 214, 215, 216, 217]), whose dispersion relation has the form:

$$\hat{\omega} = \pm c_s \hat{k} - i\Gamma(\hat{k}, \hat{d}) \, . \tag{5.5.79}$$

In (5.5.79) c_s is the speed of zero sound and Γ is the attenuation. We have integrated numerically the fluctuation equations when $\hat{d}$ is large (*i.e.* at low temperature) and we have found the value of c_s, both for the unflavored and the flavored backgrounds. The main conclusion from this calculation is that c_s is equal to the speed of the first sound u_s (given by (5.3.36)). As shown in Fig. 5.8, c_s reaches its maximal value ($c_2 = 1/\sqrt{2}$) when $m/\mu = 0$, where the system is conformally invariant. In the unflavored case c_s is always positive and vanishes at the quantum critical point at $\mu = m$ (see Fig. 5.8, left). When dynamical quarks are included c_s becomes imaginary when μ reaches its minimal value, which occurs when the Minkowski embeddings are thermodynamically favored.

At higher temperature (*i.e.* with small $\hat{d}$) the system enters into the hydrodynamic diffusive regime. The dominant mode in this case has purely imaginary frequency and a spectrum of the form:

$$\hat{\omega} = -i\hat{D}\,\hat{k}^2 \, , \tag{5.5.80}$$

where $\hat{D}$ is the rescaled diffusion constant,

$$\hat{D} = r_h D \, . \tag{5.5.81}$$

As in the zero sound case, this dynamic calculation of the diffusion constant yields the same result as the static one. Indeed, the results obtained by numerical integration of (5.5.75) and (5.5.76) coincide with the ones obtained from the Einstein relation (5.4.63), as shown in Fig. 5.11.

Let us finish this section with the following observation. A careful reader would had expected some discussion on the possible instability as the WZ action has a term $C_1 \wedge F \wedge F \wedge F$ which is the source of striping via a generic mechanism introduced in [184]. Indeed, the occurrence of tachyonic fluctuations have been confirmed in similar brane models [181, 182], with the subsequent construction of the striped ground state [188]. In the current work, we analyzed the fluctuations of the transverse gauge field, where such an instability is expected. In this sector, one needs to analyze the coupled fluctuations of the internal gauge field a and the transverse Minkowski gauge field a_y at non-vanishing momentum. The corresponding equations of motion are presented in appendix 5.A.1. While we did see the precursor of the instability, a purely imaginary mode first ascending towards the upper half of the complex ω plane and then descending as a function of k, we were unsuccessful to finding parameter values for which case the mode would had actually become unstable. We expect that in the case in which an internal flux is turned on at the unperturbed level, where the contribution of the pullback of $\hat{C}_1$ at the background level is non-vanishing, the relevant WZ term can become sizable and thus implies striping in some range of parameters.

5.6   Discussion

In this chapter we studied the phase diagram of a D6-brane probe with non-vanishing charge density in a background dual to the ABJM Chern-Simons matter theory with dynamical massless flavors at zero temperature. We analyzed the phase transition between black hole and Minkowski embeddings at zero temperature and non-vanishing chemical potential. This transition is a holographic model of a conductor-insulator phase transition between a gapless (black hole) phase and a gapped (Minkowski) phase.

In the unflavored background we found that this transition occurs when the charge density vanishes and is of second order. Moreover, we were able to characterize the scaling behavior of the probe near the critical point. Interestingly, we found logarithmic multiplicative corrections. In the background with dynamical quarks the transition of the probe is of first order and takes place when the density is non-zero. Therefore, we have shown that, even if the change of the metric due to the backreaction to the flavor is seemingly mild, the physical effects are very important.

It is interesting to compare our results with the one corresponding to the (2+1)-dimensional D3-D5 intersection [195, 208]. When the mass m of the quarks is zero, the gravitational descriptions of both systems are equivalent and have the same thermodynamic quantities. However, for non-conformal embeddings with $m \neq 0$, the ABJM probe action gets a non-trivial contribution from the Wess-Zumino term. This term is responsible for the different critical behaviors of the systems even in the absence of backreaction.

Let us now discuss some possible extensions of the work performed in this chapter. First of all, it would be interesting to extend our study of the Minkowski-black hole embedding phase transition to non-zero temperature, in order to completely determine the phase diagram of the model. In the absence of the chemical potential $\mu = 0$, this analysis was performed in [136]. Another possible generalization would be to consider the case of massive dynamical

quarks presented in chapter 3. recall that this solution contains a scale (the mass of the sea quarks) and it would be very interesting to explore how it affects the results found here.

Turning on a suitable NSNS flat B field in the ABJM supergravity solution we get the so-called ABJ background, which is dual to a Chern-Simons matter theory with gauge group $U(N + M) \times U(N)$ [61]. The B field breaks parity in 2+1 dimensions. The embedding of flavor brane probes in the ABJ background has been analyzed in chapter 4 and the relation to the quantum Hall effect was doped out. It would be interesting to analyze possible quantum phase transitions in this ABJ system.

One of the main motivations of this work was the analysis of the effects of the dynamical quarks in the phase diagram of holographic compressible matter. We achieved this objective only partially since our backreacted background did not include the effect of the charge density on the flavor brane. On general grounds, one would expect having a Lifshitz geometry in the IR of such a background. Indeed, this is precisely what happens in the geometry recently found in [74], corresponding to an intersection of color D2-branes and flavor D6-branes. The study of the quantum phase transitions, as well as the collective excitations of the flavor brane, in this background is of great interest.

5.A   Appendix

5.A.1   Fluctuation analysis

Let us consider fluctuations of the gauge field A and the embedding function θ as in (5.5.65). We expand the induced metric g and the gauge field strength as:

$$g = g^{(0)} + g^{(1)} + g^{(2)} , \qquad F = F^{(0)} + f , \qquad (5.A.1)$$

where $g^{(0)}$ is the metric written in (5.2.1) and $F^{(0)}$ is the field strength of the unperturbed gauge connection (5.2.2), while $f = L^2 da$ and the first and second order induced metrics $g^{(1)}$ and $g^{(2)}$ are given by:

$$g_{ij}^{(1)} \, d\zeta^i \, d\zeta^j = \frac{L^2}{b^2} \left[2 \, \theta' \, (\lambda' \, dr + \partial_t \lambda \, dt + \partial_x \lambda \, dx) dr + \lambda \sin(2\theta) \, (d\psi + \cos\alpha \, d\beta)^2 \right]$$

$$g_{ij}^{(2)} \, d\zeta^i \, d\zeta^j = \frac{L^2}{b^2} \left[(\lambda' \, dr + \partial_t \lambda \, dt + \partial_x \lambda \, dx)^2 + \lambda^2 \cos(2\theta) \, (d\psi + \cos\alpha \, d\beta)^2 \right] . (5.A.2)$$

Let us next write the inverse of the zeroth-order DBI matrix $g^{(0)} + F^{(0)}$ as:

$$\left(g^{(0)} + F^{(0)} \right)^{-1} = \mathcal{G}^{-1} + \mathcal{J} , \qquad (5.A.3)$$

where $\mathcal{G}^{-1}$ is the symmetric part (the inverse open string metric) and $\mathcal{J}$ is the antisymmetric part. In order to write the different elements of $\mathcal{G}$ and $\mathcal{J}$ it is quite convenient to introduce the quantity Δ defined in (5.4.59). In terms of Δ, the equation for the embedding takes the form:

$$\partial_r \left[\frac{r^4 \, h \, \sin\theta}{\sqrt{\Delta}} \, \theta' \right] - r^2 \sin\theta \cos\theta \left[3 - 2b + \frac{\sqrt{\Delta}}{\sin\theta} \right] = 0 . \qquad (5.A.4)$$

Then, the non-vanishing components of the open string metric are:

$$\mathcal{G}^{tt} = -\frac{b^2 + r^2\, h\, \theta'^{\,2}}{L^2\, r^2\, h\, \Delta}\,, \qquad\qquad \mathcal{G}^{xx} = \mathcal{G}^{yy} = \frac{1}{L^2\, r^2}\,,$$

$$\mathcal{G}^{rr} = \frac{b^2\, r^2\, h}{L^2 \Delta}\,, \qquad \mathcal{G}^{\alpha\alpha} = \frac{b^2}{L^2\, q}\,, \qquad \mathcal{G}^{\beta\beta} = \frac{b^2}{L^2\, q\, \sin^2\alpha}\,,$$

$$\mathcal{G}^{\beta\psi} = -\frac{b^2\cos\alpha}{L^2\, q\, \sin^2\alpha}\,, \qquad \mathcal{G}^{\psi\psi} = \frac{b^2}{L^2 q}\left(\cot^2\alpha + \frac{q}{\sin^2\theta}\right). \qquad (5.A.5)$$

The only non-vanishing components of the antisymmetric tensor are:

$$\mathcal{J}^{tr} = -\mathcal{J}^{rt} = -\frac{d\, b}{L^2\, r^2\, \sin\theta\sqrt{\Delta}}\,. \qquad (5.A.6)$$

At second order in the fluctuations, the DBI action is:

$$S_{DBI}^{(2)} = -T_{D6}\int d^7\zeta\, e^{-\phi}\sqrt{-\det(g^{(0)} + F^{(0)})}\Bigg[\frac{1}{2}Tr\big(\mathcal{G}^{-1}g^{(2)}\big) + \frac{1}{8}\Big(Tr\big(\mathcal{G}^{-1}g^{(1)}\big) + Tr\big(\mathcal{J}f\big)\Big)^2$$

$$-\frac{1}{4}Tr\Big[\big(\mathcal{G}^{-1}\,g^{(1)}\big)^2 + \big(\mathcal{J}\,g^{(1)}\big)^2 + 4\,\mathcal{G}^{-1}\,g^{(1)}\,\mathcal{J}\,f + \big(\mathcal{G}^{-1}\,f\big)^2 + \big(\mathcal{J}\,f\big)^2\Big]\Bigg]. \qquad (5.A.7)$$

To evaluate this expression we use:

$$Tr\big(\mathcal{G}^{-1}\,g^{(2)}\big) = \frac{L^2}{b^2}\,\mathcal{G}^{mn}\partial_m\lambda\,\partial_n\lambda + \big(\cot^2\theta - 1\big)\lambda^2\,,$$

$$Tr\big(\mathcal{G}^{-1}\,g^{(1)}\big) = \frac{2L^2}{b^2}\,\theta'\,\mathcal{G}^{rr}\,\lambda' + 2\cot\theta\,\lambda\,,$$

$$Tr\Big[\big(\mathcal{G}^{-1}\,g^{(1)}\big)^2\Big] = \frac{4L^4}{b^4}\,\theta'^{\,2}\,(\mathcal{G}^{rr})^2\,(\lambda')^2 + 4\cot^2\theta\,\lambda^2 + \frac{2L^4}{b^4}\,\theta'^{\,2}\,\mathcal{G}^{rr}\,\mathcal{G}^{mn}\,\partial_m\lambda\partial_n\lambda\,, \qquad (5.A.8)$$

where the indices n and m run over the Minkowski and radial directions. After integrating over the internal angles, we get the following second-order DBI lagrangian:

$$\mathcal{L}_{DBI}^{(2)} = -\mathcal{N}r^2\sin\theta\sqrt{\Delta}\Bigg[\frac{1}{4}\mathcal{G}^{nm}\mathcal{G}^{pq}f_{mq}f_{np} + \frac{L^2}{2b^2}\Big(1 - \frac{L^2}{b^2}\theta'^2\mathcal{G}^{rr}\Big)\mathcal{G}^{mn}\partial_m\lambda\partial_n\lambda - \frac{1}{2}\lambda^2 \qquad (5.A.9)$$

$$+\frac{L^2}{b^2}\theta'\cot\theta\mathcal{G}^{rr}\lambda\partial_r\lambda - \frac{1}{2}\Big(\frac{A'_t\theta'}{\Delta}\Big)^2(\partial_t\lambda)^2 + \frac{A'_t\theta'}{\Delta}\mathcal{G}^{mn}\partial_m\lambda f_{nt} + \frac{b^2}{L^2}\frac{A'_t}{\Delta}\cot\theta\lambda f_{tr}\Bigg].$$

The WZ term at second order yields the following lagrangian density:

$$\mathcal{L}_{WZ}^{(2)} = \mathcal{N}\,r^2\,b\left[\frac{r}{b}\cos(2\theta)\,\lambda\partial_r\lambda + \Big(\cos(2\theta) - \frac{r}{b}\sin(2\theta)\,\theta'\Big)\lambda^2\right]. \qquad (5.A.10)$$

Let us now simplify these expressions. First of all, we should eliminate A'_t. With this purpose we notice that:

$$\frac{A'_t}{\Delta} = \frac{d}{b\,r^2\,\sin\theta\sqrt{\Delta}}\,. \qquad (5.A.11)$$

Secondly, we rewrite the terms with $\lambda \partial_r \lambda$ by integrating by parts and neglecting the total derivative generated in this process. In the WZ lagrangian we use

$$\frac{r^3}{b} \cos(2\theta)\, \lambda \partial_r \lambda \;=\; \left(\frac{r^3}{b} \sin(2\theta)\, \theta' \,-\, \frac{3}{2}\frac{r^2}{b}\cos(2\theta)\right) \lambda^2 \;+\; \partial_r\left[\frac{1}{2}\frac{r^3}{b}\cos(2\theta)\,\lambda^2\right] . \qquad (5.A.12)$$

The resulting WZ lagrangian takes the form:

$$\mathcal{L}^{(2)}_{WZ} \;=\; \mathcal{N}\, r^2\, b\left(1-\frac{3}{2b}\right)\cos(2\theta)\,\lambda^2 . \qquad (5.A.13)$$

In the DBI part, we first write:

$$\frac{r^4 \sin\theta h}{\sqrt{\Delta}}\, \theta'\,\cot\theta\,\lambda\partial_r\lambda \;=\; -\frac{1}{2}\partial_r\left(\frac{r^4 \sin\theta h}{\sqrt{\Delta}}\,\theta'\,\cot\theta\right)\lambda^2 \;+\; \partial_r\left(\frac{r^4 \sin\theta h}{2\sqrt{\Delta}}\,\theta'\,\cot\theta\,\lambda^2\right) . \qquad (5.A.14)$$

It follows that we can make the following substitution in $\mathcal{L}_{DBI}$:

$$\frac{r^4 \sin\theta h}{\sqrt{\Delta}}\,\theta'\,\cot\theta\,\lambda\partial_r\lambda \;\to\; -\partial_r\left(\frac{r^4 \sin\theta h}{2\sqrt{\Delta}}\,\theta'\,\cot\theta\right)\lambda^2 = -\partial_r\left(\frac{r^4 \sin\theta h}{2\sqrt{\Delta}}\,\theta'\right)\cot\theta\lambda^2 + \frac{r^4 h \theta'^2}{2\sin\theta\sqrt{\Delta}}\lambda^2 ,$$
$$(5.A.15)$$

which, after using eq. (5.2.13) for $\theta(r)$, can be written as:

$$\frac{r^4 \sin\theta h}{\sqrt{\Delta}}\,\theta'\,\cot\theta\,\lambda\partial_r\lambda \;\to\; \left(\left(b-\frac{3}{2}\right)r^2\cos^2\theta \,+\, r^2\frac{r^2 h \theta'^2 - \cos^2\theta\Delta}{2\sin\theta\sqrt{\Delta}}\right)\lambda^2 . \qquad (5.A.16)$$

Taking these results into account, it is straightforward to verify that the total lagrangian density $\mathcal{L}^{(2)} = \mathcal{L}^{(2)}_{DBI} + \mathcal{L}^{(2)}_{WZ}$ can be written as in (5.5.66).

Transverse fluctuations

We now consider fluctuations of the gauge field along the transverse direction y. It turns out that these fluctuations are coupled to those along the internal directions. Actually, we can write the following consistent ansatz:

$$A \;=\; L^2\left[A_t(r)\,dt \,+\, e^{-i\omega t + ikx}\,a_y(r)\,dy \,+\, e^{-i\omega t + ikx}\,a(r)\left(\cos\alpha\,d\beta \,+\, d\psi\right)\right] , \qquad (5.A.17)$$

where a_y and a are first-order fluctuations. The equation of motion for a_y is given by:

$$\partial_r\left(\frac{b^2\, r^2\, h\,\sin\theta}{\sqrt{\Delta}}\,a_y'\right) \,+\, \frac{\sin\theta}{r^2\, h\sqrt{\Delta}}\left[\omega^2(b^2 + r^2\, h\theta'^2) - k^2\, h\,\Delta\right]a_y$$
$$+\frac{2i\, k\, d\,\cot\theta}{r^2}\,\frac{b^2(2-q)\eta}{q(q+\eta)}\sqrt{\Delta}\,a \;=\; 0 , \qquad (5.A.18)$$

whereas that for a is:

$$\partial_r\left(\frac{b\, q\, r^4\, h}{\sin\theta\sqrt{\Delta}}\,a'\right) \,+\, 3b\, r^2\, a \,-\, \frac{b}{q}\, r^2\sin\theta\,\sqrt{\Delta}\,a \,+\, \omega^2\frac{q}{b}\frac{b^2 + r^2\, h\,\theta'^2}{\sin\theta\, h\,\sqrt{\Delta}}\,a$$
$$-k^2\frac{q}{b}\frac{\sqrt{\Delta}}{\sin\theta}\,a \,-\, \frac{2ikd\cot\theta}{r^2}\frac{(2-q)\eta}{(q+\eta)\,b}\sqrt{\Delta}\,a_y \;=\; 0 . \qquad (5.A.19)$$

For our purposes, it is enough to consider the fluctuations at zero momentum ($k = 0$). In this case the equation for a_y is decoupled from the internal fluctuation a and becomes:

$$\partial_r \left(\frac{b^2 \, r^2 \, h \, \sin \theta}{\sqrt{\Delta}} \, a_y' \right) + \frac{\sin \theta}{r^2 \, h \sqrt{\Delta}} \, \omega^2 (b^2 + r^2 \, h \, \theta'^2) \, a_y = 0 \; . \tag{5.A.20}$$

Explicitly, this equation for a_y can be written as:

$$a_y'' + \partial_r \log \left[\frac{\sqrt{d^2 + r^4 \sin^2 \theta}}{\sqrt{b^2 + r^2 \, h \, \theta'^2}} \, h \right] a_y' + \omega^2 \frac{b^2 + r^2 \, h \, \theta'^2}{b^2 \, r^4 \, h^2} \, a_y = 0 \; . \tag{5.A.21}$$

Let us expand this equation near $r = r_h$. First, we expand the embedding as in (5.2.23):

$$\theta(r) = \theta_h + \theta_h' \, (r - r_h) + \cdots \; , \tag{5.A.22}$$

where θ_h' is given by (see (5.2.24)):

$$\theta_h' = \frac{b \, r_h}{3} \frac{\sin \theta_h \, \cos \theta_h}{d^2 + r_h^4 \sin^2 \theta_h} \left[b \, r_h^2 + (3 - 2b) \sqrt{d^2 + r_h^4 \sin^2 \theta_h} \right] \; . \tag{5.A.23}$$

The coefficients of (5.A.21) will be expanded as:

$$\partial_r \log \left[\frac{\sqrt{d^2 + r^4 \sin^2 \theta}}{\sqrt{b^2 + r^2 \, h \, \theta'^2}} \, h \right] = \frac{1}{r - r_h} + d_1 \cdots$$

$$\omega^2 \frac{b^2 + r^2 \, h \, \theta'^2}{b^2 \, r^4 \, h^2} = \frac{A}{(r - r_h)^2} + \frac{c_2}{r - r_h} + \cdots \; , \tag{5.A.24}$$

where A, d_1, and c_2 are:

$$A = \frac{\omega^2}{9 \, r_h^2} \; ,$$

$$d_1 = -\frac{2}{r_h} \frac{d^2}{d^2 + r_h^4 \sin^2 \theta_h} + \frac{r_h^4 \sin \theta_h \, \cos \theta_h}{d^2 + r_h^4 \sin^2 \theta_h} \, \theta_h' - \frac{3 r_h}{2 b^2} \left(\theta_h' \right)^2 \; ,$$

$$c_2 = \frac{\left(\theta_h' \right)^2}{3 \, b^2 \, r_h} \, \omega^2 \; . \tag{5.A.25}$$

We now solve the equation of motion for a_y in a Frobenius series around $r = r_h$ as:

$$a_y(r) = (r - r_h)^\alpha \left(1 + \beta(r - r_h) + \cdots \right) \; , \tag{5.A.26}$$

where, for infalling boundary conditions, the exponent α is given by:

$$\alpha = -\frac{i\omega}{3 r_h} \; . \tag{5.A.27}$$

We will also perform a low frequency expansion by considering $k \sim \mathcal{O}(\epsilon)$ and $\omega \sim \mathcal{O}(\epsilon^2)$. Then one can show that $\beta \sim \mathcal{O}(\epsilon^2)$ and is given by:

$$\beta \approx -\alpha \, d_1 \; . \tag{5.A.28}$$

Let us now take the limits in opposite order. First, we consider the low frequency limit. At leading order, we can neglect the last term in (5.A.20) and write the equation for a_y as:

$$\partial_r \left(\frac{b^2\, r^2\, h\, \sin\theta}{\sqrt{\Delta}}\, a_y' \right) = 0 \ . \tag{5.A.29}$$

This equation can be immediately integrated:

$$a_y' = C\, \frac{\sqrt{\Delta}}{b^2\, r^2\, h\, \sin\theta} \equiv \frac{C}{G(r)} \ , \tag{5.A.30}$$

where C is a constant of integration and, in the last step, we have defined the function $G(r)$. This solution can be expanded near the horizon $r = r_h$ as:

$$a_y' = C\, \frac{r_h}{3b\, \sqrt{d^2 + r_h^4\, \sin^2\theta_h}}\, \frac{1}{r - r_h} + \cdots \ . \tag{5.A.31}$$

Let us now compare this near-horizon expansion with the one written in (5.A.26) for low frequency. First, we compute a_y' by direct differentiation of the expansion (5.A.26):

$$a_y' = \alpha(r - r_h)^{\alpha-1} \left(1 + \beta(r - r_h) + \cdots \right) + (r - r_h)^\alpha (\beta + \cdots) \ . \tag{5.A.32}$$

Taking into account that $\alpha \sim \mathcal{O}(\epsilon^2)$ and $\beta \sim \mathcal{O}(\epsilon^2)$, we get, at leading order in ϵ, that:

$$a_y' = \frac{\alpha}{r - r_h} + \cdots \ . \tag{5.A.33}$$

Thus, matching (5.A.33) and (5.A.31), we get that the constant C is given by:

$$C = \frac{3b}{r_h}\, \sqrt{d^2 + r_h^4\, \sin^2\theta_h}\, \alpha = -i\, \frac{b}{r_h^2}\, \sqrt{d^2 + r_h^4\, \sin^2\theta_h}\, \omega \ . \tag{5.A.34}$$

Therefore, we can write

$$a_y' = -\frac{i}{G(r)}\, \frac{b}{r_h^2}\, \sqrt{d^2 + r_h^4\, \sin^2\theta_h}\, \omega \ . \tag{5.A.35}$$

Let us now obtain the $\langle J_y\, J_y \rangle$ correlator from these results. The term in the lagrangian density depending on a_y is given by:

$$\mathcal{L}(a_y) = -\mathcal{N}\, r^2\, \sin\theta\, \sqrt{\Delta}\, \mathcal{G}^{yy}\, \mathcal{G}^{rr} \left(f_{yr} \right)^2 \ . \tag{5.A.36}$$

Taking into account that $f_{ry} = L^2\, a_y'$ and that:

$$r^2\, \sin\theta\, \sqrt{\Delta}\, \mathcal{G}^{yy}\, \mathcal{G}^{rr} = \frac{G(r)}{L^4} \ , \tag{5.A.37}$$

we arrive at:

$$\mathcal{L}(a_y) = -\mathcal{F} \left(a_y' \right)^2 \ , \tag{5.A.38}$$

where $\mathcal{F}$ is given by:

$$\mathcal{F} = -\mathcal{N}\, G(r)\,. \tag{5.A.39}$$

Therefore, the on-shell boundary action of a_y is:

$$S_{\text{on--shell}}(a_y) = \int d^3x\, \left(\mathcal{F}\, a_y\, a_y'\right)_{r\to\infty}\,. \tag{5.A.40}$$

The two-point function of the transverse currents, at zero momentum, is given by:

$$\langle J_y(k)\, J_y(-k)\rangle\Big|_{k=0} = \left(\mathcal{F}\, a_y'\right)_{r\to\infty} \equiv \mathcal{N}\,\Gamma_\omega\, i\,\omega\,, \tag{5.A.41}$$

where we have defined the quantity Γ_ω. From the explicit expressions of $\mathcal{F}$ and a_y, we get:

$$\mathcal{F}\, a_y' = \mathcal{N}\,\frac{b}{r_h^2}\,\sqrt{d^2 + r_h^4\,\sin^2\theta_h}\; i\omega\,. \tag{5.A.42}$$

Thus Γ_ω is given by:

$$\Gamma_\omega = \frac{b}{r_h^2}\,\sqrt{d^2 + r_h^4\,\sin^2\theta_h}\,. \tag{5.A.43}$$

From this result we get the DC conductivity, namely:

$$\sigma = \mathcal{N}\,\Gamma_\omega = \mathcal{N}\,\frac{b}{r_h^2}\,\sqrt{d^2 + r_h^4\,\sin^2\theta_h}\,, \tag{5.A.44}$$

which is just the result written in (5.4.62).

Chapter 6

Conclusions

In this thesis we have studied new cases of the AdS/CFT correspondence by using non-abelian T-duality and by including fundamental matter. Furthermore, we have constructed new holographic models of condensed matter physics systems.

- In the first chapter we gave a general introduction to the gauge/gravity duality. We reviewed the basic aspects of supergravity and T-duality. Moreover, we have introduced the AdS/CFT correspondence and how to add flavor to it. Finally, we commented on some applications of the AdS/CFT duality.

- In the second chapter we have reviewed some applications of non-abelian T-duality. In the context of type IIA/B supergravity, the non-abelian T-duality is used to obtain new solutions from previously know solutions. We have obtained new interesting cases of the gauge/gravity duality, in particular, new AdS_3 fixed points. Furthermore, we have analyzed the field theory duals of the new supergravity solutions, through the computation of some observables.

- In the third chapter we have constructed a new type IIA supergravity background with D6-branes sources, whose field theory dual corresponds to a generalization of the ABJM theory that includes unquenched massive flavors. We have analyzed several observables, and the results confirmed a RG flow between two fixed points at the IR and the UV

- In the fourth chapter we have constructed a supergravity solution based on the ABJM model that presents quantum Hall states. We have introduced D6-flavor branes with non-trivial worldvolume gauge fields. This set up allowed to have Hall states, and the filling fraction was computed. We have found supersymmetric Hall states for particular values of the parameters.

- In the fifth chapter we have obtained a supergravity solution based on the ABJM model, dual to a field theory exhibiting quantum phase transitions. The fundamental matter was introduced via D6-branes, and charge density was turned on. In the ABJM background, the fundamental matter undergoes a second order phase transition at zero charge density. In the partially backreacted ABJM solution, the phase transition becomes first order, and takes place at a finite value of the charge density.

Chapter 7

Summary

In this thesis we reviewed some results on the generalization of the gauge/gravity duality to new cases by using T-duality and by including fundamental matter, and we found applications to condensed matter physics. First, we constructed new supersymmetric solutions of type IIA/B and eleven-dimensional supergravity using non-abelian T-duality. Second, we obtained a type IIA supergravity solution with D6-sources, dual to an unquenched massive flavored version of the ABJM theory. Third, we studied a probe D6-brane with worldvolume gauge fields in the ABJM background, obtaining the dual description of a quantum Hall system. Finally, we considered a system of a probe D6-brane in the ABJM background and studied quantum phase transitions of its dual theory.

Contextualization

In the twentieth century it took place the consolidation of two fundamental developments in physics. On the one hand, the theory of general relativity was constructed to explain gravity, one of the four fundamental forces of nature, and became very successful describing macroscopic physics. On the other hand, the birth of quantum field theory gave a natural framework for elementary particle physics, which explains the other three fundamental forces of nature (weak, strong and electromagnetic) obtaining a very accurate description of the subatomic physics. The unification of these two developments is one of the most important problems of current physics. String theory is, nowadays, the best candidate to perform such unification.

Within string theory it was discovered the existence of new objects, called D-branes. D-branes are non-perturbative solutions consisting of hyperplanes where open strings can end. These open strings describe the dynamics of the branes, and their massless modes realize a gauge theory on the worldvolume of the brane. Alternatively, D-branes can be obtained as solitonic objects in the gravitational description of closed strings. The closed string interact with the branes, as they are massive objects. This open/closed dual description points towards the existence of a duality between gauge theories and string theory.

The study of D3-branes in type IIB supergravity led Maldacena to conjecture in 1997 the AdS/CFT correspondence [10]. This proposal states that the D3-branes in flat space, after taking the decoupling limit, admit two equivalent descriptions, dual to each other, one being the closed string description, corresponding to string theory on $AdS_5 \times S^5$, and the

other being the open string description, corresponding to $3+1$ dimensional $\mathcal{N} = 4$ $SU(N)$ SYM conformal field theory. The two descriptions are dual to each other in the sense that they describe the same physical theory, even if they are apparently different descriptions.

The usefulness of the conjecture lies on the fact that it is a strong/weak duality, *i.e.*, if on one side of the duality the coupling constant is weak, on the other side it is strong and vice versa. This means that if we want to compute observables in a strong coupling region of a quantum field theory, we can consider its supergravity description, were the coupling constant is weak, and perform the computations. Then, performing an easy computation in classical supergravity we can obtain results in the strong coupling regime of a quantum field theory, where other tools are limited or inexistent.

Even if the conjecture can be formulated at different levels of generality, the most useful formulation is the weak one. In its original form, it states that $\mathcal{N} = 4$ $SU(N)$ SYM in the t'Hooft limit ($N \to \infty$) and strong coupling regime ($\lambda \to \infty$) is dual to classical type IIB supergravity on the background $AdS_5 \times S^5$. This formulation is the one used along the thesis.

Soon after Maldacena's paper, new cases of the duality appeared, extending it to non-conformal and less supersymmetric solutions. Nowadays, the gauge/gravity duality has vastly extended and it has found applications in many areas: quantum chromodynamics, condensed matter physics, astrophysics, cosmology, black holes, quantum information, etc.

Non-abelian T-duality

Abelian T-duality is another important duality in string theory. It relates two apparently different theories that have an $U(1)$ isometry, but that describe the same physical theory. For example, type IIA/B string theories in Minkowski spacetime with a coordinate compactified on a circle are related by T-duality. Locally, T-duality is dictated by the Buscher rules [11], and globally it corresponds to an exchange of the Chern number of the $U(1)$ fibration and the H_3 flux on the base of the fibration [13].

On the other hand, non-abelian T-duality (NATD) was introduced in string theory in the eighties as a generalization of T-duality to solutions with non-abelian isometry groups. Locally, there is a generalization of the Buscher rules for the non-abelian case. Globally, the transformation rules are not known, and we can not access to all the features of the dual solution. This implies that we can not know all the details of the dual field theories of these new supergravity backgrounds. Along this thesis, we considered the particular case in which the isometry group is $SU(2)$.

The Buscher rules are derived from the T-dual action, via the following procedure. The idea is to start from the sigma model action for the NSNS fields, and gauge the $U(1)$ isometry $\partial \to D = \partial + A$ by introducing a gauge field A. Then, a Lagrange multiplier term is introduced, ensuring that the gauge field is not dynamical. Finally, integrating out the gauge field we are left with the dual action. The Lagrange multipliers act as the new coordinates.

The basic differences between abelian T-duality and NATD are:

- The abelian T-duality is an involution, *i.e.*, performing T-duality twice the original background is recovered. Nevertheless, NATD is not an involution, as in the NATD background the isometries are no longer present.

- For compact commuting isometries one may argue that T-duality is actually a true symmetry of string theory. There is no analogous statement for the non-abelian cases.

- The global properties of the abelian T-duality are understood. Nevertheless, for the NATD they are not known yet.

- In the abelian case we flip between type IIA and type IIB, but in the non-abelian case we might change or stay within the same theory. If the dimension of the isometry group G is odd, we flip from type IIA and II B, and if the dimension is even, we stay within the same theory.

Using this technique, in chapter 2 we obtained new solutions of type IIA/B supergravities. The idea is to obtain new solutions that are interesting in the context of the AdS/CFT correspondence. In summary, we started from a set of supergravity solutions in type IIB supergravity. In particular some of these solutions have an AdS_3 factor and are supersymmetric. All these solutions have an $SU(2)$ isometry in the compact part, and we performed non-abelian T-duality along these directions. As a result, we obtained new solutions of type IIA supergravity, and in particular new solutions with an AdS_3 factor, supersymmetric and without singularities. Moreover, starting from one of these solutions, we performed abelian T-duality back to type IIB, obtaining a new solution with an AdS_3 factor, supersymmetric, without singularities and with all supergravity fields turned on. Furthermore, the new solutions of type IIA supergravity are uplifted to eleven-dimensional supergravity.

We also proceeded to analyze the dual field theories of these new supergravity solutions. First, we compute the Page charges before and after the NATD, obtaining how the brane content of the solution changes. Moreover, we computed the central charges before and after the NATD. The quotient between the central charges before and after the NATD depends on the volume of the compact manifold after the NATD. But as the global properties are not known, neither is the volume of the involved manifolds. Finally, we also computed the entanglement entropy and the Wilson loops. In both cases, we obtained that the quotient before and after the NATD depend on global properties of the new solution, and for the solutions with non-trivial renormalization group flow, the quotient is constant along the flow.

Adding flavor to the AdS/CFT duality

In the original formulation of the AdS/CFT correspondence, the quantum field theory only has fields in the adjoint representation (in terms of QCD, only has gluons). However, in order to obtain applications in phenomenological theories, it is interesting to add matter in the fundamental representation (in terms of QCD, quarks). In the gravity side this can be achieved by adding a new type of branes, called flavor branes. If the number of flavor branes is small compared to the number of color branes, then the introduction of the new flavor branes do not modify the initial geometry. This simplification is known as the probe brane approximation. For example, in the solution $AdS_5 \times S^5$, one way to add flavor is through D7 branes extended along $AdS_5 \times S^3 \subset AdS_5 \times S^5$.

However, if the full effect of the fundamental matter has to be taken into account, then the deformation that the flavor branes create on the geometry must be considered. In this

case, a new solution must be obtained to the full problem of supergravity plus D6-brane sources. If we consider N_f flavor branes and N_c color branes, the gravity system will be modified by the flavor branes when:

$$N_c, N_f \to \infty \ , \quad N_f/N_c = constant \ . \tag{7.0.1}$$

This limit is known as the Veneziano limit. In general, a stack of flavor branes in a specific position of the geometry implies the presence of δ-functions, the loss of symmetries and dependence in several variables. In order to avoid these difficulties, we can considered the smearing technique. It consists in distributing homogeneously the flavor branes (similar to a volumic distribution of electric charge in electromagnetism, in opposition to a point charge). In this way we avoid δ-functions, we recover symmetries and the dependence only in one variable. Thus, the problem becomes easier. For a detailed review, see [73].

In chapter 3 of this thesis, we obtained a generalization of the ABJM theory which includes unquenched massive fundamental matter, using the smearing procedure. Let us review first the ABJM theory and how to introduce quenched flavor to it.

The ABJM theory

In the same way that the $\mathcal{N} = 4$ $SU(N)$ SYM theory is the best understood example of the $\text{AdS}_5/\text{CFT}_4$ correspondence, the ABJM theory is the best understood example of the $\text{AdS}_4/\text{CFT}_3$ correspondence.

In 2008 Aharony, Bergman, Jafferis and Maldacena (ABJM) [51] constructed a $2 + 1$ dimensional $\mathcal{N} = 6$ superconformal Chern-Simons-matter theory with gauge group $U(N) \times U(N)$ and opposite levels k and $-k$. The bosonic matter content of the theory is four complex scalar fields C_I ($I = 1, 2, 3, 4$) transforming in the bifundamental representation $(\mathbf{N}, \bar{\mathbf{N}})$ of the gauge group and their corresponding complex conjugate fields in the anti-bifundamental representation $(\bar{\mathbf{N}}, \mathbf{N})$.

The R symmetry of the theory is $U(4)_R = U(1)_R \times SU(4)_R$. The scalars C_I are in the fundamental $\mathbf{4}$ representation of $SU(4)_R$, and have charge $+1$ under $U(1)_R$.

One can take the t'Hooft limit in the ABJM theory, which is given by:

$$N, \ k \to \infty \quad , \quad \lambda := \frac{N}{k} = fixed \ , \tag{7.0.2}$$

where λ is the t'Hooft coupling. It turns out that in the large N limit, the degrees of freedom scale as $N^{3/2}$, a different behavior than in $\mathcal{N} = 4$ $SU(N)$ SYM, which scales as N^2.

Let us now consider the gravity dual description to the ABJM field theory. The conjecture in its strong version states that the ABJM field theory is dual to M2-branes on a $\mathbb{C}^4/\mathbb{Z}_n$ singularity in M theory. In the large N limit, the gravitational background becomes $AdS_4 \times S^7/\mathbb{Z}_k$ in eleven-dimensional supergravity. The $S^7/\mathbb{Z}_k$ space is a lens space, *i.e.*, a bundle with base $\mathbb{CP}^3$ and fiber S^1, and the possible fibrations are classified by an integer, in this case k. When the Chern-Simons level k is large ($k^5 \gg N$) the size of the fiber is small and the system is better described in terms of type IIA supergravity, after performing a dimensional reduction to ten dimensions along the Hopf fiber S^1. In the type IIA description, the

geometry is $AdS_4 \times \mathbb{CP}^3$, where $\mathbb{CP}^3$ inherits the natural metric from the total space $S^7/\mathbb{Z}_k$, known as the Fubini-Study metric. The solution also has a constant dilaton, and F_2 and F_4 forms.

The $\mathbb{CP}^3$ manifold with the Funibi-Study metric has an isometry group $U(4)$. This precisely corresponds with the R-symmetry of the ABJM field theory $U(4)_R = U(1) \times SU(4)$. The manifold $\mathbb{CP}^3$ has a spin structure, and in particular a Kähler structure with Kähler form J. The dilaton ϕ and the F_2 and F_4 forms are:

$$e^\phi = \frac{2k}{L} , \quad F_2 = 2kJ , \quad F_4 = \frac{3k}{2}L^2\Omega_{AdS_4} , \quad (7.0.3)$$

where Ω_{AdS_4} is the volume form of AdS_4 and L is the radius of AdS_4, $L^4 = 2\pi^2 N/k$.

This description of the ABJM theory in type IIA supergravity is the one considered in chapters 3, 4 and 5 of this thesis.

The ABJM theory can be generalized by including fundamental matter. The easiest way of including fundamental matter is through the probe brane approximation. If we consider the type IIA supergravity description of the ABJM theory, the addition of fundamental matter can be obtained by including N_f probe D6-branes [78], [79], embedded in $AdS_4 \times \mathbb{RP}^3 \subset AdS_4 \times \mathbb{CP}^3$, with N_f fixed in the limit $N_c \to \infty$. The resulting field theory is the original ABJM theory plus a hypermultiplet of fundamental matter in each node of the quiver diagram (see Fig. 1.2), preserving $\mathcal{N} = 3$ supersymmetry of the original $\mathcal{N} = 6$. The hypermultiplets transform in the fundamental representation $(\mathbf{N}, 1)$, $(1, \mathbf{N})$ and antifundamental representation $(\bar{\mathbf{N}}, 1)$, $(1, \bar{\mathbf{N}})$.

Unquenched massive flavored ABJM

In chapter 3 of this thesis we constructed a new solution to type IIA supergravity with flavor D6-branes, in the Veneziano limit, using the smearing technique.

Starting from the ABJM theory in the type IIA supergravity description, the $\mathbb{CP}^3$ manifold is expressed as a fibration of a S^2 sphere over a S^4 base. We consider a deformation along the fiber, which implies that the F_2 form is not closed any more, and its Bianchi identity is not vanishing, but proportional to the number of flavor branes N_f. These flavor branes are smeared, in such a way that the equations of motion only depend on the holographic coordinate and there are no δ-functions. Moreover, we imposed supersymmetry and obtained a set of BPS equations from the condition that the gravitino and dilatino vanish. The BPS equations are reduced to a single second order equation, that we proceed to solve numerically.

The interpretation of the dual field theory to this supergravity solution is the following. In the UV, the mass of the fundamental matter is negligible, and we recover the massless unquenched flavored solution of [75], which is a conformal fixed point. In the IR, the mass of the fundamental matter becomes very large and the fundamental matter decouples, and we are left with the pure ABJM theory, which is also a conformal fixed point. Thus, the complete solution smoothly interpolates between the two fixed points at the IR and UV.

Using the supergravity solution we computed some interesting observables of the dual field theory. First, we obtained the entanglement entropy for a circular surface. For that

purpose, we used the Ryu-Takayanagi holographic prescription [95]. It consists in computing the minimal surface that is hanging in the bulk and is attached to the circle at the boundary. Moreover, using the Liu-Mezei prescription, [137] we obtained a function that verifies the F theorem (the analog of the c theorem in 2+1 dimensions), *i.e.*, a function that monotonically decreases from the UV to the IR and that matches the free energy at the fixed points. Furthermore, we also obtain the two-point function for high dimensional operators, we compute the Wilson loop, and the meson spectrum. In summary, all the observables computed indicate the presence of a renormalization group flow between two fixed points at the UV and IR. This flux is smooth and monotonic, without phase transitions.

Holographic fractional Hall effect

In chapter 4 we construct a solution to type IIA supergravity based on the ABJM theory, which is dual to a quantum field theory that presents fractional Hall states.

Starting from the type IIA description of the ABJM theory, we introduced a probe D6-brane and studied its properties. We turned on gauge fields in the worldvolume of the brane. First, we switched on a gauge field on the internal compact part of the worldvolume of the brane. This gauge field is quantized and breaks parity. The parity breaking is demonstrated via helicity dependence of the meson spectrum. We also turned on gauge fields in the Minkowski part of the worldvolume of the brane which in the field theory correspond to electric and magnetic fields, currents and charge density. Once this electromagnetic set up is introduced, we compute the conductivities. For generic values of the parameters, the D6-branes reach the IR (black hole embedding) and in the field theory this corresponds to a gapless state. If the parameters verify a specific condition, we can have branes that do not reach the IR (Minkowski embeddings) and it corresponds to gapped states. The parity breaking due to the internal flux allows to have transverse current, and Hall states. Using the supergravity solution we can compute the filling fraction. Curiously, for specific values of the parameters we found supersymmetric solutions dual to Hall states.

Finally, this computations are generalized to the case in which the solution is a version of the ABJM theory which includes unquenched massless fundamental matter of [75] and also with temperature [136].

Quantum phase transitions

In chapter 5 of this thesis we constructed a gravity model and studied the quantum phase transitions of its dual field theory.

Quantum phase transitions are transitions that happen at zero temperature and that are induced by quantum fluctuations. They occur when some control parameters are varied and tuned to critical values. In this case, we constructed a system with charge density, and phase transitions occur when varying the charge density. Starting from the type IIA description of the ABJM theory, we add a probe D6-brane. In its worldvolume we turn on a gauge field which is dual to a charge density. The D6-brane undergoes a transition where the topology of the embedding changes from a black hole embedding when the charge density is grater than zero, to a Minkowski embedding when the charge density is vanishing. This transition is identified in the dual field theory with a second order phase transition,

and we compute the critical exponents. The scaling behavior near this critical point has multiplicative logarithmic corrections.

Furthermore, we generalize this construction to the version of the ABJM theory which includes unquenched massless fundamental matter of [75]. When the dynamical effect of the flavor is taken into account, the phase transition becomes first order. In this case, the phase transition happens at a charge density greater than zero. In order to characterize it, we compute the discontinuity of some physical quantities as a function of the flavor.

Chapter 8

Resumen

En esta tesis hemos generalizado la correspondencia AdS/CFT a nuevos casos mediante el uso de dualidad T y mediante la inclusión de materia fundamental. Además, se encontraron nuevas aplicaciones a la física de la materia condensada. En primer lugar, se construyeron nuevas soluciones supersimétricas de supergravedad de tipo IIA/B y de once dimensiones empleando la dualidad T no abeliana. En segundo lugar, se obtuvo una nueva solución de supergravedad de tipo IIA con D6-branas, que es dual a una versión de la teoría ABJM que incluye materia fundamental masiva y sus efectos dinámicos. En tercer lugar, se estudió una D6-brana de prueba con campos gauge no triviales en la teoría ABJM, obteniendo una descripción dual de un sistema Hall cuántico. Finalmente, se consideró una D6-brana de prueba en la teoría ABJM y se estudiaron las transiciones de fase cuánticas de su teoría de campos dual.

Contextualización

En el siglo XX se consolidan dos grandes ramas de la física, destinadas a explicar los aspectos más fundamentales de la naturaleza. Por una parte, se sedimenta la teoría de la relatividad general, que describe la fuerza de la gravedad, obteniendo resultados satisfactorios en la explicación del ámbito macroscópico. Por otra parte, se establece la teoría cuántica de campos, base del modelo estándar de la física de partículas elementales, que describe las fuerzas electromagnética, débil y fuerte, y que explica con gran precisión la física del microcosmos. La unificación de estas dos ramas es uno de los problemas abiertos más importantes de la física actual. La teoría de cuerdas es hoy en día la mejor candidata para llevar a cabo dicha unificación, y así incluir bajo un mismo marco teórico las cuatro fuerzas fundamentales.

Dentro de la teoría de cuerdas se descubrieron objetos de carácter no perturbativo llamados D-branas. Por una parte, las D-branas son soluciones que consisten en hiperplanos donde las cuerdas abiertas apoyan sus extremos. Estas cuerdas abiertas describen la dinámica de las branas, y los modos de masa cero se corresponden con una teoría gauge. Por otra parte, las branas se pueden describir como objetos gravitatorios no perturbativos desde el punto de vista de las cuerdas cerradas. Esta doble descripción de cuerdas abiertas/cerradas apunta hacia una relación entre teorías gauge y teorías de cuerdas.

En particular, el estudio de las D3-branas en teoría de cuerdas de tipo IIB condujo a la conjetura de Maldacena en 1997. Esta conjetura establece que la teoría cuántica de campos

conforme $\mathcal{N} = 4$ $SU(N)$ super-Yang-Mills es dual a la teoría de cuerdas de tipo IIB en la geometría $AdS_5 \times S^5$. Se dice que las dos teorías son duales en el sentido de que se trata de dos descripciones alternativas de la misma teoría física, aunque aparentemente sean muy diferentes.

La dualidad resulta de gran utilidad porque se trata de una dualidad débil/fuerte, es decir, es una dualidad en la que si en una teoría la constante de acoplamiento es fuerte, entonces en su descripción dual la constante de acoplamiento es débil. De este modo, la dualidad permite realizar cálculos en teorías de campos en régimen de acoplamiento fuerte, pasando a su descripción dual en términos de gravedad clásica, donde los cálculos son más fácilmente tratables.

Aunque la dualidad se puede formular en diferentes niveles de generalidad, la formulación más útil es su versión débil, que es la que se ha empleado en el desarrollo de esta tesis. En su forma original, ésta establece que $\mathcal{N} = 4$ $SU(N)$ SYM en el límite de t'Hooft ($N \to \infty$) y régimen de acoplamiento fuerte ($\lambda \to \infty$) es dual a supergravedad clásica de tipo IIB en la solución $AdS_5 \times S^5$.

Tras la publicación de Maldacena pronto aparecieron nuevos ejemplos de la dualidad gravedad/gauge extendiéndose a casos en los que la teoría de campos no es conforme y que preservan menos supersimetrías. Hasta la actualidad, el campo de la dualidad holográfica ha crecido enormemente, y ha encontrado aplicaciones en muchas áreas: cromodinámica cuántica, física de la materia condensada, astrofísica, cosmología, agujeros negros, información cuántica, etc.

Dualidad T no abeliana

La dualidad T abeliana es otra dualidad importante en el ámbito de la teoría de cuerdas. Ésta relaciona dos teorías que poseen una isometría $U(1)$, aparentemente diferentes, pero que describen la misma teoría física. Por ejemplo, las teorías de cuerdas de tipo IIA y IIB en el espacio de Minkowski con una coordenada compactificada en un círculo, están relacionadas por dualidad T. Localmente, la dualidad T está dictada por las reglas de Buscher [11], y globalmente corresponde a un intercambio del número de Chern de la fibración del círculo y el flujo de H_3 en su base [13].

Por otra parte, la dualidad T no abeliana fue introducida a finales de los años ochenta como una generalización de la dualidad T a soluciones con grupos de isometría no abelianos. Localmente, existe una generalización de las reglas de Buscher para el caso no abeliano. Globalmente, las reglas de la transformación no se conocen, y por tanto no se podrá acceder a todas las características de la solución dual. Esto implica que tampoco podrán conocerse todos los detalles de las teorías de campos duales a esas soluciones de supergravedad. A lo largo de esta tesis se ha considerado el caso particular en el que el grupo de isometrías es $SU(2)$.

Las reglas de Buscher se obtienen a través de la acción dual T mediante el siguiente procedimiento. Primero, se empieza desde el modelo sigma para los campos NSNS, y se hace gauge la isometría mediante la introducción de un campo gauge A y las correspondientes derivadas covariantes $\partial \to D = \partial + A$. A continuación, se introduce un término que actúa

como multiplicador de Lagrange, que introduce la condición de que el campo gauge A es no dinámico. Finalmente, integrando el campo gauge A se obtiene la acción dual T.

Las diferencias fundamentales entre dualidad T abeliana y no abeliana son:

- La dualidad T abeliana es una involución, es decir, realizando dualidad T dos veces se recupera la solución inicial. Sin embargo, la dualidad T no abeliana no es una involución, pues en la solución dual las isometrías iniciales ya no están presentes.

- Para isometrías compactas que conmutan se puede argumentar que la dualidad T es una simetría en teoría de cuerdas. Sin embargo, no existe un argumento similar para la dualidad T no abeliana.

- Las propiedades globales de la dualidad T abeliana son conocidas, mientras que las de la dualidad T no abeliana no se conocen.

- La dualidad T abeliana pasa de supergravedad de tipo IIA a IIB o viceversa, pero la dualidad T no abeliana puede cambiar de teoría o permanecer en la misma. Más precisamente, si el grupo de isometrías es de dimensión impar, se cambia de teoría, si es de dimensión par, se permanece en la misma teoría.

Empleando estas reglas en supergravedad de tipo IIA y IIB, se pueden obtener nuevas soluciones que podrían tener especial interés en la correspondencia AdS/CFT. En el capítulo 2 de esta tesis se construyeron nuevas soluciones empleando esta técnica. En resumen, partimos de varias soluciones en supergravedad de tipo IIB, entre las cuales tienen especial interés las soluciones con factores AdS_3 supersimétricas. Las soluciones completas tienen isometrías $SU(2)$ en la parte compacta, y efectuamos dualidad T no abeliana a lo largo de esas direcciones. Como resultado, obtuvimos nuevas soluciones en supergravedad de tipo IIA, en particular nuevas soluciones AdS_3 supersimétricas y sin singularidades. Además, partiendo de una de estas nuevas soluciones, realizamos dualidad T abeliana para obtener una nueva solución en supergravedad de tipo IIB con un factor AdS_3, supersimétrica, sin singularidades y con todos los campos de supergravedad encendidos. Además, las nuevas soluciones en supergravedad de tipo IIA se suben a supergravedad de once dimensiones, obteniendo también nuevas soluciones.

Además de obtener nuevas soluciones en supergravedad, hemos procedido a analizar sus teorías de campos duales de acuerdo con la correspondencia AdS/CFT. En primer lugar, calculamos las cargas de Page antes y después de la dualidad T, obteniendo cómo cambia el contenido de branas de las soluciones. Esto permite extraer alguna conclusión acerca de las teorías de campos duales a las nuevas soluciones. Además, calculamos las cargas centrales antes y después de la dualidad T. El cociente entre las cargas centrales antes y después de la dualidad T queda en función del volumen de la variedad compacta después de la dualidad T, pues al no conocerse las propiedades globales de estas nuevas soluciones, tampoco se conoce el volumen de las variedades involucradas. Finalmente, también calculamos la entropía de entrelazamiento y círculos de Wilson. En ambos casos, obtuvimos que el cociente antes y después de la dualidad T depende de características globales de la nueva solución, y que en las soluciones con grupo de renormalización no trivial, dicho cociente es constante a lo largo del flujo.

Adición de sabor a la dualidad AdS/CFT

En la formulación original de la correspondencia AdS/CFT, la teoría cuántica de campos únicamente presenta campos en la representación adjunta (en términos de QCD, sólo posee gluones). Sin embargo, con objetivo de obtener aplicaciones fenomenológicas, resulta interesante añadir campos de materia en la representación fundamental (en términos de QCD, quarks). En el sector gravitatorio esto se puede conseguir añadiendo un tipo adicional de branas, llamadas branas de sabor. Si el número de branas de sabor que añadimos es pequeño comparado con las branas de color, entonces la introducción de las branas de sabor no modifica la geometría inicial. Esta aproximación se llama aproximación de brana de prueba. Por ejemplo, en la solución $AdS_5 \times S^5$, una forma de añadir sabor es mediante branas D7 de prueba extendidas a lo largo de $AdS_5 \times S^3 \subset AdS_5 \times S^5$.

Sin embargo, si se quiere tener en cuenta el efecto completo de la materia fundamental, entonces debe considerarse la deformación que las branas de sabor generan sobre la geometría inicial. En este caso, hay que obtener una nueva solución al problema conjunto de supergravedad con fuentes (las branas de sabor). Si se toma un número de branas de sabor N_f y un número de branas de color N_c, el sistema gravitatorio se verá modificado por la presencia de las branas de sabor cuando:

$$N_c, N_f \to \infty , \quad N_f/N_c = constante . \tag{8.0.1}$$

Este límite se conoce como el límite de Veneziano. De forma genérica, la presencia de una pila de branas de sabor en un punto de la geometría implica la presencia de funciones δ, rotura de simetrías y dependencia en varias variables en el problema a resolver. Para evitar estas dificultades, se considera el método de distribución uniforme, que consiste en repartir de forma homogénea las branas de sabor (similar a una distribución volúmica de carga eléctrica en electromagnetismo clásico, en oposición a una carga puntual). De esta forma, se evitan las funciones δ, se recuperan las simetrías y la dependencia en una sola variable. Así, el problema se vuelve más accesible. Para una revisión detallada de este procedimiento de distribución uniforme, véase [73].

En el capítulo 3 de esta tesis, se obtuvo una generalización de la teoría ABJM que incluye materia fundamental masiva y sus efectos dinámicos mediante el método de distribución uniforme. Recordemos en primer lugar qué es la teoría ABJM y cómo introducir sabor en ella mediante branas de prueba.

La teoría ABJM

Del mismo modo que la teoría $\mathcal{N} = 4$ $SU(N)$ SYM es el ejemplo mejor entendido de la correspondencia AdS_5/CFT_4, la teoría ABJM es el ejemplo mejor entendido de la correspondencia AdS_4/CFT_3.

En 2008 Aharony, Bergman, Jafferis y Maldacena (ABJM) [51] construyeron una teoría en $2 + 1$ dimensiones, $\mathcal{N} = 6$ superconforme, de tipo Chern-Simons con materia, con grupo gauge $U(N) \times U(N)$ y niveles opuestos k y $-k$. El contenido de materia bosónico de la teoría son cuatro campos escalares complejos C_I ($I = 1, 2, 3, 4$) que transforman en la representación

bifundamental $(\mathbf{N}, \bar{\mathbf{N}})$ del grupo gauge y sus correspondientes campos complejos conjugados que transforman en la representación anti-bifundamental $(\bar{\mathbf{N}}, \mathbf{N})$.

La simetría R de la teoría es $U(4)_R = U(1)_R \times SU(4)_R$. Los escalares C_I transforman en la representación fundamental $\mathbf{4}$ de $SU(4)_R$, y tienen carga $+1$ bajo $U(1)_R$.

El límite de t'Hooft de la teoría ABJM viene dado por:

$$N,\ k \to \infty \quad , \qquad \lambda := \frac{N}{k} = constante\ , \tag{8.0.2}$$

donde λ es la constante de t'Hooft. En el límite de t'Hooft los grados de libertad de la teoría ABJM escalan como $N^{3/2}$, a diferencia de la teoría $\mathcal{N} = 4\ SU(N)$ SYM, donde escalan como N^2.

Consideremos ahora el dual gravitatorio de la teoría de campos ABJM. La conjetura en su versión fuerte establece que la teoría de campos ABJM es dual a M2 branas en la singularidad $\mathbb{C}^4/\mathbb{Z}_n$ en teoría M. En el límite $N \to \infty$, esto corresponde a $AdS_4 \times S^7/\mathbb{Z}_k$ en supergravedad en once dimensiones. El espacio $S^7/\mathbb{Z}_k$ es un espacio lenticular, es decir, un fibrado con base $\mathbb{CP}^3$ y fibra S^1, y las posibles fibraciones están clasificadas por un entero, precisamente k. Cuando el nivel de Chern-Simons k es grande ($k^5 \gg N$) el tamaño de la fibra es pequeño y el sistema está mejor descrito en términos de supergravedad de tipo IIA mediante reducción dimensional a diez dimensiones a lo largo de la fibra de Hopf S^1. En la descripción en supergravedad de tipo IIA, la geometría es $AdS_4 \times \mathbb{CP}^3$, donde $\mathbb{CP}^3$ hereda la métrica natural del espacio total $S^7/\mathbb{Z}_k$, y esta métrica se conoce como métrica de Fubini-Study. La solución también posee un dilatón constante y formas no triviales F_2 y F_4.

El grupo de isometrías de $\mathbb{CP}^3$ con la métrica de Fubini-Study es $U(4)$. Éste precisamente se corresponde con la simetría R de la teoría de campos ABJM, *i.e.*, $U(4)_R = U(1) \times SU(4)$.

La variedad $\mathbb{CP}^3$ tiene una estructura de Spin, y en particular una estructura Kähler con forma de Kähler J. En la descripción de la teoría ABJM en supergravedad de tipo IIA, el dilatón y las formas F_2 y F_4 vienen dadas por:

$$e^\phi = \frac{2k}{L}\ , \qquad F_2 = 2kJ\ , \qquad F_4 = \frac{3k}{2}L^2\Omega_{AdS_4}\ , \tag{8.0.3}$$

donde Ω_{AdS_4} es la forma de volumen de AdS_4 y L es el radio de AdS_4, $L^4 = 2\pi^2 N/k$.

Esta descripción de la teoría ABJM en supergravedad de tipo IIA es la que se ha empleado en los capítulos 3, 4 y 5 de esta tesis.

La teoría ABJM se puede generalizar incluyendo materia fundamental. La forma más sencilla de incluir materia fundamental es mediante la aproximación de brana de prueba. Si consideramos la descripción de la teoría ABJM en supergravedad de tipo IIA, la adición de materia fundamental se puede obtener incluyendo N_f D6-branas de prueba [78], [79], encajadas en $AdS_4 \times \mathbb{RP}^3 \subset AdS_4 \times \mathbb{CP}^3$, con N_f fijo en el límite $N_c \to \infty$. La teoría de campos resultante es la teoría ABJM original con un hipermultiplete de materia fundamental en cada nodo del diagrama quiver (tal como se muestra en la Fig. 1.2) preservando $\mathcal{N} = 3$ supersimetría de la original $\mathcal{N} = 6$. Los hipermultipletes transforman en la representación fundamental $(\mathbf{N}, 1)$, $(1, \mathbf{N})$ y antifundamental $(\bar{\mathbf{N}}, 1)$, $(1, \bar{\mathbf{N}})$.

ABJM con sabor masivo y sus efectos dinámicos

En el capítulo 3 de esta tesis se construyó una nueva solución de supergravedad de tipo IIA con D6-branas de sabor, en el límite de Veneziano, empleando la técnica de distribución uniforme.

Partiendo de la solución ABJM en términos de supergravedad de tipo IIA, se describe a la variedad $\mathbb{CP}^3$ como una fibración de una S^2 con base S^4. A continuación, se considera una deformación a lo largo de la fibra, lo cual permite que la forma F_2 sea no cerrada, y así su identidad de Bianchi no es cero, sino que es proporcional al número de branas de sabor. Estas branas se toman distribuidas uniformemente, de tal forma que las ecuaciones del movimiento sólo dependen de la coordenada holográfica y no hay funciones δ. Además, para obtener la solución se impone supersimetría, y se obtienen unas ecuaciones BPS de la condición de que las variaciones del gravitino y el dilatino son cero. Las ecuaciones BPS se reducen a una sola ecuación de segundo orden, que procedemos a resolver numéricamente.

La interpretación de la teoría de campos dual a esta solución gravitatoria es la siguiente. En el ultravioleta, la masa de la materia fundamental se vuelve despreciable, y recuperamos la solución sin masa de [75], que es un punto fijo conforme. En el infrarrojo, la masa de la materia fundamental se vuelve muy grande, y la materia fundamental desacopla, dejándonos puramente con la teoría ABJM, que también es un punto fijo conforme. Por tanto, la solución completa interpola suavemente entre estos dos puntos fijos en el ultravioleta y el infrarrojo.

Mediante la solución de supergravedad hemos procedido a calcular algunos observables interesantes de la teoría de campos dual. En primer lugar obtuvimos la entropía de entrelazamiento para una superficie con forma circular. Para ello empleamos la prescripción holográfica de Ryu-Takayanagi [95], que consiste en considerar la superficie de área mínima en la teoría de gravedad cuyo contorno coincide con el círculo en la frontera. Además, empleando la prescripción de Liu y Mezei [137], obtuvimos una función que verifica el teorema F (el análogo del teorema c en 2+1 dimensiones), *i.e.*, una función que decrece monotónicamente desde el ultravioleta hacia el infrarrojo y que coincide con la energía libre en los puntos fijos. También obtuvimos el correlador de dos puntos para operadores de dimensión grande, calculamos el círculo de Wilson (de donde se obtiene el potencial quark-antiquark) y el espectro de mesones. En resumen, todos los observables calculados indican la presencia de un flujo del grupo de renormalización entre dos puntos fijos en el infrarrojo y ultravioleta. Se trata de un flujo suave y monotónico sin transiciones de fase.

Efecto Hall holográfico

En el capítulo 4 de esta tesis se construyó una solución de supergravedad de tipo IIA basada en la teoría ABJM que es dual a una teoría de campos que describe un sistema Hall cuántico fraccionario.

Partiendo de la descripción de la teoría ABJM en términos de supergravedad de tipo IIA, introducimos una D6-brana de prueba y estudiamos sus propiedades. En el interior de la D6-brana encendemos campos gauge. En primer lugar, encendemos un campo gauge en la parte compacta del volumen de universo de la brana. Este campo gauge está cuantizado, y en la teoría gauge dual se corresponde con un término que rompe paridad. Esta rotura de paridad se hace explícita en el cálculo del espectro de mesones, donde se observa una

dependencia con la helicidad. A continuación encendemos campos gauge en la parte de Minkowski del volumen de universo de la brana, que en la teoría de campos se corresponden con campos eléctricos y magnéticos, corrientes y densidad de carga. Una vez introducida esta configuración electromagnética, calculamos las conductividades. Para valores genéricos de los parámetros, las D6-branas alcanzan el infrarrojo (encajamientos de tipo agujero negro) y en la teoría dual esto se corresponde con estados conductores. Si los parámetros verifican una cierta condición, se podrán tener D6-branas que no alcanzan el infrarrojo (encajamiento de tipo Minkowski) y que se corresponde con estados aislantes en la teoría dual. La ruptura de paridad introducida por el flujo interno permite la presencia de una corriente transversa, y estos estados se corresponden con estados de Hall. A través de la solución gravitatoria calculamos la fracción de llenado. Cabe destacar que existen ciertos valores de los parámetros para los que existen soluciones supersimétricas duales a estos estados de Hall.

Finalmente, estos cálculos se generalizaron al caso en el que la solución es la versión de ABJM que incluye materia fundamental dinámica sin masa de [75] y con temperatura [136].

Transiciones de fase cuánticas

En el capítulo 5 de esta tesis se construyó un modelo gravitatorio y se estudiaron transiciones de fase cuánticas en su teoría de campos dual.

Las transiciones de fase cuánticas son transiciones de fase que tienen lugar a temperatura cero y que suceden al variar algún parámetro físico. En este caso, construimos un sistema con densidad de carga, y las transiciones de fase tienen lugar al variar la densidad de carga. Partiendo de la descripción de la teoría ABJM en supergravedad de tipo IIA, añadimos una D6-brana de prueba. En el volumen de universo de esta brana encendemos un campo gauge que es dual a una densidad de carga. La D6-brana efectúa una transición en la que cambia la topología del encajamiento, desde un encajamiento de agujero negro (es decir, que alcanza el infrarrojo) cuando la densidad de carga es mayor que cero, a un encajamiento de Minkowski (es decir, que no alcanza el infrarrojo) cuando la densidad de carga es cero. Esta transición se identifica en la teoría de campos dual con una transición de fase de segundo orden, y se calculan los correspondientes exponentes críticos. Curiosamente, el comportamiento de escala cerca del punto crítico presenta términos multiplicativos logarítmicos.

Además, esta construcción se generalizó a la versión de ABJM que incluye sabor dinámico de masa cero [75]. Al incluir los efectos dinámicos del sabor, la transición de fase pasa a ser de primer orden. En este caso, la transición de fase tiene lugar a densidad mayor que cero. Para caracterizar dicha transición, calculamos la discontinuidad de ciertas magnitudes físicas como función del sabor dinámico de la solución.

Bibliography

[1] G. Veneziano, "Construction of a crossing-symmetric, Regge behaved amplitude for linearly rising trajectories", Nuovo Cim. A57 (1968) 190

[2] Y. Nambu, "Lectures at the Copenhagen symposium", unpublished (1970); T. Goto, "Relativistic quantum mechanics of one-dimensional mechanical continuum and subsidiary condition of dual resonance model", Prog.Theor.Phys. 46 (1971) 1560.

[3] P. Ramond, "Dual theory for free fermions", Phys.Rev. D3 (1971) 2415; A. Neveu and J. H. Schwarz, "Factorizable dual model of pions", Nucl.Phys. B31 (1971) 86.

[4] J. Scherk and J. H. Schwarz, "Dual models for nonhadrons", Nucl.Phys. B81 (1974) 118.

[5] F. Gliozzi, J. Scherk and D. Olive, "Supergravity and the spinor dual model", Phys.Lett. 65B (1976) 282; "Supersymmetry, supergravity theories and the dual spinor model", Nucl.Phys. B122 (1977) 253.

[6] D. J. Gross, J. A. Harvey, E. Martinec and R. Rohm, "Heterotic string theory", Nucl.Phys. B256 (1985) 253; Nucl.Phys. B267 (1986) 75

[7] E. Witten, "String theory dynamics in various dimensions", Nucl.Phys. B443 (1995) 85, hep-th/9503124.

[8] W. Nahm, "Supersymmetries and their Representations," Nucl. Phys. B **135** (1978) 149.

[9] E. Cremmer, B. Julia and J. Scherk, "Supergravity in eleven dimensions", Phys. Lett. 76B (1978), 409-412.

[10] J. M. Maldacena, "The Large N limit of superconformal field theories and supergravity," Int. J. Theor. Phys. **38** (1999) 1113 [Adv. Theor. Math. Phys. **2** (1998) 231] hep-th/9711200.

[11] T. Buscher, "A symmetry of the string background field equations", Phys. Lett. B194 (1987) 59-62; T. Buscher, "Path integral derivation of quantum duality in nonlinear sigma models", Phys. Lett. B201 (1988) 466-472.

[12] E. Bergshoeff, C. M. Hull and T. Ortin, "Duality in the type II superstring effective action," Nucl. Phys. B **451** (1995) 547, hep-th/9504081.

[13] P. Bouwknegt, J. Evslin and V. Mathai, "T duality: Topology change from H flux," Commun. Math. Phys. **249** (2004) 383, hep-th/0306062.

[14] X. C. de la Ossa and F. Quevedo, "Duality symmetries from non-abelian isometries in string theory", Nucl. Phys. B **403**, 377 (1993)

[15] K. Sfetsos and D. C. Thompson, "On non-abelian T-dual geometries with Ramond fluxes", Nucl. Phys. B **846** (2011) 21

[16] A. Karch and E. Katz, "Adding flavor to AdS / CFT," JHEP **0206** (2002) 043, hep-th/0205236.

[17] Y. Bea, E. Conde, N. Jokela and A. V. Ramallo, "Unquenched massive flavors and flows in Chern-Simons matter theories," JHEP **1312** (2013) 033, arXiv:1309.4453 [hep-th].

[18] Y. Bea, N. Jokela, M. Lippert, A. V. Ramallo and D. Zoakos, "Flux and Hall states in ABJM with dynamical flavors," JHEP **1503** (2015) 009, arXiv:1411.3335 [hep-th].

[19] Y. Bea, J. D. Edelstein, G. Itsios, K. S. Kooner, C. Nunez, D. Schofield and J. A. Sierra-Garcia, "Compactifications of the Klebanov-Witten CFT and new AdS$_3$ backgrounds," JHEP **1505** (2015) 062, arXiv:1503.07527 [hep-th].

[20] Y. Bea, N. Jokela and A. V. Ramallo, "Quantum phase transitions with dynamical flavors," Phys. Rev. D **94** (2016) no.2, 026003, arXiv:1604.03665 [hep-th].

[21] J. Figueroa-O'Farrill , "Maximal supersymmetry in ten and eleven dimensions", http://www.maths.ed.ac.uk/ jmf/CV/Seminars/Bonn.pdf

[22] Karoubi, Max. "Algebres de Clifford et K-theorie." Annales scientifiques de l'Ecole Normale Superieure 1.2 (1968): 161-270

[23] M. F. Atiyah, R. Bott and A. Shapiro, "Clifford modules," Topology **3** (1964) S3.

[24] J. M. Figueroa-O'Farrill, P. Meessen and S. Philip, "Supersymmetry and homogeneity of M-theory backgrounds," Class. Quant. Grav. **22** (2005) 207, hep-th/0409170.

[25] J. Figueroa-O'Farrill and A. Santi, "Spencer cohomology and eleven-dimensional supergravity," arXiv:1511.08737 [hep-th].

[26] A. Moroianu, "Parallel and Killing Spinors on Spin^c Manifolds", Commun. Math. Phys. 187 417-427

[27] J. M. Figueroa-O'Farrill and G. Papadopoulos, "Maximally supersymmetric solutions of ten-dimensional and eleven-dimensional supergravities," JHEP **0303** (2003) 048, hep-th/0211089.

[28] U. Gran, J. Gutowski, G. Papadopoulos and D. Roest,"N=31, D=11," JHEP **0702** (2007) 043, hep-th/0610331.

[29] J. M. Figueroa-O'Farrill and S. Gadhia, "M-theory preons cannot arise by quotients," JHEP **0706** (2007) 043, hep-th/0702055.

[30] U. Gran, J. Gutowski and G. Papadopoulos, "M-theory backgrounds with 30 Killing spinors are maximally supersymmetric," JHEP **1003** (2010) 112, arXiv:1001.1103 [hep-th].

[31] J. Figueroa-O'Farrill and N. Hustler, "The homogeneity theorem for supergravity backgrounds," JHEP **1210** (2012) 014, arXiv:1208.0553 [hep-th].

[32] M.Y. Wang, "Parallel spinors and parallel forms", Ann. Global Anal. Geom. 7(1) (1989), 59-68

[33] C. Bär, "Real Killing spinors and holonomy", Comm. Math. Phys. 154 (1993), 509-521.

[34] I. R. Klebanov and E. Witten, "Superconformal field theory on three-branes at a Calabi-Yau singularity", Nucl. Phys. B **536**, 199 (1998)

[35] L. Martucci, J. Rosseel, D. Van den Bleeken and A. Van Proeyen, "Dirac actions for D-branes on backgrounds with fluxes", Class. Quant. Grav. **22** (2005) 2745

[36] M. J. Duff, H. Lu and C. N. Pope, "$AdS_5 \times S^5$ untwisted," Nucl. Phys. B **532** (1998) 181, hep-th/9803061.

[37] A. Giveon and M. Rocek, "On nonAbelian duality", Nucl. Phys. B **421**, 173 (1994), hep-th/9308154.

[38] E. Alvarez, L. Alvarez-Gaume, J. L. F. Barbon and Y. Lozano, "Some global aspects of duality in string theory", Nucl. Phys. B **415**, 71 (1994), hep-th/9309039. E. Alvarez, L. Alvarez-Gaume and Y. Lozano, "On nonAbelian duality", Nucl. Phys. B **424**, 155 (1994), hep-th/9403155. E. Alvarez, L. Alvarez-Gaume and Y. Lozano, "A Canonical approach to duality transformations", Phys. Lett. B **336**, 183 (1994), hep-th/9406206.

[39] C. Klimcik and P. Severa, "NonAbelian momentum winding exchange", Phys. Lett. B **383**, 281 (1996), hep-th/9605212.

[40] J. Borlaf and Y. Lozano, "Aspects of T duality in open strings", Nucl. Phys. B **480**, 239 (1996), hep-th/9607051.

[41] F. Quevedo, "Duality and global symmetries", Nucl. Phys. Proc. Suppl. **61A**, 23 (1998), hep-th/9706210.

[42] G. Itsios, C. Nunez, K. Sfetsos and D. C. Thompson, "Non-Abelian T-duality and the AdS/CFT correspondence:new N=1 backgrounds", Nucl. Phys. B **873**, 1 (2013), arXiv:1301.6755.

[43] Ö. Kelekci, Y. Lozano, N. T. Macpherson and E. Ó. Colgáin, "Supersymmetry and non-Abelian T-duality in type II supergravity", Class. Quant. Grav. **32** (2015) 3, 035014, arXiv:1409.7406.

[44] Y. Kosmann, "A note on Lie-Lorentz derivatives", Annali di Mat. Pura Appl. **(IV) 91** (1972) 317.

[45] S. S. Gubser, I. R. Klebanov and A. M. Polyakov, "Gauge theory correlators from noncritical string theory," Phys. Lett. B **428** (1998) 105, hep-th/9802109.

[46] E. Witten,"Anti-de Sitter space and holography," Adv. Theor. Math. Phys. **2** (1998) 253, hep-th/9802150.

[47] I. R. Klebanov and A. A. Tseytlin, "Gravity duals of supersymmetric SU(N) x SU(N+M) gauge theories," Nucl. Phys. B **578** (2000) 123, hep-th/0002159.

[48] I. R. Klebanov and M. J. Strassler, "Supergravity and a confining gauge theory: Duality cascades and chi SB resolution of naked singularities", JHEP **0008**, 052 (2000), hep-th/0007191.

[49] K. Pilch and N. P. Warner, "N=2 supersymmetric RG flows and the IIB dilaton," Nucl. Phys. B **594** (2001) 209, hep-th/0004063.

[50] J. M. Maldacena and C. Nunez, "Supergravity description of field theories on curved manifolds and a no go theorem", Int. J. Mod. Phys. A **16**, 822 (2001), hep-th/0007018.

[51] O. Aharony, O. Bergman, D. L. Jafferis and J. M. Maldacena,"N=6 superconformal Chern-Simons-matter theories, M2-branes and their gravity duals," JHEP **0810**, 091 (2008), arXiv:0806.1218 [hep-th].

[52] J. H. Schwarz, "Superconformal Chern-Simons theories," JHEP **0411** (2004) 078, hep-th/0411077.

[53] A. Guarino, D. L. Jafferis and O. Varela, "String Theory Origin of Dyonic N=8 Supergravity and Its Chern-Simons Duals," Phys. Rev. Lett. **115** (2015) no.9, 091601, arXiv:1504.08009 [hep-th].

[54] J. Bagger and N. Lambert, "Comments on multiple M2-branes," JHEP **0802** (2008) 105, arXiv:0712.3738 [hep-th].

[55] J. Bagger and N. Lambert, "Gauge symmetry and supersymmetry of multiple M2-branes," Phys. Rev. D **77** (2008) 065008, arXiv:0711.0955 [hep-th].

[56] J. Bagger and N. Lambert, "Modeling Multiple M2's," Phys. Rev. D **75** (2007) 045020, hep-th/0611108.

[57] A. Gustavsson, "Algebraic structures on parallel M2-branes," Nucl. Phys. B **811** (2009) 66, arXiv:0709.1260 [hep-th].

[58] A. Gustavsson, "Selfdual strings and loop space Nahm equations," JHEP **0804** (2008) 083, arXiv:0802.3456 [hep-th].

[59] M. Van Raamsdonk, "Comments on the Bagger-Lambert theory and multiple M2-branes," JHEP **0805** (2008) 105, arXiv:0803.3803 [hep-th].

[60] N. Drukker, M. Marino and P. Putrov, "From weak to strong coupling in ABJM theory," Commun. Math. Phys. **306** (2011) 511, arXiv:1007.3837 [hep-th].

[61] O. Aharony, O. Bergman and D. L. Jafferis, "Fractional M2-branes," JHEP **0811** (2008) 043, arXiv:0807.4924 [hep-th].

[62] D. Gaiotto and A. Tomasiello, "The gauge dual of Romans mass," JHEP **1001** (2010) 015, arXiv:0901.0969 [hep-th].

[63] D. Gaiotto and A. Tomasiello, "Perturbing gauge/gravity duals by a Romans mass," J. Phys. A **42** (2009) 465205, arXiv:0904.3959 [hep-th].

[64] J. Gomis, D. Rodriguez-Gomez, M. Van Raamsdonk and H. Verlinde, "A Massive Study of M2-brane Proposals," JHEP **0809** (2008) 113, arXiv:0807.1074 [hep-th].

[65] Y. Imamura and K. Kimura, "On the moduli space of elliptic Maxwell-Chern-Simons theories," Prog. Theor. Phys. **120** (2008) 509, arXiv:0806.3727 [hep-th].

[66] D. L. Jafferis and A. Tomasiello, "A Simple class of N=3 gauge/gravity duals," JHEP **0810** (2008) 101, arXiv:0808.0864 [hep-th].

[67] Y. Imamura and S. Yokoyama, "N=4 Chern-Simons theories and wrapped M-branes in their gravity duals," Prog. Theor. Phys. **121** (2009) 915, arXiv:0812.1331 [hep-th].

[68] D. Martelli and J. Sparks, "Moduli spaces of Chern-Simons quiver gauge theories and AdS(4)/CFT(3)," Phys. Rev. D **78** (2008) 126005, arXiv:0808.0912 [hep-th].

[69] A. Hanany and A. Zaffaroni, "Tilings, Chern-Simons Theories and M2 Branes," JHEP **0810** (2008) 111, arXiv:0808.1244 [hep-th].

[70] H. Ooguri and C. S. Park, "Superconformal Chern-Simons Theories and the Squashed Seven Sphere," JHEP **0811** (2008) 082, arXiv:0808.0500 [hep-th].

[71] M. Benna, I. Klebanov, T. Klose and M. Smedback, "Superconformal Chern-Simons Theories and AdS(4)/CFT(3) Correspondence," JHEP **0809** (2008) 072, arXiv:0806.1519 [hep-th].

[72] G. Veneziano, "Some Aspects of a Unified Approach to Gauge, Dual and Gribov Theories," Nucl. Phys. B **117** (1976) 519.

[73] C. Nunez, A. Paredes and A. V. Ramallo, "Unquenched Flavor in the Gauge/Gravity Correspondence," Adv. High Energy Phys. **2010** (2010) 196714, arXiv:1002.1088 [hep-th].

[74] A. F. Faedo, A. Kundu, D. Mateos, C. Pantelidou and J. Tarrio, "Three-dimensional super Yang-Mills with compressible quark matter," JHEP **1603** (2016) 154, arXiv:1511.05484 [hep-th].

[75] E. Conde and A. V. Ramallo, "On the gravity dual of Chern-Simons-matter theories with unquenched flavor," JHEP **1107**, 099 (2011), arXiv:1105.6045 [hep-th].

[76] J. P. Gauntlett, G. W. Gibbons, G. Papadopoulos and P. K. Townsend, "Hyper-Kahler manifolds and multiply intersecting branes," Nucl. Phys. B **500** (1997) 133, hep-th/9702202.

[77] F. Bigazzi, R. Casero, A. L. Cotrone, E. Kiritsis, A. Paredes, "Non-critical holography and four-dimensional CFT's with fundamentals," JHEP **0510**, 012 (2005), hep-th/0505140.

[78] S. Hohenegger, I. Kirsch, "A Note on the holography of Chern-Simons matter theories with flavour," JHEP **0904**, 129 (2009), arXiv:0903.1730 [hep-th].

[79] D. Gaiotto, D. L. Jafferis,"Notes on adding D6 branes wrapping RP3 in AdS(4) x CP3", arXiv:0903.2175 [hep-th].

[80] M. Ammon, J. Erdmenger, R. Meyer *et al.*, "Adding Flavor to AdS(4)/CFT(3)," JHEP **0911**, 125 (2009), arXiv:0909.3845 [hep-th].

[81] J. Polchinski, "Tasi lectures on D-branes," hep-th/9611050.

[82] J. Simon, "Brane Effective Actions, Kappa-Symmetry and Applications," Living Rev. Rel. **15** (2012) 3, arXiv:1110.2422 [hep-th].

[83] M. Cederwall, A. von Gussich, B.E.W. Nilsson, P. Sundell and A. Westerberg, "The Dirichlet super-p-branes in Type IIA and IIB supergravity", Nucl. Phys. B490 (1997) 179, hep-th/9611159; E. Bergshoeff and P.K. Townsend, "Super D-branes", Nucl. Phys. B490 (1997) 145, hep-th/9611173; M. Aganagic, C. Popescu and J.H. Schwarz, "D-brane actions with local kappa symmetry", Phys. Lett. B393 (1997) 311, hep-th/9610249; "Gauge-invariant and gauge-fixed D-brane actions", Nucl. Phys. B495 (1997) 99, hep-th/9612080.

[84] K. Becker, M. Becker and A. Strominger, "Fivebranes, membranes and non-perturbative string theory", Nucl. Phys. B456 (1995) 130, hep-th/9507158; E. Bergshoeff, R. Kallosh, T. Ortin and G. Papadopulos, "kappa-symmetry, supersymmetry and intersecting branes", Nucl. Phys. B502 (1997) 149, hep-th/9705040; E. Bergshoeff and P.K. Townsend, "Solitons on the supermembrane", JHEP 9905 (1999) 021, hep-th/9904020.

[85] T. Sakai and S. Sugimoto,"Low energy hadron physics in holographic QCD," Prog. Theor. Phys. **113** (2005) 843, hep-th/0412141.

[86] M. Attems, J. Casalderrey-Solana, D. Mateos, D. Santos-Oliván, C. F. Sopuerta, M. Triana and M. Zilhão, "Collisions in Non-conformal Theories: Hydrodynamization without Equilibration," arXiv:1604.06439 [hep-th].

[87] F. Bigazzi, A. L. Cotrone and R. Sisca,"Notes on Theta Dependence in Holographic Yang-Mills," JHEP **1508** (2015) 090, arXiv:1506.03826 [hep-th].

[88] J. M. Pons, J. G. Russo and P. Talavera, "Semiclassical string spectrum in a string model dual to large N QCD," Nucl. Phys. B **700** (2004) 71, hep-th/0406266.

[89] J. Casalderrey-Solana and A. Ficnar, "Holographic 3-jet events," Nucl. Part. Phys. Proc. **276-278** (2016) 115.

[90] C. Hoyos, D. R. Fernández, N. Jokela and A. Vuorinen, "Holographic Quark Matter and Neutron Stars," arXiv:1603.02943

[91] P. McFadden and K. Skenderis,"Holography for Cosmology," Phys. Rev. D **81** (2010) 021301, arXiv:0907.5542 [hep-th].

[92] V. E. Hubeny, S. Minwalla and M. Rangamani, "The fluid/gravity correspondence," arXiv:1107.5780 [hep-th].

[93] P. M. Chesler and L. G. Yaffe, "Holography and colliding gravitational shock waves in asymptotically AdS_5 spacetime," Phys. Rev. Lett. **106** (2011) 021601, arXiv:1011.3562 [hep-th].

[94] P. M. Chesler and L. G. Yaffe, "Horizon formation and far-from-equilibrium isotropization in supersymmetric Yang-Mills plasma," Phys. Rev. Lett. **102** (2009) 211601, arXiv:0812.2053 [hep-th].

[95] S. Ryu and T. Takayanagi, "Holographic derivation of entanglement entropy from AdS/CFT," Phys. Rev. Lett. **96** (2006) 181602, arXiv:hep-th/0603001; "Aspects of holographic entanglement entropy," JHEP **0608** (2006) 045, arXiv:hep-th/0605073.

[96] E. Berkowitz, M. Hanada and J. Maltz, "A microscopic description of black hole evaporation via holography," arXiv:1603.03055 [hep-th].

[97] G. Policastro, D. T. Son and A. O. Starinets, "The Shear viscosity of strongly coupled N=4 supersymmetric Yang-Mills plasma," Phys. Rev. Lett. **87** (2001) 081601, hep-th/0104066.

[98] P. Kovtun, D. T. Son and A. O. Starinets, "Holography and hydrodynamics: Diffusion on stretched horizons," JHEP **0310** (2003) 064, hep-th/0309213, "Viscosity in strongly interacting quantum field theories from black hole physics," Phys. Rev. Lett. **94** (2005) 111601, hep-th/0405231.

[99] C. Shen and U. Heinz,"The road to precision: Extraction of the specific shear viscosity of the quark-gluon plasma," arXiv:1507.01558 [nucl-th].

[100] M. Muller, J. Schmalian, L. Fritz, "Graphene: A Nearly Perfect Fluid", Phys. Rev. Lett. 103, 025301 (2009).

[101] H. Lin, O. Lunin and J. M. Maldacena, "Bubbling AdS space and 1/2 BPS geometries", JHEP **0410**, 025 (2004), hep-th/0409174.

[102] D. Gaiotto and J. Maldacena, "The Gravity duals of N=2 superconformal field theories", JHEP **1210**, 189 (2012), arXiv:0904.4466.

[103] D. Gaiotto, "N=2 dualities", JHEP **1208**, 034 (2012), arXiv:0904.2715.

[104] Y. Tachikawa, "N=2 supersymmetric dynamics for pedestrians", Lect. Notes Phys. **890**, 2014, arXiv:1312.2684.

[105] G. Itsios, C. Nunez, K. Sfetsos and D. C. Thompson, "On Non-Abelian T-Duality and new N=1 backgrounds", Phys. Lett. B **721**, 342 (2013), arXiv:1212.4840.

[106] N. T. Macpherson, C. Núñez, L. A. Pando Zayas, V. G. J. Rodgers and C. A. Whiting, "Type IIB supergravity solutions with AdS_5 from Abelian and non-Abelian T dualities", JHEP **1502** (2015) 040, arXiv:1410.2650.

[107] G. Itsios, Y. Lozano, E. O Colgain and K. Sfetsos, "Non-Abelian T-duality and consistent truncations in type-II supergravity", JHEP **1208** (2012) 132, arXiv:1205.2274. Y. Lozano, E. O Colgain, D. Rodriguez-Gomez and K. Sfetsos, "Supersymmetric AdS_6 via T Duality", Phys. Rev. Lett. **110**, no. 23, 231601 (2013), arXiv:1212.1043. A. Barranco, J. Gaillard, N. T. Macpherson, C. Nunez and D. C. Thompson, "G-structures and Flavouring non-Abelian T-duality", JHEP **1308**, 018 (2013), arXiv:1305.7229. N. T. Macpherson, "Non-abelian T-duality, generalised geometry and holography", J. Phys. Conf. Ser. **490**, 012122 (2014), arXiv:1309.1358. N. T. Macpherson, "Non-Abelian T-duality, G_2-structure rotation and holographic duals of $N = 1$ Chern-Simons theories", JHEP **1311**, 137 (2013), arXiv:1310.1609. Y. Lozano, E. O. O Colgáin and D. Rodriguez-Gomez, "Hints of 5d Fixed Point Theories from Non-Abelian T-duality", JHEP **1405**, 009 (2014), arXiv:1311.4842. J. Gaillard, N. T. Macpherson, C. Nunez and D. C. Thompson, "Dualising the Baryonic Branch: Dynamic SU(2) and confining backgrounds in IIA", Nucl. Phys. B **884**, 696 (2014), arXiv:1312.4945.

[108] A. Buchel and J. T. Liu, "Gauged supergravity from type IIB string theory on $Y^{p,q}$ manifolds", Nucl. Phys. B **771** (2007) 93, hep-th/0608002.

[109] J. P. Gauntlett, S. Kim, O. Varela and D. Waldram, "Consistent supersymmetric Kaluza-Klein truncations with massive modes", JHEP **0904**, 102 (2009), arXiv:0901.0676. J. P. Gauntlett and O. Varela, "Universal Kaluza-Klein reductions of type IIB to N=4 supergravity in five dimensions", JHEP **1006**, 081 (2010), arXiv:1003.5642.

[110] A. Kehagias and J. G. Russo, "Hyperbolic spaces in string and M theory", JHEP **0007** (2000) 027, hep-th/0003281.

[111] J. P. Gauntlett, O. A. P. Mac Conamhna, T. Mateos and D. Waldram, "Supersymmetric AdS(3) solutions of type IIB supergravity", Phys. Rev. Lett. **97**, 171601 (2006), hep-th/0606221.

[112] A. Donos and J. P. Gauntlett, "Flowing from AdS_5 to AdS_3 with $T^{1,1}$", JHEP **1408**, 006 (2014), arXiv:1404.7133.

[113] A. Donos, J. P. Gauntlett and N. Kim, "AdS Solutions Through Transgression", JHEP **0809**, 021 (2008), arXiv:0807.4375.

[114] C. Nunez, I. Y. Park, M. Schvellinger and T. A. Tran, "Supergravity duals of gauge theories from F(4) gauged supergravity in six-dimensions", JHEP **0104**, 025 (2001), hep-th/0103080.

[115] J. P. Gauntlett, O. A. P. Mac Conamhna, T. Mateos and D. Waldram, "AdS spacetimes from wrapped M5 branes", JHEP **0611**, 053 (2006), hep-th/0605146.

[116] F. Benini, Y. Tachikawa and B. Wecht, "Sicilian gauge theories and N=1 dualities", JHEP **1001**, 088 (2010), arXiv:0909.1327.

[117] Y. Lozano and N. T. Macpherson, "A new AdS$_4$/CFT$_3$ dual with extended SUSY and a spectral flow", JHEP **1411**, 115 (2014), arXiv:1408.0912.

[118] F. Benini, F. Canoura, S. Cremonesi, C. Nunez and A. V. Ramallo, "Backreacting flavors in the Klebanov-Strassler background", JHEP **0709**, 109 (2007), arXiv:0706.1238.

[119] A. B. Zamolodchikov, "Irreversibility of the Flux of the Renormalization Group in a 2D Field Theory", JETP Lett. **43**, 730 (1986) [Pisma Zh. Eksp. Teor. Fiz. **43**, 565 (1986)].

[120] J. L. Cardy, "Is There a c Theorem in Four-Dimensions?", Phys. Lett. B **215**, 749 (1988).

[121] Z. Komargodski and A. Schwimmer, "On Renormalization Group Flows in Four Dimensions", JHEP **1112**, 099 (2011), arXiv:1107.3987.

[122] E. Barnes, K. A. Intriligator, B. Wecht and J. Wright, "Evidence for the strongest version of the 4d a-theorem, via a-maximization along RG flows", Nucl. Phys. B **702**, 131 (2004), hep-th/0408156.

[123] J. D. Brown, M. Henneaux, "Central charges in the canonical realization of asymptotic symmetries: An example from three-dimensional gravity", Commun. Math. Phys. 104 (1986) 207.

[124] M. Henningson, K. Skenderis, "The Holographic Weyl Anomaly", JHEP 9807, 023 (1998), hep-th/9806087.

[125] D. Z. Freedman, S. S. Gubser, K. Pilch and N. P. Warner, "Renormalization group flows from holography supersymmetry and a c theorem", Adv. Theor. Math. Phys. **3**, 363 (1999), hep-th/9904017.

[126] E. Alvarez and C. Gomez, "Geometric holography, the renormalization group and the c theorem", Nucl. Phys. B **541**, 441 (1999), hep-th/9807226.

[127] I. R. Klebanov, D. Kutasov and A. Murugan, "Entanglement as a probe of confinement", Nucl. Phys. B **796**, 274 (2008), arXiv:0709.2140.

[128] S. Gukov, "Counting RG flows", arXiv:1503.01474.

[129] M. Gutperle and P. Kraus, "Higher Spin Black Holes", JHEP **1105**, 022 (2011), arXiv:1103.4304. M. Ammon, M. Gutperle, P. Kraus and E. Perlmutter, "Spacetime Geometry in Higher Spin Gravity", JHEP **1110**, 053 (2011), arXiv:1106.4788. S. Datta, J. R. David, M. Ferlaino and S. P. Kumar, "Universal correction to higher spin entanglement entropy", Phys. Rev. D **90**, no. 4, 041903 (2014), arXiv:1405.0015. S. Datta, J. R. David, M. Ferlaino and S. P. Kumar, "Higher spin entanglement entropy from CFT", JHEP **1406**, 096 (2014), arXiv:1402.0007

[130] T. Nishioka and T. Takayanagi, "AdS Bubbles, Entropy and Closed String Tachyons", JHEP **0701**, 090 (2007), hep-th/0611035.

[131] J. M. Maldacena, "Wilson loops in large N field theories," Phys. Rev. Lett. **80**, 4859 (1998), arXiv:hep-th/9803002.

[132] S. Beck, J. B. Gutowski and G. Papadopoulos, "Supersymmetry of IIA warped flux AdS and flat backgrounds", arXiv:1501.07620. S. W. Beck, J. B. Gutowski and G. Papadopoulos, "Supersymmetry of AdS and flat IIB backgrounds", JHEP **1502**, 020 (2015), arXiv:1410.3431.

[133] Y. Lozano and C. Nunez, "Field theory aspects of non-Abelian T-duality and $\mathcal{N} = 2$ linear quivers," JHEP **1605** (2016) 107, arXiv:1603.04440 [hep-th].

[134] T. Ortin, "A Note on Lie-Lorentz derivatives", Class. Quant. Grav. **19** (2002) L143, hep-th/0206159.

[135] M. S. Bianchi, S. Penati, M. Siani, "Infrared stability of ABJ-like theories," JHEP **1001**, 080 (2010), arXiv:0910.5200 [hep-th]; M. S. Bianchi, S. Penati, M. Siani, "Infrared Stability of N = 2 Chern-Simons Matter Theories," JHEP **1005**, 106 (2010), arXiv:0912.4282 [hep-th].

[136] N. Jokela, J. Mas, A. V. Ramallo and D. Zoakos, "Thermodynamics of the brane in Chern-Simons matter theories with flavor," JHEP **1302** (2013) 144, arXiv:1211.0630 [hep-th].

[137] H. Liu and M. Mezei, "A Refinement of entanglement entropy and the number of degrees of freedom," arXiv:1202.2070 [hep-th].

[138] R. C. Myers and A. Sinha, "Holographic c-theorems in arbitrary dimensions," JHEP **1101**, 125 (2011), arXiv:1011.5819 [hep-th]; "Seeing a c-theorem with holography," Phys. Rev. D **82** (2010) 046006, arXiv:1006.1263 [hep-th]; D. L. Jafferis, I. R. Klebanov, S. S. Pufu and B. R. Safdi, "Towards the F-Theorem: N=2 Field Theories on the Three-Sphere," JHEP **1106** (2011) 102, arXiv:1103.1181 [hep-th]; I. R. Klebanov, S. S. Pufu and B. R. Safdi, "F-Theorem without Supersymmetry," JHEP **1110** (2011) 038, arXiv:1105.4598 [hep-th]; "Entanglement Entropy of 3-d Conformal Gauge Theories with Many Flavors," JHEP **1205** (2012) 036, arXiv:1112.5342 [hep-th].

[139] H. Casini and M. Huerta, "On the RG running of the entanglement entropy of a circle," Phys. Rev. D **85** (2012) 125016 [arXiv:1202.5650 [hep-th]].

[140] R. L. Bryant and S. Salamon, "On the construction of some complete metrics with exceptional holonomy", Duke Math. J. **58**, 829 (1989); G. W. Gibbons, D. N. Page and C. N. Pope, "Einstein metrics on $\mathbb{S}^3$, $\mathbb{R}^3$ and $\mathbb{R}^3$ bundles", Commun. Math. Phys. **127**, 529 (1990).

[141] M. Atiyah and E. Witten, "M theory dynamics on a manifold of G(2) holonomy," Adv. Theor. Math. Phys. **6** (2003) 1, hep-th/0107177.

[142] R. Casero, C. Nunez, A. Paredes, "Towards the string dual of N=1 SQCD-like theories," Phys. Rev. **D73**, 086005 (2006), hep-th/0602027; "Elaborations on the String Dual to N=1 SQCD," Phys. Rev. **D77**, 046003 (2008), arXiv:0709.3421 [hep-th]; C. Hoyos-Badajoz, C. Nunez and I. Papadimitriou,"Comments on the String dual to N=1 SQCD," Phys. Rev. D **78**, 086005 (2008), arXiv:0807.3039 [hep-th]; E. Conde, J. Gaillard and A. V. Ramallo, "On the holographic dual of N=1 SQCD with massive flavors," JHEP **1110**, 023 (2011), arXiv:1107.3803 [hep-th].

[143] R. Emparan, C. V. Johnson and R. C. Myers, "Surface terms as counterterms in the AdS / CFT correspondence," Phys. Rev. D **60** (1999) 104001, hep-th/9903238.

[144] H. Casini, M. Huerta and R. C. Myers, "Towards a derivation of holographic entanglement entropy," JHEP **1105**, 036 (2011), arXiv:1102.0440 [hep-th].

[145] A. Kitaev and J. Preskill, "Topological entanglement entropy," Phys. Rev. Lett. **96** (2006) 110404, hep-th/0510092.

[146] M. Levin and X. -G. Wen, "Detecting Topological Order in a Ground State Wave Function," Phys. Rev. Lett. **96** (2006) 110405.

[147] H. Liu and M. Mezei, "Probing renormalization group flows using entanglement entropy," arXiv:1309.6935 [hep-th].

[148] S. J. Rey and J. T. Yee, "Macroscopic strings as heavy quarks in large N gauge theory and anti-de Sitter supergravity," Eur. Phys. J. C **22** (2001) 379, arXiv:hep-th/9803001.

[149] V. Balasubramanian and S. F. Ross, "Holographic particle detection," Phys. Rev. D **61** (2000) 044007, hep-th/9906226.

[150] J. Louko, D. Marolf and S. F. Ross, "On geodesic propagators and black hole holography," Phys. Rev. D **62** (2000) 044041, hep-th/0002111.

[151] P. Kraus, H. Ooguri and S. Shenker, "Inside the horizon with AdS / CFT," Phys. Rev. D **67** (2003) 124022, hep-th/0212277.

[152] Y. Hikida, W. Li, T. Takayanagi,"ABJM with Flavors and FQHE," JHEP **0907**, 065 (2009), arXiv:0903.2194 [hep-th].

[153] K. Jensen, "More Holographic Berezinskii-Kosterlitz-Thouless Transitions," Phys. Rev. **D82**, 046005 (2010), arXiv:1006.3066 [hep-th].

[154] J. G. Russo and K. Sfetsos,"Rotating D3-branes and QCD in three dimensions", *Adv. Theor. Math. Phys.* **3**(1999) 131, hep-th/9901056.

[155] E. Keski-Vakkuri and P. Kraus, "Quantum Hall Effect in AdS/CFT," JHEP **0809** (2008) 130, arXiv:0805.4643 [hep-th].

[156] K. Goldstein, S. Kachru, S. Prakash and S. P. Trivedi, "Holography of Charged Dilaton Black Holes," JHEP **1008** (2010) 078, arXiv:0911.3586 [hep-th].

[157] K. Goldstein, N. Iizuka, S. Kachru, S. Prakash, S. P. Trivedi and A. Westphal, "Holography of Dyonic Dilaton Black Branes," JHEP **1010** (2010) 027, arXiv:1007.2490 [hep-th].

[158] A. Bayntun, C. P. Burgess, B. P. Dolan and S. S. Lee, "AdS/QHE: Towards a Holographic Description of Quantum Hall Experiments," New J. Phys. **13** (2011) 035012, arXiv:1008.1917 [hep-th].

[159] E. Gubankova, J. Brill, M. Cubrovic, K. Schalm, P. Schijven and J. Zaanen, "Holographic fermions in external magnetic fields," Phys. Rev. D **84** (2011) 106003, arXiv:1011.4051 [hep-th].

[160] M. Lippert, R. Meyer and A. Taliotis, "A holographic model for the fractional quantum Hall effect," arXiv:1409.1369 [hep-th].

[161] O. Bergman, N. Jokela, G. Lifschytz and M. Lippert, "Quantum Hall Effect in a Holographic Model," JHEP **1010** (2010) 063, arXiv:1003.4965 [hep-th].

[162] N. Jokela, M. Jarvinen and M. Lippert, "A holographic quantum Hall model at integer filling," JHEP **1105** (2011) 101, arXiv:1101.3329 [hep-th].

[163] C. Kristjansen and G. W. Semenoff, "Giant D5 Brane Holographic Hall State," JHEP **1306** (2013) 048, arXiv:1212.5609 [hep-th].

[164] N. Jokela, A. V. Ramallo and D. Zoakos, "Magnetic catalysis in flavored ABJM," JHEP **1402** (2014) 021, arXiv:1311.6265 [hep-th].

[165] A. Karch and A. O'Bannon, "Metallic AdS/CFT," JHEP **0709** (2007) 024, arXiv:0705.3870 [hep-th].

[166] G. Lifschytz and M. Lippert, "Anomalous conductivity in holographic QCD," Phys. Rev. D **80** (2009) 066005, arXiv:0904.4772 [hep-th].

[167] A. M. Dykhne and I. M. Ruzin, "Theory of the fractional quantum Hall effect: The two-phase model," Phys. Rev. B **50**, 2369 (1994).

[168] G. Zafrir, "Embedding massive flavor in ABJM," JHEP **1210** (2012) 056, arXiv:1202.4295 [hep-th].

[169] F. Preis, A. Rebhan and A. Schmitt, "Inverse magnetic catalysis in dense holographic matter," JHEP **1103**, 033 (2011), arXiv:1012.4785 [hep-th].

[170] F. Preis, A. Rebhan and A. Schmitt, "Inverse magnetic catalysis in field theory and gauge-gravity duality," Lect. Notes Phys. **871**, 51 (2013), arXiv:1208.0536 [hep-ph].

[171] V. G. Filev, C. V. Johnson, R. C. Rashkov and K. S. Viswanathan, "Flavoured large N gauge theory in an external magnetic field," JHEP **0710**, 019 (2007), hep-th/0701001.

[172] V. G. Filev and R. C. Raskov, "Magnetic Catalysis of Chiral Symmetry Breaking. A Holographic Prospective," Adv. High Energy Phys. **2010**, 473206 (2010), arXiv:1010.0444 [hep-th].

[173] V. G. Filev and D. Zoakos, "Towards Unquenched Holographic Magnetic Catalysis," JHEP **1108**, 022 (2011), arXiv:1106.1330 [hep-th].

[174] J. Erdmenger, V. G. Filev and D. Zoakos, "Magnetic Catalysis with Massive Dynamical Flavours," JHEP **1208**, 004 (2012), arXiv:1112.4807 [hep-th].

[175] E. Imeroni, "On deformed gauge theories and their string/M-theory duals," JHEP **0810**, 026 (2008), arXiv:0808.1271 [hep-th].

[176] Y. Bea, N. Jokela and A. V. Ramallo, work in progress.

[177] I.V. Kukushkin, J. H. Smet, V.W. Scarola, V. Umansky and K. von Klitzing, Science **324** no. 5930, 1044-1047 (2009).

[178] N. Jokela, G. Lifschytz and M. Lippert, "Magneto-roton excitation in a holographic quantum Hall fluid," JHEP **1102** (2011) 104, arXiv:1012.1230 [hep-th].

[179] N. Jokela, M. Jarvinen and M. Lippert, "Fluctuations of a holographic quantum Hall fluid," JHEP **1201** (2012) 072, arXiv:1107.3836 [hep-th].

[180] A. Ballon-Bayona, K. Peeters and M. Zamaklar, "A chiral magnetic spiral in the holographic Sakai-Sugimoto model," JHEP **1211** (2012) 164, arXiv:1209.1953 [hep-th].

[181] O. Bergman, N. Jokela, G. Lifschytz and M. Lippert, "Striped instability of a holographic Fermi-like liquid," JHEP **1110** (2011) 034, arXiv:1106.3883 [hep-th].

[182] N. Jokela, M. Järvinen and M. Lippert, "Fluctuations and instabilities of a holographic metal," JHEP **1302** (2013) 007, arXiv:1211.1381 [hep-th].

[183] N. Jokela, G. Lifschytz and M. Lippert, "Magnetic effects in a holographic Fermi-like liquid," JHEP **1205** (2012) 105, arXiv:1204.3914 [hep-th].

[184] S. Nakamura, H. Ooguri and C. -S. Park, "Gravity Dual of Spatially Modulated Phase," Phys. Rev. D **81** (2010) 044018, arXiv:0911.0679 [hep-th].

[185] M. Rozali, D. Smyth, E. Sorkin and J. B. Stang, "Holographic Stripes," Phys. Rev. Lett. **110** (2013) 20, 201603, arXiv:1211.5600 [hep-th].

[186] B. Withers, "Black branes dual to striped phases," Class. Quant. Grav. **30** (2013) 155025, arXiv:1304.0129 [hep-th].

[187] B. Withers, "Holographic Checkerboards," JHEP **1409** (2014) 102, arXiv:1407.1085 [hep-th].

[188] N. Jokela, M. Jarvinen and M. Lippert, "Gravity dual of spin and charge density waves," arXiv:1408.1397 [hep-th].

[189] N. Jokela, G. Lifschytz and M. Lippert, "Holographic anyonic superfluidity," JHEP **1310** (2013) 014, arXiv:1307.6336 [hep-th].

[190] D. K. Brattan and G. Lifschytz, "Holographic plasma and anyonic fluids," JHEP **1402** (2014) 090, arXiv:1310.2610 [hep-th].

[191] N. Jokela, G. Lifschytz and M. Lippert, "Flowing holographic anyonic superfluid," JHEP **1410** (2014) 21, arXiv:1407.3794 [hep-th].

[192] K. Skenderis and M. Taylor, "Branes in AdS and pp wave space-times," JHEP **0206** (2002) 025, hep-th/0204054.

[193] S. Sachdev, "Quantum Phase Transitions," Cambridge University Press, Cambridge (2011).

[194] M. Vojta, "Quantum Phase Transitions," Report on Progress in Physics **66** (2003) 2069-2100 [cond-mat/0309604].

[195] A. Karch and A. O'Bannon, "Holographic thermodynamics at finite baryon density: Some exact results," JHEP **0711** (2007) 074, arXiv:0709.0570 [hep-th].

[196] K. Jensen, A. Karch and E. G. Thompson, "A Holographic Quantum Critical Point at Finite Magnetic Field and Finite Density," JHEP **1005** (2010) 015, arXiv:1002.2447 [hep-th].

[197] K. Jensen, A. Karch, D. T. Son and E. G. Thompson, "Holographic Berezinskii-Kosterlitz-Thouless Transitions," Phys. Rev. Lett. **105** (2010) 041601, arXiv:1002.3159 [hep-th].

[198] N. Evans, A. Gebauer, K. Y. Kim and M. Magou, "Holographic Description of the Phase Diagram of a Chiral Symmetry Breaking Gauge Theory," JHEP **1003**, 132 (2010), arXiv:1002.1885 [hep-th].

[199] N. Iqbal, H. Liu, M. Mezei and Q. Si, "Quantum phase transitions in holographic models of magnetism and superconductors," Phys. Rev. D **82** (2010) 045002, arXiv:1003.0010 [hep-th].

[200] N. Iqbal, H. Liu and M. Mezei, "Quantum phase transitions in semilocal quantum liquids," Phys. Rev. D **91** (2015) no.2, 025024, arXiv:1108.0425 [hep-th].

[201] E. D'Hoker and P. Kraus, "Quantum Criticality via Magnetic Branes," Lect. Notes Phys. **871** (2013) 469, arXiv:1208.1925 [hep-th].

[202] V. G. Filev, "A Quantum Critical Point from Flavours on a Compact Space," JHEP **1408**, 105 (2014), arXiv:1406.5498 [hep-th].

[203] R. Apreda, J. Erdmenger, N. Evans and Z. Guralnik, "Strong coupling effective Higgs potential and a first order thermal phase transition from AdS/CFT duality," Phys. Rev. D **71**, 126002 (2005), hep-th/0504151.

[204] K. Y. Kim, S. J. Sin and I. Zahed, "Dense hadronic matter in holographic QCD," J. Korean Phys. Soc. **63**, 1515 (2013), hep-th/0608046.

[205] N. Horigome and Y. Tanii, "Holographic chiral phase transition with chemical potential," JHEP **0701** (2007) 072, hep-th/0608198.

[206] A. Parnachev and D. A. Sahakyan, "Photoemission with Chemical Potential from QCD Gravity Dual," Nucl. Phys. B **768** (2007) 177, hep-th/0610247.

[207] S. Kobayashi, D. Mateos, S. Matsuura, R. C. Myers and R. M. Thomson, "Holographic phase transitions at finite baryon density," JHEP **0702** (2007) 016, hep-th/0611099.

[208] M. Ammon, M. Kaminski and A. Karch, "Hyperscaling-Violation on Probe D-Branes," JHEP **1211** (2012) 028, arXiv:1207.1726 [hep-th].

[209] G. Itsios, N. Jokela and A. V. Ramallo, "Collective excitations of massive flavor branes," Nucl. Phys. B **909** (2016) 677, arXiv:1602.06106 [hep-th].

[210] R. Kenna, D. A. Johnston and W. Janke, "Scaling relations for logarithmic corrections," Phys. Rev. Lett. **96** (2006) 115701, [cond-mat/0605162]; "Self-consistent scaling theory for logarithmic correction exponents," Phys. Rev. Lett. **97**, 155702 (2006) Erratum: [Phys. Rev. Lett. **97**, 169901 (2006)] [cond-mat/0608127].

[211] A. Karch, M. Kulaxizi and A. Parnachev, "Notes on Properties of Holographic Matter," JHEP **0911** (2009) 017, arXiv:0908.3493 [hep-th].

[212] A. Karch, D. T. Son and A. O. Starinets, "Zero Sound from Holography," arXiv:0806.3796 [hep-th].

[213] A. Karch, D. T. Son and A. O. Starinets, "Holographic Quantum Liquid," Phys. Rev. Lett. **102** (2009) 051602.

[214] D. K. Brattan, R. A. Davison, S. A. Gentle and A. O'Bannon, "Collective Excitations of Holographic Quantum Liquids in a Magnetic Field," JHEP **1211** (2012) 084, arXiv:1209.0009 [hep-th].

[215] R. A. Davison and A. O. Starinets, "Holographic zero sound at finite temperature," Phys. Rev. D **85** (2012) 026004, arXiv:1109.6343 [hep-th].

[216] M. Kulaxizi and A. Parnachev, "Holographic Responses of Fermion Matter," Nucl. Phys. B **815**, 125 (2009), arXiv:0811.2262 [hep-th].

[217] M. Kulaxizi and A. Parnachev, "Comments on Fermi Liquid from Holography," Phys. Rev. D **78** (2008) 086004, arXiv:0808.3953 [hep-th].